

Electromagnetic field effects in

Drosophila melanogaster

Thesis submitted for the degree of

Doctor of Philosophy

at the University of Leicester

Giorgio Fedele
Department of Genetics
University of Leicester

December 2014

What is a scientist after all? It is a curious man looking through a keyhole, the keyhole of nature, trying to know what's going on.

– Jacques Yves Cousteau

Quando sei a un bivio e trovi una strada che va in su e una che va in giù, piglia quella che va in su. È più facile andare in discesa, ma alla fine ti trovi in un buco. A salire c'è speranza. È difficile, è un altro modo di vedere le cose, ti tiene all'erta.

– Tiziano Terzani, La fine è il mio inizio

ABSTRACT

Many higher animals have evolved the ability to use the Earth's magnetic field, particularly for orientation. However, the biophysical mechanism by which magnetoreception is achieved remains elusive. One theoretical model (the radical pair mechanism - RPM) proposes that the geomagnetic field is perceived by chemical reactions involving the blue-light photoreceptor Cryptochrome (CRY). Recent evidence supports the RPM in *Drosophila melanogaster* and reveals a mechanistic link with the circadian clock. Here I have confirmed, albeit with rather different results, that a low frequency electromagnetic field (AC-EMF) along with a Static Field (SF) exposure does affect circadian and activity behaviour in the fruit fly. Furthermore, I have developed two new assays to investigate the effects of EMF in *Drosophila melanogaster*, negative geotaxis and an additional light wavelength preference assay, revealing a net CRY-dependent response. My data support the idea of CRY mediated magnetoreception, thereby indirectly supporting the RPM.

Furthermore, I provide some striking new results that challenge our view that only the canonical clock neurons contribute to behavioural rhythms in *Drosophila melanogaster*.

ACKNOWLEDGMENTS

This work belongs to many people, no one more so than my two supervisors Bambos Kyriacou and Ezio Rosato, whose scientific curiosity and knowledge are unrivaled. Without their input and guidance this work would not have been performed.

During the course of my PhD I have met many people that, in one way or the other, have helped and supported me. Naming all of them is a difficult task and it will become a simple list of people that I worked with. However, the following people have directly contributed, both scientifically and personally, to my work and my PhD-life during these 4 years. First of all I would like to thank Carlo and Valeria. They guided and took care of me during the Erasmus and through the PhD. They taught me a lot but most importantly they made me feel at home every single day since I got to Leicester. I will always be grateful to John; he always made my *day*. I won't thank him for all the help and the scientific support he gave me in the lab but especially for the numerous beer-nights, the X-box sessions and the broken windows that characterized our friendship. Mirko, Kam and Lewis provided numerous forms of support, from intriguing scientific conversations to memorable evenings spent together. Additionally I would like to thank Celia, Daniel and Ed for their efforts and contributions to some parts of this study.

A Massive "thank-you" goes to the "Italian Family" in the department (Gen-Italia, as suggested by Bambos) whose members become terrific friends. With them I experienced some of the most memorable moments during my stay in Leicester. Angy and the attempts of learning venetian dialect made me realize how beautiful is the snow in august, Batini and the multiple uses of washing powder discussed over some beers, Ottoloni showed me how to make a toast for a marriage proposal in the middle of a rock concert, Pille enriched my knowledge with the concept of "edible laundry" less overrated than "edible lingerie", Mika and his kisses during hard-core brainstorming sessions, Pier with his "un-uniform *regalita*" and Forni with his banana

addiction will be remembered for the countless number of hours spent in developing and concealing the AQPs paper that never got published.

Special thanks go also to all my friends in Italy who, despite the distance, have been very close to me during all these years spent abroad: Bardini, Clod, Iore, Mariani, Poppe.

A significant proportion of credit goes to my family, who has provided strong support during my four years in Leicester. Last but not least, I would like to acknowledge Laura; she has been my point of strength and a pillar that helped me going through all the challenges I encountered. I owe her a lot.

TABLE OF CONTENTS

ABSTRACT.....	I
ACKNOLEDGMENTS	II
TABLE OF FIGURES	VIII
ABBREVIATIONS.....	XI
<u>1</u> <u>INTRODUCTION</u>	<u>1</u>
1.1 THE EARTH'S MAGNETIC FIELD: AN OVERVIEW	1
1.1.1 CHARACTERISTICS OF THE EARTH'S MAGNETIC FIELD	2
1.2 MAGNETORECEPTION.....	4
1.2.1 ELECTROMAGNETIC INDUCTION.....	6
1.2.2 FERROMAGNETISM	7
1.2.3 RADICAL PAIR MECHANISM (RPM)	9
1.2.4 EVIDENCE FOR PHOTORECEPTOR-BASED MAGNETO-RECEPTION	16
1.2.5 EVOLUTIONARY ORIGINS FOR THE MAGNETORECEPTION SENSE	20
1.3 CIRCADIAN CLOCKS	20
1.3.1 <i>DROSOPHILA MELANOGASTER</i> CIRCADIAN CLOCK.....	21
1.3.2 ANATOMY OF THE CLOCK	21
1.3.3 THE NEGATIVE FEEDBACK LOOP (NFL) IN <i>DROSOPHILA</i>	24
1.3.4 LIGHT ENTRAINMENT OF THE CLOCK	27
1.3.5 INSECT CRYPTOCHROMES	32
1.4 MAGNETORECEPTION IN <i>D. MELANOGASTER</i>	36
1.5 MY PROJECT.....	43
<u>2</u> <u>MATERIAL & METHODS</u>	<u>45</u>
2.1 FLY MAINTENANCE AND LINES USED	45

2.2	GENOMIC DNA EXTRACTION AND GENOTYPING PCR.....	49
2.3	WESTERN BLOT	50
2.4	CO-IMMUNOPRECIPITATION (CO-IP) AND PARTIAL PROTEOLYSIS	52
2.5	SCHUDERER APPARATUS	53
2.6	ACTIVITY EXPERIMENTS.....	55
2.7	HOME-MADE EXPOSURE SYSTEM	55
2.8	DATA COLLECTION AND ANALYSIS.....	57
3	<u>EMF EXPOSURE SHORTENS FREE-RUNNING PERIOD</u>	<u>59</u>
3.1	INTRODUCTION	59
3.2	MATERIALS AND METHODS	60
3.2.1	DROSOPHILA STRAINS	60
3.2.2	BEHAVIORAL ANALYSES	61
3.2.3	PROTEIN EXTRACTION, WESTERN BLOTS, IP, CO-IP, PARTIAL PROTEOLYSIS AND LUCIFERASE ASSAY	62
3.2.4	STATISTICAL ANALYSIS.....	62
3.3	RESULTS.....	63
3.3.1	LIGHT INTENSITY SCREENING	63
3.3.2	EXPOSURE TO EMF SHORTENS THE PERIOD	64
3.3.3	NOVEL LOCOMOTOR PHENOTYPE	69
3.3.4	HCRY AND MAGNETORECEPTION	71
3.3.5	DROSOPHILA CRY IS STABILISED BY EMF.....	72
3.3.6	CRY CONFORMATION AND CRY-PROTEINS INTERACTIONS.....	73
3.4	DISCUSSION	75
4	<u>GENETIC DISSECTION OF THE EMF-MEDIATED CIRCADIAN EFFECTS.....</u>	<u>81</u>
4.1	INTRODUCTION	81

4.2	MATERIAL AND METHODS	82
1.1.1.	FLY STOCKS	82
1.1.2.	EMF EXPOSURE	83
4.3	RESULTS.....	83
1.1.3.	EXPRESSION OF CRY IN A SUBSET OF CRY⁺ CELLS RESCUES THE EMF PHENOTYPE.	86
1.1.4.	MANIPULATING THE CLOCK AND EMF	86
1.1.5.	EYES AND ANTENNAE AS PUTATIVE STRUCTURES FOR MAGNETORECEPTION.....	87
4.4	DISCUSSION	90
5	NOVEL EMF PHENOTYPE: EMF EXPOSURE DISRUPTS NEGATIVE GEOTAXIS	94
5.1	INTRODUCTION	94
5.2	MATERIAL AND METHODS	94
5.2.1	FLY STRAIN.....	94
5.2.2	BEHAVIOURAL APPARATUS.....	95
5.3	RESULTS.....	95
5.4	DISCUSSION	99
6	SOME MISCELLANEOUS EXPERIMENTS	102
6.1	INTRODUCTION	102
6.1.1	A ‘REPPERT-LIKE’ ASSAY	102
6.1.2	IN SEARCH OF MAGNETITE.....	104
6.1.3	CRY AND AGEING	104
6.2	MATERIALS AND METHODS	105
6.2.1	T-MAZE AND EMF EXPOSURE	105
6.2.2	PARAFFIN SECTIONS AND MAGNETITE STAINING	106

6.2.3	NASONIA LOCOMOTOR ACTIVITY EXPERIMENTS	107
6.2.4	PROTEIN CARBONYLS CONTENT	107
6.3	RESULTS AND DISCUSSION.....	107
6.3.1	FLIES AVOID THE MAGNETIC FIELD UNDER BLUE LIGHT BUT SWITCH THEIR PREFERENCES UNDER GREEN LIGHT.....	107
6.3.2	DROSOPHILA DOES NOT CONTAIN MAGNETITE.....	109
6.3.3	EMF EXPOSURE AND CRY EXPRESSION REDUCE PROTEIN CARBONYLS SYNERGISTICALLY	112
7	ROLE OF PERIPHERAL CLOCKS	114
7.1	INTRODUCTION	114
7.1.1	PERIPHERAL CLOCKS.....	114
7.2	MATERIAL AND METHODS	116
7.2.1	FLY STRAINS	116
7.2.2	IMMUNOHISTOCHEMISTRY (IHC)	116
7.3	RESULTS.....	118
7.3.1	EXPRESSION OF <i>PER</i> IN THE PERIPHERY IS SUFFICIENT TO RESCUE <i>PER</i>⁰¹ PHENOTYPE	118
7.3.2	DBT MUTANTS AS A TOOL FOR STUDYING HOW PERIPHERAL CLOCKS AFFECT THE “CENTRAL PACEMAKER”	124
7.3.3	ARE THESE DRIVERS EXPRESSED IN CANONICAL CLOCK NEURONS?....	129
7.4	DISCUSSION	133
8	FINAL DISCUSSIO	136
9	APPENDIX	142
10	BIBLIOGRAPHY	152
11	PAPERS PUBLISHED	169

TABLE OF FIGURES

FIGURE 1-1 MAGNETIC FIELD COMPONENTS.....	2
FIGURE 1-2 THE EARTH'S MAGNETIC AND GEOGRAPHIC POLES AND THE EARTH'S MAGNETIC FIELD.....	3
FIGURE 1-3 MAGNETIC COMPASSES IN ANIMALS	5
FIGURE 1-4 SIMPLIFIED REACTION SCHEME FOR THE RPM	11
FIGURE 1-5 "REFERENCE-PROBE" MODEL FOR A RADICAL PAIR SENSOR.....	12
FIGURE 1-6 CRY PHOTOCYCLE AND EMF-SENSITIVE STEPS	15
FIGURE 1-7 ORIENTATION OF EUROPEAN ROBINS IN LIGHT AND DARKNESS.	18
FIGURE 1-8 OVERVIEW OF CLOCK-GENE EXPRESSING NEURONS AND ANATOMICAL LOCALIZATION WITH A CLOSE-UP TO LN_D s.....	23
FIGURE 1-9 THE THREE INTERLOCKED NEGATIVE-FEEDBACK LOOPS IN DROSOPHILA.....	27
FIGURE 1-10 LIGHT- DEPENDENT TIM-CRY DEGRADATION.....	30
FIGURE 1-11 DNA PHOTOLYASE/CRY GENE FAMILY PHYLOGENETIC TREE (ML).....	34
FIGURE 1-13 CRY IS INVOLVED IN DROSOPHILA MAGNETORECEPTION	40
FIGURE 1-14 EMF MODULATES DROSOPHILA CIRCADIAN CLOCK THROUGH CRY.....	42
FIGURE 2-1 BACKROSSING SCHEME. ♀ INDICATES FEMALE VIRGINS, ♂ INDICATES MALES AND ← INDICATES THE Y CHROMOSOME.	48
FIGURE 2-2 EXAMPLE OF RECOMBINATION USING TM8SB ¹ . ♀ INDICATES FEMALE VIRGINS, ♂ INDICATES MALES AND ← INDICATES THE Y CHROMOSOME.....	49
FIGURE 2-3 SCHEMATIC REPRESENTATION OF THE SCHUDERER APPARATUS.. ..	54
FIGURE 2-4 THE DELIVERY SYSTEM FOR EMFs CONSISTS OF A DOUBLE-WRAPPED COIL SYSTEM	57
FIGURE 3-1 RHYTHMICITY OF WILD-TYPE UNDER DIFFERENT INTENSITIES OF CONSTANT BLUE LIGHT....	63

<i>FIGURE 3-2 EMF EXPOSURE SHORTENS FREE-RUNNING CIRCADIAN PERIODS IN DIM BLUE LIGHT.....</i>	65
<i>FIGURE 3-3 - PERIOD CHANGES ARE NOT CAUSED BY MECHANICAL VIBRATION.....</i>	66
<i>FIGURE 3-4 CRY VARIANTS ALTER NORMAL CIRCADIAN RESPONSES TO EMFs.....</i>	69
<i>FIGURE 3-5 EMF INDUCED HYPERACTIVITY IN CANTON-S FLIES.....</i>	70
<i>FIGURE 3-6 EMF INDUCED HYPERACTIVITY IN CRY VARIANTS.....</i>	71
<i>FIGURE 3-7 HCRYs.....</i>	72
<i>FIGURE 3-8 EXPOSURE TO EMF INCREASED CRY STABILITY.....</i>	73
<i>FIGURE 3-9 IN-VITRO PARTIAL PROTEOLYSIS.....</i>	74
<i>FIGURE 3-10 Co-IP</i>	75
<i>FIGURE 3-11 EXPOSURE TO GREEN LIGHT LENGTHENS THE PERIOD UNDER EMF.....</i>	77
<i>FIGURE 4-1 A-B EXPRESSION OF CRY IN CRY-POSITIVE CELLS RESTORES EMF PHENOTYPES.....</i>	84
<i>FIGURE 4-2 PDF>CRY;CRY⁰² AND CLK9M>CRY;CRY⁰² FLIES FAILED TO RESPOND TO EMF.</i>	85
<i>FIGURE 4-3 CONTROL USING TIMGAL4.</i>	86
<i>FIGURE 4-4 OVEREXPRESSION OF SGG DOES NOT SHOW AN EMF EFFECT.</i>	87
<i>FIGURE 4-5 GMRGAL4 DRIVEN CRY EXPRESSION IS SUFFICIENT TO RESCUE EMF EFFECTS.....</i>	88
<i>FIGURE 4-6 R7 RHABDOMERES MEDIATE EMF EFFECTS.....</i>	88
<i>FIGURE 4-7 GLASS MUTANTS CAN RESPOND TO EMFs.</i>	89
<i>FIGURE 4-8 CRY IN THE ANTENNAE RESCUES THE PERIOD SHORTENING BUT NOT THE HYPERACTIVITY.....</i>	89
<i>FIGURE 4-9 JOGAL4 WEAKLY RESCUES EMF-INDUCED PERIOD SHORTENING.....</i>	90
<i>FIGURE 5-1 MEAN GEOTACTIC RESPONSES±SEM.....</i>	97
<i>FIGURE 5-2 GAL4/UAS CONTROLS STRAINS SHOW NORMAL EMF RESPONSES.....</i>	99

<i>FIGURE 6-1</i> NAÏVE FLIES AT WAVELENGTHS >420NM SHOW OPPOSITE RESPONSE TO FLIES EXPOSED TO >400NM AND FULL SPECTRUM LIGHT (FROM GEGEAR ET AL., 2008).....	103
<i>FIGURE 6-2</i> T-MAZE APPARATUS.....	105
<i>FIGURE 6-3</i> A CANTON-S FLIES EXHIBITED AVOIDANCE FOR THE FILED UNDER BLUE LIGHT	108
<i>FIGURE 6-4</i> A-E DROSOPHILA SECTIONS. A SAGITTAL SECTION OF DROSOPHILA.....	109
<i>FIGURE 6-5</i> AVERAGE PERIOD (A) AND LOCOMOTOR EVENTS OF ACTIVITY (B) FOR <i>NASONIA VITRIOPENNIS</i>	111
<i>FIGURE 6-6</i> PROTEIN CARBONYL CONTENTS UNDER EMF/SHAM EXPOSURE.....	112
<i>FIGURE 7-1</i> EXPRESSION OF PER USING PERIPHERAL DRIVERS.....	118
<i>FIGURE 7-2</i> EXPRESSION OF PER IN THE ANTENNAE RESCUES PER ⁰¹ LOCOMOTOR RHYTHMS.....	120
<i>FIGURE 7-3</i> EXPRESSION OF PER IN TRP CHANNELS RESCUES PER ⁰¹ ARRHYTHMIA.	121.
<i>FIGURE 7-4</i> EXPRESSION OF PER IN THE ANTENNAE AND IN THE EYES RESTORES RHYTHMICITY.....	123
<i>FIGURE 7-5</i> EXPRESSION OF DBT MUTANTS IN THE ANTENNAE IS SUFFICIENT TO TRIGGER PERIOD CHANGES.	125
<i>FIGURE 7-6</i> EXPRESSION OF DBT-VARIANTS IN THE EYES DOES NOT TRIGGER PERIOD CHANGES.....	126
<i>FIGURE 7-7</i> A OVEREXPRESSION OF DBT ^{K/R} INDUCES ARRHYTHMIA.....	127
<i>FIGURE 7-8</i> IHC SHOWING L-LN _V S LABELLED BY GFP IN <i>PdfG80</i> , <i>PAING4</i> , <i>PYXGAL4</i> AND <i>FGAL4</i> LINES... ..	130
<i>FIGURE 7-9</i> EXPRESSION OF GFP DRIVEN BY GMRGAL4. ONE L-LN _V WAS LABELLED (TOP) WHEREAS NO DORSAL NEURONS WERE LABELLED (BOTTOM) BY GFP. COURTESY OF DR HANSEN.	131.
<i>FIGURE 7-10</i> GFP-LABELLING IN THE ANTENNAE OF <i>PdfG80</i> , <i>PAING4</i> AND <i>FGAL4</i>	132.
<i>FIGURE 7-11</i> CRYOSTAT SECTIONS OF THE ANTENNAE IN <i>IAVGAL4</i> AND <i>NOMPAGAL4</i> . IMAGES ARE REPORTED AS STACKS.	132.

ABBREVIATIONS

AC- Alternate current	ELF-Extremely Low Frequency
Arnt- aryl hydrocarbon receptor nuclear translocator protein	EMF-Electro Magnetic Field
bHLH- basic Helix-Loop-Helix	EPR-Electron Paramagnetic Resonance
bZip- basic leucine Zipper	ET-Electron Transfer
CCGs- Clock Controlled Genes	FAD- Flavin Adenine Dinucleotide
CK2 –CASEIN KINASE 2	GFP- Green Fluorescent Protein
CLK-CLOCK	GMF-GeoMagnetic Field
Co-IP- CoimmunoPrecipitation	GMR-GLASS MULTIMER REPORTER
CRY- CRYPTOCHROME	hCRY- <i>Human</i> CRY
CS- Canton-S	IHC- ImmunoHistoChemistry
CTT- C-terminal tail	IP- Immuno Precipitation
CWO- CLOCKWORK ORANGE	ISC-Inter-System Crossing
CYC-CYCLE	JET-JETLAG
DBT-DOUBLE-TIME	KAY-KAYAK
DC- Direct Current	I-LN _V s-large-Lateral Ventral Neurons
dCRY- <i>Drosophila</i> CRY	LN _D s-Lateral Dorsal Neurons
DD- Constant Darkness	MTHF- Methenyltetrahydrofolate
dLL- dim Constant Light	NFL- Negative Feedback Loop
DNs-Dorsal Neurons	NMO-Nemo
EB- Exaction Buffer	O ₂ - Oxigen
	OX- Oxidised

PAS- Per-Arnt-Sim	SD- Single Domain
PBS- Phosphate Buffered Saline	SGG- SHAGGY
PDF-PIGMENT DISPERSING FACTOR	Sim- single-minded protein
PDP1 ε - PAS DOMAIN PROTEIN 1 ε	SLIMB- Supernumerary LIMbs
PER- Period	SPM - SuperParaMagnetic
Phe- Phenylalanine	TBS- Tris Buffered Saline
PHR- Photolyase Homology Region	TIM- timeless
QSM-QUASIMODO	Trp- Tryptophan
RED- Reduced	TTL- Transcriptional-Translational-Loop
RF- RadioFrequency	UAS-Upstream Activating Sequence
RPM- Radical Pair Mechanism	UV- Ultra-Violet
s-LN _{vs} -small-Lateral Ventral Neurons	VRI- VRILLE
SB- Squishing Buffer	

1 INTRODUCTION

1.1 THE EARTH'S MAGNETIC FIELD: AN OVERVIEW

The Earth is a huge magnet that produces a geomagnetic field (GMF). The intensity of this field varies from about 70 µT at the north and south poles to about 30 µT at the equator (in the UK the intensity is about 50 µT). This geomagnetic field is a magnetic dipole tilted 11 degrees from the spin axis of the Earth, with the magnetic field South Pole near the Earth's geographic North Pole and the magnetic field North Pole near the Earth's geographic South Pole; therefore the total magnetic field can be divided into several components (Figure 1-1):

- **Declination (D)** indicates the differences, in degrees, between the headings of true north and magnetic north.
- **Inclination (I)** is the angle, in degrees, of the magnetic field above or below horizontal.
- **Vertical Intensity (Z)** defines the vertical component of the total field intensity.
- **Total Intensity (F)** is the strength of the magnetic field, not divided into its component parts.

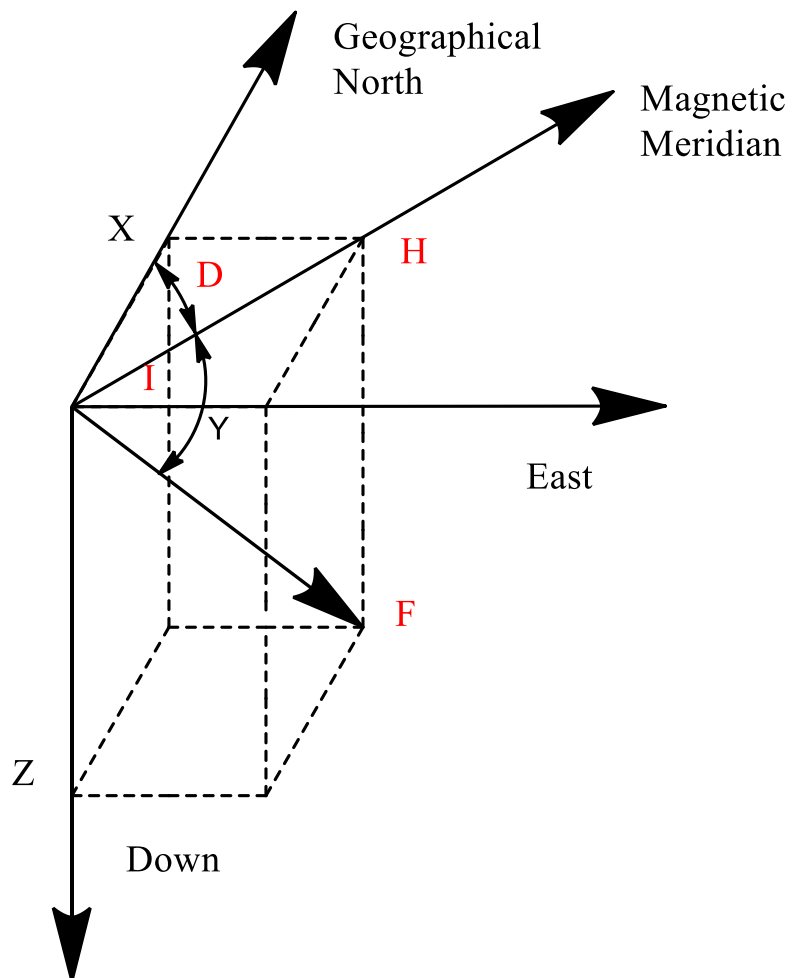


Figure 1-1 Magnetic Field Components

(X, Y, Z) define the Cartesian components (north, east, down), (H, D, Z) are the components of the magnetic field (horizontal intensity, declination, down), (I) is the inclination of the field (F) is the total intensity. Adapted from The US Geological Survey.

1.1.1 CHARACTERISTICS OF THE EARTH'S MAGNETIC FIELD

The Earth's magnetization is due to a "Dynamo Effect" (Demorest, 2001; Dormy & Le Mouël, 2008), where a conducting flowing fluid is capable of inducing an electromagnetic field (EMF) if kept in constant rotation. The convection of molten iron

in the outer liquid core of the planet, which is constantly rotating thanks to the Coriolis force, produces electric currents aligned with the rotational axis, thus inducing the GMF (Figure 1-2). Studies on paleomagnetic samples provided even further evidence for this Dynamo model. When a rock is formed, it usually acquires a magnetization parallel to the ambient magnetic field; studies of these samples revealed not only significant change of the field over time, but actual polarity flips, which cannot be explained by a simple permanent magnetization- *i.e.* a magnetite core. Those flips called *reversals* are explained by the fact that the electric currents are not constant in direction, although the underlying mechanism remains unknown (Dormy & Le Mouël, 2008).

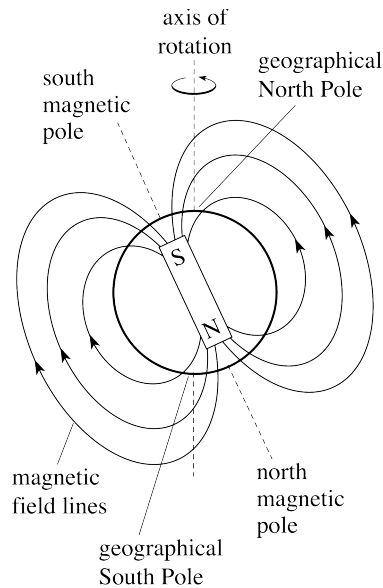


Figure 1-2 The Earth's magnetic and geographic poles and the Earth's magnetic field.
Adapted from PPLATO, University of Reading.

FIELD VARIATIONS AT DIFFERENT TIMES

As previously mentioned, the GMF is neither uniform nor constant, and along with latitudinal variations it also exhibits some predictable fluctuations of intensity and direction with a well-defined period of 24 h. These variations are caused by the interaction of the solar ionising radiation with the neutral molecules in the ionosphere.

In this region of the atmosphere, high-energy ultra-violet (UV) and X-rays from the Sun ionize the air molecules creating electric currents, which in turn induce a superimposed EMF. The result of this interaction is that the GMF is stronger during the day and weaker during the night. Consequently, the total GMF also exhibits seasonal variation; in fact in the northern hemisphere the GMF is rather stronger during the summer than during winter, a reflection of the increased photoperiod (Campbell, 2003; Kato, 2006; Gould, 2010).

In reality, this type of variation would affect the declination by no more than a few tenths of a degree. Inclination varies by less than a tenth of a degree and the total intensity is perturbed by only a few tens of nT, which represents about 0.1% of the Earth's magnetic field strength. Although these effects are very small, they are relevant for studies of animal navigation (Campbell, 2003), and they provide a rationale for invoking a role in the regulation of circadian clocks as a weak synchronizer (*Zeitgeber*) (Wever, 1973; Gould, 1984).

1.2 MAGNETORECEPTION

Despite the fluctuating nature of the GMF (reversals, regional variations), the field is a reliable source for navigation: the magnetic vector provides directional information and can be used as a compass (Wiltschko & Wiltschko, 2006), while the total intensity and/or inclination exhibits a gradient between the magnetic poles and the magnetic equator and it may be used as a component of a system indicating position (a GPS – Global Positioning System) (Wiltschko & Wiltschko, 2006). Thus, it appears plausible that organisms evolved mechanisms to detect and exploit the field's properties. The evolution of magnetic sense, in fact, has been described in a wide variety of organisms across different *taxa*. Two types of magnetic compasses have been defined in nature: a polarity and an inclination compass (Figure 1-3). The first works as a normal technical compass being able to discriminate the polarity of the GMF, distinguishing between South and North Poles. The latter, in contrast, ignores the polarity of the field but it is sensitive to the angle of the field lines with respect to the Earth's surface. It distinguishes between a *pole-ward* direction, where the lines have a downward direction, and an *equator-ward* direction if the lines have an upward

orientation (Wiltschko & Wiltschko, 2005, 2006; Winklhofer, 2010; Dodson, Hore & Wallace, 2013). A way to distinguish between the two compasses is simply by testing animal responses in a field with the vertical component inverted; rodents and spiny lobsters (Wiltschko & Wiltschko, 2006) have been shown to be able to maintain their headings while birds (Ritz, Adem & Schulten, 2000) and newts (Phillips, Jorge & Muheim, 2010a) reverse theirs, hence revealing the use of an inclination compass.

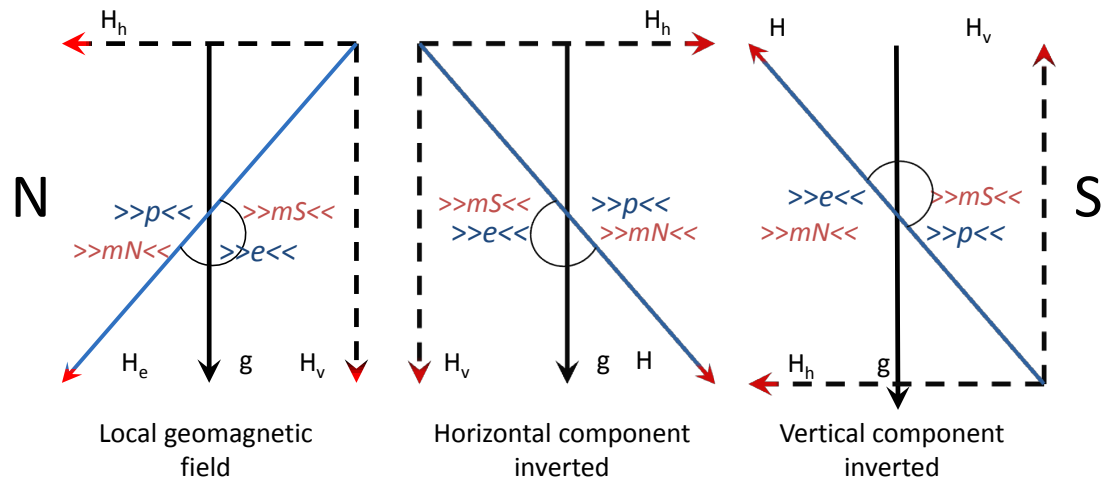


Figure 1-3 Magnetic compasses in animals

Arrows in red give the polarity of the magnetic field , the course of the field is given in blue; N, S geographic North and South, respectively; He, vector of the magnetic field; H_h, H_v, horizontal and vertical component of the field; g, gravity vector. The “polarity compass” is based on the polarity of the field lines, its readings >>mN<<, magnetic North and >>mS<<, magnetic South, these readings are given in red. The “inclination compass” is based on the course of the field lines and their inclinations, its readings >>p<<, poleward when they are pointing downward and >>e<<, equatorward, when they are pointing upward; these readings are given in blue. Left: the natural situation is represented with He pointing toward the N. In this situation, both polarity and inclination compass point in the same direction. Centre: H_h reversed, the polarity is changed (He is pointing S) and as consequence also the course of the field lines is changed pointing downward toward South, but for the “inclination compass” this situation can represent the situation in the southern hemisphere, i.e. where the field lines point downward toward the South Pole. Right: H_v is inverted; in this case the “polarity compass” is unaffected since He is still pointing North. On the contrary, the “inclination compass” is affected since the course of the lines field has been inverted. They are going upward toward the geographic poles and

downward toward the equator. Adapted from (Wiltschko & Wiltschko, 2006). In other words, if a migratory bird, which uses an inclination compass, is flying towards the South Pole, it could follow the field lines. In the Northern hemisphere, the field lines are downward, so the bird must fly in the opposite direction, i.e. equatorward direction (left panel). However when it crosses the equator, the horizontal component is now inverted and the field lines are pointing downward toward the Pole. Again the bird can follow them maintaining a southward direction (central panel). If however, the vertical component of field was inverted then the inclination compass will fail: following the field lines would assume a northward rather than a southward direction.

The existence of at least two different types of animal compasses, suggests that different physiological mechanisms must have evolved, and, over the last three decades, several pieces of evidence have hinted at the existence of at least three magnetosensing mechanisms: one model involves electromagnetic induction: a peculiar feature of marine creatures; another model relies on receptors that utilize single-domain or super-paramagnetic clusters of magnetite particles; and the last model involves electron-spin resonance interactions occurring in a specialized photoreceptor, which would result in modulation by the Electromagnetic Field (EMF) of the photoreceptor's response to light. This model is called the Radical Pair Mechanism (RPM) (Ritz *et al.*, 2000).

1.2.1 ELECTROMAGNETIC INDUCTION

Electromagnetic induction, discovered by Farady in 1831, is the production of voltages across conductors moving through an EMF (see 1.1.1). This concept has been used to explain a possible mechanism for magnetoreception in animals, and suggests that if organisms had a set of copper coil-like structures they could simply move across the GMF and measure the current this motion induces in the circuit. The amplitude of these voltages would depend on the cross-sectional area of the coil, the speed of the organism, the angle between the direction of travel and field and the resistance of the coil. Theoretical calculations have never been very encouraging for the coil model: animals move too slowly, are too small to have

sufficiently large detectors and have too much resistance in the fluids that could serve as conductors. Nevertheless, it has been showed that at least some elasmobranches use induction to judge direction, employing their *ampullae of Lorenzini* (Kalmijn, 1982; Lohmann & Johnsen, 2000; Randall, Burggren & French, 2002; Gould, 2010). These special receptors are jelly-filled canals opened to the surface by *pori* and ended blindly in a cluster of small pockets, synapsing the VII cranial nerve. These *ampullae* can sense small changes in voltage; their sensitivity is thought to be $2\mu\text{V}/\text{m}$ (Kalmijn, 1982; Randall *et al.*, 2002; Johnsen & Lohmann, 2008). It is theoretically possible that sharks and rays use electromagnetic induction as a source for magnetoreception. However, since this hypothesis was first proposed, several complications have arisen.

First of all, despite their remarkable sensitivity, the *ampullae* are thought to detect only alternating current (AC) fields, whereas the GMF is mainly static. In addition, ocean currents are also conductors, and moving through the GMF the sharks produce an electric field of their own. So the question remains, how can elasmobranches detect the GMF? Paulin suggested that sharks could solve both problems by swinging the head back and forth while swimming (Paulin, 1995). This movement will create oscillating electric fields that can be detected but also it might work as a high-pass filter, removing the background noise and helping the animals to pay attention only to the oscillating electric field that originates from its head movement. However, Walker and co-workers (2003) (Walker, Diebel & Kirschvink, 2003) demonstrated that bar magnets inserted in the nasal cavities of the short-tailed stingray, *Dasyatis brevicaudata*, lead to disorientation, whereas the same was not true for non-magnetic materials, raising the possibility that sharks could use a different system of navigation, probably magnetite (but see Molteno & Kennedy, 2009).

1.2.2 FERROMAGNETISM

The second model proposed, permanent magnetization, is based on magnetite crystals (Fe_3O_4). The idea of biological magnetite was proposed by Lowenstam (1967) (Lowenstam, 1967), when he discovered that magnetite was used by chitons (Mollusca: Polyplacophora) for hardening their *radula*, in order to graze biofilm on underwater rocks. Subsequently, Blakemore (Blakemore, 1975) described the first

magnetotactic bacteria, where magnetite clusters were found in the rostral part of the organisms and used to align the organisms with the Earth's field lines, causing these prokaryotes to swim away from the toxic oxygen-rich atmosphere. It seems likely that magnetite (the densest substance synthetized biologically) was originally utilised as a weight to pull the organism down away from the surface and subsequent evolution may have led to aligned chains, capable of orienting in the GMF.

Since these early discoveries, magnetite has then been found in many different taxa: in specific cells in honey bees (*Apis mellifera*) (Gould, Kirschvink & Deffeyes, 1978; Hsu *et al.*, 2007), in antennae in ants (*Pachycondyla marginata*) (Acosta-Avalos *et al.*, 1999; de Oliveira *et al.*, 2010) and in innervated tissues in the ethmoid sinus near the nose in many vertebrates (especially birds (Kirschvink, Walker & Diebel, 2001; Walker *et al.*, 2003; Wiltschko & Wiltschko, 2005, 2006; Cadiou & McNaughton, 2010; Eder *et al.*, 2012). Recent studies have also pointed out a possible way of formation of magnetite in bacteria (Komeili, 2007; Jogler & Schüler, 2009), indicating novel structures, called *magnetosomes*, as sites for the formation of magnetite crystals and identifying also putative genes thought to be involved in this process (Komeili, 2007).

The magnetic property of magnetite depends on the structure, size and shape of particles. The magnetism itself is generated by the spin of electrons in the substances; in atoms with an even numbers of electrons, the spins are paired and parallel, and cancel one another out. In all materials with an odd number of electrons, the unpaired spin of an electron in one-atom cancels out the oppositely oriented unpaired spin in the neighbor. But in magnetite, the crystal structure aligns the unpaired electrons in series: analogous to a pair of magnets attaching themselves in a line, N→S: N→S. The ability of magnetite to retain a permanent field depends on the crystal size: larger particles are multi-domain without a net magnetic momentum, smaller particles (hereafter called Single Domain- SD) have a stable magnetic moment thus working as tiny magnets, whereas even smaller ones (superparamagnetic- SPM) are too small to retain a magnetic momentum, due to thermal agitation. However, a SPM cluster can be magnetized in an external field, but it loses its magnetization as soon as the field disappears (Cadiou & McNaughton, 2010; Gould, 2010).

In vertebrates, SD has been found in the ethmoid sinus, located between the olfactory and optic nerves, and innervated by a branch of the trigeminal nerve, both in birds and fish; whereas, clusters of SPM have been described in the skin of the upper beak of pigeons, *Columba livia* (Wiltschko & Wiltschko, 2006; Cadiou & McNaughton, 2010) although the real nature of these clusters is still under debate (Treiber *et al.*, 2012; Lefeldt *et al.*, 2014). These findings suggest that both types of crystals are equally likely to contribute to the magnetosense in different organisms, although a definitive physiological model has yet to be proposed.

1.2.3 RADICAL PAIR MECHANISM (RPM)

This model for magnetoreception is based on a completely different mechanism that relies on chemical reactions involving specialized photoreceptors (Ritz *et al.*, 2000). Absorption of light triggers an electron transfer (ET) from a donor (D) to an acceptor (A) molecule, thus forming a radical pair (D-A) in which each partner shares an electron. The new-formed radical possesses a quantum magnetic property, which is denoted by the spin of the shared electrons (*i.e.* the angular momentum of the electron), and this quantum magnetic property can be affected by an external EMF (Figure 1-4).

The alignment of the two electrons at any given moment is denoted as the spin state of the radical pair: singlet [S] when they are paired (antiparallel) and triplet [T] if they become unpaired (parallel) and this is a determinant for their chemical reactivity. In other words, a radical in an overall singlet state can trigger reactions that are forbidden to a triplet state. Normally, radicals created in a photoreaction are typically spin-correlated (Solov'yov & Schulten, 2011) namely the spin of the unpaired electron matches the spin of the atomic nucleus, *via* hyperfine interactions, intra-radical coupling between the magnetic moment of an atomic nucleus and the magnetic moment of the unpaired electron. The magnetic forces that describe the torque of the atomic nucleus influence the “direction” of the electrons in the atom (Abeyrathne, Halgamuge & Farrell, 2010). Under the influence of the hyperfine couplings, the radicals oscillate between [S] and [T], depending on the quantum orientation of the atoms, a process called $S \leftrightarrow T$ interconversion (or intersystem crossing- ISC). The ISC

could be enhanced by an external magnetic field in the presence of anisotropic hyperfine couplings (with a preferred direction), a weak Zeeman effect, *i.e.* electronic energy line splitting that is dependent on the strength of an external magnetic field (Ashworth, 2012), and weak exchange interactions, *i.e.* interactions between the unpaired electrons of a radical that decays exponentially with the distance between the two electrons (Dodson *et al.*, 2013). In fact, if the magnetic field is weaker than hyperfine interaction, then the Zeeman splitting favours the interconversions between [S] to [T], whereas if the field is stronger, then the equilibrium between the two states is pushed toward the triplet, which has a net magnetic moment, and away from the singlet (Ritz *et al.*, 2000; Wang & Ritz, 2006; Abeyrathne *et al.*, 2010; Ma & Ritz, 2014). Similarly, when the distance between two unpaired electrons becomes negligible (*i.e.* they are sufficiently far), the exchange interactions are weak and the interconversion becomes feasible (Abeyrathne *et al.*, 2010; Ashworth, 2012; Dodson *et al.*, 2013). In other words, in order for a radical pair to be magnetically sensitive but at the same time being capable of providing directional information, five important points need to be satisfied (Solov'yov & Greiner, 2013):

- At least one of the S and T states should undergo a spin-selective reaction that the other cannot.
- There should be suitable anisotropic hyperfine interactions.
- The lifetime of the radical pair must be long enough to allow the weak magnetic field to affect the spin-dynamics.
- The Zeeman interaction can only modulate the $S \leftrightarrow T$ interconversion if inter- radical (exchange) interactions are sufficiently weak, *i.e.* the two radicals should have an optimal distance.
- To deliver directional information, the radical pairs must be aligned and immobilized and the spin system should relax sufficiently slowly.

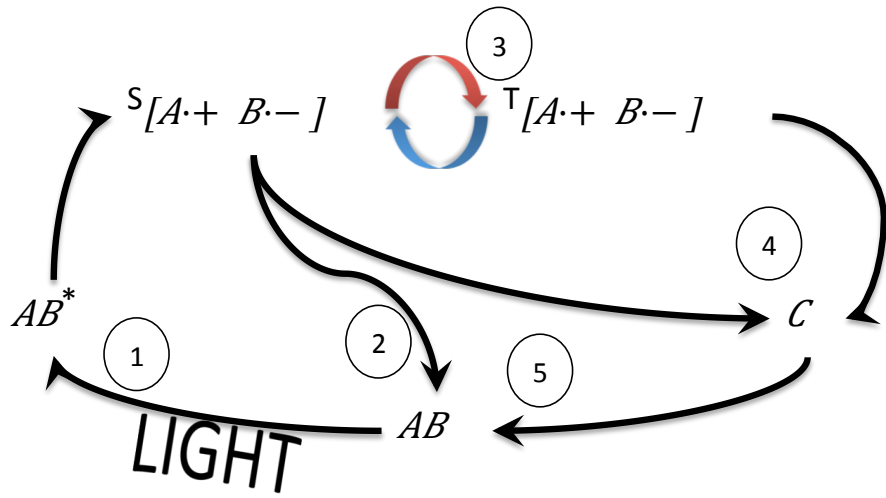


Figure 1-4 Simplified reaction scheme for the RPM

1) photon absorption excites the molecule AB to AB^* that will form the radical pair $S[A\cdot + B\cdot -]$ in an overall singlet state. (2) the radical pair $S[A\cdot + B\cdot -]$ can be re-oxidized to AB . (3) an applied EMF enhances the interconversion of $S[A\cdot + B\cdot -]$ and $T[A\cdot + B\cdot -]$, modifying the formation of C (4). Species C is either the signalling state or leads to the signalling state via subsequent chemical transformations. (5) When C is formed it can be re-oxidized to AB . (Modified from (Rodgers & Hore, 2009)).

Moreover, it has been shown that most known radicals contain either nitrogen or hydrogen atoms with very strong internal magnetic fields. These fields however are highly anisotropic, that is they are much stronger in one direction than in others, as demonstrated by Maeda and co-workers (Maeda *et al.*, 2008). This feature can therefore be exploited to design a compass; the GMF can be either aligned with the stronger or the weaker internal field. Thus the effect of an external magnetic field not only depends on its intensity but also on its direction, thereby providing magnetic directional information (Ritz *et al.*, 2000; Maeda *et al.*, 2008). To better understand how a magnetic field, as weak as the GMF, could affect the radical pair and therefore providing directional information, Ritz and co-workers (Ritz *et al.*, 2000, 2010) proposed the so-called “reference-probe” model (Figure 1-5). In this model, only one of the two radicals has strong hyperfine couplings, normally due to Nitrogen or Hydrogen atoms (called *reference*), whereas the second radical is devoid of internal

magnetic field (*probe*). In this scenario, a weak external magnetic field will have no effect on the reference but will re-orient the probe, therefore providing directional information by affecting the precession rate and direction of the electron, *i.e.* the rotational movement of the electron along its axis will be changed allowing an intersystem crossing.

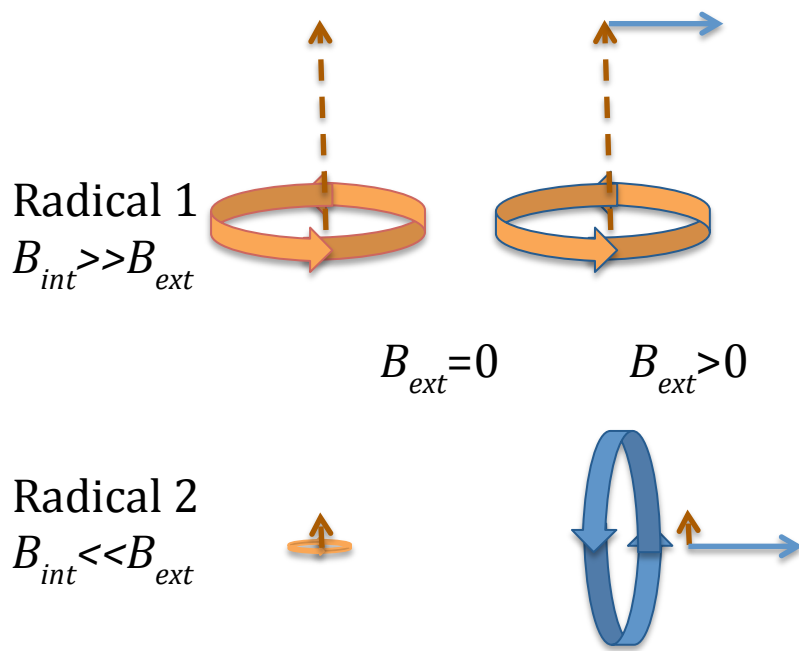


Figure 1-5 “Reference-Probe” model for a radical pair sensor

Straight arrows indicate strength and direction of internal (orange) and external (blue) magnetic fields in the ‘reference’ radical (top) and ‘probe’ radical (bottom), circular arrows illustrate the resulting electron spin motion around the combined magnetic field axis, with larger arrows indicating the main effect.. In the ‘reference’ radical (top), the spin will precess at a high rate and exposure to an external magnetic field will not perturb its movement. However, if a ‘probe’ radical (bottom) has very small or no internal magnetic fields, then the external magnetic field will completely determine the relative spin orientation to the external magnetic field. (Modified from (Ritz *et al.*, 2010)).

Although the quantum chemical mechanism that leads to magnetic information is well understood, it still remains unclear which biological molecules are capable of

undergoing such a mechanism. One class of photoreceptors that meets the requirements is Cryptochrome (CRYs), a flavoprotein ubiquitous among different taxa. CRYs are blue-photoreceptors containing two non-covalently bound chromophores: a redox active flavin adenine dinucleotide (FAD) and a light-harvesting cofactor (Ahmad *et al.*, 2007; Solov'yov, Chandler & Schulten, 2007; Oztürk *et al.*, 2008; Ozturk *et al.*, 2011; Czarna *et al.*, 2013). Their functions include entrainment of circadian clocks (see paragraph 1.3.4) and in plants regulation of growth and development. CRYs have evolved from photolyases, but they exhibit a much reduced and almost null DNA repair ability. Moreover, in contrast to photolyases, the photoactive forms of CRY seem to contain FAD in its fully oxidized redox state (FAD_{ox}). Absorption of blue light ($\lambda \leq 480$ nm) leads to the formation of the semi-reduced form, the flavosemiquinone radical ($\text{FAD}^{\bullet-}$ or the protonated neutral form FADH^{\bullet} , Figure 1-6) by a sequence of intraprotein electron transfers along a conserved chain of 3 tryptophan residues (Trp-triad) that culminates in the oxidation of the terminal Trp residue to form a $\text{Trp}^{\bullet+}$ radical that can deprotonate to form a Trp^{\bullet} radical.

When CRY is in its semi-reduced form the protein is considered in its signalling state (Figure 1-6). At this stage the magnetic field influences the rate of inter-system crossing between S and T excited states (Figure 1-6). Owing to conservation of spin, back transfer of an electron to reform the FAD_{ox} form is possible only when the RP is in an overall S state. Consequently, alignments of the magnetic field that produce a greater $S \leftrightarrow T$ mixing, and therefore, decrease the overall S character of the RP, will enhance the persistence of the radical form, *i.e.* the protein remains in its active state longer (Rodgers & Hore, 2009; Phillips, Muheim & Jorge, 2010b). Further absorption of light (at wavelength ≥ 500 nm) leads to the complete reduced form of CRY (FADH^{\bullet} , inactive state, Figure 1-6), which is subsequently converted back to the fully oxidized state in the dark (Bouly *et al.*, 2007). This re-oxidation reaction occurs by a mechanism that could also generate radical pairs (superoxide and/or peroxide radicals) and therefore is magnetically sensitive (Müller & Ahmad, 2011) (Figure 1-6). However, Muller and co-workers showed that the superoxide radicals could be formed even in the presence of light, depending on the intracellular concentration of molecular oxygen (O_2), therefore opening the possibility that upon illumination both radicals can

be formed. The superoxide radical will be in an overall triplet state due to spin conservation, molecular oxygen is triplet in its ground state; however the full re-oxidation to FAD_{ox} requires a singlet state and hence a spin-forbidden [T]-[S] conversion could be enhanced by the external EMF (Müller & Ahmad, 2011). To note, the superoxide radicals perfectly fit the reference-probe model discussed above, as one of the radicals is devoid of any hyperfine couplings (no Nitrogen or Hydrogen atoms are present in O₂). In addition, new plausible radicals have been suggested to place a role in detecting the field. Tyrosine residues, for instance, could mediate an electron transfer (ET) when of the Trp is ablated (Biskup *et al.*, 2013) suggesting that CRY could preserve ET reactions through different compensatory mechanisms. However, recent spin dynamics simulations seem to favour a radical (called Z, as the identity is unknown) (Lee *et al.*, 2014) over the canonical Trp (or Tyr) radical, which has relative strong hyperfine interactions and does not really fit with the reference-probe model (Ritz *et al.*, 2010). According to the simulations, a [FAD^{•-} Z[•]] radical pair, where Z has almost null hyperfine interactions, would be more anisotropic than a [FAD^{•-} Trp[•]] radical pair and therefore would be more sensitive to an external magnetic field as weak as the Earth's (Lee *et al.*, 2014). Still it remains unclear what is the nature of the Z radical; simulations suggest that oxygen could be a suitable candidate (Lee *et al.*, 2014) even though it would have a very fast spin relaxation rate, non-ideal for a magnetic field sensor. Speculation has focused attention on another molecules that could be a suitable radical: ascorbic acid, a common biological reductant that can reduce photo-excited flavin and Trp radicals by either hydrogen atom or electron transfer with relatively small hyperfine interaction (Lee *et al.*, 2014).

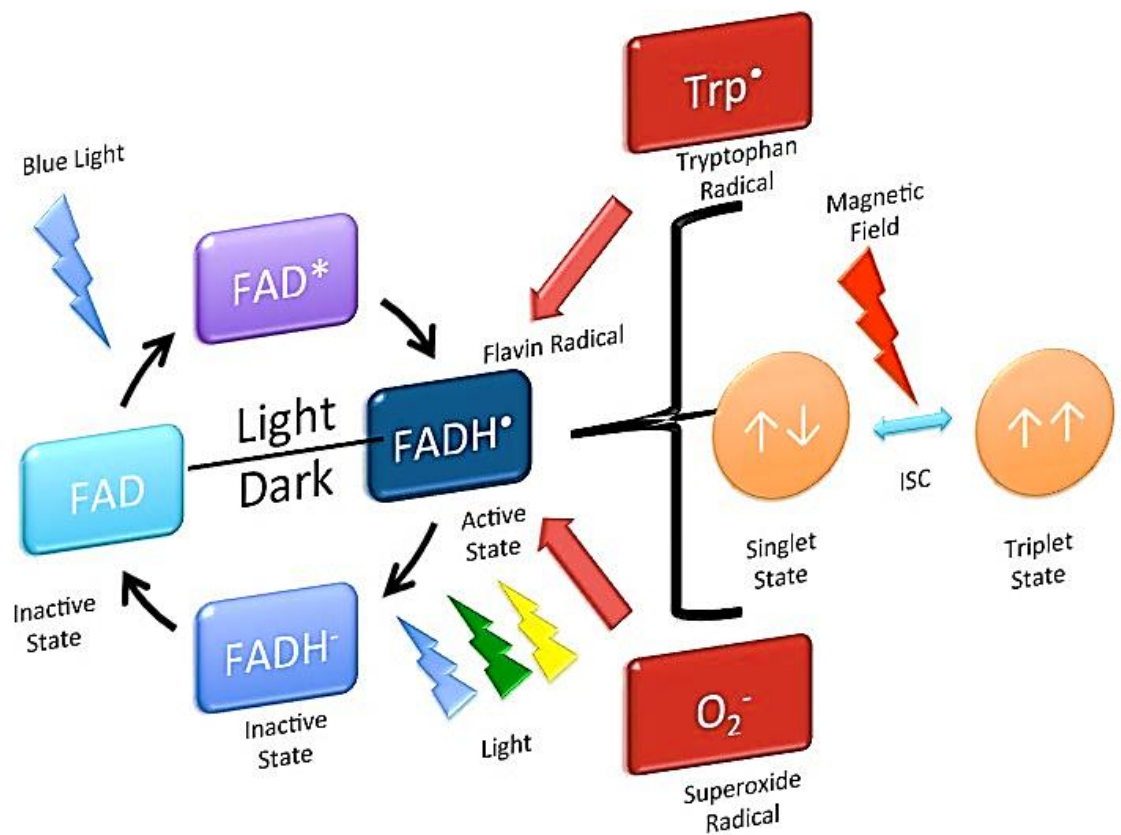


Figure 1-6 CRY photocycle and EMF-sensitive steps

In CRY, fully oxidized FAD is excited to $[FAD^*]$, which decays within picoseconds to a singlet radical pair ${}^S[FADH^\bullet \text{Trp}^\bullet]$, which corresponds to the active state of CRY. Singlet/triplet mixing of the radical pair is modulated by magnetic fields. Further absorption of light (Blue, Green and Yellow) fully reduced the FAD ($FADH^-$) allowing the reconversion of fully oxidized FAD in darkness, which inactivates CRY. Back electron transfer from the semiquinone to form the fully oxidized FAD is spin-selective and only occurs from the singlet state. Other routes by which FAD radicals are oxidized and Trp radicals reduced might be magnetically sensitive, as they require O_2^- thus forming a superoxide radical. See text for more details.

To summarize, a RPM based magnetoreception is theoretically plausible, and it could act as a magnetic compass in animals with an inclination compass rather than a polarity one. Moreover, given the function of CRY in the regulation of the circadian clocks (see below 1.3), the RPM provides a rationale for a link between the magnetic

field and circadian clock, as suggested in the past by several authors (Wever, 1973; Abeyrathne *et al.*, 2010).

1.2.4 EVIDENCE FOR PHOTORECEPTOR-BASED MAGNETORECEPTION

Light dependent magneto-reception was first documented with behavioural experiments with homing pigeons. When young inexperienced pigeons (*Columba livia*) were displaced under lighting conditions they were able to properly orient, however when displaced in total darkness they were disoriented. Further studies on bird orientation revealed that they indeed have an inclination compass. When the horizontal component of the field was inverted European robins, *Erithacus rubecula*, reversed their headings, whereas when the polarity of the field was changed, the bird's orientation was unaffected (Wiltschko & Wiltschko, 1972). The authors concluded that birds derive the magnetic north direction from interpreting the inclination of the axial direction of the GMF. Additionally, several studies have demonstrated that RP-mediated magnetoreception occurs in the eyes of the birds (Ritz *et al.*, 2010), especially the right one (Stapput *et al.*, 2010), in accordance to the predicted model of RPM. *Columba livia* wearing goggles with a clear lens on the right one and a frosty one on the left was indeed able to orient, however when the lenses were swapped the birds were disoriented.

Radio frequency (RF) fields are also used as diagnostic tool for the RPM (Henbest *et al.*, 2004). When placed in a magnetic field, a magnetic moment responds by precessing around the axis of the field with a specific frequency, the Larmor frequency, which is dependent of the intensity of the field. Behavioural experiments with birds (Ritz *et al.*, 2004, 2009) and cockroaches (Vácha, Puzová & Kvícalová, 2009) showed that RF fields at the Larmor frequency were enough to disorient the animals. Recently it has been published that anthropogenic magnetic noise in the range of 2kHz-5Mhz is enough to disrupt magnetic orientation of migratory European robins (Engels *et al.*, 2014). Remarkably, in contrast to previous studies (Ritz *et al.*, 2009), where birds were disoriented only by a vertical monochromatic RF field below 100 nT matching the Larmor frequency, the RF fields used in Engels *et al.* (Engels *et al.*, 2014)

do not match the Larmor frequency (1.363 MHz in Oldenburg, Germany where the study was assessed), but they show a rather broadband spectrum, which is the result of RF fields coming from AM radio signals and electronic equipment. The biophysical mechanism that allows such a response is still far from clear, since in order to be sensitive to such extremely weak RF fields, the spin-decoherence, of the radical pair would have to be order of magnitude slower compared to what is thought to be possible (Engels *et al.*, 2014). Moreover, it has been demonstrated that birds orient in a wavelength dependent manner (Wiltschko & Wiltschko, 2005; Wiltschko *et al.*, 2007b; Nießner *et al.*, 2013), matching the action spectrum of CRY. Interestingly, it has been found that under particular wavelengths (538, 635 nm (Nießner *et al.*, 2013) and darkness (Stapput *et al.*, 2008)) *Erithacus rubecula* exhibits an odd response, changing the normal migratory direction (southerly in spring and northerly in autumn) to a fixed westerly direction, suggesting that when the RP-compass is disrupted, the ancestral magnetite compass takes over (Figure 1-7). However, pre-exposure to 635 nm light of about 1 h was sufficient to rescue magnetoreception when the European robins were tested under red light (Wiltschko *et al.*, 2004), suggesting that birds are able to re-learn the EMF pattern. This view, however, is not consistent with the CRY-mediated magnetoreception, as the light wavelength is well above the CRY-activating spectrum, and therefore it is likely that a second unknown photoreceptor might be involved (Wiltschko *et al.*, 2004). Additionally, orientation in birds also seems to be affected by light intensity (Wiltschko *et al.*, 2007a, 2013). Under high levels of mono- and dichromatic light birds shifted their behaviour from migratory to axial directions. The mechanism underlying these changes is still unknown, but these results reinforce the idea of cross-talk between the RPM and the ancient magnetite-based navigational system. It appears that the RPM is mainly used as navigational compass, whereas the magnetite crystals are part of a navigational map (tells the actual position (Wiltschko *et al.*, 2006a)), providing information on magnetic intensity, and only under “unnatural” lighting conditions do they appear to make the birds heading a particular direction (Wiltschko *et al.*, 2006a, 2011). The “functional window” of magnetoreception in birds is not only light intensity dependent but also field intensity dependent (Wiltschko *et al.*, 2006b). European robins tested under twice the GMF intensity (92 µT in Germany) failed to orient unless they were pre-exposed to such

intensities before being tested. This is consistent with the RPM, the ability to orient in a magnetic field derives from a specific activation pattern in the retina (Ritz *et al.*, 2000); this pattern can be influenced by either field intensity or wavelength, but the system can reset to new patterns and provide EMF sensitivity (Wiltschko *et al.*, 2006b).

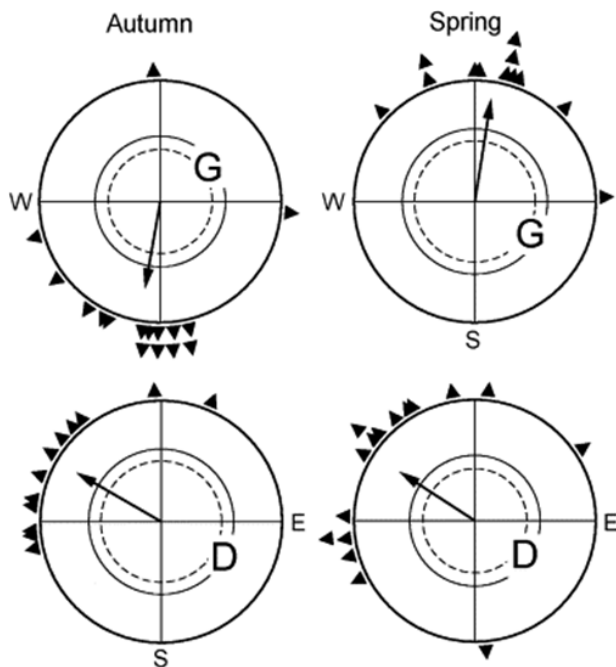


Figure 1-7 Orientation of European robins in light and darkness.

Upper diagrams: Migratory orientation under 565 nm green light (G) shows the typical directional change between autumn and spring. Lower diagrams: “fixed direction” response in absolute darkness (D), where there was no seasonal change. It is clear that when the RPM is abolished, i.e. in darkness, a magnetite based system takes over. Modified from (Stapput *et al.*, 2008).

The effects of wavelength on orientation have also been described in other animals. Eastern red-spotted newts, *Notophthalmus viridescens*, under short-wavelengths (≤ 450 nm) orient as expected towards the shoreline, but their orientation is shifted by 90° under long-wavelengths (≥ 500 nm). However, when tested under intermediate wavelengths the newts become disoriented (Phillips & Borland, 1992a, 1992b; Deutschlander, Phillips & Borland, 1999). Although at the time of these studies,

the CRY hypothesis was not available, the authors proposed a simple physiological explanation to explain how the EMF might alter the response of a photoreceptor-based system. The model anticipated that a receptor cell might contain two spectral mechanisms, a short and long-wavelength mechanism acting antagonistically on the neuronal output (Deutschlander *et al.*, 1999; Phillips *et al.*, 2010a) (see below for more details). However, the authors concluded that disorientation in newts, as in birds, could occur when the magnetic information provided by a photoreceptor cannot properly orient the “map” detector, which is likely to be magnetite-based (Deutschlander *et al.*, 1999).

Light dependent magnetoreception has been described also in insects, for example, the monarch butterflies (*Danaus plexippus*) have an inclination compass (Guerra, Gegear & Reppert, 2014). During the autumn, *D. plexippus* migrate from the US to Mexico for overwintering. This equatorward migration has also been observed in laboratory conditions using a flight simulator surrounded by coils mimicking the GMF, but only when certain light wavelengths are present (380<<420 nm), consistent with the CRY-dependent RPM. Interestingly, when the vertical component of the field was inverted by -45°, the butterflies inverted their orientation and pointed towards magnetic North, a peculiar feature of an inclination compass (Wiltschko & Wiltschko, 2006). Remarkably, it has been observed, that ablation of the antennae (coating them with black paint) resulted in a disoriented flight behaviour (Guerra *et al.*, 2014). This is the first documented evidence for an inclination compass in a long distance migratory insect. Moreover, the cockroach (*Platypedia americana*) is disoriented when exposed to a RF field (Vácha *et al.*, 2009) also suggesting that magnetic field alignment is under control of the RPM.

To conclude, light based-magnetoreception is a widespread feature among migratory or homing animals and the available evidences point towards the RPM. However, as discussed above, the RPM and magnetite-based magnetoreception could coexist. Evolution has shaped the function of the two systems, making them complementary: a magnetic compass and a magnetic map working in synchrony.

1.2.5 EVOLUTIONARY ORIGINS FOR THE MAGNETORECEPTION SENSE

The wide variety of organisms (from bacteria to vertebrates) is capable of detecting the GMF, suggests that this ability shares common origins and must have evolved prior to the radiation of the animal phyla. As mentioned above, magnetite helps micro-aerial bacteria to escape from the toxic oxygen-rich layer near the surface, due to its high density. As the early metazoans also lived in an aqueous environment, navigational abilities may have been under selection. Thus, it has been proposed that the biophysical mechanisms for magnetoreceptive transduction in the nervous system have evolved as ancestral traits, common to all animals, and not as separate entities among groups (Kirschvink *et al.*, 2001). As a consequence, it is plausible that any magnetic sensory system will be subjected to the same evolutionary pressure as other genetically controlled sensory mechanisms. Kirschvink *et al.* (2001) suggested that magnetoreception has evolved through the process of ‘exaptation’, as described by Gould and Vrba (Gould & Vrba, 1982). “This process involves the elaboration of a biological system as an ancillary survival tool to existing modalities, until eventually the new system evolves independently and distinctly from its ancestor. Hence, the magnetic sense has increased its sensitivity, through evolutionary processes, down to the thermal noise limit (as has happened for the other senses)” (Kirschvink *et al.*, 2001). The view, which I embrace, rejects the idea of magnetoreception as a by-product of electroreception or photoreception, as proposed.

1.3 CIRCADIAN CLOCKS

The 24 h cycle imposed by the rotational movement of our planet has played an important role in shaping the evolution of most living organisms (from bacteria, plants to higher vertebrates) since it affects abiotic (light and temperature) or biotic (social interactions) factors. The evolution of an endogenous 24 h circadian clock (from the Latin *circa* “about” *diem* “day”) is not surprising, as organisms need a timekeeping mechanism to anticipate these cyclical environmental changes.

1.3.1 DROSOPHILA MELANOGASTER CIRCADIAN CLOCK

The circadian clock in *Drosophila melanogaster* has been extensively studied thanks to the availability of genetic tool kits and overexpression/knockout systems (Brand & Perrimon, 1993) and much is known about its molecular components and how they interact, in order to generate and sustain rhythmicity. The identification of the first clock gene *period* (*per*) in *D. melanogaster* opened the way to the molecular dissection of the circadian clock. In 1971 Konopka and Benzer (Konopka & Benzer, 1971) identified *period* not only as the first clock gene, but also as the first gene responsible for a complex behaviour. Mutagenesis screening and analysis of locomotor activity and eclosion rhythms identified three mutants, one arrhythmic, another with a short period and the third with a long period. The locus responsible for these behaviours was mapped to the tip of the long arm of the X chromosome, and named *period* (Konopka & Benzer 1971). In 1984, *period* was cloned, the first behavioural gene defined by mutation to be molecularly identified (Bargiello, Jackson & Young, 1984; Reddy *et al.*, 1984). The second clock gene to be identified and cloned was *timeless* (*tim*) (Sehgal *et al.*, 1995). The proteins encoded by these two clock genes provide the key components of the molecular mechanism underlying the endogenous 24 h rhythm. The discovery of clock genes has led to the idea that circadian clocks must rely on cell-autonomous regulation of gene expression, whereby rhythmic behaviours or physiological and metabolic changes are under control of specific cells that can sustain their own rhythmicity. This view gave origin to the Transcriptional /Translational feedback Loop (TTL) model (Dunlap, 1999). In this model, clock genes achieve rhythmic transcription by controlling their own expression and then transmitting this rhythmicity to other genes, known as *clock controlled genes* (*ccgs*), which are not part of the clock *per se*, but provide rhythmic outputs to other pathways (Hardin, Hall & Rosbash, 1990; Hardin *et al.*, 1992; Dunlap, 1999).

1.3.2 ANATOMY OF THE CLOCK

The organization of *Drosophila*'s behavioural pacemaker system comprises ~150 neurons in the brain, which are divided into seven groups based on their location: three dorsal groups (DN_{1-3}) and three lateral ones (LN_d -Lateral Dorsal

neurons, s-LN_V- small Lateral ventral Neurons and l-LN_V-large Lateral Ventral Neurons) in the anterior brain and a lateral posterior group (LPN, Figure 1-8) (Helfrich-Förster *et al.*, 2007b). Due to the high heterogeneity of these clock neurons, a further subdivision has been made based on their main expression patterns. Of the s-LN_V four cells express the neuropeptide Pigment-Dispersing Factor (PDF) and one is PDF-negative (PDF-) called 5th s-LN_V; but all of them express CRY (Figure 1-8) (Helfrich-Förster *et al.*, 2007b). The l-LN_V makes projections into the optic lobes, making them important for rhythms observed in visual input circuits (Helfrich-Förster *et al.*, 2007a). They are also important for sleep/arousal phenotypes but they are not required for activity rhythms in constant condition (Grima *et al.*, 2004). The small cluster of LN_V is especially important for driving rhythms under constant darkness (Stoleru *et al.*, 2005). The six LN_Ds comprise a very heterogeneous group consisting of three neurons expressing CRY (CRY⁺), whereas the remaining ones do not seem to express it at high levels (Figure 1-8) (Benito *et al.*, 2008; Yoshii *et al.*, 2008; Damulewicz & Pyza, 2011; Dissel *et al.*, 2014). The LN_Ds are a very heterogeneous groups of neurons expressing different neuropeptides (Johard *et al.*, 2009). The LN_Ds neurons can be divided based on their neurotransmitter expression into groups 1, 2a-b, 3a-b and 4 (Johard *et al.*, 2009). LN_D-1 expresses the long form of neuropeptide F (NPF), which has been proposed to increase mating activity in males at dusk and being involved in feeding behaviour (Johard *et al.*, 2009), the ion transport peptide (ITP), ITP is a member of the extensive family of peptides related to crustacean hyperglycaemic hormones (CHHs) with an antidiuretic function in crustacean (Johard *et al.*, 2009; Nässel & Winther, 2010; Damulewicz *et al.*, 2013) and CRY; LN_D2a-b express the short form of neuropeptide F (sNFP), which is utilized widely as a peptide co-released with classical neurotransmitters or other peptides (Johard *et al.*, 2009), together with acetylcholine (Cha, Figure 1-8)(Nitabach & Taghert, 2008); LN_D3a-b express NPF whereas in the LN_D4 neurotransmitters have yet to be identified. Interestingly, the 5th-sLN_V also expresses ITP (together with Cha and CRY), and has been implicated in the circadian regulation of the ATP_A subunit in the glia of the lamina (Damulewicz *et al.*, 2013).

These neurons are important for determining the phase of DD behaviour, for maintaining the evening peak in LD conditions (Murad, Emery-Le & Emery, 2007;

Stoleru *et al.*, 2007) and the CRY⁺ cells apparently drive behavioural rhythms in dim LL (Helfrich-Förster *et al.*, 2007b; Rieger *et al.*, 2009).

The DN₁ consist of roughly 17 neurons (Figure 1-8). Two of these cells are peculiar as they are present even in larvae, they lack the transcription factor *glass* (*gl*) but do express IPN-amide (Figure 1-8) (Helfrich-Förster *et al.*, 2007b) and they are located in an anterior position separated from the others, therefore named DN_{1anterior} (DN_{1a}); moreover these neurons express CRY⁺. Another two DN₁ are also CRY⁺, and because of their location, named DN_{1posterior} (DN_{1p}). The DN₁ cluster has been implicated in maintaining rhythmic behaviour in LL (Murad *et al.*, 2007; Stoleru *et al.*, 2007) and for morning anticipation (Sheeba, Fogle & Holmes, 2010; Zhang *et al.*, 2010). Two other clusters of dorsal neurons have also been described: two DN₂ neurons and a cluster of 40 cells forming the DN₃, of which some express CRY and PDFR (Helfrich-Förster *et al.*, 2007b; Peschel & Helfrich-Förster, 2011). The DN neurons (DN₂ in particular) along with LPN have been implicated in temperature entrainment (Miyasako, Umezaki & Tomioka, 2007).

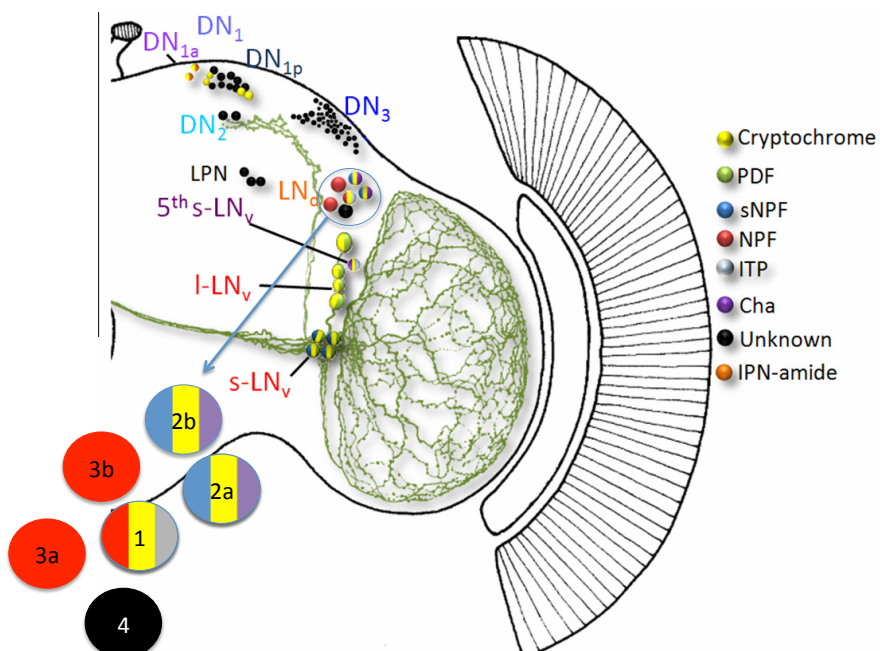


Figure 1-8 Overview of clock-gene expressing neurons and anatomical localization with a close-up to LN_{ds}s. Adapted from (Peschel & Helfrich-Förster, 2011).

1.3.3 THE NEGATIVE FEEDBACK LOOP (NFL) IN DROSOPHILA

At the molecular level *Drosophila* clock is based upon three interlocked negative TTLs (Figure 1-9). Two transcription factors CLOCK (CLK) and CYCLE (CYC, homologous to BMAL1 in other organisms,) are the main players, as they regulate both loops (Allada *et al.*, 1998; Rutila *et al.*, 1998). The two proteins heterodimerize *via* their basic Helix-Loop-Helix (bHLH) and PAS (Period circadian protein- Aryl hydrocarbon receptor nuclear translocator protein- Single-minded protein) domains and bind to the E-box of several clock genes, such as *period*, *timeless* but also *vriile* (*vri*) and *PAR domain protein 1ε* (*Pdp1ε*)- called “evening genes”, initiating their transcription (Allada *et al.*, 1998; Rutila *et al.*, 1998).

In the first loop, *per* and *tim* transcripts peak in the early hours of darkness, due to the anchored CLK-CYC complex to the respective E-box regions (Figure 1-9). PER and TIM peaks are delayed relative to their transcripts by ~4-6 h due to post transcriptional modifications, in particular phosphorylation (Hardin *et al.*, 1992; Edery, Rutila & Rosbash, 1994; Myers *et al.*, 1995). PER is a target for many kinases, including CASEIN KINASE 2 (CK2) which phosphorylates PER (possibly at Ser 151-153(Lin, Schroeder & Allada, 2005) facilitating its nuclear entry (Lin *et al.*, 2002, 2005; Akten *et al.*, 2003) and eventually playing a role in repressing CLK activity (Szabó *et al.*, 2013). NEMO (NMO) is a recently discovered kinase that mediates phosphorylation of PER at Ser596. This triggers the phosphorylation of the so called phosphocluster by the Casein Kinase 1e homologue DOUBLE-TIME (DBT, Thr583, Ser585 and Ser589 (Kloss *et al.*, 1998; Chiu, Ko & Edery, 2011)) that slows down PER cytoplasmic accumulation. The phosphorylation of the phosphocluster delays the phosphorylation by DBT of Ser47; which is the key phosphoevent, as it increases the binding affinity of SLIMB (SUPERNUMERARY LIMBS, a E3-ubiquitin ligase) to PER leading to its degradation by the proteasome (Ko *et al.*, 2010; Chiu *et al.*, 2011). This delay reinforces PER repression on CLK (Nawathean & Rosbash, 2004). The relative abundance of TIM during the night (see below) helps protect PER from being degraded (Figure 1-9). TIM is the main target of CK2 (Meissner *et al.*, 2008), which regulates its abundance and together with

SHAGGY (SGG), a GLYCOGEN SYNTHASE KINASE-3b (GSK-3b), it promotes nuclear translocation (Martinek *et al.*, 2001).

PER-TIM dimers enter the nucleus and suppress CLK-CYC activity thereby inhibiting their own transcription early in the morning, (Lee, Bae & Edery, 1998) (Figure 1-9). The inhibition of CLK activity is due to high phosphorylation levels. The current model proposes that CLK hyper-phosphorylation is mediated somehow by the NMO-DBT-PER-TIM complex (Figure 1-9). DBT seems to function as a bridge between PER and CLK whereas NMO is thought to progressively phosphorylate CLK leading to its molecular instability, although there is no direct evidence for this (Yu *et al.*, 2009; Yu, Houl & Hardin, 2011). Interestingly, new findings revealed that CK2 also increases CLK phosphorylation in a PER-dependent manner. However, overexpression of CK2 resulted in a more stable CLK with reduced transcriptional activity. Since both DBT and CK2 show a preferential association with CLK in the morning-*i.e.* when PER is more abundant, they might counteract each other to control CLK degradation and recycling for the next transcription cycle (Szabó *et al.*, 2013). This entire process takes roughly 24 h.

The second loop is much less clear compared to the previous one, and is mainly based on the circadian regulation of CLK (bear in mind that despite the misleading name, *cycle* is not rhythmically expressed). Experimental data revealed that the transcripts of *Cik* and *cry* peak in the late night-early morning (Allada *et al.*, 1998; Emery *et al.*, 1998), when CLK-CYC repression is at its maximum, suggesting that additional factors might be involved. It has been observed that the peak of expression of VRI, a basic leucine Zipper (bZip) protein, coincides with the lowest expression of *Cik*, making it one of the possible negative regulators (Blau & Young, 1999). VRI forms homodimers that binds to the V/P box of morning genes (*Cik* and *cry*, Figure 1-9).

For every negative regulator, there must be a positive one; and in fact, another protein has been found to oscillate similarly to VRI, PDP1 ϵ . The transcripts of both *vri* and *Pdp1\epsilon* are under CLK-CYC control and accumulate in the late day/early morning. However, VRI and PDP1 ϵ have different peaks: VRI accumulates more quickly and inhibits *Cik* transcription; after ~4 h, PDP1 ϵ accumulates and releases the inhibition of

VRI. Moreover, the α isoform of the *Drosophila* FOX homologue KAYAK (KAY), a bZip transcription factor is required for normal circadian behaviour as it regulates VRI and CLK-CYC activity (Ling, Dubruille & Emery, 2012). KAY is able to form a dimer with VRI, probably through the bZip domain, and this dimer is no longer able to bind to any VRI targets. Moreover, it has been shown that although there is no direct interaction between KAY and CLK, it can decrease CLK transactivation potential through a yet unidentified repressor (Ling *et al.*, 2012). Given the exquisite function of CLK (*i.e.* regulating the expression on TIM/PER together with its own expression VRI/PDP1 ϵ) it becomes clear that the two loops are interconnected and share common elements (Figure 1-9).

A newly discovered transcription factor *clockwork orange* (*cwo*), a bHLH ORANGE protein rhythmically expressed by CLK-CYC activity, has been implicated as a new core clock component, which synergises with PER and inhibits CLK-mediated transcription especially during the late night (Kadener *et al.*, 2007), consistent with the low amplitude of evening transcripts (*per*, *tim*, *vri* and *Pdp1 ϵ*) in *cwo* mutants, together with period lengthening (Kadener *et al.*, 2007). However, in *cwo* mutants, the evening transcripts showed a significant decreased in the early night or midnight peak and a subsequent loss of oscillation (Richier *et al.*, 2008), suggesting that CWO is required for the oscillation of CLK-targets genes by promoting their evening peaks (Richier *et al.*, 2008). Conversely, in those mutants the levels of *cwo* are constitutively high (Kadener *et al.*, 2007; Richier *et al.*, 2008), confirming CWO as strong repressor of its own transcription, but at the same time it can act as transcriptional activator in the evening when PER levels are low and a transcriptional repressor in the morning when PER is mostly nuclear (Richier *et al.*, 2008) (Figure 1-9). This view provides a new interlocked loop in the circadian clock mechanism of *D. melanogaster*.

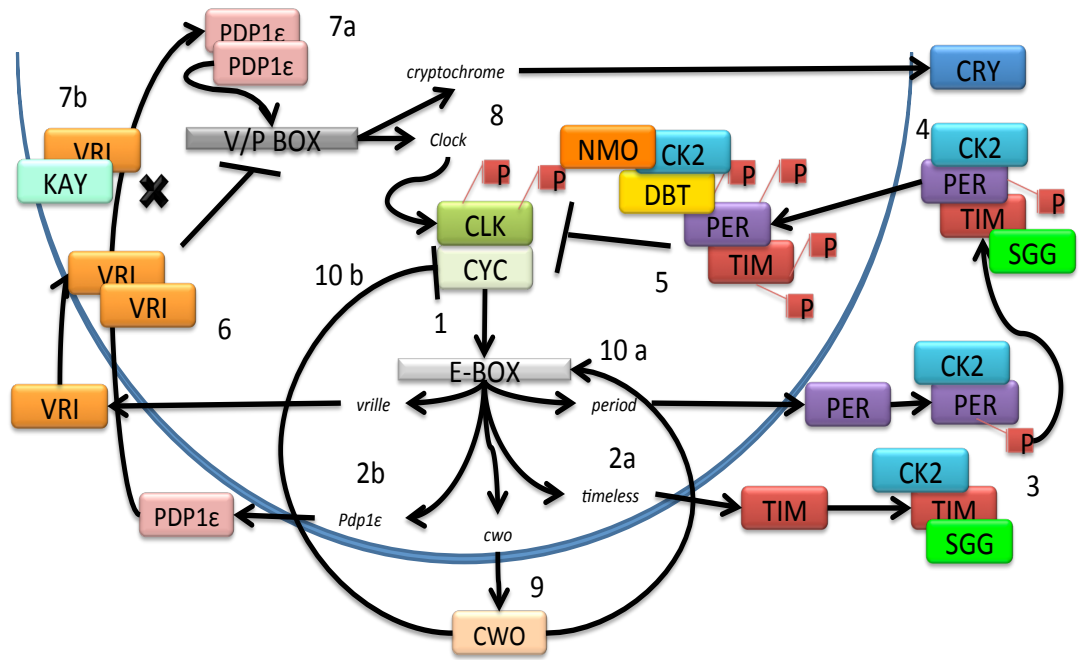


Figure 1-9 The three interlocked negative-feedback loops in *Drosophila*.

1 CLK -CYC dimer enhances the transcription of CCGs by binding to the E-box. In the first loop per and tim transcription is activated by CLK-CYC (2a, 2b). (3). PER and TIM proteins accumulate in the cytoplasm where they undergo posttranslational modification (phosphorylation mediated by CK2 and SGG). (4) phosphorylated PER and TIM proteins heterodimerise and re-enter the nucleus, where they inhibit CLK-CYC activity by hyperphosphorylating CLK with the help of DBT, NMO and CK2. 5. In the second loop *Pdp1ε* and *vriile* transcripts are transcribed by CLK-CYC dimers (2b). VRI dimers inhibit Clk transcription (6). 4h later, *PDP1ε* dimer antagonizes VRI repression (7a) and binds to the V/P box starting the transcription of *Clk* and *cry* (8). KAY binds to VRI and making it unable to bind to any targets (7b). The third interlocked loop involves CWO (9), whose transcription is under CLK-CYC control. CWO enhances transcription of evening clock genes in the evening (10 a) and synergies with PER to repress CLK-CYC activity in the morning (10 b). Blue curved line symbolises the nuclear membrane, boxed Ps represent phosphorylation. See text for more details.

1.3.4 LIGHT ENTRAINMENT OF THE CLOCK

As mentioned above, an evolutionary stable circadian clock must confer advantages to the organisms that eventually lead to an increase in fitness. One of the key points for a “functional” circadian clock is therefore the ability to be perfectly

synchronized with the external environment, in order to be entrained but also predict new environmental conditions. One of the most evident changes is the cycle of day and night, the by-product of the rotational movement of our planet along its axis. Biological clocks have therefore evolved the ability to be entrained to the photoperiod.

Taking into consideration the TIM/PER loop described above, during the day, TIM levels are quite low and DBT is able to hyper phosphorylate PER leading to its degradation, thus removing the PER-TIM inhibition on CLK-CYC activity. This simple view can be used to explain how the light sensitivity of the clock is achieved. Every time the light is switched on regardless of the phase, TIM levels are reduced and the clock stops for the entire duration of the light exposure. Moreover, under constant lighting conditions (LL), the constant degradation of TIM and PER is responsible for arrhythmia.

A breakthrough in understanding circadian light entrainment came with the discovery of CRY. Flies carrying a hypomorphic allele with a point mutation at the flavin binding site (Asp 410 Asn) that makes the protein unstable, *cry^{baby}* (*cry^b*), were still rhythmic in LL (Stanewsky *et al.*, 1998). This led to the idea that *Drosophila*-CRY (dCRY), a blue photoreceptor, may be the key molecule responsible for the resetting of the clock.

When CRY is activated by light, it undergoes a conformational change that allows the protein to bind to TIM, inducing posttranslational modifications (Peschel *et al.*, 2009). These modifications are required for the formation of a complex between TIM and an E3-ubiquitin ligase protein, JETLAG (JET), which targets TIM for proteasomal degradation (Figure 1-10). JET can also dimerize with CRY, once activated, but it has stronger affinity with TIM, and since the CRY-TIM interaction is required for JET activity, the flavoprotein is then targeted to the proteasome (Koh, Zheng & Sehgal, 2006). As result, under lighting conditions, the levels of CRY and TIM are generally low, indicating protein degradation. In addition to the JET-CRY interaction, Ozturk and co-workers (Ozturk *et al.*, 2013b) identified a mutation in *Ramshackle* the fly homologue of human BRDW1, that attenuates light degradation of CRY, suggesting BRWD3 is a substrate for CRY ubiquitin-mediated degradation (Figure 1-10). Another step in the

light entrainment process and light degradation of TIM, is that SGG binds to CRY, increasing its stability and preventing the CRY-TIM interaction (Stoleru *et al.*, 2007), while phosphorylating TIM and promoting its nuclear entry (Martinek *et al.*, 2001). Overexpression of SGG resemble a *cry^b* phenotype in LL (Stoleru *et al.*, 2007).

Natural polymorphisms in *tim* generate different isoforms of TIM via an upstream insertion of a *G* nucleotide that leads to a haplotype (*ls-tim*), which has two in-frame start codons, producing a long TIM isoform (L-TIM) from the upstream *ATG* and a 23 amino acid shorter isoform (S-TIM) from the downstream *ATG*. Flies without this insertion produce the ancestral form, S-TIM, plus a 19 amino acid amino terminal truncated peptide (Tauber *et al.*, 2007). Interestingly the two natural variants lead to different photosensitivities. The long isoform is less sensitive to light because it binds poorly to CRY; whereas, S-TIM is very light sensitive and strongly binds to CRY (Sandrelli *et al.*, 2007; Tauber *et al.*, 2007; Peschel *et al.*, 2009). Similarly, a new genetic variant, *Veela* (Peschel, Veleri & Stanewsky, 2006), has been described having an abnormal rhythmic behaviour in constant light. This is due to the simultaneous presence of the *ls-tim* allele and a *jet* variant called *jet^c* (*jet* ‘common’ (Koh *et al.*, 2006), which encodes a mutant form of the F-box protein JET (Phe 209 Ile substitution). The *jet^c* mutation, together with *jet^r* (rare, Ser 220 Leu substitution), are both adjacent to the Leucine-Rich Repeats (LRR) region of JET, a protein-protein interaction domain thought to be involved in target recognition (Koh *et al.*, 2006). The abnormal LL phenotype of *jet^c* was only observed in the presence of *ls-tim* but not *s-tim* (Peschel *et al.*, 2006).

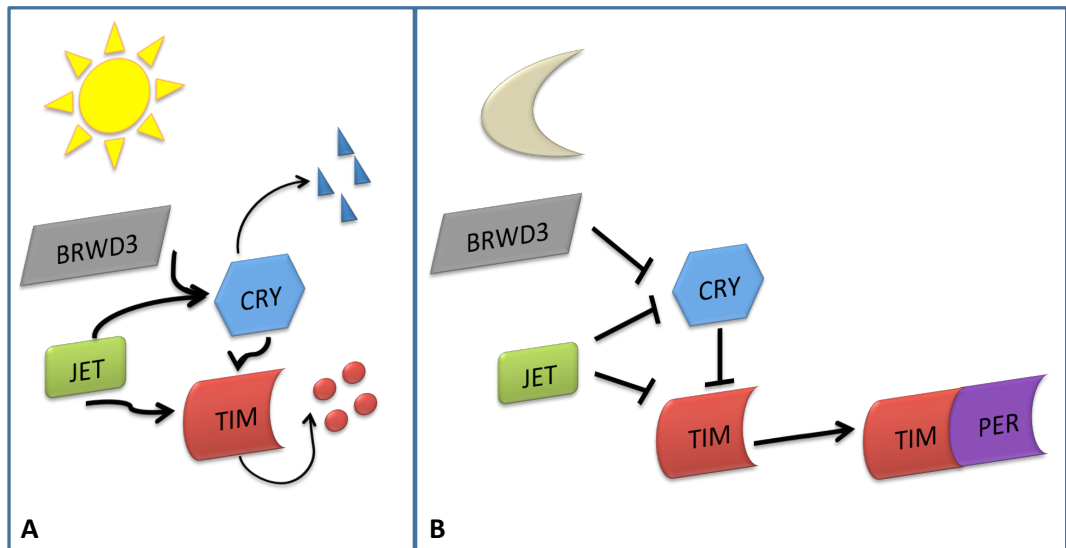


Figure 1-10 Light- dependent TIM-CRY degradation

In presence of light, CRY is activated promoting the interaction with JET and TIM, which eventually leads to the proteosomal degradation (A). In darkness, CRY is inactive and non-degraded TIM can form a dimer with PER.

A cell-autonomous light-dependent degradation of TIM appears to be the cause of entrainment, but there are some discrepancies with this model. Both *cry^b* and *cry-null* (Dolezelova, Dolezel & Hall, 2007) mutants, although rhythmic under LL, are still able to entrain to LD cycles, and are still able to phase shift (Kistenpfennig *et al.*, 2012) under certain lighting conditions. In addition the molecular clock in the LN_s is still entrainable even in a *cry* mutant background (Stanewsky *et al.*, 1998). Circadian blindness can be achieved only after disruption of all retinal structures (compound eyes and ocelli- (Stanewsky *et al.*, 1998; Helfrich-Förster *et al.*, 2001; Kistenpfennig *et al.*, 2012) along with Hofbauer-Buchner eyelets (Helfrich-Förster *et al.*, 2001)), as described by Helfrich-Förster *et al.* (2001) where flies homozygous for the loss-of-function allele *gl^{60j}* and *cry^b* failed to re-entrained to a LD cycle, due a PER/TIM asynchrony in the brain (Helfrich-Förster *et al.*, 2001). These observations suggest that photopigments other than CRY are expressed in clock neurons and can compensate for *cry^b* (Helfrich-Förster *et al.*, 2001), allowing CRY-mutant flies to entrain in LD. New findings suggest that a CRY-independent phase shift and TIM degradation could be

induced by the neuronal activity of s-LN_vs cells, *via* PDF (Guo *et al.*, 2014). PDF expression from M cells is likely to activate a PDFR-CUL3 (E3 ubiquitin ligase component) pathway that reduces cytoplasmic TIM accumulation in the early night (Guo *et al.*, 2014).

A further component of the light entrainment pathway is QUASIMODO (QSM), a zona pellucida type of protein likely attached to the extracellular side of the cell membrane through a glycosyl phosphatidylinositol membrane anchor (Chen *et al.*, 2011). *qsm* transcription is under clock control, but the protein seems to be under light control as the levels increase after lights on (Chen *et al.*, 2011). Interestingly knocking down *qsm* resulted in abnormal rhythmicity under LL conditions and increased stability of TIM and PER (Chen *et al.*, 2011). Moreover, overexpression of QSM resulted in TIM reduction (in light) even in *cry*-null flies, suggesting that QSM could function independently from CRY, but still in a light-dependent manner. Although there is no clear idea for QSM function, given the predicted membrane localization, it is possible that QSM could be activated by a membrane-bound photoreceptor (rhodopsin perhaps) and signal light information to the network (Chen *et al.*, 2011).

Intercellular communication

Overall, the model of the NFL supports the idea of a cell autonomous clock (Allada *et al.*, 1998; Rutila *et al.*, 1998; Kilman & Allada, 2009), where different clock-neurons, each with a cell autonomous pacemaker capability, are coupled to each other creating a network (Chang, 2006). However, new evidence has cast doubt on this hierarchical view of the structure of the circadian clock. Current models propose that this network is organised in two coupled oscillators: the PDF⁺ cells that control the morning peak of activity (therefore called Morning cells (Grima *et al.*, 2004)) and the remaining more dorsal neurons that control the evening peak of activity (Evening cells). In this view, PDF⁺ cells (s-LN_v) serve as the main pacemaker that resets the PDF⁻ cells daily *via* PDF expression, even in absence of external stimuli, acting as cellular *Zeitgeber* (Stoleru *et al.*, 2005). Expression of SGG using a *Pdf-GAL4* drivers not only resulted in a shorter period, as predicted (Martinek *et al.*, 2001), but also revealed an advanced E-peak of locomotor activity, suggesting that the manipulation in the s-LN_v

also altered the E-cells (Stoleru *et al.*, 2005), while when the expression was targeted to the E-cells only, *tim-GAL4/Pdf-GAL80;UAS-SGG* flies, the overall rhythm was 24 h (Stoleru *et al.*, 2005). However, this model is now under revision as a recent study revealed a more complicated situation. Among all the PDF⁻ cells, only half of them express the PDF Receptor (PDFR), suggesting that the morning cells modulate only a small portion of the evening neurons (Im & Taghert, 2010; Im, Li & Taghert, 2011). Expression of DBT^L (variant of DBT with reduced kinase activity that prolongs PER expression by diminishing phosphorylation (Preuss *et al.*, 2004)) allowed Yao and co-workers (2014) to study how a cluster of PDF⁻ neurons (LN_ds and the 5th s-LN_v, Figure 1-8) responds to PDF. Three independent oscillators have been observed among the lateral dorsal ‘evening’ neurons, whose output relies on specific neurotransmitters: 2 PDFR⁺ sNPF⁺ LN_ds strongly coupled to the PDF cells; a single LN_d and the 5th s-LN_v, both expressing ITP, less strongly coupled to the PDF neurons; the remaining 3 PDFR⁻ cells, which were not coupled with the morning cells (Yao & Shafer, 2014). In addition new findings revealed a more important role for some E cells (5th-sLN_v and 4 LN_ds) in controlling all aspects of circadian rhythms and locomotor activity, suggesting that TIM levels changes in these cells in response to the M cells neuronal firing, making a major contribution to the resulting phase changes, an pinpointing them as main contributors for the timekeeping mechanism in LD (Guo *et al.*, 2014). The clock neuronal network appears to consist of multiple independent oscillators interacting with each other, rather than a single cluster of pacemaker neurons (Dissel *et al.*, 2014).

1.3.5 INSECT CRYPTOCHROMES

As mentioned above, CRY proteins are components of the light-resetting mechanism, so are not canonical components of the circadian system. Phylogenetic analyses show at least two rounds of gene duplication at the base of the metazoan radiation, as well as several losses, giving rise to two *cry* gene families in insects, a *Drosophila*-like *cry1* family and a vertebrate-like *cry2* family. At the molecular level, the central circadian clock in *D. melanogaster* is driven by a negative transcriptional feedback loop (see 1.3.1) and CRY functions mainly as a blue-light photoreceptor involved in photic entrainment (Peschel *et al.*, 2009; Peschel & Helfrich-Förster, 2011;

Czarna *et al.*, 2013). Based on studies of the two mouse CRY proteins (both of which belong to the *cry2* gene family), the mammalian CRYs work within the clock itself as potent repressor of CLK-BMAL1 mediated transcription in a light-independent manner (Yuan *et al.*, 2007).

A second *cry* gene was discovered in insects, which is present in all non-drosophilid species so far examined (Zhu *et al.*, 2005). This second *cry* encodes a vertebrate-like protein designated insect CRY2, which is a potent transcriptional repressor of CLK:CYC-mediated transcription in *Drosophila* cells but is not light sensitive (Zhu *et al.*, 2005). Insect CRY2 has been found in mosquitos and butterflies (Zhu *et al.*, 2005) together with insect CRY1; surprisingly, the honeybee *Apis mellifera* and the beetle *Tenebrio castaneum* encode only CRY2, suggesting two evolutionary possibilities (Zhu *et al.*, 2005). First, the core oscillator in insects has itself evolved so that at least three kinds of clocks exist, one utilising a photosensitive *Drosophila* CRY1 only, those containing both CRY1 and CRY2 as in the monarch butterfly (Zhu *et al.*, 2005) and those containing only CRY2. Second, in insects containing only CRY2, the cryptochrome may serve dual functions, as both photoreceptor and transcriptional repressor (Zhu *et al.*, 2005). However further analyses showed that light has no significant effect on insect CRY2 to inhibit CLK:CYC mediated transcription in cell culture, therefore suggesting that CRY2, like vertebrate-like CRY2, cannot act as photoreceptor (Yuan *et al.*, 2007; Vieira *et al.*, 2012), but see (Hoang *et al.*, 2008).

Phylogenetic analyses of *cryptochrome*/DNA photolyase genes indicated that both insect *cry1* and *cry2* homologues existed at the base of metazoan radiation, and at least two gene duplication events occurred leading to the evolution of the *cry2* cluster (Figure 1-11). The first duplication led to the insect *cry1* cluster and a second duplication led to the evolution of the vertebrate *cry* and insect *cry2* cluster. *cry1* appears to have been lost in the lineage of *Tribolium* and *Apis*, whereas *cry2* in *Drosophila* was lost sometime after the split between that lineage and mosquitoes, 223-240 MYA (Wiegmann *et al.*, 2003).

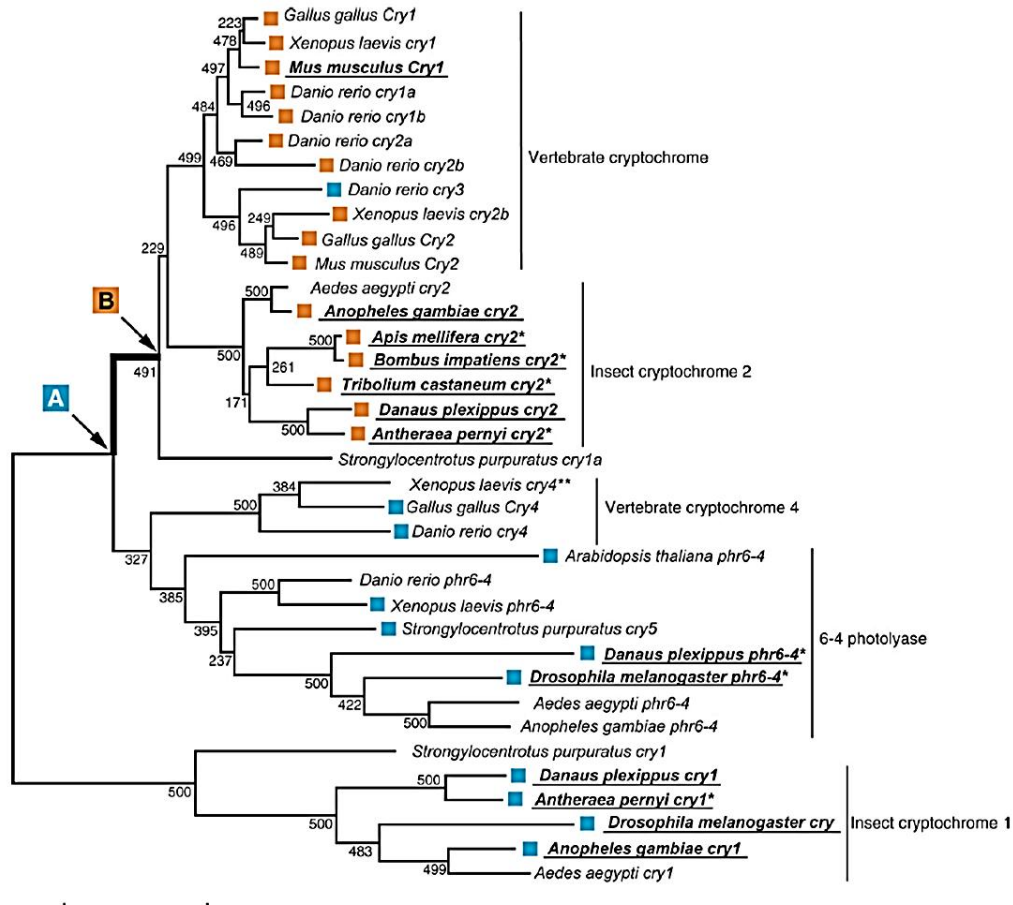


Figure 1-11 DNA photolyase/cry gene family phylogenetic tree (ML)

Orange squares indicate the function of circadian clock repressor; blue squares indicate proteins that lack this function. (Modified from (Yuan *et al.*, 2007))

Photosensitive CRY

Light-sensitive *dcry* encodes a 542 aa protein belonging to the DNA photolyase class-1 family but without photolyase activity (Cashmore, 2003). CRY and related proteins (*i.e.* photolyases) share a chromophore binding photolyase homology region (PHR), which consists of an $\alpha\beta$ N-terminal domain, probably containing a light-harvesting chromophore such as methenyltetrahydrofolate (MTHF (Berndt *et al.*, 2007) and a C-terminal helical domain that binds FAD in a U-shape (Czarna *et al.*, 2013). In addition to the PHR, cryptochromes have a regulatory C-terminal tail (CTT) of variable length and sequence (Cashmore, 2003; Berndt *et al.*, 2007; Chaves *et al.*, 2011).

dCRY is thought to bind oxidized flavin (FAD_{ox}) in darkness, which is then converted to an anionic $\text{FAD}^{\bullet-}$ after blue light illumination (Berndt *et al.*, 2007). An electron cascade involving three highly conserved Trp residues 342, 397 and 420 (the Trp triad, see 1.2.3) mediates the photoreduction of the flavin and the formation of a radical pair (Hoang *et al.*, 2008). This may induce a conformational change of the CTT (Ozturk *et al.*, 2011) that allows the PHR to interact with TIM and JET, leading to the resetting of the clock (Peschel *et al.*, 2009). A similar scenario is predicted by the crystallographic structure of dCRY that reveals basic (dTIM) and acidic (JET) regions near the CTT (Czarna *et al.*, 2013). In other words, flavin photoreduction seems to be required for CRY activation (Vaidya *et al.*, 2013). During the dark phase, the completely reduced FAD (FAD^{RED}) is then re-oxidized and CRY becomes inactive again (Figure 1-6). The displacement of the CTT may therefore provide the key step for CRY activation. In support of this view, deletion of 20 aa in the CTT (called CRY Δ) makes CRY constitutively active, *i.e.* capable of binding TIM in a light-independent manner (Rosato *et al.*, 2001; Dissel *et al.*, 2004).

Although this model has been experimentally evaluated, there are still some uncertainties regarding the actual oxidation state of the FAD at the beginning of the photocycle. Studies suggest that the oxidation of the flavin during the dark phase is an artefact of the protein purification method used (Ozturk *et al.*, 2011). Also, new evidence suggests that none of the highly conserved Trps are required for the photoactivation of CRY. Trp to Phe substitutions block photoreduction but they do not affect either the photosensory function of CRY in *Drosophila* cells as measured by light-induced proteolysis of dCRY (Oztürk *et al.*, 2008; Ozturk *et al.*, 2011) or magnetoreception in flies as measured by behavioural assays (Gegear *et al.*, 2010) (see below). Furthermore, it has been showed that that light excitation of dCRY::FAD can cause functionally relevant conformational change even in the absence of flavin reduction (Ozturk *et al.*, 2013a). These new findings challenge our current understanding of the CRY photocycle and ultimately of the RPM.

To summarise, dCRY acts as the main circadian photoreceptor capable of resetting the clock through light-dependent degradation of TIM and it is also able to regulate neuronal firing, again, in a light dependent fashion (Fogle *et al.*, 2011), possibly through potassium channels (Holmes, pers.comm), implying that CRY is involved in cellular communication (Dissel *et al.*, 2014). However, these are not the only functions that CRY plays in *Drosophila*. It has been shown that in the non-pacemaker cells, dCRY acts a circadian repressor (Collins *et al.*, 2006), rather similarly to CRY2 molecules (Kume *et al.*, 1999; Okamura *et al.*, 1999). *per*, *tim*, *Pdp1ε* and *vri* RNA levels are in fact derepressed in *cry^b* mutant larvae, suggesting an increased transcriptional activity of CLK-CYC. Additionally, overexpression of both PER and CRY in the eyes results in reduced *tim* and *vri* expression (Collins *et al.*, 2006). Finally *per⁰¹;cry^b* double mutants show ectopic TIM expression consistent with an upregulation of *Cik*. Interestingly, CRY repression only occurs in synergy with PER. CRY interacts *in vivo* with PER via TIM so it is possible that CRY and PER control different steps in CLK-CYC repression (Collins *et al.*, 2006).

Moreover, CRY has been shown to mediate some transcriptional responses (stress response genes) in flies under DD conditions, revealing a common ancient mechanism for CRY2 proteins (Vieira *et al.*, 2012). Finally, CRY delays age-related dampening of clock gene oscillations by delaying ageing through a yet unknown pathway (Rakshit & Giebultowicz, 2013).

1.4 MAGNETORECEPTION IN *D. MELANOGASTER*

Magnetoreception in *D. melanogaster* was documented for the first time in 1970 by Wehner and co-workers (Wehner & Labhart, 1970), who demonstrated an interaction of the geomagnetic field on the direction of geotactic orientation. Twenty years later, Phillips & Sayeed (Phillips & Sayeed, 1992) showed that flies trained in the ambient magnetic field to a horizontal gradient of 365 nm light emanating from one of the four cardinal compass directions, were able to orient into a radial 8-arm maze in which the magnetic field alignment could be varied, under the same light conditions (Phillips & Sayeed, 1992). Similar responses were also observed in second instar larvae (Dommer *et al.*, 2008; Painter *et al.*, 2013). Surprisingly, flies showed similar photo-

magnetic response to those observed in newts (Phillips & Borland, 1992a, 1992b). When tested in the same maze but under a 500 nm light, they exhibited a 90° clockwise shift in magnetic compass orientation relative to the trained direction, reinforcing the idea of an antagonistic effect of light, probably mediated by two photoreceptors (Figure 1-12). In order to explain this wavelength-dependent effect of light, Phillips and co-workers proposed that the change in wavelength had a non-specific effect on the flies' behaviour. Under long wavelengths, flies may simply be switching to a different form of orientation behaviour. Recently, other retinula cells (R7y and R8y in the seventh rhabdomere) have been proposed as photoreceptors specialized for detection of the Earth's magnetic field. In particular R7y cells have been proposed to provide a short-wavelength (400nm) input whereas the R8y cells a long-wavelength (500 nm) input. Moreover it is noteworthy that within these rhabdomeres, the microvilli of R7y and R8y are aligned perpendicularly, suggesting that the summation of outputs after light excitation of those groups of cells onto a second-order cell could reinforce the magnetic field effect (Phillips *et al.*, 2010a).

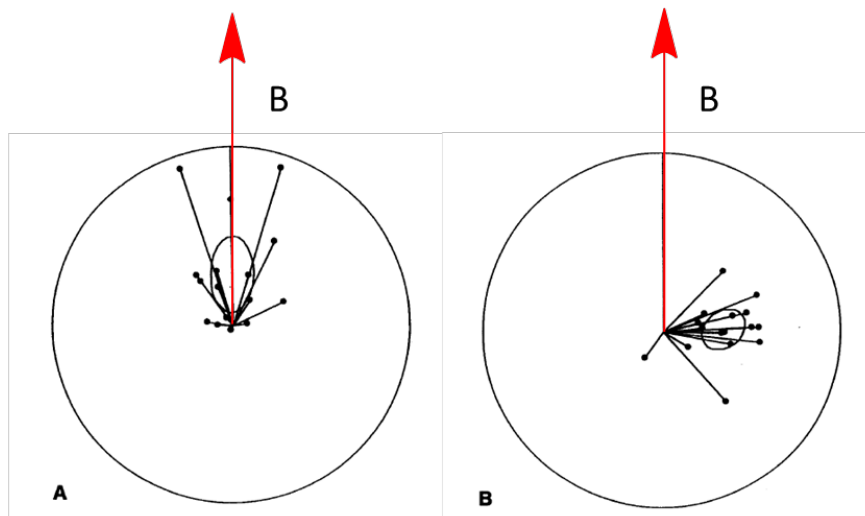


Figure 1-12 Magnetic compass orientations in *D.melanogaster* under (A) 365 and (B) 500 nm.

Flies tested under 365 nm light exhibited unimodal magnetic orientation in the training direction (red arrow), whereas under 500 nm light they showed a unimodal magnetic orientation which was shifted 90° clockwise of the training direction. Modified from (Phillips & Sayeed, 1992).

A similar experiment was performed, where flies were trained to associate an EMF with a sucrose reward and tested in a binary-choice behavioural T-maze revealed a possible involvement of CRY in *D. melanogaster*'s magnetoreception (Gegear *et al.*, 2008). As mentioned before, Drosophila-like CRY (CRY1) proteins are sensitive to UV-blue light and act primarily as photoreceptors that synchronize the circadian clock (Emery *et al.*, 1998, 2000; Stanewsky *et al.*, 1998). On the other hand, vertebrate-like CRY proteins (CRY2) act mainly as repressors of the *Clock* and *Bmal1* transcription factors (Kume *et al.*, 1999; Okamura *et al.*, 1999). In an illuminated apparatus, flies experienced an EMF generated by an electrical coil system, where it was possible to produce a magnetic field on one side of the T-maze while producing no field on the opposite side (Figure 1-13A). Flies were tested either in the naïve state or after a training session in which, following a Pavlovian paradigm, the field was paired with a sucrose reward. Wild-type flies showed significant naïve and trained responses to a magnetic field under full spectrum of light (300-700 nm) but did not respond to the field when wavelengths in the CRY -sensitive, UV-A/blue part of the spectrum (< 420 nm) were blocked (Figure 1-13B-C). However, even if there was not a significant naïve/trained response under long wavelength (>420 nm) lighting conditions, naïve flies showed a reverse response compared to flies tested under full spectrum and under wavelengths below < 420 nm. This was consistent with the idea of an antagonistic effect of the magnetic field as proposed by Phillips and co-workers (Phillips *et al.*, 2010a). Furthermore, CRY deficient (*cry*⁰²) mutant flies, where the entire *cry* coding sequence has been replaced with *mini-white*⁺ in *cry*-null flies (Dolezelova *et al.*, 2007), and *cry*^b mutants (Stanewsky *et al.*, 1998), showed a complete lack of magnetic sense (Gegear *et al.*, 2008) suggesting a putative role of CRY in magnetoreception (Figure 1-13D).

CRY interacts with the critical circadian clock protein TIM to reset the circadian clock mechanism (Figure 1-10), so Gegear and co-workers used clock mutants to show that an intact circadian system was not necessary for the CRY-dependent magnetosensitive responses in wild-type flies. Subsequent work from this group, has shown that both CRY1 and CRY2 molecules from the monarch butterfly, *D. plexippus*, and *human* CRY2 (*hCRY2*), when transformed into *cry* mutant *Drosophila*, can rescue

the fly's sensitivity to EMF in a *cry^b* background under full-spectrum and UV-A/blue light (Geegear *et al.*, 2010; Foley, Geegear & Reppert, 2011) (Figure 1-13E). Interestingly, the result with CRY2 (both *DpCRY* and *hCRY*) was not expected given that these molecules are not believed to be light-responsive in a circadian context (Vieira *et al.*, 2012) (but see (Hoang *et al.*, 2008)). These findings do not fit the widely held view that the tryptophan triad-generated radical pairs mediate the ability of CRY to sense a magnetic field, since 450 nm light is sufficient for the photoreduction of oxidized flavin (Berndt *et al.*, 2007; VanVickle-Chavez & Van Gelder, 2007). Further studies performed using mutant flies in which the tryptophan residues were substituted with phenylalanine (Phe), structurally similar to Tryptophan but unable to transfer electrons have shown a “normal” naïve and trained responses to the EMF, suggesting that CRY-magneto sensing does not depend on the presence of Trp-triad-mediated radical pairs (Geegear *et al.*, 2010) opening the possibility of a different radical partner (Müller & Ahmad, 2011; Biskup *et al.*, 2013; Lee *et al.*, 2014).

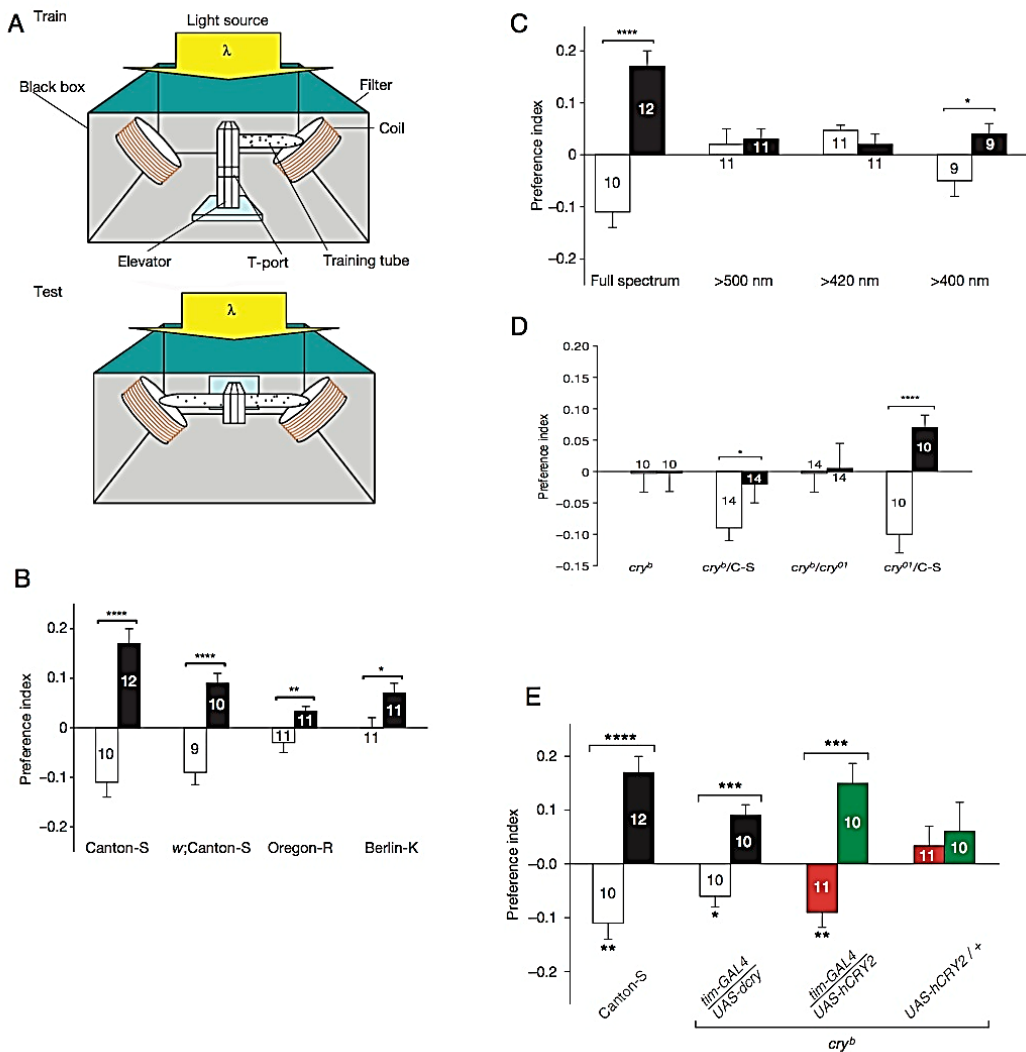


Figure 1-13 CRY is involved in *Drosophila* magnetoreception

A set-up used for training and testing flies. B Wild type flies show a significant response to the magnetic field. C a magnetic field response is observed only under full spectrum of light and when wavelength < 420 nm were present. However, naïve flies exposed to wavelengths >500 nm or > 400 nm exhibit an opposite response, as hypothesized by the antagonistic effect. D *cry* mutants do not show any EMF response. E hCRY2 rescues EMF sensitivity in *Drosophila*. White and red bars = naïve flies, Black and green bars= trained flies. A-B-C-D adapted from (Gegear *et al.*, 2008); E adapted from (Foley *et al.*, 2011)

As discussed in section 1.3.4, CRY in *Drosophila* mediates direct light input to reset the clock. Thus, if the RPM works through CRY it is plausible that a magnetic field can alter the circadian clock output. Therefore, free-running periods and rhythm strengths were measured in flies exposed to different intensities of EMF (Yoshii, Ahmad & Helfrich-Förster, 2009). Flies were kept under constant dim light (dLL) in order to maintain their rhythmicity, light intensity was set at $0.18 \mu\text{W}/\text{cm}^2$ both in blue (465 nm) and red (645 nm) light. By using two Helmholtz coils, a constant magnetic field was applied during the activity experiment of different intensities (0-150-300 and 500 μT - approx. 0-3 and 6-10 times stronger than the Earth's magnetic field). Applying the EMF resulted in a change of the free-running period (40% of the flies showed a longer period, although 12% also show shorter cycles - the rest (about half) showed no change in period, Figure 1-14A-B). The EMF response occurred only under blue light and not in red light, suggesting a possible involvement of CRY (Figure 1-14C).

Interestingly, the response to the EMF was dependent on the strength of the magnetic field, since the maximum response was obtained when a 300 μT EMF was applied, but no effects were observed under 1 mT, in accordance to the theoretical prediction (see 1.2.3, Figure 1-14C). To confirm the hypothesis of a CRY-mediated response, CRY-deficient flies (cry^b and cry^M , cry null mutant) were tested together with CRY over-expressing flies (using GAL4-UAS system, *timGAL4-UAScry*, Figure 1-14D). As expected, the vast majority (76-84%) of CRY-deficient flies showed no effects of EMF exposure whereas flies over-expressing CRY in all clock neurons showed an amplified response resulting in arrhythmia in 66% of the flies. It is worth noting that the absence of any EMF effect in *cry* mutants flies is not surprising because the initial blue light induced change in period which acts as the substrate for the EMF, is itself CRY-dependent. Consequently *cry*-null flies free-run with ~24 h period as they are insensitive to dim blue light. Overexpression of CRY however does reveal an EMF phenotype, and in the 8 flies that remained rhythmic, period was very variable, but generally longer than non-exposed flies. These findings are consistent with the RPM and suggest that the magnetic field intensifies the effects of blue light on the clock by virtue of the arrhythmicity in *tim>cry* flies. This provides the first evidence of a mechanistic link between CRY and magnetic sensitivity in the circadian clock of fruit

flies, which could conceivably play a role in fly orientation, as has been shown for the sun compass orientation in *D. plexippus* (Zhu *et al.*, 2005; Merlin, Gegear & Reppert, 2009).

Reppert's group has also suggested that CRY expression in the antennae may play a role in EMF detection in monarch butterflies (Merlin *et al.*, 2009; Guerra *et al.*, 2014), in ants (de Oliveira *et al.*, 2010) and bees (Lucano *et al.*, 2006). Although, the presence of CRY in fly antennae has been observed (Hares, 2013), and that *cry* mutations disrupt circadian antennal phenotypes (Krishnan *et al.*, 2001), very little is known about CRY localization in the fly antennae which are known to provide the location of several receptors, including Johnston's Organ, which detects geotaxis and vibrations, and olfactory receptors (North & Greenspan, 2007; Sun *et al.*, 2009; Yorozu *et al.*, 2009).

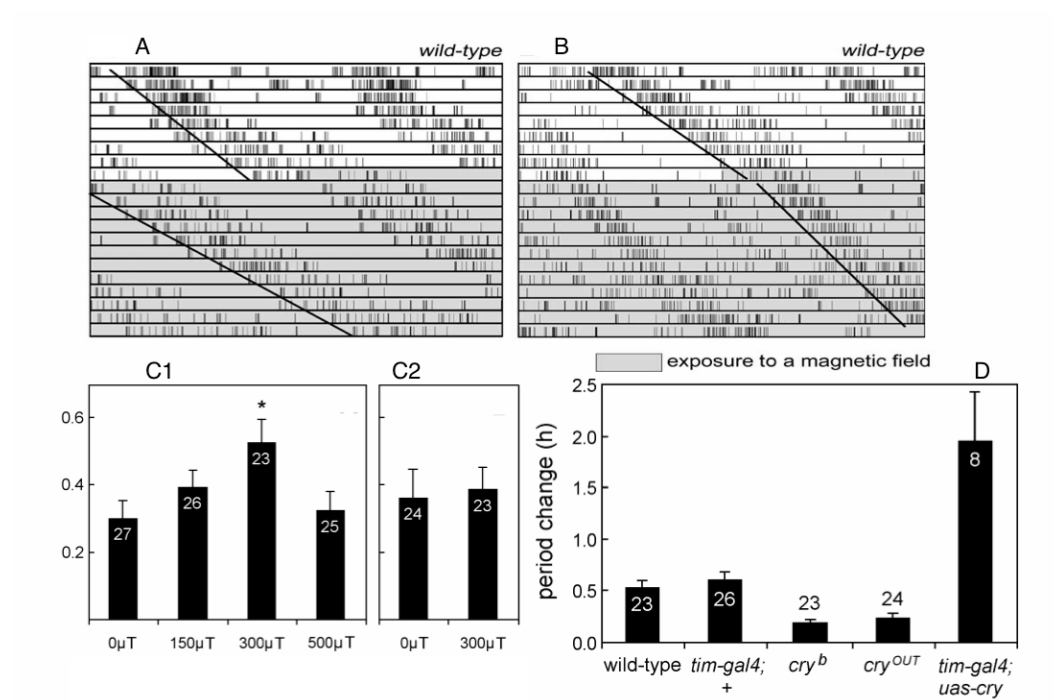


Figure 1-14 EMF modulates *Drosophila* circadian clock through CRY.

Exposure to a 300 μT static field significantly changes the period of wild-type flies, giving both longer (A) or shorter (B) periods. The effects are observed only under blue light and under a 300 μT field (C1) but not under red light (C2). *cry* mutants do not show any response whereas CRY overexpressing flies show an even more pronounced effect (D). Adapted from (Yoshii *et al.*, 2009).

In conclusion, studies conducted on *D. melanogaster* have demonstrated its ability to perceive the magnetic field in a wavelength-dependent manner, and this is compromised when CRY is not functional. This is consistent with the model proposed by Ritz (Ritz *et al.*, 2000) although, flies can respond to EMF without apparently generating radical pairs through the Trp-triad, which is thought to be the critical element of a CRY-based magnetoreception. It is not clear yet whether fly CRY functions as the actual magnetoreceptor or whether it is an essential component downstream of the receptor, nor how magnetosensitive chemical reactions are generated and transduced into neural signals.

1.5 MY PROJECT

This study was aimed to better understand the role of CRY in magnetoreception in *D. melanogaster*. Despite several pieces of evidence in the literature, the actual biological mechanism and adaptive implications of CRY in detecting EMFs is still far from clear. As mentioned above, very strong and clear evidence of a light-dependent compass in the fruit fly are provided by the Phillips Lab (Dommer *et al.*, 2008; Painter *et al.*, 2013), however, the lack of genetic manipulation in these studies does not clarify a role for CRY. On the other hand, the observations of Yoshii and coworkers together with the studies from the Reppert lab, describe an effect of EMF on CRY, albeit very weak. In particular, in Yoshii *et al.* (2009), the assumptions that dCRY is a potential magnetoreceptor have been based on the fact that *cry-null* flies did not show any EMF effect but as mentioned above this does not provide a critical test. The real indication that CRY could be involved in the RPM, comes from CRY-overexpressing flies, which show an enhanced EMF response compared to wild-type, *i.e.* increased levels of arrhythmia and a greater period lengthening. Moreover, in this study, the authors showed that under red light, the period changes were similar to those under blue light in the absence of a magnetic field which creates further difficulties.

Consequently I decided to try and replicate Yoshii's observations (Yoshii *et al.*, 2009) using a more controlled EMF exposure system, the Schuderer apparatus (Schuderer *et al.*, 2004). In Chapter 3, I assayed the response of wild type and *cry*

mutants flies to different intensities and frequencies of EMF, and I observed very consistent circadian and non-circadian locomotor responses under these conditions. Given these robust responses in Chapter 4, I used different combinations of GAL4-GAL80 drivers in an attempt to localize the relevant EMF responsive clock neurons and external brain structures involved in magnetoreception. In Chapter 5 I established a new clock independent assay for magnetoreception based on negative geotaxis (Toma *et al.*, 2002), and in Chapter 6 I provide a third independent assay for magnetoreception in flies, which was originally conceived by inspecting some of the results from the work of Gegear and coworkers (Gegear *et al.*, 2008, 2010; Foley *et al.*, 2011). Finally, in Chapter 7, which is not strictly EMF relevant, I show some striking results that challenge our view that only the Lateral and Dorsal clock neurons contribute to behavioural rhythms.

2 MATERIAL & METHODS

2.1 FLY MAINTENANCE AND LINES USED

Drosophila stocks were reared in culture vials with maize food (72 gr/L maize meal, 80 gr/L glucose, 50 gr/L brewer's yeast, 8.5 gr/L agar, 2 gr/L of Nipagine, dissolved in 10 ml 100% ethanol) and kept at 25°C in a temperature-controlled room where a 12:12 LD regime was applied. Flies for activity experiments were loaded in activity tubes with maize food.

The lines used in this study are:

- *Canton-S*, the common laboratory wild-type strain
- w^{1118} ; *white-eyed mutant*(Lindsley & Zimm, 1992)
- *CyO/Sco;TM6B/MKRS* Double Balancer Line (DBL) used for balancing the second and third chromosome (Lindsley & Zimm, 1992)
- *FM7 α* used for balancing the X chromosome (Lindsley & Zimm, 1992)
- *cry⁰²* *cry* knock-out strain, where the *cry* CDS?? has been replaced by the *mini-white* marker (Dolezelova, Dolezel & Hall, 2007)
- *Clk^{irk}* dominant allele (Allada *et al.*, 1998)
- *Antp^R* hypomorphic allele (Johnston *et al.*, 1998)
- *glass^{60j}* (Helfrich-Förster *et al.*, 2001)
- *eya²*; 322bp deletion 581bp upstream of the transcription start site of the type I *eya* transcript (Zimmerman *et al.*, 2000)
- *Pdf⁰¹* null mutation (Renn *et al.*, 1999)
- *per⁰¹* amorphic allele (Konopka & Benzer, 1971)

For the drivers (GAL4/GAL80):

- *Clk9M>GAL4* expresses GAL4 in DNs and s-LN_s (Kaneko *et al.*, 2012)

- *cry₁₃>GAL4* expresses GAL4 under the control of *cry* promoter (Dissel *et al.*, 2004, 2014; Stoleru *et al.*, 2007)
- *cry>GAL80_{2e3m}* expresses GAL80 under the control of *cry* promoter (Stoleru *et al.*, 2007; Dissel *et al.*, 2014)
- *FGAL4* expresses GAL4 under the control of *Nanchung* promoter, a TRPV channel (Kim *et al.*, 2003)
- *gmr>GAL4* expresses GAL4 under the control of *Glass Multimer Reporter* promoter (Wernet *et al.*, 2003)
- *iav>GAL4* expresses GAL4 under the control of *inactive* promoter, involved in calcium channel activity (Sun *et al.*, 2009)
- *Jo15>GAL4* expresses GAL4 under the control of *Hobo* enhancer trap promoter in the Johnston's Organ (Sharma *et al.*, 2000; Kamikouchi, Shimada & Ito, 2006),
- *nompA>GAL4* expresses GAL4 under the control of *non mechanical perception A* promoter, a TRP channel involved in sensory perception (Eberl & Boekhoff-Falk, 2007)
- *pain>GAL4* expresses GAL4 under the control of *painless* promoter, line R21B03 (Bloomington)
- *Pdf>GAL4* expresses GAL4 under the control of *Pdf* promoter (Dissel *et al.*, 2004, 2014; Stoleru *et al.*, 2007)
- *Pdf>GAL80_{96a}* expresses GAL80 under the control of *Pdf* promoter (Dissel *et al.*, 2004, 2014; Stoleru *et al.*, 2007)
- *pyx>GAL4* expresses GAL4 under the control of *Pyrexia* promoter, a TRP channel involved in thermal noninception (Sun *et al.*, 2009; Simoni *et al.*, 2014)
- *R7>GAL4* Expresses GAL4 in all R7 cells under the control of portions of the *rhodopsin 3* and *4* promoters (Mollereau *et al.*, 2000)
- *Rh5>GAL4* (GAL4 driven by the *rhodopsin 5* promoter in R8 cells (Tahayato *et al.*, 2003)

- *Rh6>GAL4* GAL4 driven by the *rhodopsin 6* promoter in R8 cells (Chen *et al.*, 2014)
- *tim>GAL4* expresses GAL4 under the control of *tim* promoter (Dissel *et al.*, 2004, 2014; Stoleru *et al.*, 2007)

For the reporters (UAS):

- *UAS-GFP-C-terminal-CRY* (Made by Dr John Hares in Ezio Rosato's laboratory)
- *UAS-luciferase-cry* (gift from Prof R. Stanewsky, UCL)
- *UAScry24b* (Emery *et al.*, 2000)
- *UAScryW342F* (Gegear *et al.*, 2010)
- *UAScryΔ_{14.6}* on the first Chromosome (Dissel *et al.*, 2004, 2014)
- *UASdbt^{K/R}* (Preuss *et al.*, 2004; Muskus *et al.*, 2007)
- *UASdbt^{Long}* (Preuss *et al.*, 2004; Muskus *et al.*, 2007)
- *UASdbt^{Short}* (Preuss *et al.*, 2004; Muskus *et al.*, 2007)
- *UASGFP* (Dissel *et al.*, 2014)
- *UASHAcry* (Dissel *et al.*, 2004)
- *UASmychCRY1* (gift from Prof S. Reppert, UMass)
- *UASmychCRY2* (Foley *et al.*, 2011)
- *UASNaChBac* (a bacterial depolarization-activate sodium channel (Nitabach *et al.*, 2006))
- *UASper* (Collins *et al.*, 2006)
- *UASSgg* (Stoleru *et al.*, 2007)

All the lines used in this study were backcrossed for at least 7 generations into a *w¹¹¹⁸* background, with the exception of the *DBT* mutant reporters (*UASdbt^{long}*, *UASdbt^{short}*), the drivers *pyxGAL4*, *iavGAL4*, *nompAGAL4* and *FGAL4* and *Cik^{Jrk}* and *per⁰¹* strains. A general backcrossing scheme is given below (Figure 2-1).

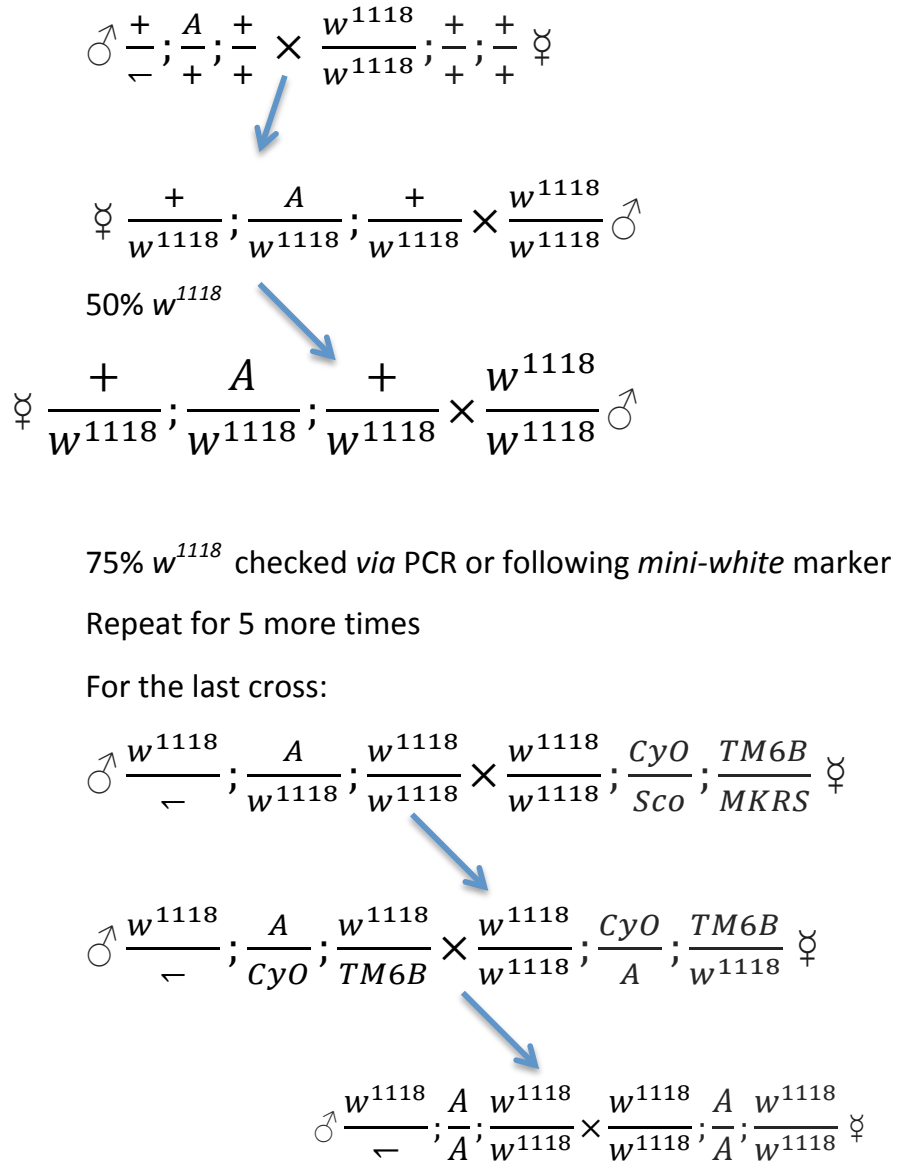


Figure 2-1 Backcrossing scheme. ♀ indicates female virgins, ♂ indicates males and - indicates the Y chromosome.

cryG80,cry⁰², *painG4,cry⁰²* and *Jo15G4,cry⁰²* flies were obtained by recombination or using *TM8Sb¹*, *cry⁰²/TM6B* flies. *TM8Sb¹* flies carry an inversion that balances the third chromosome except the cytological regions 87C-92D-E (Lindsley & Zimm, 1992). *cry* maps to 91F (Lindsley & Zimm, 1992) and therefore recombination was possible. A stock carrying *TM8Sb¹*, *cry⁰²/TM6b* was then used for recombination following the *mini-white* eye marker of *cry⁰²* and the marker *Sb¹* (Lindsley & Zimm, 1992), see example below (Figure 2-2).

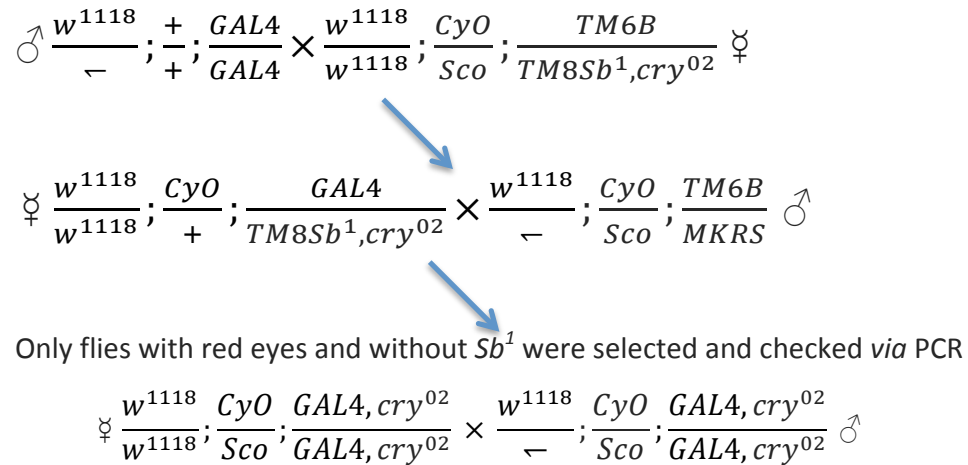


Figure 2-2 Example of recombination using $TM8sb^1$. ♀ indicates female virgins, ♂ indicates males and – indicates the Y chromosome.

2.2 GENOMIC DNA EXTRACTION AND GENOTYPING PCR

Genomic DNA was extracted either from whole flies or wings in Squishing Buffer (SB, Table 9-1) and 200 μ g/ml of ProteinaseK (Sigma) added fresh before use. Individual flies or pairs of wings were placed in a 0.5 ml PCR tube and mashed up using a pipette tip containing 50 μ l of SB (or 100 μ l in case of wings). Incubation at 37° C for 1h (or overnight for wings) was followed by Proteinase K inactivation at 95°C for 2 min. The DNA extraction was followed by PCR amplification using a G-Storm ThermoCycler.

The reaction mix was: 4 μ l of 5X PCR Buffer (Table 9-1) 2 μ l of Genomic DNA, 1 μ l of Primer Forward, 1 μ l of Primer Reverse, 0.2 μ l of KAPA Taq DNA Polymerase and 11.8 μ l of H₂O. The primers used for cry^{02} , eya^2 , Pdf^{01} , $GAL4$, $GAL80$ and UAS are reported in Table 9-2 together with annealing temperature. Based on the strategy used for generating the cry^{02} strains (Dolezelova *et al.*, 2007), a multiplex PCR strategy was used for genotyping: two reverse primers one binding to the 5' of the *mini-white* gene and the other one to 5' of *cry* gene span (after the ATG codon), whereas the unique forward primer was specific for the 3' of the *cry* promoter

region. This strategy allowed discrimination of homozygous mutant, heterozygous and negative (wild-type) flies.

Moreover, flies were genotyped for the *ls/s-tim* variants (Sandrelli *et al.*, 2007; Tauber *et al.*, 2007) using a multiplex PCR assay as described in (Tauber *et al.*, 2007) and resulted to carry the *s-tim* allele only (Table 9-2).

2.3 WESTERN BLOT

Flies for western blots analyses were collected at specific time points and flash frozen in liquid nitrogen. A set of sieves with different sizes (Fisher Scientific) was used to separate heads from bodies after vortex agitation. Heads were collected in 1.5 ml centrifuge tubes and stored at -80°C until processed.

For the EMF or sham blots, flies were harvested after 5 days under the control of constant dim blue light and constant darkness (DD) controls were generated by using flies in vials wrapped in aluminium foil and placed inside the same boxes so exposed to the same EMF or sham conditions. A pool of 100 heads, collected at ZT14, was homogenized in 1.5X volume of extraction buffer (EB, Table 9-1). Western blots on the *UAS-GFP-C-terminal-CRY*, *UAScryW342F* and *UASmychCRY1* crossed to *timGAL4* were performed by keeping 10-15 flies in DD for 3 days and collecting them during the fourth subjective night (ZT 20-22). Proteins were extracted as described above

After quantification *via* the Bradford (Sigma) assay, 15 µL of protein was heated 95°C for 5 min together with 15 µL of 2X Laemli sample buffer (Table 9-1), loaded on a 10% SDS-page (Table 9-1) and transferred to a nitrocellulose membrane (GE HealthCare) for 4 h at 4°C (Table 9-1). After transfer, the membranes were checked with Ponceau solution (Sigma) and blocked for 2 h at room temperature (or at 4°C overnight) using 5% milk/TBS-T solution (1XTBS with 0.1% Tween20, Table 9-1). Immunoblotting was performed using different primary (Table 2-1) and secondary antisera (Table 2-1) diluted in 5% milk/TBS-T solution. Signals were

obtained by chemiluminescence (ECL, GE HealthCare) and quantified with GelAnalyser 2010 (GelAnalyser.com, Dr Istvan Lazar). Three biological replicates with three technical replicates were performed.

Table 2-1 List of primary and secondary (HRP conjugated) antisera used .

Antibody	Concentration	Host	Brand
α -MYC	1:3,000	Mouse	Invitrogen
α -TUB α	1:10,000	Mouse	Sigma
α -HA	1:6,000	Mouse	Sigma
α -GFP	1:3,000	Rabbit	Invitrogen
α -CRY	1:1,000	Guinea Pig	Own
α -HSP70	1:50,000	Mouse	Sigma
α -Guinea Pig	1:10,000	Goat	ABCam
α -Mouse	1:6,000	Goat	Sigma
α -Rabbit	1:3,000	Goat	Invitrogen

2.4 CO-IMMUNOPRECIPITATION (CO-IP) AND PARTIAL PROTEOLYSIS

Flies were collected as before but protein extraction was performed immediately after flash freezing in liquid nitrogen. The extraction buffer consisted of 1 volume of TBS-NP40 (1XTBS with 0.5% NP-40, Table 9-1) together with protease inhibitor tablets (Thermo Scientific). After homogenization, pestle proteins were spun for 10 min at 4°C at maximum speed (17,000 G) and the supernatant collected.

95 µL of protein extract were diluted in 400 of 1XTBS (Table 9-1). 50 µL of the resulting dilution were used as input control. Agarose beads conjugated with primary antibody (anti-HA and anti-GFP) obtained from Thermo Scientific were washed 3 times using 1 mL of cold TBS and centrifuged at 2,500 G for 2 min at 4°C and the supernatant removed. After the last wash the beads were diluted in 750 µL and aliquoted into three separate 1.5 mL centrifuge tubes. Beads and 250 µL of proteins were incubated on a rotating wheel overnight at 4° C followed by wash and elution steps using elution buffer (Thermo Scientific). The flow-through from the washes was used as the negative loading control. Protein concentration was determined using a Qubit Assay (Life Technology) and after heat denaturation (95°C for 5 min) 30 µL were loaded on a 4-20% SDS-page (Precast BioRad, Table 9-1) with 2x reducing sample buffer (Thermo Scientific) with the addition of 15% β-mercaptoethanol. Both semi-dry blotting (BioRad) and wet blotting were used for transferring the proteins to a nitrocellulose membrane (GE Healthcare).

After blotting, the membranes were equilibrated in 7% acetic acid- 10% methanol solution for 15 min, stained with Sypro Ruby Blot Stain (Life Technology) and visualised using a LAX-4000 Digital Imager (Fujifilm).

For partial proteolysis, almost 30,000 *tim>HAcry* flies (from a stable line) were kept in darkness for 10 days and proteins were extracted as described in (Ozturk *et al.*, 2011). After immunoprecipitation (IP) using HA- agarose beads (Thermo Scientific) and competent elution (HA peptide, Thermo Scientific) proteins were concentrated using VivaSpin 50kDa columns (GE Healthcare).

5 µg of proteins were aliquoted in an eppendorf containing 1x PBS in a total volume of 50 µL and reactions were initiated with the addition of 5 µL of trypsin (Promega) at final trypsin:protein ratio of 1:800 and 1:100 (w:w). Tubes were exposed to EMF or Sham conditions under the control of blue light for 45 min. Reactions were stopped with the addition of 15 µL of 5xSDS buffer (Table 9-1) and resolved by a 4-20% SDS-page (BioRad) and transferred using wet-blotting (Table 9-1) for 1.5 h. Normal immunostaining and detection was then performed.

All the steps for both Co-IP and IP, were also performed under red lighting conditions and at 4°C until ready to be loaded.

2.5 SCHUDERER APPARATUS

To perform activity experiments under the control of EMF exposure I used the Schuderer apparatus (Schuderer *et al.*, 2004), which allows EMF exposure through a computer controlled random (blind) decision maker. There is also complete isolation between exposure and sham chambers and also continuous monitoring of all environmental and technical parameters.

The setup is based on two identical coil systems that are placed beside each other inside a normal incubator; each coil system consists in a 4 quadratic Helmholtz coils (Schuderer *et al.*, 2004) which are optimized to produce a homogeneous magnetic field over the area of the TriKinetics© monitors in which the flies are located (Figure 2-3). The field is perpendicular to the plane of the flies. The entire 4-coil system is placed inside a µ-metal box that serves to shield the ambient incubator extremely-low frequency (ELF) fields and to isolate the sham group so that both coil system can be kept inside the same incubator and do not influence each other (Figure 2-3).

The magnetic field that is produced by the coils is an oscillating ELF field ranging from 3 Hz to 1.2 kHz and intensity ranging from 90 µT to 3 mT. Temperature rise due to electric currents is avoided by a ventilation system placed on the side of each chamber and controlled by a PC unit. Elastic/rubber feet minimize vibrations.

The exposure is initialized and controlled by MS-Windows-based user software, and the decision of which chamber is ELF exposed and which is sham exposed is taken randomly by the PC. All exposure settings like signal type, frequency, duration, etc. can be defined. During exposure, all sensor signals and commands are stored in 10 s intervals. The software is able to self-detect malfunctions by tracing and handling ~60 types of errors (Schuderer *et al.*, 2004). It generates warnings or abortions if required (the software has been programmed in order to abort an experiment if differences in temperature between the two chambers are greater than 0.8 °C and if the actual temperature reaches 27°C). After completion of the experiment, all data is stored in an encoded file, which can be decoded only by a dedicated program. Decoding is performed by a collaborator in Zurich (Dr Manuel Murbach, ETH) after locomotor activity data evaluation in order to guarantee the blind study design.

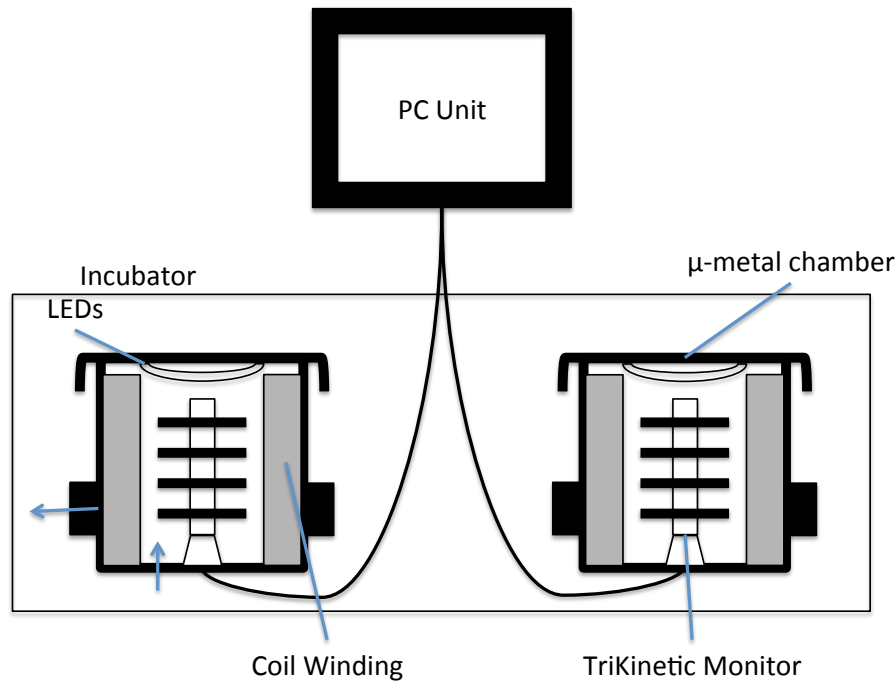


Figure 2-3 Schematic representation of the Schuderer Apparatus. The two μ -metal chambers are placed side by side inside the incubator. Within each chamber one Trikinetic monitor is placed. Light is provided by a LEDs array placed on top of the chamber outside the coil radius to minimize interferences. Blue arrows represent airflow. Adapted from Fedele *et al.* in press.

2.6 ACTIVITY EXPERIMENTS

All the activity experiments were performed using TriKinetics® monitors and software (TriKinetics Inc). Each male fly (1-3 days old) was loaded into a 10 cm long glass tube containing maize food at one end (sealed with a plastic cap to avoid desiccation) and cotton bung at the other.

Each tube was placed in the monitoring apparatus (32 tubes/monitor), which consists of an infrared emitter and detector. Every time the fly breaks the beam, one unit of locomotor activity is recorded by a computer. The number of times the beam is interrupted within a 30 min window is recorded as the locomotor activity of that specific time bin. The average activity histogram (Actograms) was plotted using Microsoft Excel by considering only flies that survived until the end of the experiment.

The monitors were place in light boxes or (into the Schuderer apparatus chambers) equipped with 15 to 30 dimmable LEDs that were programmed to turn on or off using timers. The light boxes were placed into incubator (Sanyo Electric Co. Ltd) that maintained constant temperature. All the activity experiments were performed at 20°C.

The light intensities inside each light box (or chamber) were measured using a radiometer/photometer (LOT-Oriel Group) connected to an irradiance detector (LOT-Oriel Group). In order to decrease light intensities neutral density filters (ROSCO Ltd) were applied on each lighting plate.

2.7 HOME-MADE EXPOSURE SYSTEM

In order to perform both negative geotaxis and Reppert-like (Gegear *et al.*, 2008, 2010; Foley *et al.*, 2011) assays, a dedicated apparatus has been built in the Biomedical Joint Workshops (University of Leicester), based on a design from my laboratory. The exposure systems consist of dual-coils (50 windings each, 10 cm radius, Figure 2-4A) able to produce a static magnetic field that can be shifted from one side to the other of the maze or creating uniform magnetic field between the

coils. The coil system is based on the double-wrapped coil system described in (Kirschvink, 1992): two coils are wrapped with two copper wires in the same direction in one coil and in antiparallel direction in the other to generate sham exposure.

Considering the two wires wrapped on one coil as a pair, magnetic fields generated by equal and opposite currents flowing through them will cancel each other out, producing no measurable fields, even a few wire diameters away (Kirschvink, 1992). Connecting the coils in series guarantees that the currents are equal. On the other hand, if the current directions are parallel, their magnetic fields will add together and produce fields in the surrounding space. Such configuration will allow, through a double-pole double-throw (DPDT) switch, to invert the electric current's flux in one of the two wires thus producing or not detectable magnetic fields in only one coil. The coils are hosted inside a dual-layer aluminium box, and they can be moved back and forth to increase or decrease the intensity of the field (Figure 2-4A). A power pack supplies the coils with DC currents. The system is illuminated by two LED plates, supplied by an adjustable power pack that can be used to change the light intensity. Four different wavelengths have been chosen: blue (450 ± 20 nm), green (500 ± 20 nm) red (645 ± 10 nm) and white (400nm – 750 nm) (Figure 2-4A).

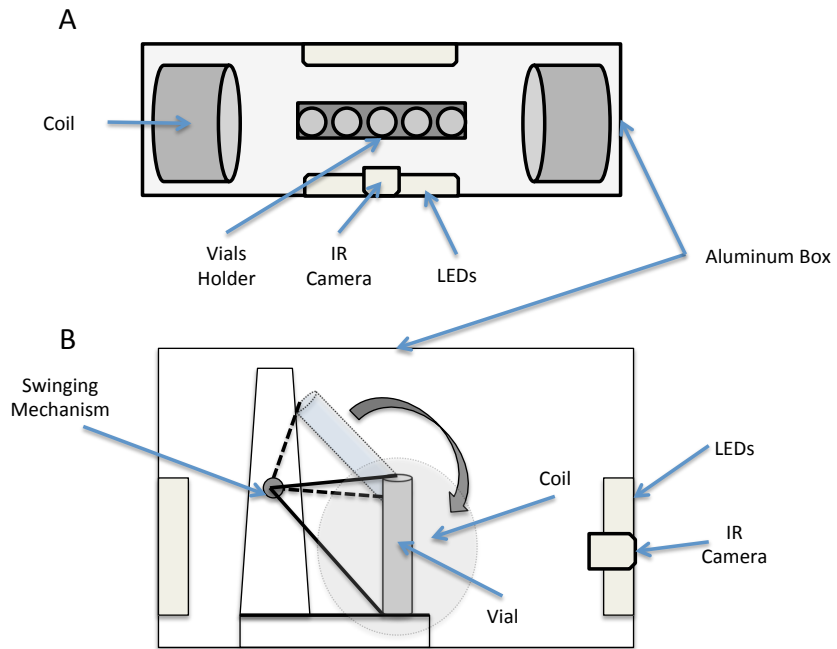


Figure 2-4 The delivery system for EMFs consists of a double-wrapped coil system (a, top view), and a custom-made swinger apparatus (b, side view) that allows tapping three vials simultaneously with equal force so the flies fall to the bottom of the tube. IR, infrared. Adapted from (Fedele *et al.*, 2014).

NEGATIVE GEOTAXIS

For the negative geotaxis assay (Fedele *et al.*, 2014) flies were placed in a plastic vial and tapped to the bottom by means of a custom-made ‘swinger’ that allowed three vials to be tapped to the bottom simultaneously with exactly equal force (Figure 2-4B). An infrared webcam (Logitech) was used to film the flies.

2.8 DATA COLLECTION AND ANALYSIS

The TriKinetics monitors were connected to a PC and the data was collected using DAMSystem2.1.3 software (TriKinetics Inc). The period of each individual fly was calculated by Autocorrelation (cross-correlation of a signal with itself) and using Python 22 for high resolution spectral analysis using the CLEAN algorithm (Roberts *et al.*, 1987). Monte Carlo simulations were used to generate the confidence limits of 95% and 99% by performing 100 randomizations on the data for each fly. The data

obtained after CLEAN was assembled together and further processed using a collection of BeFly! macros generated in our laboratory by Dr. Edward Green (Allebrandt *et al.*, 2013). Flies were considered rhythmic if they presented a clear and significant autocorrelation and spectral analysis. If an individual showed a single peak above the 99% confidence limit in the CLEAN analysis, this was taken as the period. Individuals with multiple peaks above 99% confidence limit were considered having multiple rhythms, whereas individuals with all peaks falling below the 99% confidence limit were considered arrhythmic if this was confirmed by autocorrelation.

For the statistical methods used for negative geotaxis and Reppert-like assay please refer to the corresponding Chapters. Other statistical analyses (ANOVA, post-hoc and χ^2 -square tests) were performed using STATISTICA (StatSoft, Inc. 1996) and GraphPad Prism version 6.00 (GraphPad Software, San Diego California USA).

3 EMF EXPOSURE SHORTENS FREE-RUNNING PERIOD

The majority of the data and part of the text presented in this chapter have been adapted from Fedele *et al.*, 2014.

3.1 INTRODUCTION

The RPM states that CRY could mediate magnetoreception in a light dependent manner (Ritz, Adem & Schulten, 2000), and it could serve as magnetic map, used by migratory animals. Although direct evidence is still missing, several observations coming both from *in vitro* (Maeda *et al.*, 2008; Abeyrathne, Halgamuge & Farrell, 2010) and *in vivo* (Wiltschko & Wiltschko, 2006; Vácha, Puzová & Kvícalová, 2009; Phillips, Jorge & Muheim, 2010a; Wiltschko, Wiltschko & Ritz, 2011; Wiltschko *et al.*, 2013; Nießner *et al.*, 2013) studies support this CRY-centric model. CRY is also one of the main players in the regulation of the circadian clocks in different organisms; in mammals CRY (both CRY1 and CRY2) acts as clock repressor helping PER inhibiting CLK-BMAL1 transcriptional activity (Kume *et al.*, 1999), whereas in *D. melanogaster* it is the circadian photoreceptor that allows the clock to be reset every day (Peschel & Helfrich-Förster, 2011). This dual nature of CRY provides a rationale for the use of magnetic field as plausible *Zeitgeber* for the circadian clock. In other words, if exposure to a magnetic field has an effect on CRY, this should be reflected as a modulated output of the circadian clock.

The first (and only) mechanistic link between magnetoreception and circadian clock has been described in *D. melanogaster* by Yoshii and co-workers in 2009 (Yoshii, Ahmad & Helfrich-Förster, 2009). In this study, flies exposed to constant dim blue light significantly changed their free running period when exposed to a 300 µT static field, resulting in an overall period lengthening (Yoshii *et al.*, 2009). According to the authors, this effect is CRY-dependent as under red light (*i.e.* when CRY is inactive) and

in *cry*-mutant flies it is abolished, and more importantly overexpression of CRY in clock neurons leads to a significant decrease in rhythmicity and a enhancement of the period changes during EMF exposure (Yoshii *et al.*, 2009).

In this chapter I sought to re-examine the effects of EMF on circadian behaviour using the Schuderer apparatus, in which responses to EMF can be studied without interference from the Earth's natural magnetic field or from other local magnetic/radiofrequency fields (Schuderer *et al.*, 2004). Under these more controlled and stringent conditions, I observe a highly robust and consistent CRY-dependent period response to extremely low frequency and static EMFs as well as an additional novel locomotor phenotype.

3.2 MATERIALS AND METHODS

3.2.1 DROSOPHILA STRAINS

Flies were raised at 25 °C on standard yeast-maize medium under a light-dark (LD 12:12) cycle. All strains, mutants, GAL4 and UAS transgenes were backcrossed into a *w¹¹¹⁸* background for 5-7 generations. *UASmychCRY1/2* and *UAScryW342F* were obtained from Steven Reppert (UMass). *timGAL4*, *UAScry24b* (Emery *et al.*, 1998), *UASHAcry* and *UAScryΔ14.6* have been described elsewhere (Dissel *et al.*, 2004). *UASluciferase-cry* was a gift from Prof Stanewsky (UCL).

UASGFPcryCT cloning: This chimeric *cry* construct contains the C-terminal CRY residues 491-542 fused downstream of the *GFP* gene with an N-terminus tagged with Strep(II) and was generated by John Hares (Hares, 2013). This was done by amplifying the GFP sequences using a forward primer (*primer-Af*) containing a start codon and the Strep(II) tag and a reverse primer possessing the relevant GFP sequence plus an additional stretch of bases complementary to the *cry* C-terminal sequence. A second amplification used a forward primer encoding a tract of complementary GFP nucleotides and the start of the *cry*- C-terminus with the reverse primer (*primer-Br*) completing the *cry* sequences plus stop codons to terminate translation. The products of the two amplifications were added together after gel-extraction with

primer-Af and *primer-Br* to generate the chimeric construct. This was sequenced to check for errors before being inserted into pUAST and outsourced for injection (BestGene, CA, USA).

3.2.2 BEHAVIORAL ANALYSES

Circadian locomotor activity was recorded with *Drosophila* Trikinetics Monitors (Waltham, MA) and analysed using spectral analysis and autocorrelograms (Rosato & Kyriacou, 2006). For the fly experiments I initially chose a 300 μ T EMF, the intensity at which the maximal responses had been previously observed (Yoshii *et al.*, 2009), oscillating at 3Hz and in constant blue light (LL) at an intensity of 0.25 μ Wcm⁻² (LED wavelength 450 nm, 40 nm broad range, RS Component).

The experimental design was as follows: two groups of flies of the same genotype were studied for seven days under constant dim blue light (LL, hereafter termed pre-exposure) followed by eight days under the same illumination but exposed either to an EMF (EMF exposure) or a sham EMF (sham exposure). The circadian locomotor period was then calculated separately for the pre-exposure and exposure days for each fly and compared. Experiments were performed using a static field, 3Hz, 50 Hz each at 300 μ T, and also at 90 μ T and 1mT at 3 Hz. Under the RPM, the effect of a superimposed EMF should not be different for static or extremely low frequency fields at the same field intensity, since the oscillations of the field are longer by several orders of magnitude than the radicals' lifetime, which is in the order of microseconds (Kato, 2006).

The period was determined during the pre-exposure and during the EMF or sham exposure. Statistical analyses were performed on flies that were rhythmic throughout the experiment, however for some experiments, especially when only a few flies were rhythmic both before and after the exposure, all flies that were rhythmic either before or after the exposure were included in the analysis. General activity levels were calculated for every 30 min bin regardless of period, but only rhythmic flies were included.

It is noteworthy that the GAL4/UAS controls in this experimental design were omitted since every lines had its own internal control (Sham vs Exposed/ Preexposure vs Exposure). This decision was also driven by the extremely low throughput of the Schuderer apparatus (*i.e.* 1 Trikinetics monitor every 3 weeks).

3.2.3 PROTEIN EXTRACTION, WESTERN BLOTS, IP, CO-IP, PARTIAL PROTEOLYSIS AND LUCIFERASE ASSAY

Protein extraction, Western blots, IP, Co-IP, Partial proteolysis procedures are described in the Material and Methods section. Western blot analyses were performed to check the expression of *UASGFPcryCT* *UAShCRY1* and *UAScryW342F* and are reported in the Appendix.

tim>LUC-cry;cry⁰² flies were harvested after 5 days under constant dim blue light and constant darkness (DD) controls were generated by using flies in vials wrapped in aluminium foil and placed inside the same boxes so exposed to the same EMF/sham conditions. Protein extraction was performed according to the Promega Luciferase Assay system manual (Promega Corporation, Madison, Wisconsin, USA). 20 heads are placed in 1 volume of cell lysis buffer and homogenised by grinding. Protein amounts are quantified using Bradford (Sigma) assay and determined against a standard BSA curve using the micro-assay protocol as described by the manufacturer.

20 µl of protein (at normalised concentration) are loaded in a white 96-well plate together with 100 µl of LAR II reagent (Promega Corporation, Madison, Wisconsin, USA) and quantified using a BMG Plate Reader. Values are normalised against samples kept in DD after being blank and background corrected. Three biological replicates with three technical replicates are performed.

3.2.4 STATISTICAL ANALYSIS

Statistical analyses were performed using spectral analysis implemented in the custom-written BeFly! package (Rosato & Kyriacou, 2006; Allebrandt *et al.*, 2013). Further analyses were carried out using GraphPad Prism version 6.00 for Windows,

(GraphPad Software, La Jolla California USA, www.graphpad.com) and STATISTICA (data analysis software system, version 8.0 StatSoft, Inc. 2008, www.statsoft.com).

3.3 RESULTS

3.3.1 LIGHT INTENSITY SCREENING

Initially, flies responses to dim light were studied by performing activity experiments at different intensities of 450 nm blue light in order to obtain an intensity at which at least 50% of the flies showed rhythmicity with considerable longer rhythms compared to DD. Among four different light intensities (0.16, 0.18, 0.25 and 0.40 μWcm^{-2}) 0.25 μWcm^{-2} was chosen as experimental intensity since 60% of flies remained rhythmic (Figure 3-1 A). In addition, the free-running period of the rhythmic flies in dim blue light was significantly longer (27.5 ± 0.6 h) compared to flies kept in DD (24.1 ± 0.4 h, Figure 3-1B), so any putative effects of EMF on rhythmicity could be observed in both directions.

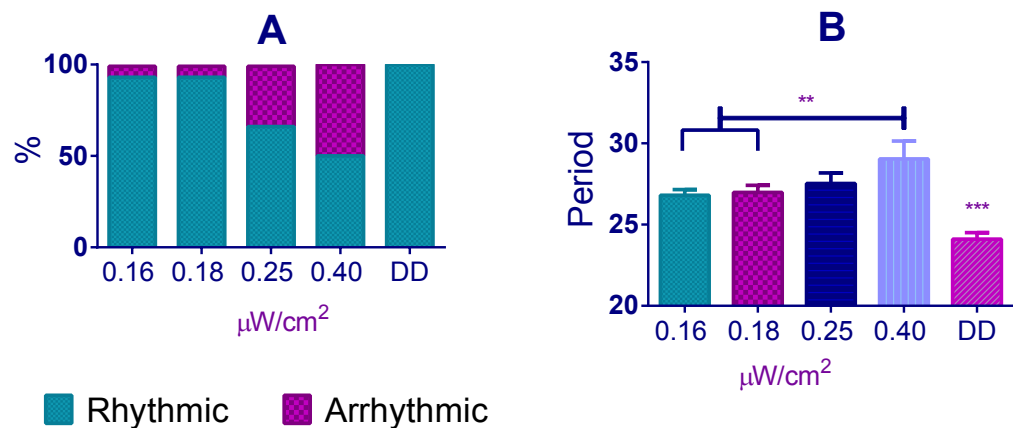


Figure 3-1 Rhythmicity of wild-type under different intensities of constant blue light.

A % of rhythmic CS under different blue light intensities. Heterogeneity $\chi^2_{(4)}=16.19$, $p=0.0028$. (B) Period lengthening of CS flies under different blue light intensities. $F_{(4,53)}=6.79$, $p<0.001$. $0.16 \mu\text{Wcm}^{-2}=26.80 \pm 0.35$, $N=14$; $0.18 \mu\text{Wcm}^{-2}=26.97 \pm 0.44$, $N=16$; $0.25 \mu\text{Wcm}^{-2}=27.53 \pm 0.64$, $N=12$; $0.40 \mu\text{Wcm}^{-2}=29.04 \pm 1.10$, $N=8$; DD= 24.1 ± 0.40 , $N=8$. (post-hoc * $p<0.05$, ** $p<0.01$, *** $p<0.001$). Mean \pm sem. Adapted from Fedele *et al.*, 2014.

3.3.2 EXPOSURE TO EMF SHORTENS THE PERIOD

EMF responses of flies were examined using a standard field intensity of 300 μT (the intensity at which Yoshii and co-workers detected the maximal response) with stationary, 3Hz or 50 Hz frequencies (Figure 3-2 A-C), or using a standard 3Hz frequency with field intensities of 90, 300 or 1000 μT (1 mT, Figure 3-2 C-E). Interestingly, while sham-exposed Canton-S exhibited a lengthening in period between Pre- and Exposure due to the constitutive activation of CRY irrespective of frequency and intensity of the field (Dissel *et al.*, 2004), the EMF-exposed flies showed a shorter period compared both to their previous LL behavioural cycle, but also compared to the corresponding sham-exposed control flies. A three way ANOVA revealed significant effects for EMF frequency ($F_{(2,294)} = 37.28$, $p \sim 0$), exposure to EMF/sham ($F_{(1,294)} = 14.81$, $p < 0.001$), and for the two-way interaction between pre-exposure and EMF/sham ($F_{(1,294)} = 21.73$, $p < 0.01$). Importantly, there was no significant three-way interaction ($F_{(2,294)} = 1.01$, $p = 0.36$), revealing that a similar pattern is revealed at all three frequencies at 300 μT (Figure 3-2 A-C). Exposure to a 50 Hz oscillating field under 0.25 μWcm^{-2} led to a rate of arrhythmicity in the flies well above 50% and so the blue light intensity was reduced to 0.09 μWcm^{-2} . The 50 Hz EMF interfered with the circuit for the LEDs causing them to flicker and thereby raising their effective intensity. Three way ANOVA also revealed significant effects for intensity ($F_{(2,272)} = 23.59$, $p < 0.001$) exposure to EMF/sham ($F_{(1,272)} = 16.69$, $p < 0.001$) and for the pre-exposure x EMF/sham interaction ($F_{(1,272)} = 19.38$, $p < 0.001$). There was no significant 3-way interaction ($F_{(2,272)} = 0.04$, $p = 0.96$) showing that the flies were responding in a similar manner to these exposures at 3 Hz (Figure 3-2 C-E,Table 9-3).

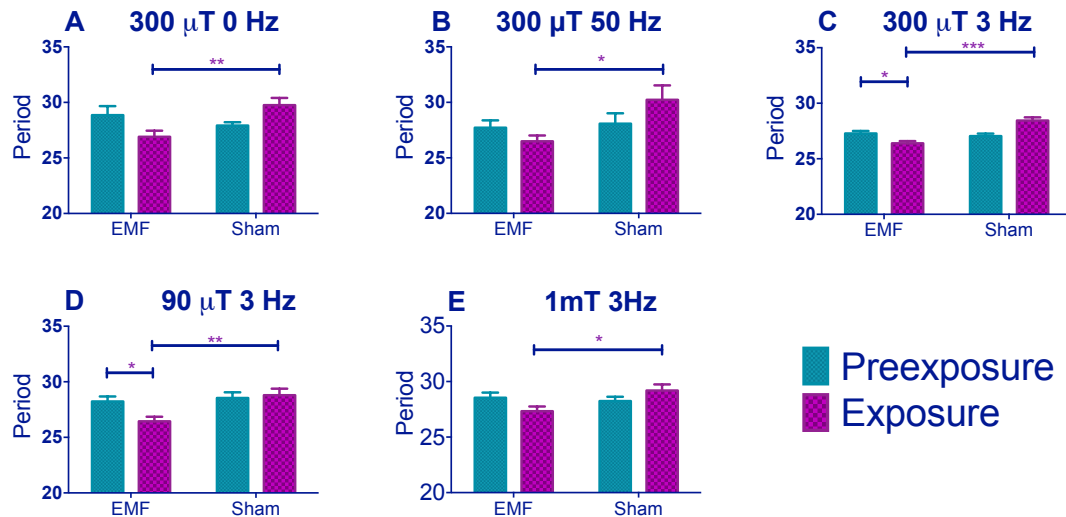


Figure 3-2 EMF exposure shortens free-running circadian periods in dim blue light.

Mean circadian periods (h) \pm sem are shown for the EMF and sham-exposed groups. Note how periods are considerably longer than 24 h (A-C) period changes in CS flies under static, 50 and 3 Hz field respectively at 300 μ T (C-E) period changes in CS flies under 300, 90 and 1000 μ T (1mT) field respectively at 3 Hz. EMF-exposed flies show significant period shortening. For period and N see Table 9-3. (*post-hoc* *p<0.05, **p<0.01, ***p<0.001). Adapted from Fedele *et al.*, 2014.

To study whether these effects could be due to any artifacts associated with the experimental procedures, I analysed possible sources of external contamination, including vibration and light exposure. I evaluated the possibility that vibrations produced by the electric current flowing through the coils and the turning of the fans, could be strong enough to affect the flies' behaviour. Flies were therefore assayed for the locomotor activity by having one group of flies in one of the Schuderer's boxes, connected to the amplifier (*i.e.* fans were on and Sham electric current was flowing) and the second group, placed inside the second box but disconnected from the amplifier (*i.e.* fans were off and no electric current, with the only possible source of vibration was the background such as the incubator, and building). The experiment resulted in similar activity patterns, with no significant difference in period (Figure 3-3 A). Similarly, when both chambers were set as sham, flies showed similar activity patterns, revealing that the amount of vibration in both chambers is similar (Figure 3-3 B).

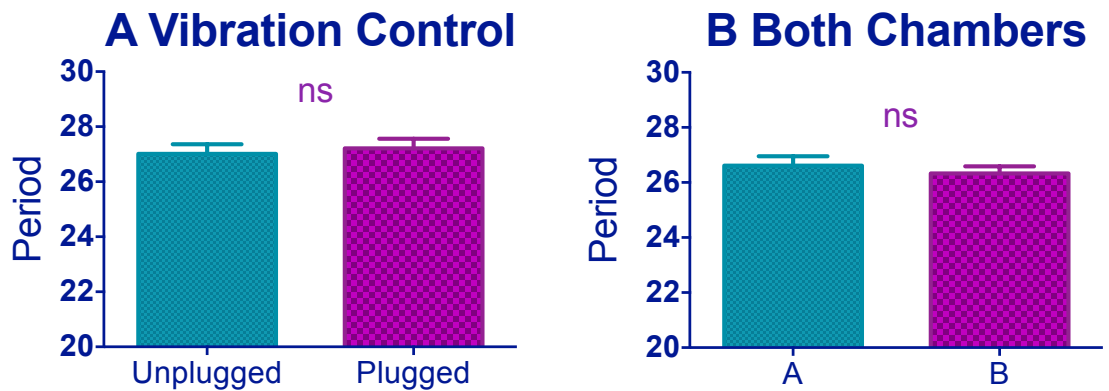


Figure 3-3 - Period changes are not caused by mechanical vibration.

A. When one of the two fans was unplugged from the mains to reduce vibration in one chamber, there were no differences observed in period under dim blue light between wild-type flies in the two chambers ($F_{(1,31)}=0.17$, $p= 0.68$, $N=16$ for both conditions) B. When both fans were plugged in for a sham exposure condition, there were no differences observed in period under dim blue light ($F_{(1, 36)}=1.7$, $p=0.27$, $N=18$ and 19). Mean \pm sem. For period and N see Table 9-3. Adapted from Fedele *et al.*, 2014.

I then pursued my analyses by using a 300 μ T 3Hz EMF to study any effect of the *cry*⁰² null mutant (Dolezelova *et al.*, 2007). The response to the EMF was abolished in *cry*⁰² flies (Figure 3-4 A, Table 9-3), consistent with a possible role for CRY in determining this phenotype (pre-exposure x EMF/sham exposure interaction $F_{(1,52)}=2.93$, $p = 0.09$). However, CRY is required in order to generate the initial blue light-dependent lengthening of period and so these results are not informative in determining whether CRY is the magnetoreceptor. *cry*⁰² flies did show a slight lengthening of period between the pre- and exposure conditions of about 0.5 h ($F_{(1,52)}=108.4$, $p < 0.001$, Table 9-3) suggesting an ageing effect over the ~15 day observation (Rakshit & Giebultowicz, 2013). Indeed I observed a similar period lengthening in CS flies exposed to DD for the same number of days during which CRY would not be light-activated ($F_{(1,54)} =14.40$, $p < 0.001$, Figure 3-4A, Table 9-3). ANOVA revealed no significant three-way interaction when I compared CS in DD to *cry*⁰² in LL (genotype x pre-exposure x EMF/sham exposure, $F_{(2, 106)} = 0.07$, $p = 0.79$), supporting the view that the slight lengthening of period was due to ageing. Consequently, an ageing effect must be taken in consideration also in CS flies in sham condition under dim blue LL, where a dramatic period lengthening was observed (1-2 h, Figure 3-2 A-E). The shortening of period in wild-type flies exposed to EMF is therefore observed in spite of

a natural tendency of the flies to increase their period over the duration of the experiment due to ageing (Figure 3-2 A-E).

I also tested *cry*-overexpressing flies using *timgal4* driver and observed that ~55% the *timgal4>cry* flies in a wild-type background became arrhythmic during the initial pre-exposure days. However, EMF-exposure abrogated arrhythmicity to ~20%, suggesting a disruption of CRY signalling under these conditions, whereas sham exposure flies maintained 67% arrhythmicity ($\chi^2_{(3)}=13.96$, $p < 0.05$, Figure 3-4B, Table 9-3). Furthermore, the flies that stayed rhythmic throughout the *timgal4>cry* experiment again revealed a significant shortening in the period under EMF compared to the sham controls (pre-exposure x EMF/sham exposure interaction ($F_{(1,79)}= 6.23$, $p = 0.015$, Figure 3-4C, Table 9-3).

Taken together these results so far seem to suggest a crucial role of CRY in mediating an EMF response in accordance to the RPM. I also tested the UAS construct carrying a Trp to Phe amino acid substitution in one of the Trp forming the Trp-triad (342), thought to abolish the EMF response, under *timgal4* control in a *cry*-null mutant. I observed that this mutant is light responsive and significantly lengthens its period in dim blue light (Figure 3-4D, Table 9-3). However, a significant period shortening in EMF exposed compared to sham flies (pre-exposure x EMF/sham exposure interaction $F_{(1,54)} = 4.15$, $p < 0.05$, Figure 3-4E, Table 9-3) was observed. Consequently mutation of Trp-342 in the triad does not significantly disrupt the circadian response to EMF, indicating that other radicals must be formed.

The *cryΔ* mutant in which the final 20 residues of the C-terminal have been deleted was also tested. These flies are reported to behave as if CRY is constitutively active in constant darkness with a long period, but CRY Δ can be further activated by blue light (Dissel *et al.*, 2004). Flies expressing CRY Δ under *tim* promoter control were tested in a *cry*-null background under constant dim light and darkness. These analyses revealed a significant response to light that corresponded to period lengthening ($F_{(1,34)} = 6.53$, $p < 0.01$, Figure 3-4F, Table 9-3). However, they did not show any significant period changes under EMF exposure (pre-exposure x EMF/sham Exposure $F_{(1,174)}=0.74$, $p = 0.39$, Figure 3-4G, Table 9-3) implicating the C-terminal of CRY (CT) in the response

to EMF. I therefore tested flies expressing a GFP-CRY-CT fusion in a *cry*⁰² genetic background. This construct carries only the CRY C-terminal residues 491-542 fused to GFP. Remarkably, these flies were still able to respond to light (Figure 3-4H) and also show a modest response to the EMF ($F_{(1,118)} = 4.9$, $p < 0.02$; Figure 3-4I, Table 9-3) confirming the importance of the CRY-CT in the EMF response. While the same experiment in DD did not show any significant EMF effect (pre-exposure x EMF/sham exposure $F_{(1,82)} = 0.1$, $p = 0.81$, Figure 3-4I) a significant ageing effect on period was detected (pre-exposure vs exposure $F_{(1,82)} = 4.2$, $p < 0.05$, Figure 3-4I). Consequently the CRY C-terminal appears to play a role in the EMF circadian phenotype.

These observations need to be further analysed in order to understand the biochemical and molecular mechanism through which the EMF is acting. Two possible scenarios are plausible: It is possible that the GFP, which is capable of absorbing blue photons, could allow the electron transfer to the CRY-C-terminus, required by the RPM (Bogdanov *et al.*, 2009). If the interaction between GFP and CRY-C-terminal is negligible, then another possible explanation could be that the C-terminus is actually the EMF effector, *i.e.* it is the protein domain capable of transmitting the magnetic information downstream, probably by interactions with downstream molecules not identified yet.

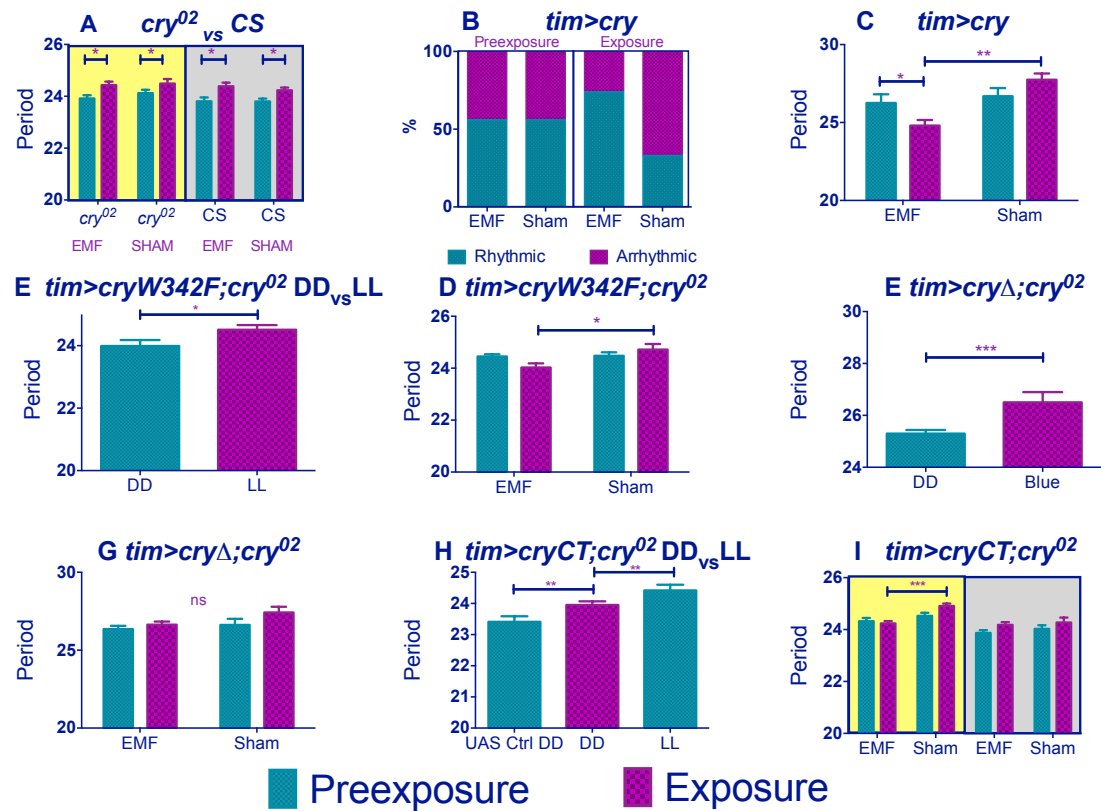


Figure 3-4 *cry* variants alter normal circadian responses to EMFs.

Circadian periods (h) in dim blue LL are shown for EMF and sham-exposed groups. Mean periods \pm sem. (A) *cry⁰²* flies exposed to EMF show only ageing effects on period (yellow shaded box). Wild-type flies kept in DD (grey shaded box) show similar ageing effects (B) *tim>cry* % rhythmic/arrhythmic flies during pre-exposure and exposure to EMF or sham. Exposure to EMF dramatically increases the proportion of rhythmic flies. (C) *tim>cry* period for EMF exposed and sham flies before and during exposure (D) light response *tim>cryW342F; cry⁰²* (E)EMF response of *tim>cryW342F; cry⁰²* (F) light response of *tim>cryΔ; cry⁰²*. (G) EMF response of *tim>cryΔ; cry⁰²*. (H) Light response of *tim>GFPcryCT; cry⁰²*. UAS Ctrl indicates *UASGFP-CRY-CT/w¹¹¹⁸*. (I) EMF response of *tim>GFPcryCT; cry⁰²* both in LL (yellow shaded box) and DD (grey shaded box). (See Table 9-3, post-hoc *p<0.05, **p<0.01, ***p<0.001). Adapted from Fedele *et al.*, 2014.

3.3.3 NOVEL LOCOMOTOR PHENOTYPE

Further analysis of the locomotor activity data revealed a significant hyperactivity of EMF-exposed wild-type flies. Comparison of static to 3 and 50 Hz at 300 μ T fields revealed significant Frequency ($F_{(2,294)}= 42.35$, $p\sim 0$), sham/EMF ($F_{(1,294)}=6.75$, $p<0.01$), pre-exposure/exposure ($F_{(1,294)}= 7.98$, $p<0.01$) and pre-exposure x EMF/sham exposure interaction ($F_{(1,294)}= 7.93$, $p<0.001$), but no significant three-way interaction ($F_{(2,294)}=0.17$, $p=0.83$) illustrating that all frequencies gave a similar pattern of EMF mediated hyperactivity (Figure 3-5A-C, Table 9-4). When 90, 300 and 1000 μ T at

3Hz were compared, no significant Intensity effect ($F_{(2,272)}=2.14$, $p=0.1$) was observed, but sham/EMF ($F_{(1,272)}=4.66$ $p<0.05$), pre-exposure/exposure ($F_{(1,272)}=8.133$, $p<0.05$) and pre-exposure x EMF/sham exposure interactions ($F_{(1,227)}=3.71$, $p=0.05$) were all significant (Figure 3-5C-E, Table 9-4). Post-hoc tests revealed a significant hyperactivity in EMF exposed flies compared to sham at 90 and 300 μ T, but not at 1mT, but this difference was not sufficient to generate a significant three-way interaction ($F_{(2,272)}=0.71$, $p=0.5$).

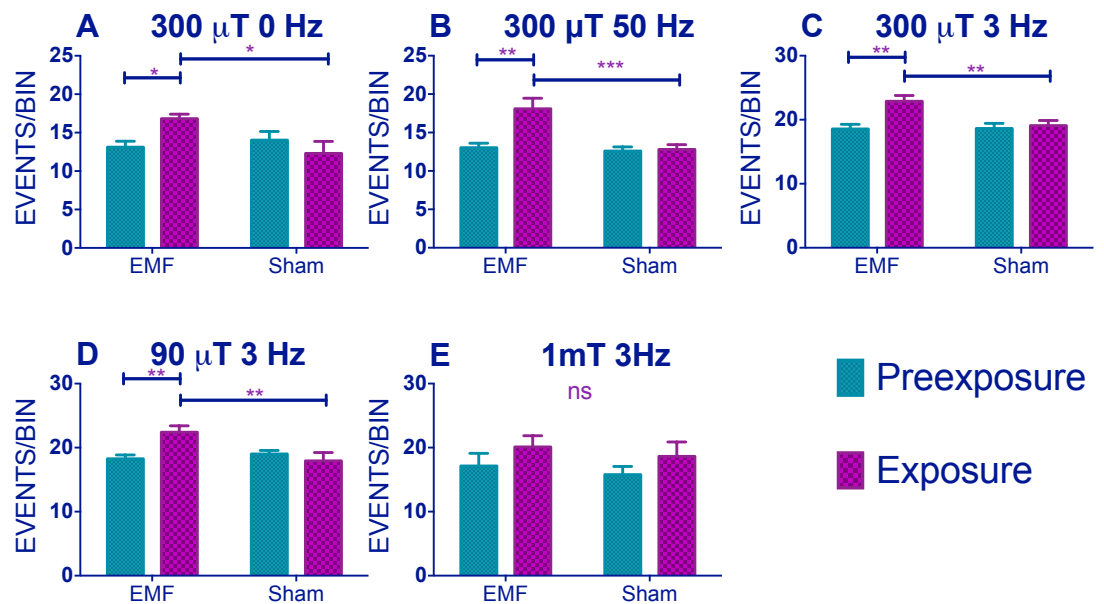


Figure 3-5 EMF induced hyperactivity in Canton-S flies.

(A-C) Hyperactivity in EMF-exposed CS under static, 50 and 3 Hz field respectively at 300 mT. C-E Hyperactivity in CS flies under 300, 90 and 1000 μ T field respectively at 3Hz. N's are the same as in Figure 3-2. Mean activity events per 30 min time bin (\pm sem). For average activity and N refer to Table 9-4 (post-hoc * $p<0.05$, ** $p<0.01$, *** $p<0.001$). Adapted from Fedele *et al.*, 2014.

Similar results were obtained for *timgal4>cry* overexpressing flies (pre-exposure x EMF/sham exposure interaction ($F_{(1,79)}= 4.021$, $p<0.05$, Figure 3-6A, Table 9-4) revealing that EMF-exposed flies showed enhanced hyperactivity compared to sham and pre-exposed flies. More surprisingly, *timgal4>cryΔ* flies also expressed this hyperactivity under EMF exposure (pre-exposure x EMF/sham Exposure interaction $F_{(1,174)}=11.28$, $p<0.01$, Figure 3-6B, Table 9-4) whereas no locomotor differences were detected in *cry⁰²* (pre-exposure x EMF/sham exposure interaction, $F_{(1,52)}=0.04$, $p=0.95$,

Figure 3-6C, TableS2) nor in *cry-CT* (pre-exposure x EMF/sham interaction, $F_{(1, 118)} = 0.51$, $p = 0.46$, Figure 3-6D, Table 9-4). Furthermore flies expressing the *cryW342F* mutation also exhibited the hyperactivity associated with EMF exposure ($F_{(1, 54)} = 11.9$ $p < 0.01$, Figure 3-6E, Table 9-4). I therefore conclude that while robust EMF-induced shortening of circadian period requires the CRY C-terminus, the hyperactivity appears to be determined via the N-terminal photolyase-like domain and is not susceptible to disruption by the Trp-342 mutation, indicating that alternative routes are available for the RPM.

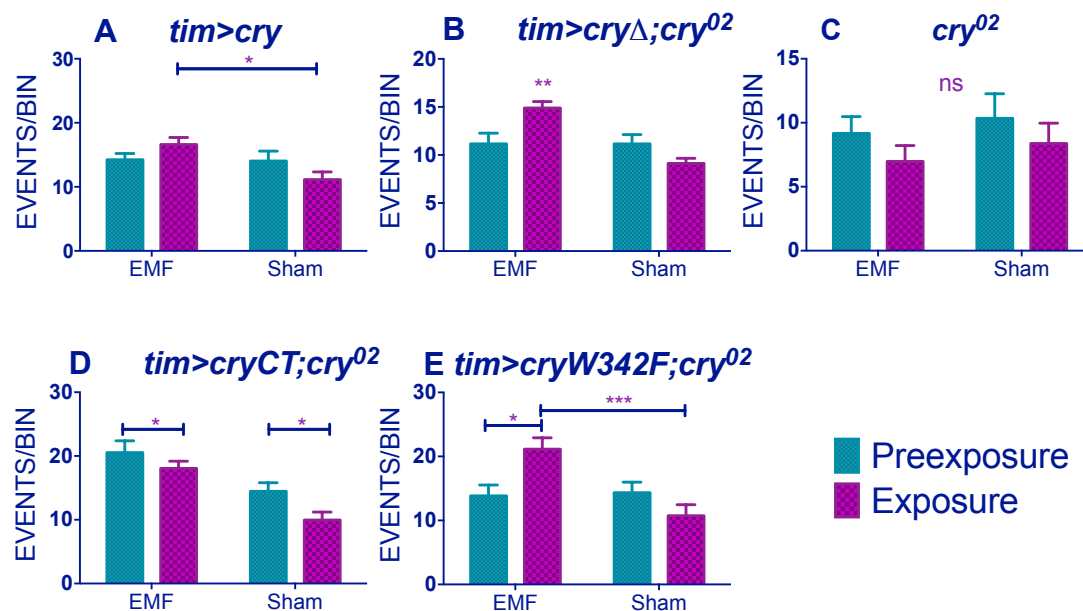


Figure 3-6 EMF induced hyperactivity in *cry* variants.

(A) *tim>cry* (B) *tim>cryΔ;cry02* (C) *cry02* (D) *tim>cryCT;cry02* (E) *tim>cryW342 F;cry02* N's are the same as in Figure 3-4. Mean \pm sem. (see Table 9-4, post-hoc * $p < 0.05$, ** $p < 0.01$, *** $p < 0.001$). Adapted from Fedele *et al.*, 2014.

3.3.4 HCRY AND MAGNETORECEPTION

Flies expressing vertebrate non-photoreceptor *hCRY2* are reported to exhibit light-dependent magnetoreception in a conditioning assay (Foley, Gegear & Reppert, 2011). By separately expressing *tim-GAL4> hCRY1* or *hCRY2* on a *cry02* background, I observed no significant differences in period between exposed and sham flies (Figure 3-7A, B, Table 9-3). Indeed, the *hCRY1/2* flies behaved as if they did not respond to

dim blue LL because their circadian period did not lengthen in LL compared to DD (Figure 3-7C), although hCRY proteins have been shown to be light degraded in flies (Hoang *et al.*, 2008) and *hCRY2* has been implicated in mediating EMF response in a light dependent manner (Foley *et al.*, 2011). Nevertheless and somewhat surprisingly, flies expressing *hCRY2* but not *hCRY1* showed the EMF-induced hyperactivity phenotype (*hCRY2* pre-exposure x sham interaction $F_{(1,54)} = 5.69$ $p < 0.05$, Figure 3-7D, E, Table 9-4).

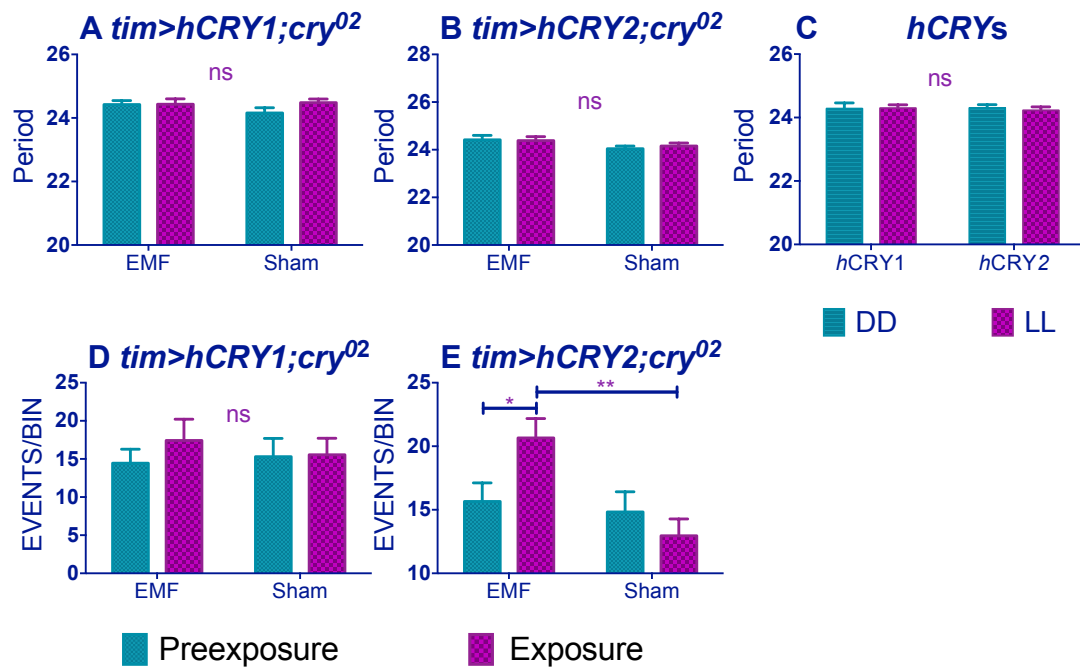


Figure 3-7 *hCRYs*.

(A) *tim>hCRY1; cry⁰²* or (B) *tim>hCRY2; cry⁰²* transformants do not show period shortening under EMF (pre-exposure*EMF/sham interaction *hCRY1* $F_{(1,48)}=1.41$, $p=0.3$ *hCRY2* $F_{(1,54)}=0.2$, $p=0.63$ (see Table 9-3). (C) *hCRY1/2* flies do not show period increase in dim blue LL compared to DD ($F_{(1,82)}=0.125$, $p = 0.72$) (D) *hCRY1* are not hyperactive under EMF ($F_{(1,48)}=0.33$, $p=0.56$). (E) *hCRY2* are hyperactive under EMF exposure. Mean \pm sem (see Table 9-4, post hoc * = $p < 0.05$, ** = $p < 0.01$). Adapted from Fedele *et al.*, 2014.

3.3.5 DROSOPHILA CRY IS STABILISED BY EMF

Western analysis revealed, that levels of CRY in DD were significantly elevated compared to sham in dim blue light as expected (Emery *et al.*, 1998), but I also observed that under EMF exposure, CRY was significantly more abundant compared to sham ($p < 0.001$, Figure 3-8A-B). EMF therefore appears to reduce CRY degradation,

which in turn would suggest that CRY signalling is compromised. Similarly, I quantified the expression of CRY using a CRY-LUC construct which expression is driven by *tim* promoter, in a *cry*⁰² background. Again the levels of luciferase were significantly higher in flies under EMF compared to Sham ($p < 0.05$, Figure 3-8C).

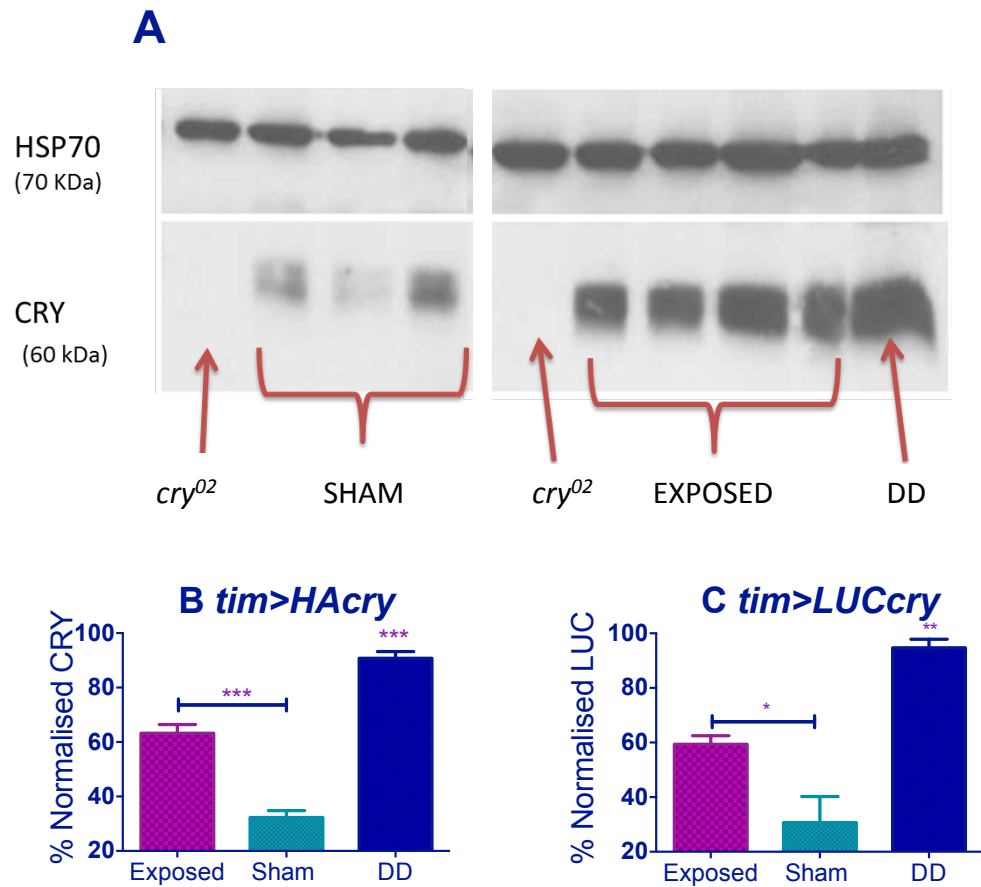


Figure 3-8 Exposure to EMF increased CRY stability.

[A] Western blots for CRY using anti-dCRY in wild-type flies exposed to EMF or sham in dim blue LL with *cry*⁰² and DD control. HSP is used as loading control. [B]. Quantification based on 3 biological replicates each with 3 technical replicates (repeated measures ANOVA $F_{(2,6)}=113.1$, $p < 0.001$, *post hoc* *** $p < 0.001$). [C] Luciferase assay, quantification based on 3 biological replicates with 3 technical replicates (repeated measures ANOVA $F_{(2,6)}=27.87$, $p < 0.001$, *post hoc* *** $p < 0.001$) Mean \pm sem. Adapted from Fedele *et al.*, 2014.

3.3.6 CRY CONFORMATION AND CRY-PROTEINS INTERACTIONS

Intrigued by the results presented above, I performed some preliminary assays in order to investigate the biochemical effects of the EMF exposure on CRY. As a first

step, a partial- in solution- proteolysis has been performed on purified CRY during exposure to EMF. The idea behind this assay is to detect different protein conformations. The trypsin cleavage sites (K-T) become more available when CRY is light activated and opens the CT (Ozturk *et al.*, 2011; Vieira *et al.*, 2012; Czarna *et al.*, 2013). Albeit very preliminary, partial proteolysis revealed different cleavage sites in CRY exposed to EMF or Sham, supporting the idea of a different protein conformation that might explain the behavioural data (Figure 3-9). Interestingly, the cleavage profile under EMF resembles the profile under DD (only one additional band was observed). Unfortunately, Mass-Spec data are not yet available and further experiments will be performed in the future.

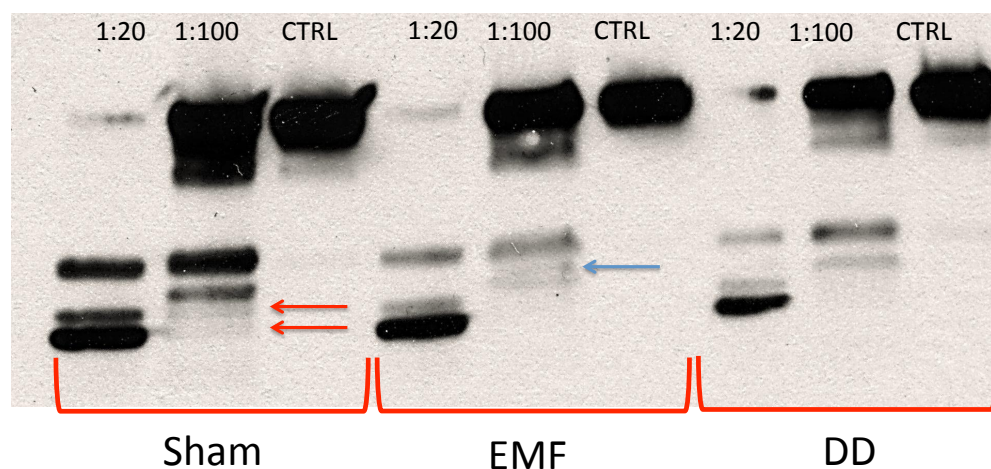


Figure 3-9 *In-vitro* partial proteolysis.

Purified CRY from *tim>HAcry* (See Material&Methods Section) was cleaved by trypsin at different concentration (1:20, 1:100 w/w and control). Red arrows indicate two cleaved band which are present only under Sham but not under EMF and DD. Blue arrow indicates an additional cleaved band present only under EMF. Immunoblotting performed with α CRY raised in guinea pig.

Moreover, I tried to identify possible CRY interactors under EMF exposure by Co-IP both with *tim>cry-CT;cry⁰²* and *tim>HAcry* (Figure 3-10). In both cases I observed different band patterns suggesting that under EMF conditions the binding affinity/interactions of CRY are changing, maybe due to protein conformational changes *per se*. Mass Spec will be performed in the future.

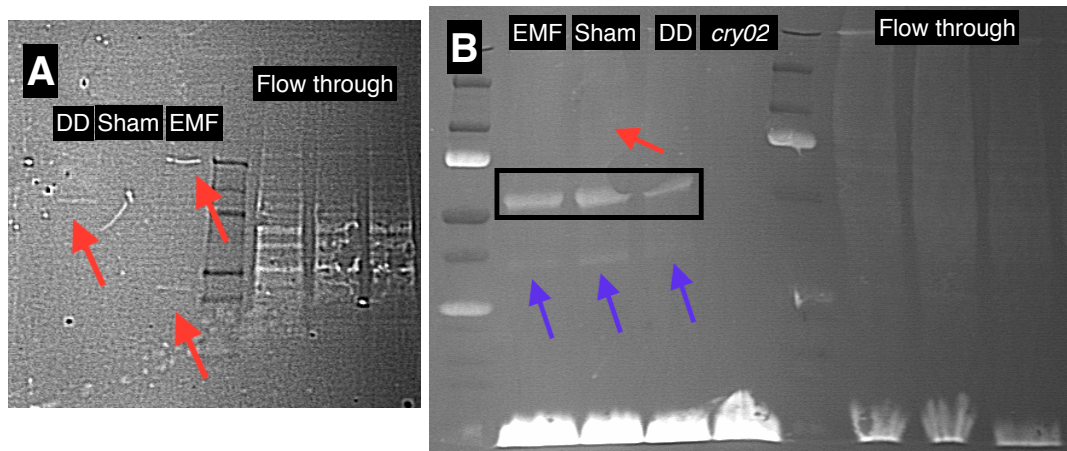


Figure 3-10 Co-IP .

A *tim>cryCT;cry⁰²* red arrows indicate bands present only in DD or under EMF exposure. B *tim>HAcry* red arrow indicates a band present only under Sham condition. Blue arrows indicate common bands present in all three conditions (EMF, Sham and DD). Boxed bands indicate CRY stained with anti-CRY antisera. *cry⁰²* flies was loaded as negative control.

3.4 DISCUSSION

I have identified two light-dependent and robust behavioural responses to EMF in the fly: shortening of circadian period and locomotor hyperactivity. My findings are consistent with an underlying CRY-dependent magneto-response and importantly confirm and extend the most relevant observation of Yoshii et al (2009), which was that overexpression of CRY in clock neurons enhances the circadian response to EMF. This was observed in two ways, by an increase in the proportion of rhythmicity under EMF in flies overexpressing CRY (80 v. 37%), as well as in the associated shortening of circadian period between sham- and EMF-exposed conditions. However these results contrast sharply with those of Yoshii et al., who observed a significant decrease in the proportion of rhythmic CRY-overexpressing flies under EMF and a predominant lengthening of period. While both sets of results indirectly support the RP hypothesis (Ritz et al., 2000), it is unlikely that these differences are solely due to the considerably more controlled EMF environment generated by the Schuderer apparatus.

This contradiction may be resolved by considering the action spectrum of CRY (Berndt et al., 2007; Hoang et al., 2008) and the ‘antagonistic effect’ of the magnetic field in response to light (Phillips, Muheim & Jorge, 2010b; Nießner et al., 2013). Under this proposal, the alignment of the magnetic field would produce inverse or

complementary responses under different wavelengths and is dependent on the initial ratio of singlet-triplet states of the radical. This antagonistic effect of wavelength was observed in flies, which under green light (500 nm) showed a 90°shift in their alignment compared to flies tested under violet light (365 nm) (Phillips & Sayeed, 1993). This has also been proposed to explain why in the EMF conditioning experiments of Gegear *et al.* (2008), flies failed to exhibit a response to EMF under full spectrum light when wavelengths below 420 nm were filtered out (Phillips *et al.*, 2010b). As pointed out by Phillips and co-workers, this failure could be due to a change in the nature of the response rather than an inability of the flies to sense the field. Indeed, the response of naïve flies to EMF under full spectrum and full spectrum > 420 nm has opposite directions (Gegear *et al.*, 2008). Therefore, it is possible that the different wavelength used in this study (450nm, range 410-490 nm) allowed specific singlet-triplet inter-conversions that resulted in an opposite response compared to the previous work which was reported to be carried out in a very narrow 465-470 nm range (Yoshii *et al.*, 2009). In order to solve this contradiction, a preliminary experiment under green light (500 ± 20 nm) was performed with Canton-S flies. As predicted by the “antagonistic effect” model, under these longer wavelengths EMF-exposed flies exhibited a significant period lengthening compared to Preexposure and Sham-Exposed flies (EMF/Sham Exposure $F_{(1,141)} = 5.12$, $p < 0.05$ and pre-exposure/exposure $F_{(1,141)} = 8.77$, $p < 0.01$, Figure 3-11). It is worth noting however, that the overall effects although significant, are weaker compared to blue light (Figure 3-2A-E) and resemble the results obtained by Yoshii and coworkers (Yoshii *et al.*, 2009). Further experiments using wavelengths cut-off filters will be performed in the future in order to investigate the switch point.

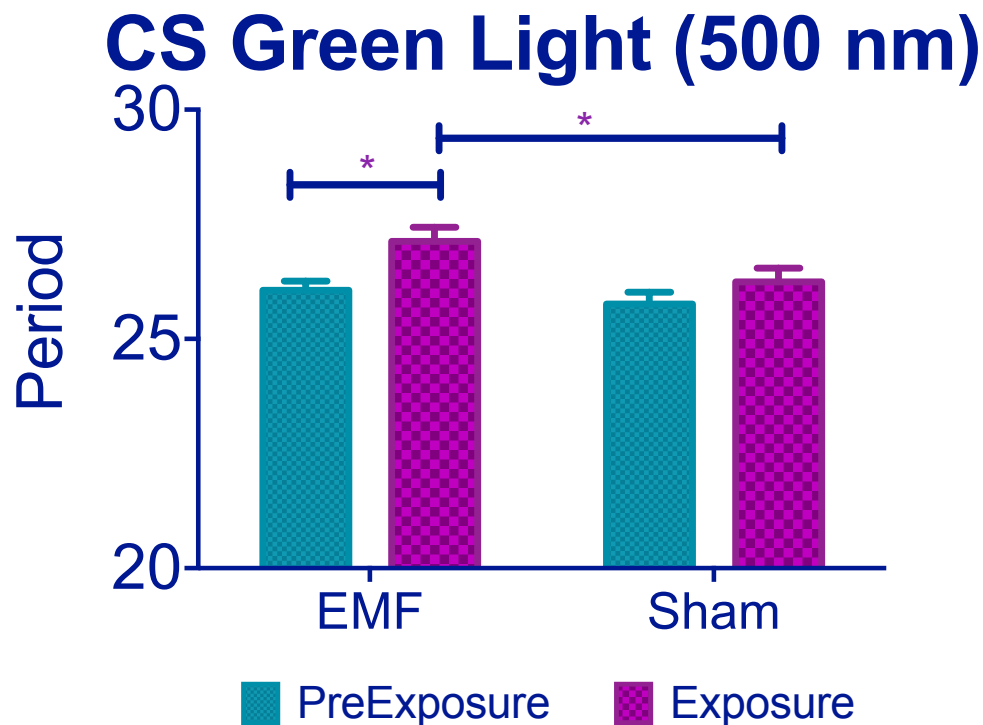


Figure 3-11 Exposure to green light lengthens the period under EMF.

CS flies kept under 500 nm show period lengthening when exposed to EMF compared to sham flies. (See Table 9-3, *post-hoc* * $p<0.05$, ** $p<0.001$). Mean \pm sem. Adapted from Fedele *et al.*, 2014.

Dim LL lengthens circadian period because activation of CRY alters PER and TIM dynamics, so that nuclear accumulation of these proteins is delayed in s-LNv pacemaker neurons, generating a longer period (Dissel *et al.*, 2004). The shortening of circadian period observed under EMF thus suggests a partial inactivation of CRY. This is supported by western blot analyses, which showed a more stable/abundant CRY under EMF. Upon light absorption, CRY undergoes conformational changes leading to its activation and ultimately to its degradation, which is mediated by E3-ubiquitin ligases (Emery *et al.*, 1998, 2000; Peschel *et al.*, 2009; Ozturk *et al.*, 2011, 2013b). Displacement of the CRY C-terminal tail (CT) induced by light may increase the binding affinity of CRY to its partners, generating more extended positively and negatively charged regions (Czarna *et al.*, 2013). Thus significantly more abundant CRY under EMF is likely to be due to CRY maintaining a more inactive conformation that

attenuates its light-mediated degradation and prevents period-lengthening (Vaidya *et al.*, 2013).

Interestingly, I observed a different cleavage pattern of purified CRY under EMF and Sham, casting a rationale for different protein conformational changes induced by light and EMF together therefore modifying CRY activity. In addition, a preliminary Co-IP assay revealed different binding interactors not yet identified. It is therefore possible that the “inactivation” of CRY under EMF could be induced both by conformational changes and by different binding affinities either with activators or inactivators of CRY. Recent work performed in my laboratory (Hares, 2013) aimed to study the function of a novel gene called *day* (darkness active in yeast), which seems to bind CRY in darkness preventing it from signalling. Although direct evidences of these physical interactions are still elusive, DAY becomes a suitable candidate to study how CRY behaves in the presence of EMF.

By using the CRY Δ construct, I was also able to decouple the phenotypic effects of EMF. The period-lengthening requires the C-terminus, whereas the hyperactivity can be mediated by the N-terminal sequences. Thus at least one of the two EMF-induced phenotypes is intact in either wild-type CRY or CRY Δ so if one accepts the RP model, it is difficult to postulate disruption to the Trp triad as a factor in EMF-mediated shortening of circadian period. Indeed the classical Trp cascade includes Trp residues W342, W397 and W420 that lie close to the FAD and are not included in the CRY Δ deletion that removes CRY residues 521-540 (Rosato *et al.*, 2001; Dissel *et al.*, 2004; Hemsley *et al.*, 2007). It has been recently suggested, however, that although the Trp triad is required for photoreduction of CRY (Berndt *et al.*, 2007; Czarna *et al.*, 2013) but see (Oztürk *et al.*, 2008; Ozturk *et al.*, 2013a; Vaidya *et al.*, 2013), the substitution of Cys523 could alter the photoreduction state of the FAD by Met421 and Cys337, possibly by producing a destabilising effect on the packing of the CT against the N-terminal (Czarna *et al.*, 2013). So it may be possible that by deleting the CT, the molecule, although functional, is destabilised and is not able to maintain the wild-type protein-protein interactions implicated in the period shortening.

It has also been shown that Trp536 originally thought to lie in close proximity to the FAD, if mutated along with Phe534 and Phe535, drastically reduces CRY stability (Czarna *et al.*, 2013). These residues are deleted in CRY Δ , which is less stable than CRY (Dissel *et al.*, 2004). Yet CRY Δ still responds to the EMF with hyperactivity but not with period shortening. My results therefore suggest a model in which these C-terminal residues are required to promote a more robust electron transfer (ET) that can mediate both EMF phenotypes. When they are ablated, the classic Trp triad is sufficient but not necessary to maintain the EMF-induced hyperactivity, because the results with the *cryW342F* mutant suggest that Trp342 is dispensable for both EMF phenotypes (as it is also for the conditioning EMF phenotype Gegear *et al.*, 2010). I cannot exclude the possibility that another residue such as tyrosine may complete the ET (Biskup *et al.*, 2013), or that a photolyase-like photocycle could be involved (Oztürk *et al.*, 2008; Ozturk *et al.*, 2011).

The importance of the CRY-CT for the EMF-induced acceleration of the circadian rhythm was further demonstrated by the GFP-CRY-CT fusion, which does not appear to contain an FAD binding site but it is still able to respond to light. The GFP-CRY-CT fusion was not able to restore the EMF-induced hyperactivity phenotype, again consistent with the role of the N-terminal region of CRY mediating that phenotype. A protein-protein interaction study is therefore required at this point to better understand the molecular function of the CT. Preliminary Co-IP revealed that the CT is interacting with different proteins under EMF and Sham. Once identified these interactors could provide more insights on how the EMF effects are translated in protein modifications and ultimately in behavioural changes.

CRY Δ binds to both PER and TIM in a light-independent manner (Rosato *et al.*, 2001; Dissel *et al.*, 2004), so the dimerization of these two negative clock regulators to CRY/CRY Δ is not sufficient for generating EMF-induced shortening of period, but it may be important for EMF-induced hyperactivity. Furthermore, of the two hCRYs, both of which have conserved N-terminals but diverged C-terminals compared to dCRY, hCRY2 was able to rescue the EMF-induced hyperactivity. At the primary sequence level, hCRY2 is marginally more similar to dCRY than hCRY1 (40.4% v 39.4%) in the N-terminal 500 residues, but whether this translates to more similarity in protein

structure, remains to be resolved (Czarna *et al.*, 2013). Although my observations are constant and robust, the actual mechanism through which the EMF can affect CRY is still unclear. Several different experiments need to be performed, in particular a protein interaction study with a protein-sequencing assay. Also, I suggest performing an *in vivo* Electron Paramagnetic Resonance (EPR) assay, which will be able, hopefully, to give more insights on the actual REDOX state of CRY under low frequency EMF. Additionally radio-frequency (RF) exposure is required as diagnostic test for the RPM (Henbest *et al.*, 2004; Ritz *et al.*, 2004, 2009; Vácha *et al.*, 2009; Engels *et al.*, 2014; Kirschvink, 2014), together with a well-defined frequency/intensity dose response.

4 GENETIC DISSECTION OF THE EMF-MEDIATED CIRCADIAN EFFECTS

4.1 INTRODUCTION

In the previous chapter, general effects of EMF-exposure on the clock were described. Flies exposed to EMF showed an overall period shortening and an increased hyperactivity. However, little is known about the anatomical structures responsible for these effects, as the mutants were tested only using *timGAL4* as the driver (*i.e.* expression in all the clock neurons). In this chapter, I will describe a brief genetic dissection of the phenotypes observed.

From an anatomical point of view, the clock neurons forming the “central pacemaker” in *Drosophila* are grouped according their position, but a more generalised division could be made based on their gene expression patterns. In particular, based on CRY expression, it is possible to group the neurons into CRY⁺ (CRY-positive, which are labelled with *cryGAL4*) (Stoleru *et al.*, 2007; Dissel *et al.*, 2014) or CRY⁻ (CRY-negative, partially labelled with *timGAL4,cryGAL80* driver) cells (Stoleru *et al.*, 2007; Dissel *et al.*, 2014). Within the CRY⁺ cells, however, some distinctions need to be made according to the function of individual neuronal clusters based on the expression of the neuropeptide PDF (Ozkaya & Rosato, 2012; Dissel *et al.*, 2014). I therefore focused my attention in evaluating the role of PDF-expressing cells to establish whether or not they might have different responses EMFs. In addition to this genetic dissection, I also altered the molecular properties of the circadian network using the bacterial depolarization-activating sodium channel (NaCHBac) (Nitabach *et al.*, 2006) and overexpressing the kinase SHAGGY, SGG a homologue of GSK-3 (Martinek *et al.*, 2001; Stoleru *et al.*, 2007).

Additionally, it has been demonstrated in other organisms that external structures, other than the brain, are important for detecting EMFs. In particular, in *Danaus plexippus* the antennae play a crucial role (Guerra, Gegear & Reppert, 2014). Ablation of one antenna only is sufficient to disorient the butterfly (Guerra *et al.*, 2014). Similarly, magnetite clusters have been found to be abundant in the antennae of hymenoptera (bees, ants and *Nasonia vitripennis* –Fedele G unpublished)(Acosta-Avalos *et al.*, 1999; Lucano *et al.*, 2006; de Oliveira *et al.*, 2010). However, ablation of antennae in the American cockroach *Platypanopeta americana* does not affect the response to EMF (Vácha, Půžová & Drštka, 2008). I therefore tested whether antennae in *Drosophila* could represent magnetoreceptors by expressing CRY in Johnston's Organ (JO) a collection of sensory cells involved in detecting gravity, vibrations and hearing (Sun *et al.*, 2009). Moreover, I also focused my attention to the eyes, that are responsible for oriented flight in migratory birds such as European robins (*Erythacus rubecula*)(Nießner *et al.*, 2013) and pigeons (*Columba livia*)(Stappert *et al.*, 2010). In addition to specific eye-drivers (*gmr>GAL4* and *R7>GAL4*), used to express CRY only in the compound eyes, the loss-of-function allele *glass^{60J}* mutant - homozygous flies are devoid of ocelli and all photoreceptor cells (Helfrich-Förster *et al.*, 2001)- was also tested in order to verify the contribution of functional eyes to the observed EMF phenotype.

4.2 MATERIAL AND METHODS

1.1.1. FLY STOCKS

Flies were raised at 25 °C on standard yeast-maize medium under a light-dark (LD 12:12) cycle. All strains, mutants, GAL4 and UAS transgenes were backcrossed into a *w¹¹¹⁸* background for 5-7 generations. *timGAL4*, *UAScry24b* (Emery *et al.*, 1998); *cry₁₃GAL4* (hereafter called *cryGAL4*) and *PdfGAL4* (Stoleru *et al.*, 2007); *Clk9mGAL4* (Kaneko *et al.*, 2012); *gmrGAL4* (Damulewicz, Rosato & Pyza, 2013); *R7GAL4* (Mollereau *et al.*, 2000); *UASsgg* (Martinek *et al.*, 2001); *UASNChBac* (Nitabach *et al.*, 2006) and *glass^{60J}* (Helfrich-Förster *et al.*, 2001) have been described elsewhere. *painlessGAL4* (line R21B03) was obtained from the Bloomington Stock Center (Indiana, USA). Drivers

and reporters were further crossed into a *cry*⁰² background (Dolezelova, Dolezel & Hall, 2007), with the exclusion of *tim>sgg*, *tim>dbt* and *tim>NaChBac*. *cryGAL80_{2e3m}* (hereafter called *cryGAL80*) (Stoleru *et al.*, 2007) and *J015GAL4* (hereafter called *JOGAL4*) (Sharma *et al.*, 2000) were recombined into a *cry*⁰² background and validated by PCR. For the crossing schemes and primers used please refer to Chapter 2.

1.1.2. EMF EXPOSURE

EMF was set at 300 µT 3Hz for all the experiments using the same experimental set up described in Chapter 3.

4.3 RESULTS

1.1.3. EXPRESSION OF CRY IN A SUBSET OF CRY⁺ CELLS RESCUES THE EMF PHENOTYPE.

Overexpression of CRY driven by the *cryGAL4* driver in a *cry*⁰² genetic background generated significant period shortening (pre-exposure X EMF/Sham exposure interaction $F_{(1,28)} = 7.95$, $p < 0.01$; EMF vs Sham $F_{(1,28)} = 5.57$, $p < 0.05$, Figure 4-1A) and enhanced hyperactivity (preexposure X EMF/Sham exposure interaction $F_{(1,28)} = 7.96$, $p < 0.01$; EMF vs Sham $F_{(1,28)} = 6.47$, $p < 0.05$, Figure 4-1B) when flies were exposed to EMF.

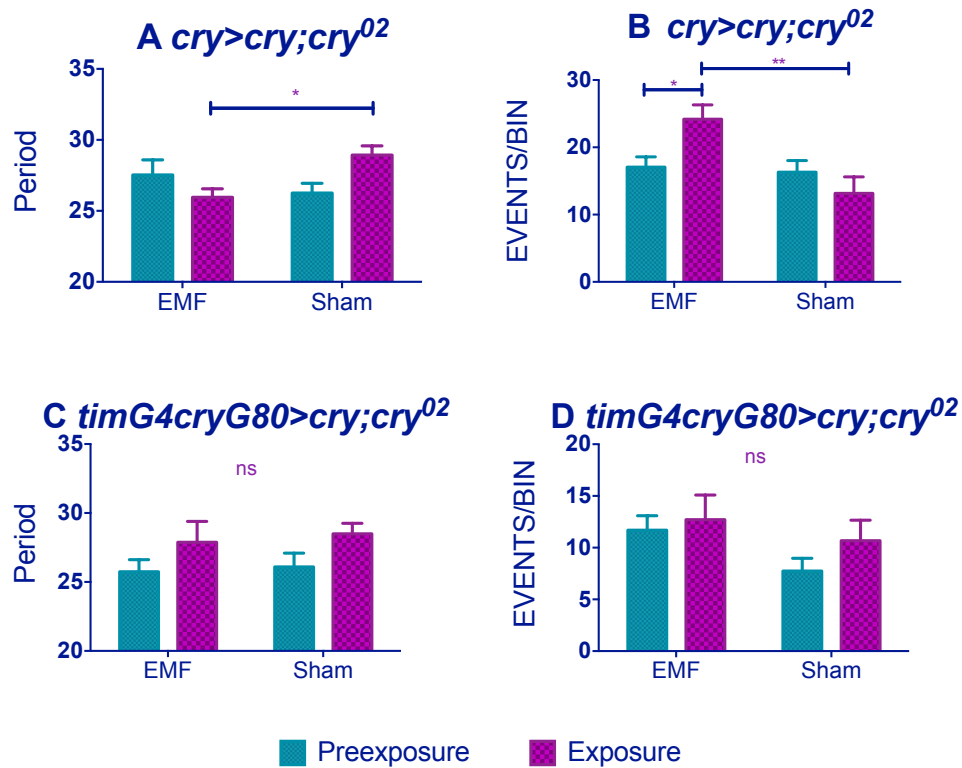


Figure 4-1 A-B Expression of CRY in CRY-positive cells restores EMF phenotypes.

A. Mean circadian periods (h) \pm SEM are shown for the EMF and sham-exposed groups. B. Hyperactivity (events per bin) \pm SEM. C-D. Expression of CRY in CRY-negative cells does not rescue EMF responses. C. Mean circadian periods (h) \pm SEM are shown for the EMF and sham-exposed groups. For period and Ns see Table 9-3. D. Hyperactivity (events per bin) \pm SEM. For activity levels and Ns see Table 9-4. (post-hoc *p<0.05, **p<0.01, ***p<0.001).

timG4cryG80>cry; cry⁰² flies failed to respond to EMF both in terms of period (pre-exposure X EMF/Sham exposure $F_{(1,36)} = 0.01$, p= 0.91, Figure 4-1C) and hyperactivity (pre-exposure X EMF/Sham exposure $F_{(1,36)} = 0.29$, p= 0.58, Figure 4-1D).

When CRY-expression was restricted to the LN_vs (*Pdf>cry; cry⁰²*) no period shortening was observed (pre-exposure X EMF/Sham exposure $F_{(1,33)} = 1.48$, p= 0.23; Figure 4-2A) nor hyperactivity was observed (pre-exposure X EMF/Sham exposure $F_{(1,33)} = 1.67$, p= 0.20; Figure 4-2B).

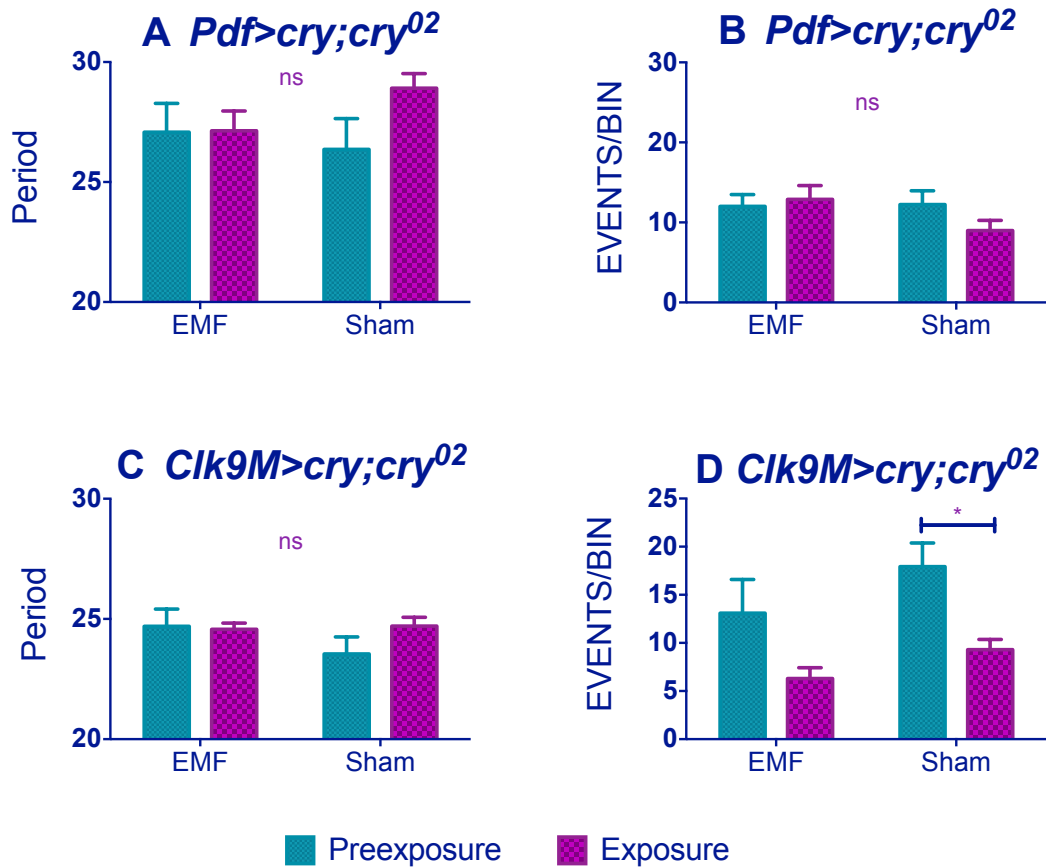


Figure 4-2 *Pdf>cry;cry⁰²* and *Clk9M>cry;cry⁰²* flies failed to respond to EMF.

A Mean circadian periods (h) \pm SEM are shown for the EMF and sham-exposed groups. B Hyperactivity (Events of activity/ Bins) \pm SEM. C-D Expression of CRY DN₂s and s-L_NVs is not sufficient to trigger the response. C. Mean circadian periods (h) \pm SEM are shown for the EMF and sham-exposed groups. D Hyperactivity (Events of activity/ Bins) \pm SEM. For period and Ns see Table 9-3. For activity levels and Ns see Table 9-4. (post-hoc *p<0.05, **p<0.01, ***p<0.001).

Similarly, expression of CRY in dorsal neurons (*Clk9M>cry;cry⁰²*) was not sufficient to rescue the EMF phenotype (pre-exposure X EMF/Sham exposure $F_{(1,32)} = 1.43$, p= 0.24, Figure 4-2C) nor the hyperactivity (pre-exposure X EMF/Sham exposure $F_{(1,32)} = 0.16$, p= 0.69, Figure 4-2D). It is worth noting that this driver expresses only in the DN₂ and s-L_NVs neurons (Kaneko *et al.*, 2012), reinforcing my results that the small PDF⁺ neurons are not responsible for the EMF phenotype.

tim>cry;cry⁰² flies revealed the usual period shortening under EMF- compared to pre-exposed and Sham-exposed flies (preexposure X EMF/Sham exposure $F_{(1,21)} = 7.74$, p<0.05; EMF vs Sham $F_{(1,21)} = 4.66$, p< 0.05, Figure 4-3A) and a significant rescue

of rhythmicity levels ($\chi^2_{(1,32)} = 4.57$, $p<0.05$, Figure 4-3B). Hyperactivity was also observed (2 way ANOVA preexposure X EMF/Sham exposure $F_{(1,21)} = 6.29$, $p<0.05$; EMF vs Sham $F_{(1,21)} = 5.84$, $p<0.05$, Figure 4-3C).

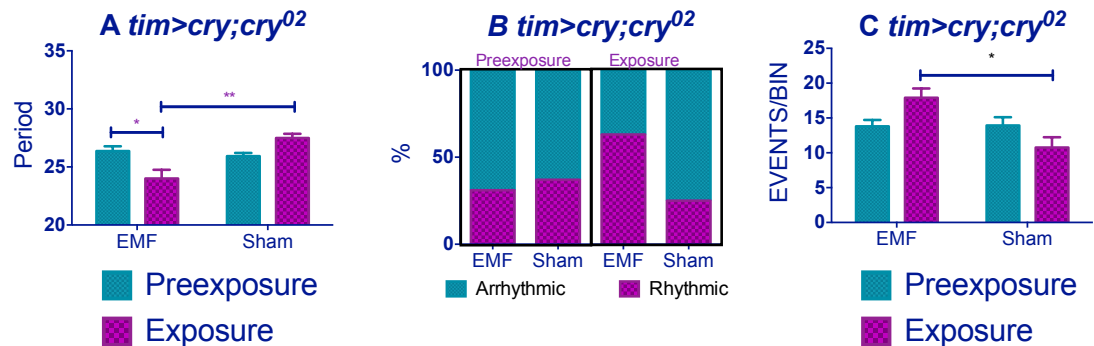


Figure 4-3 Control using *timGAL4*.

A. Mean circadian periods (h) \pm SEM are shown for the EMF and sham-exposed groups. For period and Ns see Table 9-3. B. Rescue of rhythmicity levels. C. Hyperactivity (Events of activity/ Bins) \pm SEM. For activity levels and Ns see Table 9-4. (post-hoc * $p<0.05$, ** $p<0.01$, *** $p<0.001$).

1.1.4. MANIPULATING THE CLOCK AND EMF

Expression of the neuronal activator NaChBac resulted in completely arrhythmic flies throughout the whole experiment (preexposure and exposure) as a consequence of elevated neuronal firing within the circadian network (data not shown). Similar arrhythmia has been observed in *tim>NaChBac* flies tested under total darkness (Dissel *et al.*, 2014).

The kinase SGG has been observed to stabilise CRY under LL conditions resulting in ~50% rhythmicity rather than the arrhythmicity usually observed under LL (Stoleru *et al.*, 2007). However, under my conditions of dim blue light, the majority of the flies were arrhythmic under pre-exposure conditions. For the rhythmic flies, no period differences were observed (pre-exposure X EMF/Sham exposure $F_{(1,22)} = 0.98$, $p=0.33$, Figure 4-4A). Activity levels were significantly decreased in Sham conditions while under EMF the levels remained similar to preexposure (pre-exposure X EMF/Sham exposure $F_{(1,22)} = 6.73$, $p<0.05$; EMF vs Sham $F_{(1,22)} = 5.25$, $p<0.05$, Figure 4-4).

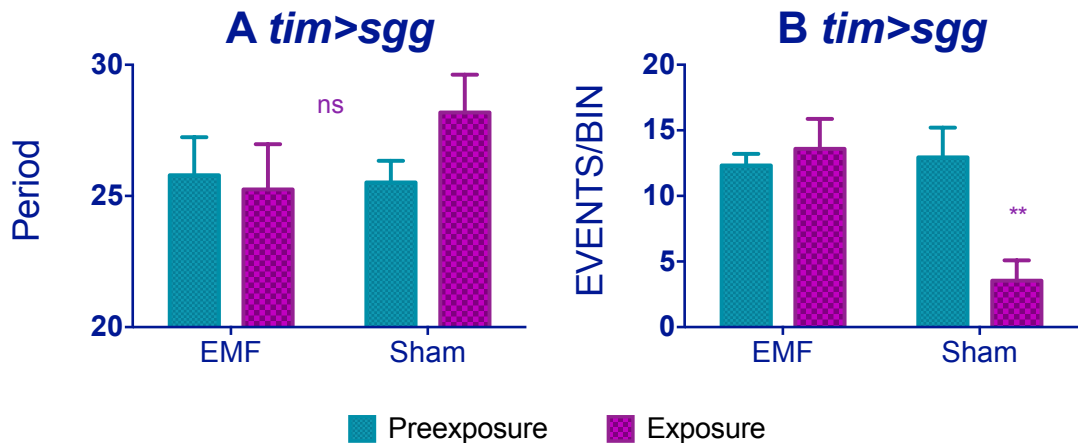


Figure 4-4 Overexpression of SGG does not show an EMF effect.

A Mean circadian periods (h) \pm SEM are shown for the EMF and sham-exposed groups. For period and Ns see Table 9-3. B Hyperactivity (Events of activity/ Bins) \pm SEM. For activity levels and Ns see Table 9-4. (*post-hoc* * $p<0.05$, ** $p<0.01$, *** $p<0.001$).

1.1.5. EYES AND ANTENNAE AS PUTATIVE STRUCTURES FOR MAGNETORECEPTION

I overexpressed CRY in the eyes using *gmrGAL4* and *R7GAL4* and subsequently in the antennae, with *painGAL4* and *JO15GAL4* in *cry*-null mutants. I observed that the eyes contributed to the EMF induced period-shortening, (*gmr>cry;cry*⁰² preexposure X EMF/Sham exposure $F_{(1,29)}=5.61$, $p<0.05$, Figure 4-5A) and to the associated hyperactivity (preexposure X EMF/Sham exposure $F_{(1,29)} =4.63$, $p<0.05$; EMF vs Sham $F_{(1,29)}=4.88$, $p<0.05$, Figure 4-5B).

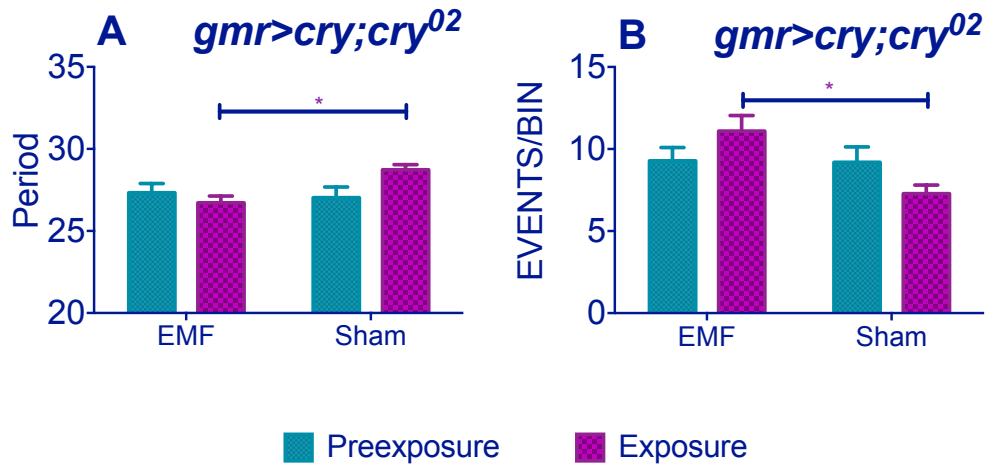


Figure 4-5 *gmrGAL4* driven CRY expression is sufficient to rescue EMF effects.

A Mean circadian periods (h) \pm SEM are shown for the EMF and sham-exposed groups. For period and Ns see Table 9-3. B. Hyperactivity (Events of activity/ Bins) \pm SEM. For activity levels and Ns Table 9-4. (*post-hoc* *p<0.05, **p<0.01, ***p<0.001).

When the expression of CRY was restricted to the R7 rhabdomeres (*R7GAL4*), (Phillips, Jorge & Muheim, 2010a), flies exhibited period shortening (preexposure X EMF/Sham exposure $F_{(1,105)} = 5.01$, p<0.05, Figure 4-6A) but no significant hyperactivity (preexposure X EMF/Sham exposure $F_{(1,105)} = 0.02$, p= 0.87; EMF vs Sham $F_{(1,105)} = 0.14$, p=0.7 but pre- vs exposure $F_{(1,105)} = 9.8$, p<0.01, Figure 4-6B).

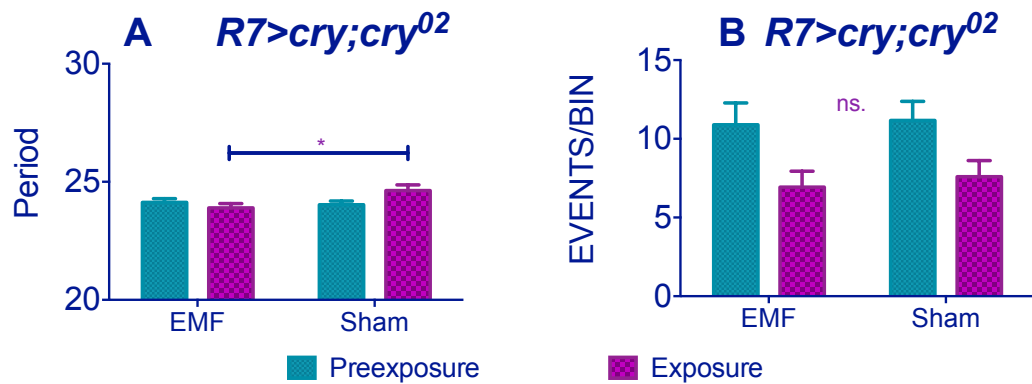


Figure 4-6 R7 rhabdomeres mediate EMF effects.

A. Mean circadian periods (h) \pm SEM are shown for the EMF and sham-exposed groups. For period and Ns see Table 9-4. B. Hyperactivity (Events of activity/ Bins) \pm SEM. For activity levels and Ns see Table 9-3. (*post-hoc* *p<0.05, **p<0.01, ***p<0.001).

In addition, *glass*^{60j} mutants showed a significant period shortening under EMF (preexposure X EMF/Sham exposure interaction $F_{(1,35)} = 5.34$, $p < 0.05$; EMF vs Sham $F_{(1,35)} = 19.40$, $p < 0.001$, Figure 4-7A) and hyperactivity (preexposure X EMF/Sham exposure $F_{(1,35)} = 4.71$, $p < 0.05$; EMF vs Sham $F_{(1,35)} = 4.22$, $p < 0.05$, Figure 4-7B) suggesting that rhodopsin may not play a role in EMF-mediated phenotypes.

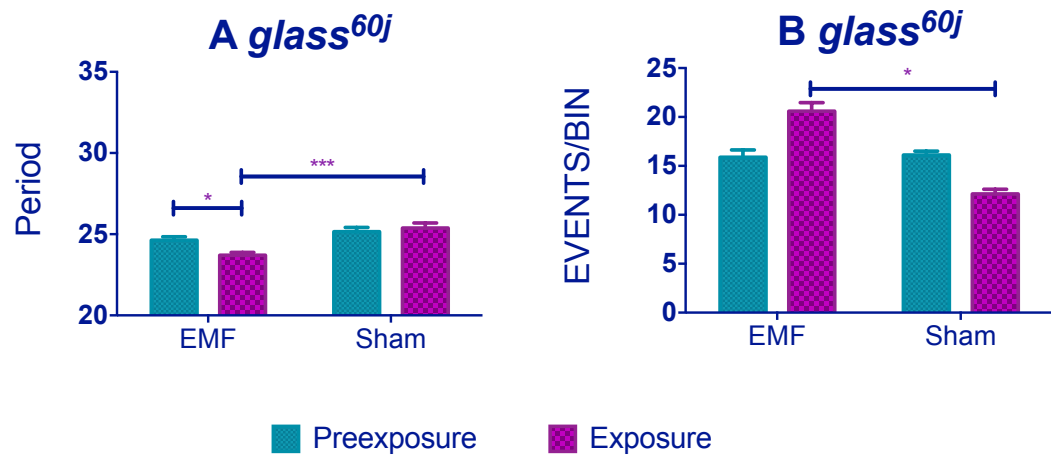


Figure 4-7 *glass* mutants can respond to EMFs.

A Mean circadian periods (h) \pm SEM are shown for the EMF and sham-exposed groups. For period and Ns see Table 9-3. B Hyperactivity (Events of activity/ Bins) \pm SEM. For activity levels and Ns see Table 9-4. (*post-hoc* * $p < 0.05$, ** $p < 0.01$, *** $p < 0.001$).

Expression of CRY in the JO was sufficient to rescue at least the period-shortening effects (*pain>cry;cry*⁰²): preexposure X EMF/Sham exposure $F_{(1,62)} = 4.5$, $p < 0.05$, EMF vs Sham $F_{(1,62)} = 6.81$, $p < 0.01$, Figure 4-8A; Activity levels, preexposure X EMF/Sham exposure $F_{(1,62)} = 0.08$, $p < 0.77$, EMF vs Sham $F_{(1,62)} = 3.09$, $p = 0.08$, Figure 4-8B).

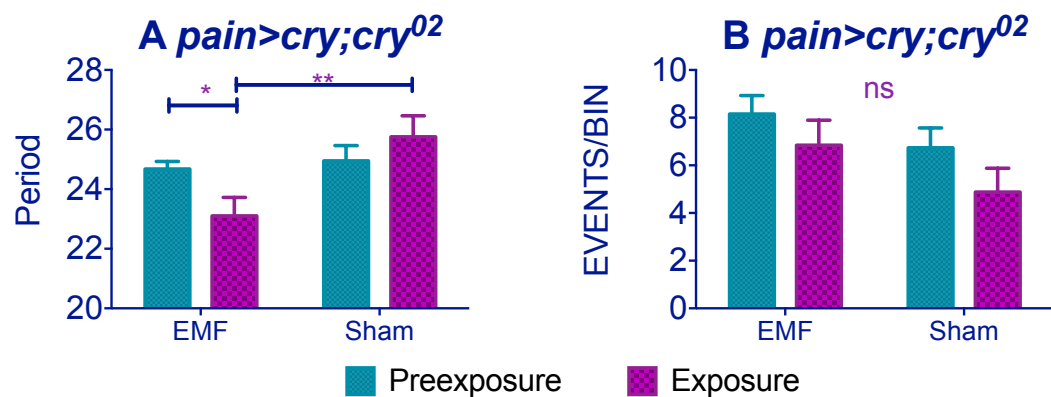


Figure 4-8 CRY in the antennae rescues the period shortening but not the hyperactivity.

A Mean circadian periods (h) \pm SEM are shown for the EMF and sham-exposed groups. For period and Ns see Table 9-3. B Hyperactivity (Events of activity/ Bins) \pm SEM. For activity levels and Ns see Table 9-4. (post-hoc *p<0.05, **p<0.01, ***p<0.001). B.

JO>cry;cry⁰² flies however, showed a weak EMF response (pre-exposure X EMF/Sham exposure $F_{(1,20)} = 2.59$, p= 0.12; EMF vs Sham $F_{(1,20)} = 12.01$, p<0.01, Figure 4-9A). During the exposure days both groups exhibited period lengthening, however in EMF exposed flies this was not significantly different from pre-exposed flies but still significantly shorter compared to Sham-exposed. No hyperactivity was observed (preexposure X EMF/Sham exposure $F_{(1,20)} = 0.24$, p=0.6, Figure 4-9B).

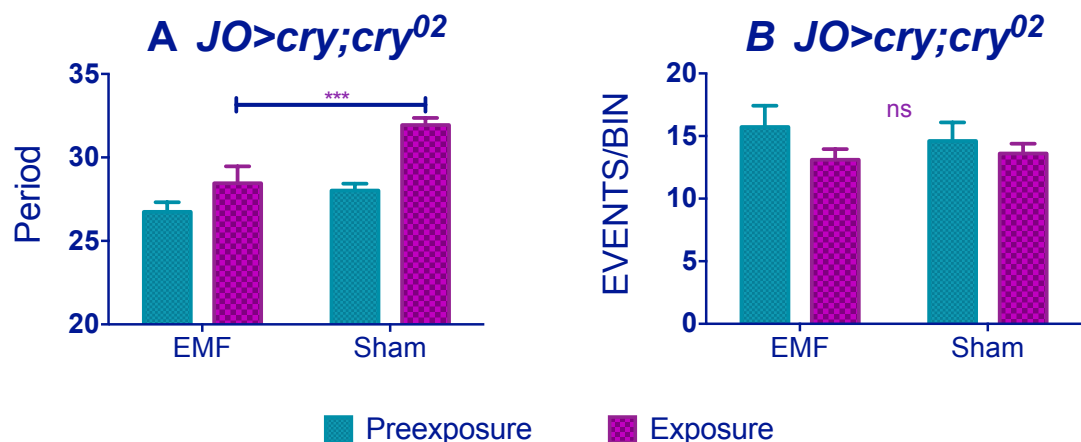


Figure 4-9 *JOGAL4* weakly rescues EMF-induced period shortening.

A Mean circadian periods (h) \pm SEM are shown for the EMF and sham-exposed groups. For period and Ns see Table 9-3. B Hyperactivity (Events of activity/ Bins) \pm SEM. For activity levels and Ns see Table 9-4. (post-hoc *p<0.05, **p<0.01, ***p<0.001).

4.4 DISCUSSION

In this chapter I have attempted to anatomically dissect the EMF locomotor phenotype. I observed that a general ectopic expression of CRY is not sufficient to trigger an EMF response. In contrast I found that only a few clock neurons retain the ability to be magneto-sensitive, perhaps the three CRY⁺ LN_ds and the 5th s-LN_v. This observation is perhaps not surprising since the magnetic field effects I observe strongly depend on the ability of the flies to retain rhythmicity under dim light conditions, that has been suggested to be a property of these cells under these lighting

conditions (Rieger *et al.*, 2009). I also observed that the expression of CRY using the *Pdf*-promoter did not trigger the EMF response, indicating that the PDF⁺ neurons might not be involved.

However, although I can exclude the s-LN_Vs (see results with *Clk9MGAL4*), I cannot rule out that the large PDF expressing cells, the I-LN_Vs are not playing a role. The PDF-expressing cells are an heterogeneous cluster of neurons: the s-LN_Vs express the PDF receptor (PDFR) at high levels whereas the large LN_Vs express it very weakly (Im & Taghert, 2010). Consequently the neuronal activation induced by CRY (Fogle *et al.*, 2011; Dissel *et al.*, 2014) together with PDF, may strongly inhibit the dorsal cells *via* activation of the CRY⁺ LN_Ds, which express the highest levels of PDFR, and this would result in period lengthening (Dissel *et al.*, 2014). For an account of how this would work via de-repression of the s-LN_Vs endogenously longer period by the inhibition of the DNs please see the recent paper by Dissel et al (2014). The PDF-induced neuronal activation could however amplify this repression by feeding back into the small neurons (expressing PDFR) and activating them even more. On the other hand the I-LN_Vs send projections to a distant layer of medulla of the optic lobe (Im & Taghert, 2010) and their activation will be restricted to the expression of CRY (together with the endogenous PDF). This organization could therefore lead to activation disequilibrium between small and large PDF⁺ cells masking any effects that are occurring in the large PDF-expressing cells only. Additionally, the fact that the eyes are capable of triggering the response could be further evidence suggesting the I-LN_Vs as important cells. Further experiments using different (not yet available drivers such as a *PDFRGAL80*) are therefore required.

I also observed that expression of CRY in the eyes and antennae is sufficient to trigger an EMF response, supporting findings from different species showing the importance of these structures in magnetoreception (Stapput *et al.*, 2010; Guerra *et al.*, 2014). However, the neuronal circuit underlying these responsive still remains to be analysed. I can speculate that probably the large PDF-expressing cells could be involved (see above) together with some CRY⁺ dorsal neurons (labelled with *gmrGAL4*). Additionally, *glass*^{60J} does not compromise the response to the magnetic field in either of my phenotypes. Mutation in the transcription factor *glass* results in the absence of

at least all external photoreceptor pigments (Helfrich-Förster *et al.*, 2001), in particular flies homozygous for the loss-of-function allele *glass*^{60J} are devoid of ocelli and all photoreceptor retinal cells plus the primary and secondary pigment cells in the compound eye (Lindsley & Zimm, 1992) but retain a functional CRY (Helfrich-Förster *et al.*, 2001)

R7y rhabdomeres together with R8y cells have been implicated in the detection EMFs in *Musca domestica* and *Calliphora vicina* (Phillips *et al.*, 2010a) and consequently rhodopsins were also proposed as suitable candidates for magnetoreception, acting in concert with CRY (Stoneham *et al.*, 2012). The proposed model suggests that a light-excited S radical pair may decay to form long-lived T radicals that can be achieved through a charge transfer to a Tyr residue. The electric field resulting from a population of T dipoles in the retina, might be sufficient to trigger the photoisomeration of 11-cis-retinal (or 11-cis 3-hydroxyretinal in *Drosophila*) (Tian *et al.*, 2012) to all-trans-retinal therefore providing a visual information of the field (Stoneham *et al.*, 2012) and ultimately a sense of direction. In my circadian assay, however, it is not possible to test whether or not rhodopsins are required for compass information, but I can confirm that they are not necessary for triggering my EMF period-shortening response.

Nevertheless, I can speculate that under green light conditions the observed “antagonistic” effect (Phillips & Sayeed, 1992; Phillips *et al.*, 2010a) could be partially mediated by the activation of different photoreceptors cells resulting in different neuronal outputs. Anatomical orientation of the microvilli in R7 and R8 rhabdomeres is orthogonal (Phillips, Muheim & Jorge, 2010b). Therefore, activation of one group of cells only will trigger a directional response in reflecting the orientation of the microvilli (Phillips *et al.*, 2010b). A way to test this model might be to restrict the expression of rhodopsin and CRY either to the R7y or R8y rhabdomeres and test the flies for their orientation behaviour (Dommer *et al.*, 2008; Gegear *et al.*, 2008, 2010; Foley, Gegear & Reppert, 2011; Painter *et al.*, 2013). This could be achieved by reintroducing the retinal isomerase *ninaB* (Voolstra *et al.*, 2010) only in those cells together with CRY and testing for orientation preferences (eg *ninaB*¹*cry*⁰² double mutants expressing *ninaB* driven by *actinGAL4;Rh1GAL80* and *cry* by *R7/R8LexA* would

reintroduce functional rhodopsins and CRY only in R8/R7 cells). If my suggestion is correct I could confirm a possible CRY-dependent isomerization of rhodopsins, which might be EMF-sensitive (S-T ratio mixing) and ultimately leading to opposing directional responses. In general, the expression of CRY in external structures is not sufficient to trigger hyperactivity, suggesting that the two EMF phenotypes are not interdependent but may require different neuronal networks.

In conclusion, this brief and preliminary genetic dissection of the circadian effects due to EMF exposure further suggests the importance of CRY in mediating these responses. However, the expression of CRY alone is not sufficient to rescue the response, implying that tissue specific protein-protein interactions with yet unidentified partners must be occurring. As discussed in the previous chapter, the binding pattern of CRY under EMF-exposure differs substantially from Sham-exposed flies; these differences could be due to a conformational change of CRY under an EMF which allows the protein to change its interacting partners or to other EMF-sensitive/light-sensitive proteins acting in concert with CRY. Deep protein sequencing is therefore required to identify putative candidates, along with a full structural analysis of CRY under such conditions (*in vivo* EPR?). Alternatively, it is conceivable that the absence of EMF responses due to specific localised expression of CRY, could be a masking effect due to altered organization of the circadian neuronal circuit (Dissel *et al.*, 2014).

5 NOVEL EMF PHENOTYPE: EMF EXPOSURE DISRUPTS NEGATIVE GEOTAXIS

The majority of the data and part of the text presented in this chapter have been adapted from Fedele *et al.*, 2014.

5.1 INTRODUCTION

Due to the very low throughput of the Schuderer apparatus (only 1 Trikinetics Monitor/Experiment could be loaded every ~3 weeks), a faster and equally reliable assay for studying EMF effects in *Drosophila* needed to be developed.

Negative geotaxis in flies (their ability to climb against gravity) has been studied by both traditional quantitative genetic and modern genomic methods (Toma *et al.*, 2002). Artificial selection for flies that show high and low levels of geotaxis has been allied to transcriptomic analyses to reveal that CRY may play a significant role in this phenotype (Toma *et al.*, 2002) and CRY's role in fly climbing behaviour has recently been confirmed (Rakshit & Giebultowicz, 2013), although the actual pathway is still unknown. I therefore suspected that this phenotype could be wavelength dependent and if so, applying an EMF might compromise it. I show here that negative geotaxis provides a reliable method for studying behavioural responses to EMFs.

5.2 MATERIAL AND METHODS

5.2.1 FLY STRAIN

Flies were maintained in LD 12:12 at 25°C. Canton-S (CS) flies, *cry*⁰² and all *gal4* drivers and mutants were backcrossed into a *w¹¹¹⁸* background for up to 7 generations. All the strains were described in Chapter 2.

5.2.2 BEHAVIOURAL APPARATUS

An EMF delivery system was described in the Materials and Methods section. Ten, 2-3 day old males were placed in a plastic vial and tapped to the bottom by means of a custom-made ‘swinger’ that allowed three vials to be tapped to the bottom simultaneously with exactly equal force. An infra-red webcam (Logitech) was used to film the flies. Flies that were able to reach a vertical height of 15 cm in 15s were counted as ‘climbers’ and each tube was tested 10 times, with 30s between each of the first 5 trials, then after a 15 min rest, another 5 trials were performed. The static EMF (500 μ T) or sham was applied at random after every group of 10 trials. Each set of 10 trials on the swinger ran three different genotypes simultaneously in the three tubes. Experiments were run at 25°C either in dim blue (450 nm, 40 nm range) or dim red light (635nm, 20 nm range) using LEDs with an intensity at the surface of the vials of 0.25 μ Wcm⁻². Three biological replicates were used for each genotype and data was analysed using a multifactorial ANOVA with repeated measures (RM ANOVA). All statistical analyses in this study were performed using GraphPad Prism, (GraphPad Software, La Jolla California)

5.3 RESULTS

Climbing ability was measured as the percentage of flies that could climb 15 cm in 15 s at different wavelengths under EMF or sham exposure. Interestingly, under blue-light (450 nm), the proportion of wild-type Canton-S sham ‘climbers’ is significantly higher than in corresponding EMF exposed flies (*a posteriori* p=0.0004; Figure 5-1A), whereas in red-light (635 nm) and in *cry*⁰² flies climbing is substantially and equally suppressed under both sham and EMF exposure (RM ANOVA, Genotype F_(2,12)= 16.48, p= 0.00036, Exposure F_(1,12)=8.67, p 0.012, GXE interaction F_(2,12)=9.86, p=0.002), suggesting that negative geotaxis requires both blue-light activation and the presence of CRY (Toma *et al.*, 2002; Rakshit & Giebultowicz, 2013) and that this phenotype can be disrupted by a static EMF (Figure 5-1A).

Overexpression of CRY under different drivers on a *cry*⁰² background partially restored high levels of climbing in sham, which was significantly reduced in EMF

conditions, as in the wild-type, whereas *Pdf*⁰¹-mutants showed reduced climbing activity and consequently did not show any EMF reduction in their climbing score (RM ANOVA, Genotype $F_{(7,32)}=4.18$, $p= 0.002$, Exposure $F_{(1,32)}=32.8$, $p\approx 0$, GxE interaction $F_{(7,32)}=3.18$, $p=0.011$; Figure 5-1B). In particular, overexpression of CRY under *tim>GAL4* or *cry>GAL4* rescued the EMF phenotype to a level similar to CS (Figure 5-1B). However when CRY expression was restricted further by using the *Pdf>GAL4* driver which expresses in the LN_s subset of clock neurons (Dissel *et al.*, 2014), intermediate levels of climbing were observed which were not further disrupted under EMF (Figure 5-1B). A similar scenario prevailed when the *timGAL4;cryGAL80* combination was used to drive CRY expression predominantly in the dorsal neurons plus three normally CRY negative LN_ds (Dissel *et al.*, 2014), with again levels of climbing observed that were similar to those obtained with *tim>cry* and *cry>cry*, but no significant reduction of geotaxis under EMF. In contrast to these restricted patterns of CRY expression, *Mai*¹⁷⁹>*cry* that expresses in three CRY positive LN_d neurons (Yoshii *et al.*, 2008) generated intermediate levels of climbing which were nevertheless susceptible to an EMF. Consequently it appears that among the canonical clock neurons only when the LN_d clock cells are expressing CRY is there observed a robust EMF response, similar to the effects observed in the circadian assay (Chapter 4). As expected, *Pdf*⁰¹ flies showed no EMF response, their climbing levels were not different from *cry*⁰². *Pdf* is in fact responsible for negative geotaxis (Toma *et al.*, 2002).

As reported in the previous chapter, major peripheral tissues in the head, namely the eyes and antennae that normally express CRY, have been shown to contribute to EMF sensitivity. Specific rhodopsin promoters driving GAL4: *Rh5>cry*, *Rh6>cry* and *R7>cry*, were therefore tested. These drivers all restored normal levels of climbing to *cry*⁰² mutants that were significantly reduced under EMF (RM ANOVA, Genotype $F_{(8,36)}= 5.45$, $p=0.00016$, Exposure $F_{(1,36)}=99.4$, $p\approx 0$, GxE interaction $F_{(8,36)}=3.25$, $p=0.007$; Figure 5-1C) confirming a role of these structures in mediating EMF-effects. On the contrary, the *eyes-absent* mutant, *eya*², which has a complete absence of eyes, showed a significant reduction in climbing and no further reduction under EMF (Figure 5-1C).

Regarding the antennae, the same two antennal drivers used in the previous chapter were also tested for their climbing activity. *JO15>cry* and *Pain>cry* also rescued the sham/EMF response on a *cry⁰²* background (RM ANOVA, Genotype $F_{(8,36)}=5.45$, $p=0.00016$, Exposure $F_{(1,36)}=99.4$, $p\approx0$, GxE interaction $F_{(8,36)}=3.25$, $p=0.007$; Figure 5-1C), in spite of the fact that in *JO>cry*, the initial level of climbing was significantly reduced compared to CS ($p=0.0005$) and no higher than that of *eya²*. Furthermore, the *Antp^R* mutant significantly reduced the climbing score under sham, but did not reduce it further under EMF (Figure 5-1C). These results suggest that antennae also play significant roles in climbing and in the response to EMFs.

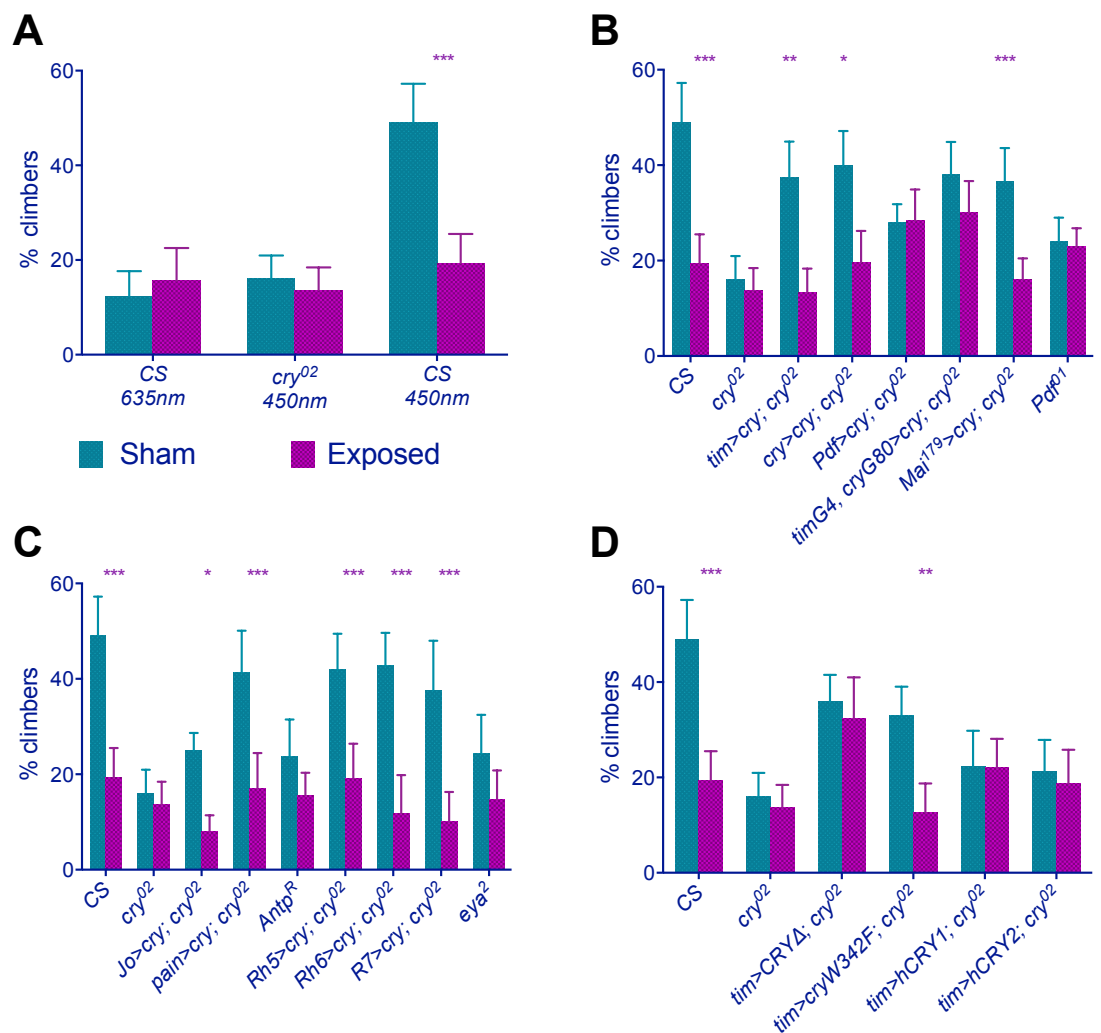


Figure 5-1 Mean geotactic responses \pm SEM.

Based on three biological replicates. Green bars, sham exposed; purple bars, EMF exposed. The results from Canton-S (CS) and *cry⁰²* were used as positive and negative controls for all analyses and b-d represent experiments performed only at 450 nm. (a) Response of CS and *cry⁰²* exposed to different wavelengths of light. Post hoc tests revealed significant

differences only between CS in blue light under sham compared with all the other conditions ($P<0.001$). (b) Responses of clock *GAL4/UAScry* genotypes on a *cry⁰²* background with *Pdf⁰¹* flies as control. *Post hoc* tests reveal no significant differences between sham *tim>cry*, *cry>cry*, *timG4,cryG80>cry* or *Mai¹⁷⁹>cry* compared with CS, nor for EMF exposure with the exception of *Mai¹⁷⁹>cry* ($p=0.02$). For sham, *Pdf>cry* vs *cry⁰²* $p=0.11$, vs CS $p=0.008$; *timG4,cryG80>cry* vs *cry⁰²* $p=0.007$; *Pdf⁰¹* vs *cry⁰²* $p=0.56$, vs CS $p=0.004$; for EMF *Pdf>cry* vs *cry⁰²* $p=0.06$, vs CS $P=0.23$, *timG4,cryG80>cry* vs *cry⁰²* $=0.04$, vs CS $p=0.16$. *Pdf⁰¹* vs *cry⁰²* $p=0.49$, vs CS $p=0.91$. (c) Responses of eye and antennal genotypes (*GAL4>cry* on *cry⁰²* background) *Post hoc* for sham, CS was not significantly different from sham *pain*, *rh5*, *rh6*, *R7>cry*, but *J0>cry* vs *cry⁰²* $p=0.18$, vs CS $p=0.0005$. For EMF, none of the genotypes were significantly different from CS or *cry⁰²*. (d) Responses of *cry* variants driven by *tim>GAL4* (RM ANOVA, Genotype $F_{(5,24)}=6.89$, $p=0.0004$, Exposure $F_{(1,24)}=16.8$, $p=0.0005$ and GxE interaction $F_{(5,24)}=4.13$, $p=0.008$). Both *hCRY* constructs did not show a significant EMF effect. *Post hoc* sham *tim>cryΔ;cry⁰²* vs *cry⁰²* $p=0.007$, vs CS $p=0.04$, *tim>cryW342F;cry⁰²* vs *cry⁰²* $p=0.02$, vs CS $=0.017$; for EMF *tim>cryΔ;cry⁰²* vs *cry⁰²* $p=0.01$, vs CS $=0.06$, t *tim>cryW342F;cry⁰²* vs *cry⁰²* $p=0.2$, vs CS $p=0.33$). Duncan's *post hoc* * $P<0.05$, ** $P<0.01$, *** $P<0.001$. Adapted from (Fedele *et al.*, 2014).

Finally, in order to maintain parallelism between circadian experiments and the climbing assay, the same *cry* variants used previously (with the exception of *tim>cryCT;cry⁰²* that will be tested in the future) were tested on the *cry⁰²* background using *tim>GAL4*. *hCRY1* and *hCRY2*, previously reported to restore light dependent magnetoreception in the conditioning assay (Foley, Gegear & Reppert, 2011) and enhance the activity levels under EMF (Chapter 3 and Fedele *et al.*, in Press) did not appear able to rescue the climbing phenotype beyond that of *cry⁰²*, so they are not competent to respond to EMF (*a posteriori* for Sham *tim>hCRY1* vs *cry⁰²* $p=0.37$; *tim>hCRY2* vs *cry⁰²* $p=0.44$; for EMF *tim>hCRY1* vs *cry⁰²* $p=0.24$; *tim>hCRY2* vs *cry⁰²* $p=0.45$; Figure 5-1D). In contrast, the Trp to Phe mutation (*cryW342F*) generated intermediate levels of climbing which were significantly further reduced on EMF exposure (Figure 5-1D). *tim>cryΔ;cry⁰²* flies were also tested and interestingly, under both sham and EMF conditions, this mutant showed intermediate levels of climbing but with no difference between the two conditions. As with *cryW342F*, the *cryΔ* mutants retained the ability to climb but were not responsive to EMF, reconfirming a role for the CRY CT in magneto-sensing (Figure 5-1D).

All *GAL4* and *UAS* control strains showed normal EMF response under blue light revealing a significant Exposure effect (RM ANOVA $F_{(1,64)}=217.52$, $p=0.0004$) but no effect of Genotype ($F_{(15,64)}=0.818$, $p=0.65$) nor a G x E interaction ($F_{(15,64)}=0.60$, $p=0.86$), so all genotypes responded in the same way to the EMF (Figure 5-2).

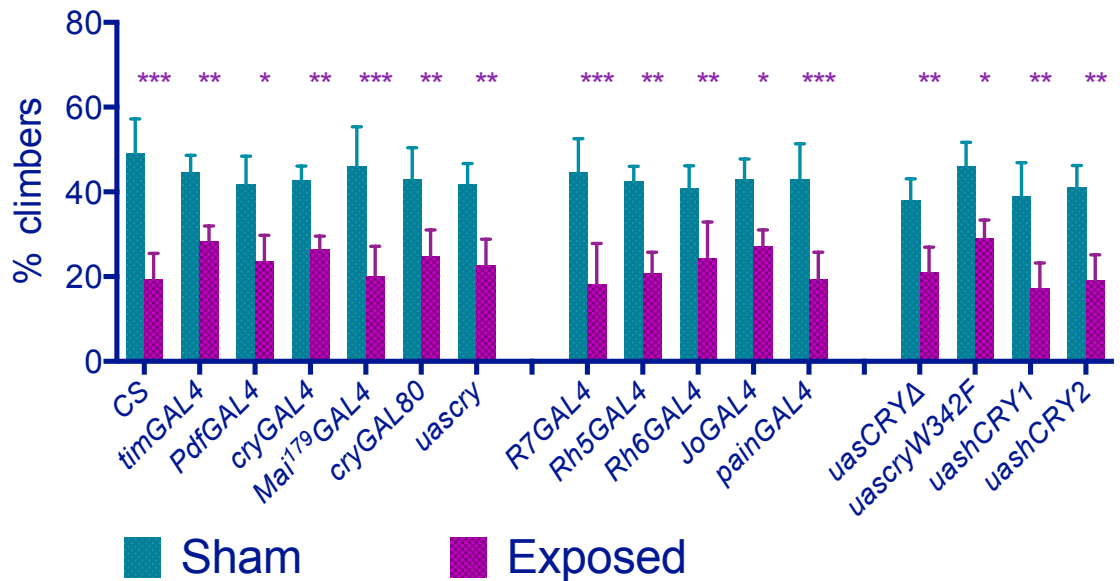


Figure 5-2 GAL4/ UAS controls strains show normal EMF responses.

Mean climbing scores (\pm s.e.m.) under blue light based on three biological replicates. Duncan's *post hoc* *P<0.05, **P<0.01, ***P<0.001. Adapted from (Fedele *et al.*, 2014).

5.4 DISCUSSION

It has been demonstrated previously that *Drosophila* requires a functional CRY molecule for a normal negative geotaxis behaviour (Toma *et al.*, 2002; Rakshit & Giebultowicz, 2013) providing a novel assay for studying EMF effects on CRY. I have observed that under blue light, the climbing of wild-type flies exposed to a 500 μ T static EMF is significantly reduced compared to sham exposure, whereas in red light, flies exposed to sham or EMF suppress their climbing, so negative geotaxis is wavelength-dependent, thereby implicating the fly's dedicated blue-light circadian photoreceptor, *cryptochrome*. As consequence *cry-null* mutants fails to climb also in sham conditions but this ability could be rescued by overexpressing CRY in a number of different neuronal types that include clock neurons, antennae and eyes. These results are consistent with our circadian clock data, and they all suggest a putative role for CRY in mediating the effects of EMFs, possibly through the RPM, albeit with some amendments. The strongest evidence comes from the *tim>cryΔ;cry⁰²* flies. These mutants failed to respond to EMF, but in contrast to a *cry-null* mutant, the *tim>cryΔ;cry⁰²* flies retain the ability to climb to levels comparable to wild-type,

indicating, as previously postulated, that the C-terminal domain of CRY is required for triggering an EMF-induced response.

Moreover, as with the circadian phenotypes described in Chapters 3 and the conditioning assay (Geegear *et al.*, 2010), the Trp to Phe amino acid substitution in position 342 that should interfere with the normal electron transfer and therefore abolish EMF effects, is still able to rescue the EMF-reduced climbing ability of the flies, indicating that other radical partners are involved.

While both the climbing and conditioning assays reveal consistent effects for the terminal Trp mutant, the same could not be stated for hCRY2. In the conditioning assay (Foley *et al.*, 2011) and to some extent in my locomotor activity, hCRY2 is EMF-sensitive, but in the climbing assay, hCRY1 and hCRY2 behave very similarly to *cry*⁰², suggesting that they are not capable of transmitting light information in this assay, as in the previous circadian assay (Chapter 3).

I also obtained EMF phenotypes when I varied the expression patterns of CRY. Under the control of different clock drivers, I observed that as I reduced expression from *tim>cry* expressed in nearly all clock cells) to *cry>cry* (only CRY expressing cells), to *Pdf>cry* (expressed in LN_Vs) and *timG4;cryG80>cry* (predominantly dorsal neurons, DNs and three LN_Ds that do not normally express CRY (Dissel *et al.*, 2014)), I noticed that under sham conditions the proportion of climbers was generally either intermediate between the mutant and wild-type values or not statistically different from the value of the wild type. For example, *timG4;cryG80 >cry* gave 38% climbers compared to *cry*⁰² 16% and wild-type, 49%. Yet for *Pdf>cry* and *timG4;cryG80>cry* there were no significant differences between the sham and EMF conditions, so the EMF response had been lost. However, *Mal¹⁷⁹>cry*, which expresses in the three strongly CRY-positive LNd cells (Yoshii *et al.*, 2008), restored the intermediate levels of climbing under sham control as well as the EMF suppression. Comparing this result with that of the *timG4;cryG80 >cry* driver combination, it would appear that CRY expressed in the three CRY positive LN_D neurons could be sufficient for restoring both climbing and the EMF responses. The LN_d cluster are involved in circadian locomotor

responses under light conditions (Stoleru *et al.*, 2007), providing a rationale for why they may play an important role in the climbing phenotype under blue- light.

The clock neurons are not the only relevant cells for mediating the effects of EMFs. CRY expression in the R8 photoreceptors of pale ommatidia (via *Rh5>cry*), or in the R8 yellow ommatidia and the Hofbauer-Buchner eyelet (*Rh6>cry*) or in the R7 cell, is sufficient for robust climbing and EMF responses, as it is for the locomotor activity assay. Johnston's organ (JO), which is located in the second antennal segment, has been previously implicated in negative geotaxis (Sun *et al.*, 2009) and our results with *JO15>cry* which expresses specifically in the JO (Kamikouchi, Shimada & Ito, 2006), and *pain>cry* which is more widely expressed in the antennae and some central neurons (Sun *et al.*, 2009), suggest that CRY expression in JO is sufficient for mediating the effects of EMF.

6 SOME MISCELLANEOUS EXPERIMENTS

6.1 INTRODUCTION

This chapter will cover several miscellaneous experiments concerning magnetoreception including a new assay developed for studying magnetic field effects in flies based on the positive conditioning assay used in the Reppert laboratory (Gegear *et al.*, 2008, 2010; Foley, Gegear & Reppert, 2011). In addition, attempts were made to localize magnetite crystals in the fly and finally a biochemical assay was designed to study the effects of EMF exposure on ageing, a CRY controlled response (Rakshit & Giebultowicz, 2013).

6.1.1 A ‘REPPERT-LIKE’ ASSAY

From 2008 the Reppert laboratory published three studies describing the ability of *Drosophila* to associate a positive reward (*i.e.* sucrose) with the presence of an external magnetic field, and suggesting that CRY mediates light-dependent magnetoreception. Flies were starved for 24 h and then loaded into a L-maze where a food reward was present at the end of the arm (Gegear *et al.*, 2008). During the training phases, the food reward was always associated with the presence of an external magnetic field of 5 G. After training, flies were then loaded into a T-maze in which the field was present at only one end of the two horizontal arms. A significant proportion of flies learned to associate the field to the food by moving to one end of the maze or the other according to the presence of the field. Trained flies were also compared to naïve flies, which without training exhibited an avoidance response to the field. This ability to associate positive reinforcement with the EMF was CRY dependent, in that *cry-null* flies showed a low preference index ($PI \sim 0$). In contrast, transgenic *cry-null* flies expressing *D.plexippus* or *H.sapiens* CRY2, rescued the wavelength- dependent

conditioning phenotype. According to the authors, when wavelengths below 420 nm were blocked (Figure 6-1) trained flies were unable to follow the field (Gegear *et al.*, 2008, 2010; Foley *et al.*, 2011).

However, wild type naïve flies at wavelengths >420 nm showed opposite responses to EMF compared to flies tested under full spectrum or blue light only (420 nm; Figure 6-1) (Gegear *et al.*, 2008; Foley *et al.*, 2011). Thus under longer wavelengths the flies' preference to move towards the field rather than escape from it, would likely mask any positive conditioning as in both naïve and conditioning tests flies would move in the same direction. Moreover, in their 2008 paper, Gegear and co-workers showed that w^{1118} flies exhibited a preference for the magnetic field rather than an avoidance (under full spectrum light) and concluded that this apparent difference was due to the genetic background (Gegear *et al.*, 2008).

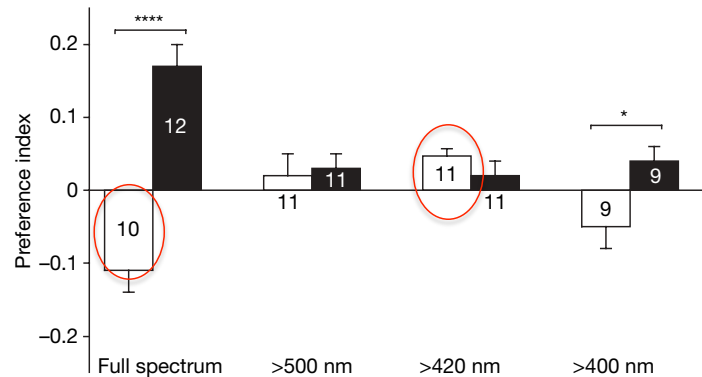


Figure 6-1 Naïve flies at wavelengths >420nm show opposite response to flies exposed to >400nm and full spectrum light (from Gegear *et al.*, 2008). Red circles highlight the opposite response. Although the raw data are not available, based on the SEMs of the bars in the graph I can presume that under longer wavelengths (> 420 nm) flies significantly prefer the field.

This apparent opposite magnetic response under different wavelengths was first described by Phillips and Sayeed in 1992 (Phillips & Sayeed, 1992). In their original paper, the authors hypothesized the existence of two EMF-sensitive photoreceptors located in the R7-R8 rhabdomeres with different light sensitivities, one more sensitive to shorter wavelengths and the other to longer ones. After the initial idea of CRY acting

as a magnetoreceptor was developed, Phillips and co-workers amended their original idea and proposed a model through which different wavelengths could lead to a different initial singlet-triplet ratio leading to changes in the EMF responses (Phillips & Sayeed, 1992; Phillips, Jorge & Muheim, 2010). Here, I will provide some preliminary evidence for this antagonistic effect.

6.1.2 IN SEARCH OF MAGNETITE

As mentioned in the introduction, one of the mechanisms described for magnetoreception in animals relies on magnetite crystals (Lohmann & Johnsen, 2000; Wiltschko *et al.*, 2002, 2010; Wiltschko & Wiltschko, 2006; Cadiou & McNaughton, 2010; Gould, 2010; Kirschvink, Winklhofer & Walker, 2010; Ma & Ritz, 2014). This iron-mineral-based structure is found within nerve cells in birds' upper beak and was originally proposed as the magnetoreceptor (Fleissner *et al.*, 2003). However this view has been seriously challenged by a report showing that these cells could actually be macrophages ((Mouritsen, 2012; Treiber *et al.*, 2012) but see (Lefeldt *et al.*, 2014)), immune cells involved in iron homeostasis (Wang & Pantopoulos, 2011). It now appears that many organisms, even non-migratory ones, contain magnetite (Stanley, 2014) but so far, there have been no reports of magnetite in *Drosophila*.

6.1.3 CRY AND AGEING

It has been recently shown that low CRY expression enhances ageing through an unknown mechanism. I decided to test the levels of reactive oxygen species (ROS) in EMF exposed and Sham exposed flies. My previous results (Chapter 3), revealed higher levels of CRY under EMFs compared to Sham, providing a rationale for a suspension of ageing, which is one interpretation of m locomotor activity data. Under an EMF, more CRY could mean less ageing, and as ageing generates a longer period, then the arrest of ageing could conceivably produce the shorter periods observed on exposure (Chapter 3).

6.2 MATERIALS AND METHODS

6.2.1 T-MAZE AND EMF EXPOSURE

I used a population of flies placed inside a T-maze and tested them for their naïve responses. A *Drosophila* plastic vial was wrapped in aluminum foil and used as the starting point for the T-maze. A plastic T-tube connector was then inserted into the vial and connected to two plastic frames sealed with a commercial mosquito net that I used as collection chambers. Plastic pipette tips were used as valves so that once a fly entered the collection chamber it was then unable to exit (Figure 6-2). A different maze was also tested (Section 9-2).

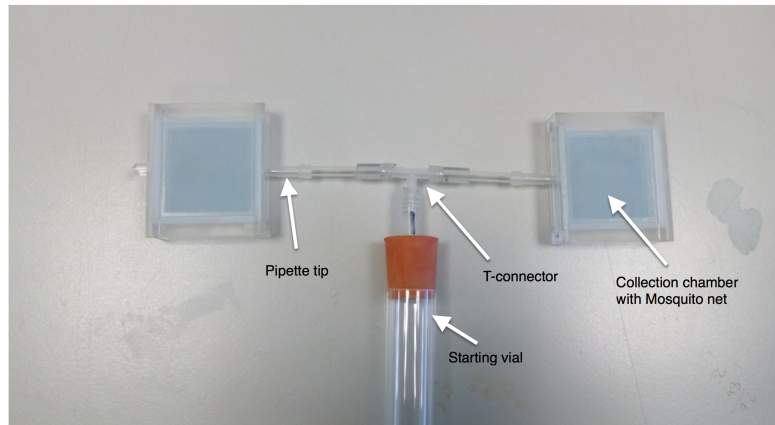


Figure 6-2 T-maze apparatus

Flies were free to enter the T-maze and choose one of the two arms for 45 to 75 min in the presence of EMF exposure at only one end of the maze. 50 to 100 flies were tested for each trial, with at least 3 trials per strain. As controls, flies were also tested in the absence of a superimposed EMF. The preference index (PI) was calculated as in (Gegear *et al.*, 2008): $(Pm - 0.5) \div [(Pm + 0.5) - (2Pm \times 0.5)]$; where Pm is the proportion of flies moving towards the EMF side of the T-port. All the *t*-tests performed are one sample *t*-test " $t = (x - \mu) / (s / \sqrt{n})$ "; where x is the sample mean, μ is a specific value (in this case 0), s is the sample standard deviation and n the sample size. The strains used in this assay were previously described.

The magnetic field was provided using the same apparatus as for the climbing experiments but with a wiring modification that provided the EMF only on one coil but not the other. The magnetic field was measured using a gaussmeter (GM-1-HS, AlphaLab Inc. USA) both at the end of the chambers ($700\text{ }\mu\text{T}$ towards the active coil/ $40\text{ }\mu\text{T}$ towards the sham exposed coil, which is comparable to the ambient magnetic field inside the room ($36\text{ }\mu\text{T}$) and in the middle of the T-maze ($100\text{ }\mu\text{T}$, only the horizontal component was measured). The entire apparatus was placed in a temperature-controlled room (25°C) and away from any other electrical appliances that could interfere with the magnetic field.

6.2.2 PARAFFIN SECTIONS AND MAGNETITE STAINING

Whole bodies of Canton-S flies and of the parasitic wasp, *Nasonia vitripennis* were collected during the day regardless of their circadian time and immediately incubated in 4% PFA for 4 h at room temperature. After two washes in 1X PBS pH 7.4 for 15 min each (for buffer formulation refer to table XX in the appendix), the samples were incubated in PBS with 25% sucrose (cryoprotectant) overnight. Specimens were subsequently placed in a mould, embedded with O.C.T. compounds (Sigma) and frozen using a mix of Dry Ice and ethanol and then stored at -80 C until dissection. 15 μm sections were obtained using a cryostat (Leica). Each section was collected onto a glass slides coated with poly-lysine (Thermo Scientific) for improving tissue adherence.

Slides were subsequently washed twice for 15 min each and soaked in equal volumes of 20% aqueous solution of hydrochloric acid (Sigma) and 10% aqueous solution of potassium ferrocyanide (Sigma) for 30 min. Any ferric ion (Fe^{+3}) present in the tissue combines with the ferrocyanide and results in the formation of a bright blue pigment, Prussian blue, or ferric ferrocyanide. After three washes in distilled water (15 min each) the slides were then soaked in nuclear fast red solution (counterstaining for nuclei) and finally washed twice in distilled water (15 min each). Slides were then covered with coverslip and resinous mounting media (clear nail polish). Mounted slides were observed using a Nikon light microscope and images were taken using a Canon camera.

6.2.3 NASONIA LOCOMOTOR ACTIVITY EXPERIMENTS

1-4 day old males were collected and place inside a glass activity tube containing a sucrose jelly. The experimental set up was the same used for *Drosophila* EMF exposure (300 μ T, 3 Hz). Locomotor activity data were analysed as described previously.

6.2.4 PROTEIN CARBONYLS CONTENT

Colony-S, *cry*⁰² and *tim>cry* male flies were kept for 6-7 days under constant dim 0.25 Wcm⁻² blue light (450 nm) and exposed either to EMF (300 μ T, 3Hz) or Sham conditions. At ZT 14 flies were flash frozen in liquid nitrogen and assayed according to manual of the OxiSelectTM Protein Carbonyl Fluorometric Assay (Cells Biolabs) for protein carbonyls contents. Fluorescent levels were measured using a BMG plate reader and after normalization using standard curve and protein concentration, the nmol/mg of protein carbonyls were plotted and analysed according to manufacture instructions. Three biological replicates were performed for each condition.

6.3 RESULTS AND DISCUSSION

6.3.1 FLIES AVOID THE MAGNETIC FIELD UNDER BLUE LIGHT BUT SWITCH THEIR PREFERENCES UNDER GREEN LIGHT

I observed similar results to Gegear et al (2008), in that wild type CS flies showed a significant avoidance to EMF under blue light (450 nm, $t_{(2)}= 5.06$, $p<0.05$;

Figure 6-3A) whereas Sham flies showed a PI that was not significantly different from 0 ($t_{(2)}= 0.91$, $p=0.45$ and $t_{(4)}=4.572$, $p<0.05$; Figure 6-3A). *cry*⁰² did not show a significant preference index ($t_{(2)}= 0.69$, $p=0.56$; Figure 6-3B). Additionally, flies overexpressing CRY (*tim>cry*) were also tested and they exhibited similar responses to wild type ($t_{(2)}= 8.70$, $p<0.05$; Figure 6-3B). Similarly, *Cik*^{Jrk} (Allada et al., 1998) flies

showed a naïve avoidance for the field ($t_{(2)}= 9.43$, $p<0.05$; Figure 6-3B) suggesting that a functional clock is not required for EMF detection, at least in this assay.

Interestingly however when flies were tested under longer wavelengths (green, 500 ± 20 nm) I observed in Canton-S and *tim>cry* flies a significant preference for the field compared to Sham flies (ANOVA $F_{(2,6)}= 34.88$, $p< 0.001$; Figure 6-3C and ANOVA $F_{(3,9)}=24.48$, $p<0.001$; Figure 6-3D) further supporting the idea of an antagonistic effect.

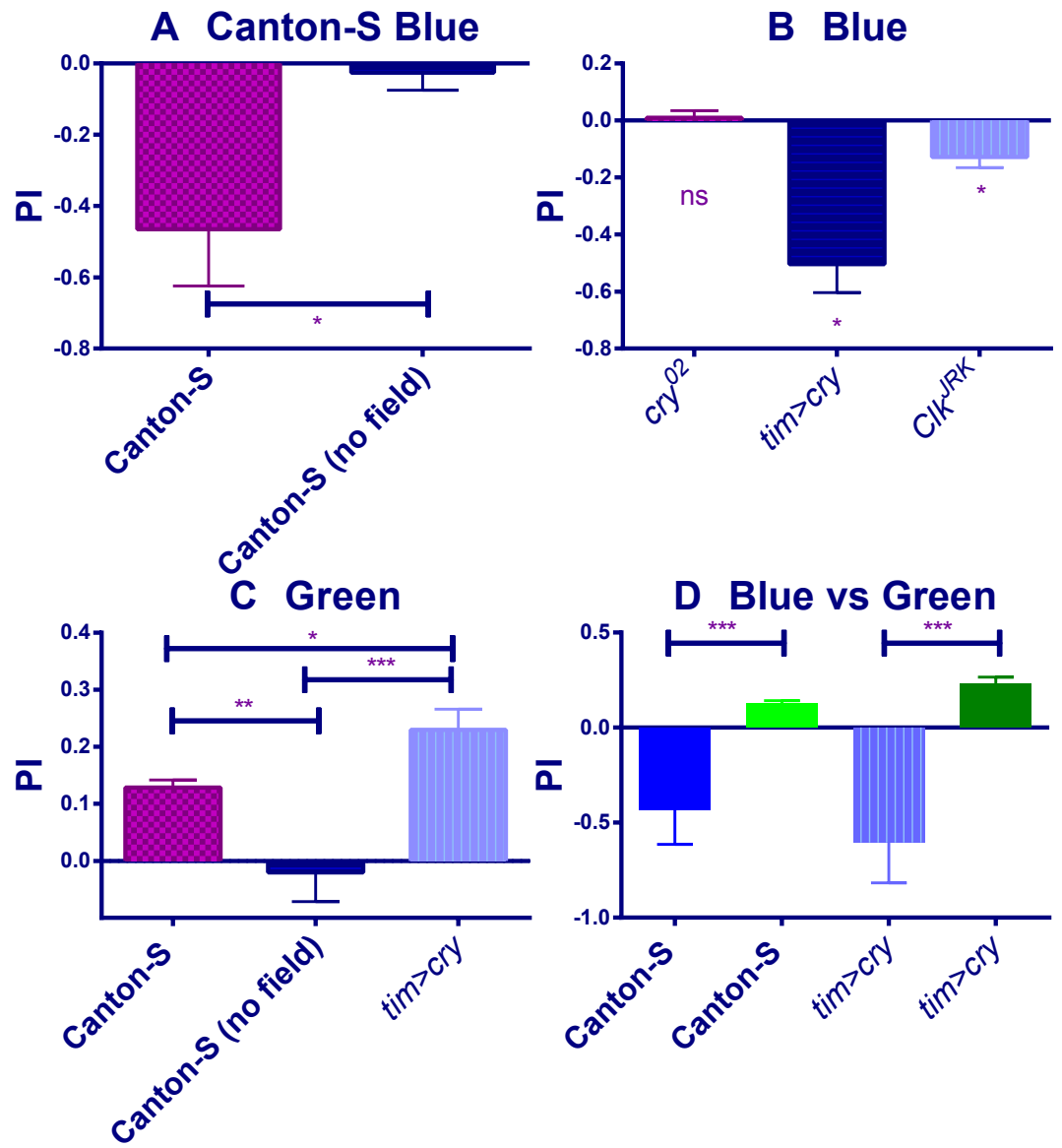


Figure 6-3 A Canton-S flies exhibited avoidance for the filed under blue light (450 nm). B PI of *cry⁰²*, *tim>cry*, *Clk^{Jrk}* flies exposed to EMF under 450 nm, t-test used for testing significance from 0. C Responses of Canton-S and *tim>cry* flies under green light (500 nm). Exposed Canton-S and *tim>cry* flies both showed a significant preference compared to 0 (CS: $t(2)= 17.70$, $p<0.05$ and *tim>cry*: $t(2)= 11.05$, $p<0.01$) whereas Sham flies did not ($t(2)= 0.68$, $p=0.53$). D Opposite response under blue and green light. Mean \pm SEM. (post-hoc * $p<0.05$, ** $p<0.01$, *** $p<0.001$).

6.3.2 DROSOPHILA DOES NOT CONTAIN MAGNETITE

Staining of several sections did not reveal the presence of magnetite in the fly's body (Figure 6-4A-E), whereas iron-containing clusters were observed in *Nasonia vitripennis* eyes and abdomen (Figure 6-4F-I). Absence of staining in *Drosophila* is not enough to exclude magnetite, as a more sophisticated assays would be required (Lefeldt *et al.*, 2014) such as X-ray electron microscopy diffraction or the use of SQUID magnetometers (Acosta-Avalos *et al.*, 1999), which are not currently available in my institution.

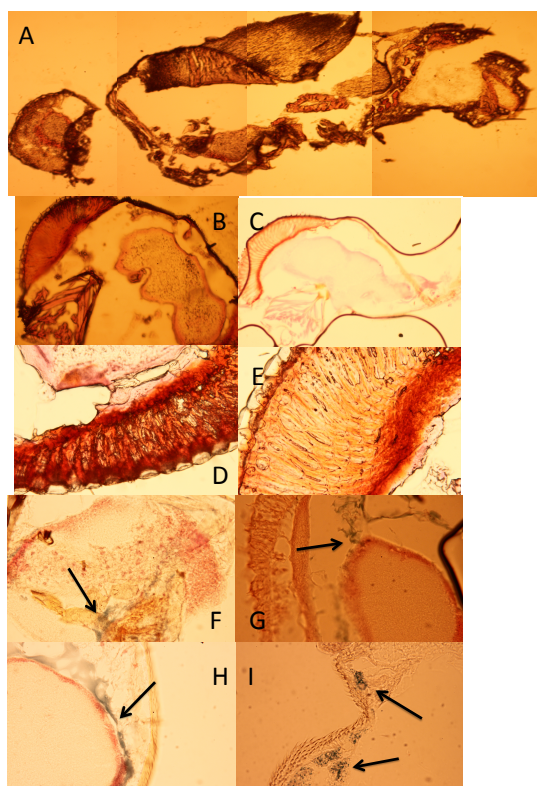


Figure 6-4 A-E Drosophila sections. A Sagittal section of Drosophila.

B-C Transversal section of Drosophila head. D-E Close-up to the eyes. None of the samples revealed presence of magnetite. F-I *Nasonia* sections. F-G-H Iron-granules near the eyes (transversal section). I Abundance of iron-containing particles in the abdomen (sagittal section). Arrows indicate iron granules stained by Prussian Blue. Red staining indicates nuclei.

Light-dependent magnetoreception could also occur through magnetite if the crystals are linked to a light activated ion channel (TRPL for instance) (Cadiou & McNaughton, 2010). Moreover, recent data suggest that a broadband RF spectrum, rather than a single RF matching the Larmor frequency is required for bird orientation (Engels *et al.*, 2014). These recent results do not require the RPM, as the orientation

effects could be explained by involvement of iron-clusters large enough to detect small electric and magnetic vectors arising from the radio-frequency radiation (Kirschvink *et al.*, 2010; Engels *et al.*, 2014; Kirschvink, 2014).

In conclusion, more sensitive analyses are required to exclude the possibility of magnetite in *Drosophila*. Nevertheless CRY or magnetite –mediated magnetoreceptors are not mutually exclusive and may actually coexist as shown in birds and other animals (Stapput *et al.*, 2008; Kirschvink *et al.*, 2010).

The presence of iron clusters in the eyes and abdomen of *N. vitripennis* raises the possibility that this parasitoid wasp could perceive EMF, although the exact nature of these ferric clusters is unknown. A preliminary experiment with male wasps using the circadian assay, did not observe any period difference between EMF and Sham exposed wasps (Interaction pre-exposure *vs* EMF/Sham Exposure $F_{(1,101)}=0.006$, $p=0.93$; pre-exposure *vs* exposure $F_{(1,101)}=13.12$, $p<0.001$; Figure 6-5A) nor hyperactivity (Interaction pre-exposure *vs* EMF/Sham Exposure $F_{(1,101)}=0.06$, $p=0.8$; Figure 6-5B). It might be interesting to assay *Nasonia* in the newly developed orientation assay (see Paragraph 6.1.1) in future.

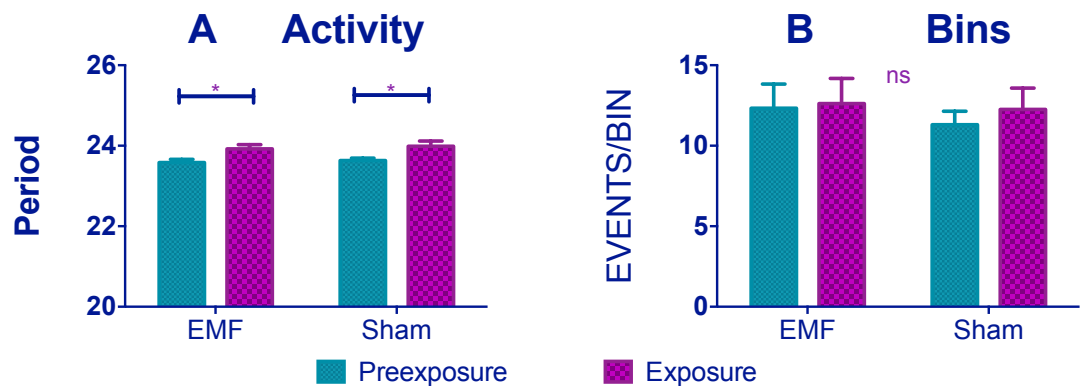


Figure 6-5 Average period (A) and locomotor events of activity (B) for *Nasonia vitripennis*. Mean \pm SEM. (*post-hoc* *= $p<0.05$). For values and Ns please refer to Tables 9-3 and 9-4.

6.3.3 EMF EXPOSURE AND CRY EXPRESSION REDUCE PROTEIN CARBONYLS SYNERGISTICALLY

In this assay the content of protein carbonyls, biomarkers of oxidative stress (Dalle Donne *et al.*, 2005) were significantly lower in EMF exposed flies compared to Sham exposed flies for wild-type and *tim>cry* strains (2 way ANOVA interaction Genotype *vs* EMF/Sham Exposure $F_{(2,12)}=18.17$, $p<0.001$; EMF *vs* Sham $F_{(1,12)}=32.73$, $p<0.001$ and a Genotype effect $F_{(2,12)}=69.02$, $p<0.001$; Figure 6-6) whereas in *cry⁰²* no differences were observed (*a posteriori* Newman-Keuls test $p=0.13$).

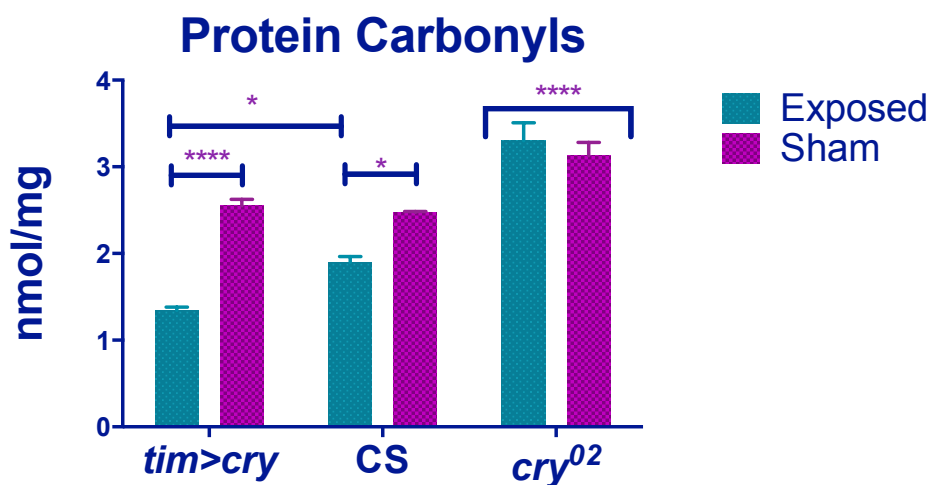


Figure 6-6 Protein carbonyl contents under EMF/Sham exposure.

In presence of EMF the overall levels of protein carbonyls is significantly reduced in function of the presence of CRY. CS= Canton-S. Mean \pm SEM shown. (*post-hoc* * $p<0.05$, ** $p<0.01$, *** $p<0.001$)

Further *post hoc* tests revealed a significant difference between EMF exposed wild-type *vs* *tim>cry* flies ($p<0.05$) in accordance with the hypothesis that higher levels of CRY (in *tim>cry*) should promote lifespan, by indirectly reducing ROS species (Rakshit & Giebultowicz, 2013). This assay provides further indirect evidence that normal CRY signaling is modified under EMF, resulting in more abundant CRY protein levels (see Results Chapter 3), which will reduce ROS levels, partially suspend ageing,

and as period gets longer with age, this may contribute to the period shortening effect observed in my locomotor activity experiments. Of course, higher levels of CRY under EMF would also reduce period as light-signaling is also compromised. Thus two separate phenomena could contribute to the period effects observed under EMF.

7 ROLE OF PERIPHERAL CLOCKS

7.1 INTRODUCTION

The central clock in the brain of *D.melanogaster* consists of ~150 neurons clustered in different groups in relation to their anatomical position (Nitabach & Taghert, 2008; Peschel & Helfrich-Förster, 2011; Ozkaya & Rosato, 2012). Historically, the circadian clock of *Drosophila* was considered as clusters of cell-autonomous clock neurons, organised in a hierarchical structure, with the PDF-expressing cells acting as pacemakers and driving the 24 h cycle (Chang, 2006; Allada & Chung, 2010) by synchronising the PDF⁻ cells *via* PDF expression (Stoleru *et al.*, 2005). However, recent work has suggested that the neuronal organization of the clock is based on multiple oscillators integrated into a flexible network (Dissel *et al.*, 2014; Yao & Shafer, 2014). Alteration of single neuronal clusters does not abolish the cycle but rather it modifies the intracellular communications among clusters (Dissel *et al.*, 2014). While these studies provide a new understanding of the central pacemaker, less is known about peripheral neuronal clocks and what, if any role they might play in the regulation of the pacemaker.

7.1.1 PERIPHERAL CLOCKS

Peripheral clocks have been detected in many tissues such as legs, proboscis, wing and antennae by a PER-driven luciferase reporter (Plautz *et al.*, 1997). Cells of the ring gland and Malpighian tubules continue to express *per* in a rhythmic fashion *in vitro*, without communication from the central clock (Hege *et al.*, 1997). Furthermore, Malpighian tubule cells transplanted into host flies maintain their own original phase of PER oscillation, despite the host flies being entrained to a reverse Light/Dark cycle (Giebultowicz *et al.*, 2000). The molecular clock of peripheral oscillators seems to differ slightly from that of the central clock, with CRY suggested to function as a core component of the molecular clock (Ivanchenko, Stanewsky & Giebultowicz, 2001; Krishnan *et al.*, 2001b; Collins *et al.*, 2006).

Expressing clock genes only in antennal neurons proved to be necessary and sufficient for rhythmic olfaction in *Drosophila* (Tanoue *et al.*, 2004), but both central and peripheral clocks were necessary for eclosion rhythms (Myers, Yu & Sehgal, 2003). This suggests that peripheral clocks may be important for some circadian events (Myers *et al.*, 2003). Additionally, functional Chordotonal organs (ChO, collection of sensory neurons distributed throughout the body) (Sun *et al.*, 2009; Kavlie & Albert, 2013) have been recently described as necessary for temperature (Sehadova *et al.*, 2009) and vibration (Simoni *et al.*, 2014) entrainment of the circadian clock. I therefore decided to test whether peripheral oscillators might be sufficient to promote rhythmic locomotor activity.

In this chapter, I will provide striking and unexpected evidence for a novel role for peripheral clocks in generating rhythmic locomotor activity in *per⁰¹* flies. In particular, I focused my attention on the antennae. To do this I used a collection of drivers expressing GAL4 in TRP (Transient Receptor Potential) channels (Venkatachalam & Montell, 2007) located mostly in the antennae and in particular in the Johnston's Organ (JO), a collection of chordotonal neurons involved in hearing (Eberl & Boekhoff-Falk, 2007), geotaxis (Sun *et al.*, 2009) and temperature (Simoni *et al.*, 2014). TRP channels are a superfamily of highly conserved six-trans membrane domain cation channels that play a crucial role in the responses to external stimuli (Venkatachalam & Montell, 2007) such as light, temperature and vibrations (Venkatachalam & Montell, 2007). In particular, in this study I have used the already described *TRPA* channel *painless* (*painGAL4*) together with another *TRPA* channel, *pyrexia* (*pyxGAL4*), both involved in negative geotaxis and temperature detection (Sun *et al.*, 2009); two *TRPV* channels *nanchung* (*FGAL4*) and *inactive* (*iavGAL4*) both involved in hearing and negative geotaxis (Sun *et al.*, 2009) and a *TRPN* channel *nompA* (*nompAGAL4*) involved in mechanical transduction in the JO (Venkatachalam & Montell, 2007).

7.2 MATERIAL AND METHODS

7.2.1 FLY STRAINS

All the strains used in this chapter have been described previously with the addition of *UASdbt* variants (dbt^{Short} ; dbt^{Long} and $dbt^{K/R}$); which confer a short, long and long-arrhythmic phenotype respectively (Mus�us *et al.*, 2007).

7.2.2 IMMUNOHISTOCHEMISTRY (IHC)

All the drivers were crossed to *UASGFP* flies kept in LD12:12 and collected at ZT23.

WHOLE MOUNT

After collection, flies were immediately fixed in 4% paraformaldehyde (PFA) in PBS (phosphate buffered saline) with 0.1% Triton and 0.5%DMSO for 4 h at room temperature. After 3 x 15 min washes in PBST (PBS with 0.5% Triton), flies were dissected using a normal dissection microscope (Nikon) under red light conditions and washed again 3 x 15 min in PBST. Blocking was performed overnight with 10% goat serum (Sigma) diluted in PBST. The staining was done accordingly to Table 7-1. All the *antisera* were diluted in blocking solution. After secondary staining, the brains were equilibrated in Anti-fade mounting media (20% w/v n-propyl gallate in DMSO diluted in 1X PBS- glycerol) for 24 h and the mounted on a glass slide and observed under the confocal microscope (Olympus FV1000).

Table 7-1 List of *antisera* used for IHC.

Antibody	Host	Concentrati on	Brand
α-21A6	Mouse	1:50	DSHB
α-GFP	Mouse	1:1000	Invitrogen

α-GFP	Rabbit	1:1000	Molecular Probes
α-Mouse	Goat	1:1000	ABCam
Cy5			
α-PER	Rabbit	1:500	Santa Cruz
α-Rabbit	Goat	1:1000	ABCam
Cy3			

ANTENNAE

After collection, the antennae were immediately dissected and the auto-fluorescence of GFP was checked. Whenever the auto-fluorescence signal was not detectable, cryostat sections of the antennae were performed (Mishra, 2014). Head and proboscis were removed from anaesthetised flies and incubated in 4% PFA for 3 h at room temperature. After fixation the heads were washed 3X20 minutes in PBS pH7.4 followed by incubation in PBS containing 10 % sucrose for 1 h and an additional incubation in PBS with 25% sucrose overnight at 4C. Heads were then transferred to a sectioning mould and embedded in OTC mounting medium and allowed to freeze. 12 µm slices were obtained using a cryostat (Leica). After sectioning slices were transferred to polylysine slides and washed 3 times 15 min each in PBS containing 1% Tween-20 (PBS-Tw) and blocked in TBS-Tw with 5% goat serum for 2 h at room temperature. Immunostating was performed with primary *antisera* against GFP and *Eyes shut* (*Eys*, labelled by α-21A6) a gene required for the formation of matrix-filled scolopale (Husain *et al.*, 2006; Mishra, 2014) and respective secondary antibodies (Table 7-1). Slices were then mounted in Anti-fade mounting media and observed under the confocal microscope (Olympus FV1000).

7.3 RESULTS

7.3.1 EXPRESSION OF *PER* IN THE PERIPHERY IS SUFFICIENT TO RESCUE *PER*⁰¹ PHENOTYPE

Expression of *per* using several antennal drivers significantly rescued the arrhythmic phenotype of *per*⁰¹ flies (Figure 7-1 and Table 7-2). In particular *per* expression driven by the *painG4* (Sun *et al.*, 2009) in a *PdfG80* background (indicated in the figures as *G80,G4>per*) to ensure that there was no spurious *per* expression in the PDF neurons, restored high levels of rhythmicity compared to controls (77% $\chi^2_{(6)}=38.08$, $p < 0.0001$; Figure 7-2A and Table 7-2). This rescue was reduced to 18% in the corresponding genotype when I surgically removed the antennae with fine forceps ($\chi^2_{(1)}=70.44$, $p < 0.0001$ compared to intact *per*⁰¹; *PdfG80,painG4>per*, Figure 7-2A and Table 7-2) but still significantly different from *per*⁰¹ flies ($\chi^2_{(1)}=6.4$, $p < 0.05$ data not shown, Table 7-2). It is worthy to note that all the drivers and reporter tested in a *per*⁰¹ background were not significantly different from *per*⁰¹ flies (data not shown).

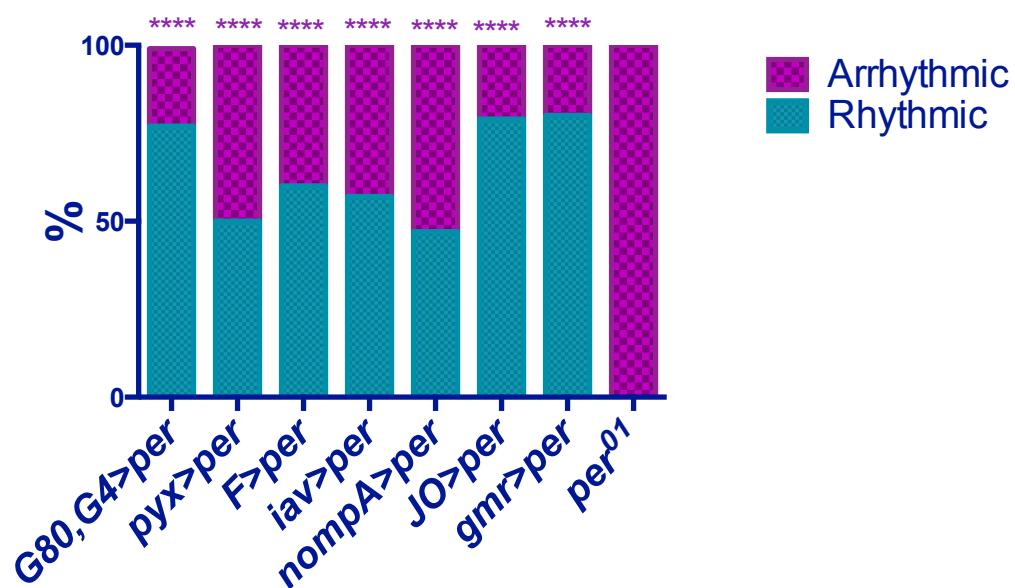


Figure 7-1 Expression of *per* using peripheral drivers.

Driving *per* overexpression either in the antennae or the eyes gave a significant increase in rhythmicity compared to *per*⁰¹. The line *PdfG80,painG4>per* has been abbreviated to *G80,G4>per*. All the lines showed in the figure are in a *per*⁰¹ background. χ^2 tests were performed individually for each genotype. *PdfG80,painG4>per* vs *per*⁰¹ $\chi^2_{(1)}=48.65$, $p < 0.0001$; *pyx>per* vs *per*⁰¹ $\chi^2_{(1)}=18.16$, $p < 0.0001$; *F>per* vs *per*⁰¹ $\chi^2_{(1)}=27.05$,

$p < 0.0001$; $iav>per$ vs per^{01} $\chi^2_{(1)} = 23.64$, $p < 0.0001$; $nompA>per$ vs per^{01} $\chi^2_{(1)} = 18.00$, $p < 0.0001$; $J0>per$ vs per^{01} $\chi^2_{(1)} = 40.74$, $p < 0.0001$ and $gmr>per$ vs per^{01} $\chi^2_{(1)} = 42.54$, $p < 0.0001$. For Ns please refer to Table 7-2..

Given that *cry* in the periphery is believed to work as a clock repressor (Collins *et al.*, 2006) I also expressed tested *PdfG80,painG4>per* on a $per^{01};;cry^{02}$ background. Remarkably, the double mutant background did not produce any significant reduction in the levels of rhythmicity (75%; Figure 7-2A and Table 7-2) but did exhibit a longer period compared to the $per^{01};;cry^+$ flies (ANOVA $F_{(6, 118)} = 16.41, p < 0.001$; Figure 7-2B and Table 7-2). However, expression of PDF is required for this rescue because $per^{01};;Pdf^{01}$ double mutants flies carrying *PdfG80,painG4>per* were mostly arrhythmic compared to controls ($\chi^2_{(3)} = 13.49$, $p < 0.01$) whereas the rhythmicity levels were not significantly different from *Pdf*⁰¹ flies ($\chi^2_{(1)} = 1.24$, $p = 0.26$; Figure 7-2C and Table 7-2). Additionally, the few rhythmic flies showed a significant period lengthening compared to controls (*UAS, GAL4* and *Pdf*⁰¹flies $F_{(3, 31)} = 9.28$, $p < 0.001$; Figure 7-2D and Table 7-2).

Another TRPA channel driver, *pyrexia* (*pyxGAL4*) (Sun *et al.*, 2009), showed a more modest, yet still highly significant increase in rhythmicity compared to controls (50% rhythmicity, $\chi^2_{(5)} = 31.47$, $p < 0.0001$; Figure 7-2E and Table 7-2) with a considerable reduction to 17% rhythmicity with antennae removed ($\chi^2_{(1)} = 24.44$, $p < 0.0001$, compared to intact $per^{01};;pyx>per$; Figure 7-2E and Table 7-2). Expression of *per* triggered longer rhythms compared to controls (ANOVA $F_{(4, 48)} = 14.14$, $p < 0.001$; Figure 7-2F and Table 7-2).

Three other TRP channel promoters that drive expression in the ChOs were also used, two TRPV channels involved in calcium activity and responsible for hearing (Sun *et al.*, 2009) *F-GAL4* (*Nanchung*, Figure 7-3A-B) (Kim *et al.*, 2003) and *inactive* (*iavG4*; Figure 7-3C-D) and one TRPN channel *no mechano potential A* (*nompA*, Figure 7-3E-F) involved in mechanical transduction (Venkatachalam & Montell, 2007). All of these drivers substantially rescued the *per*⁰¹ arrhythmia (Figure 7-1) to almost 50% with again, longer periods compared to controls (Figure 7-3 B-D-E and Table 7-2).

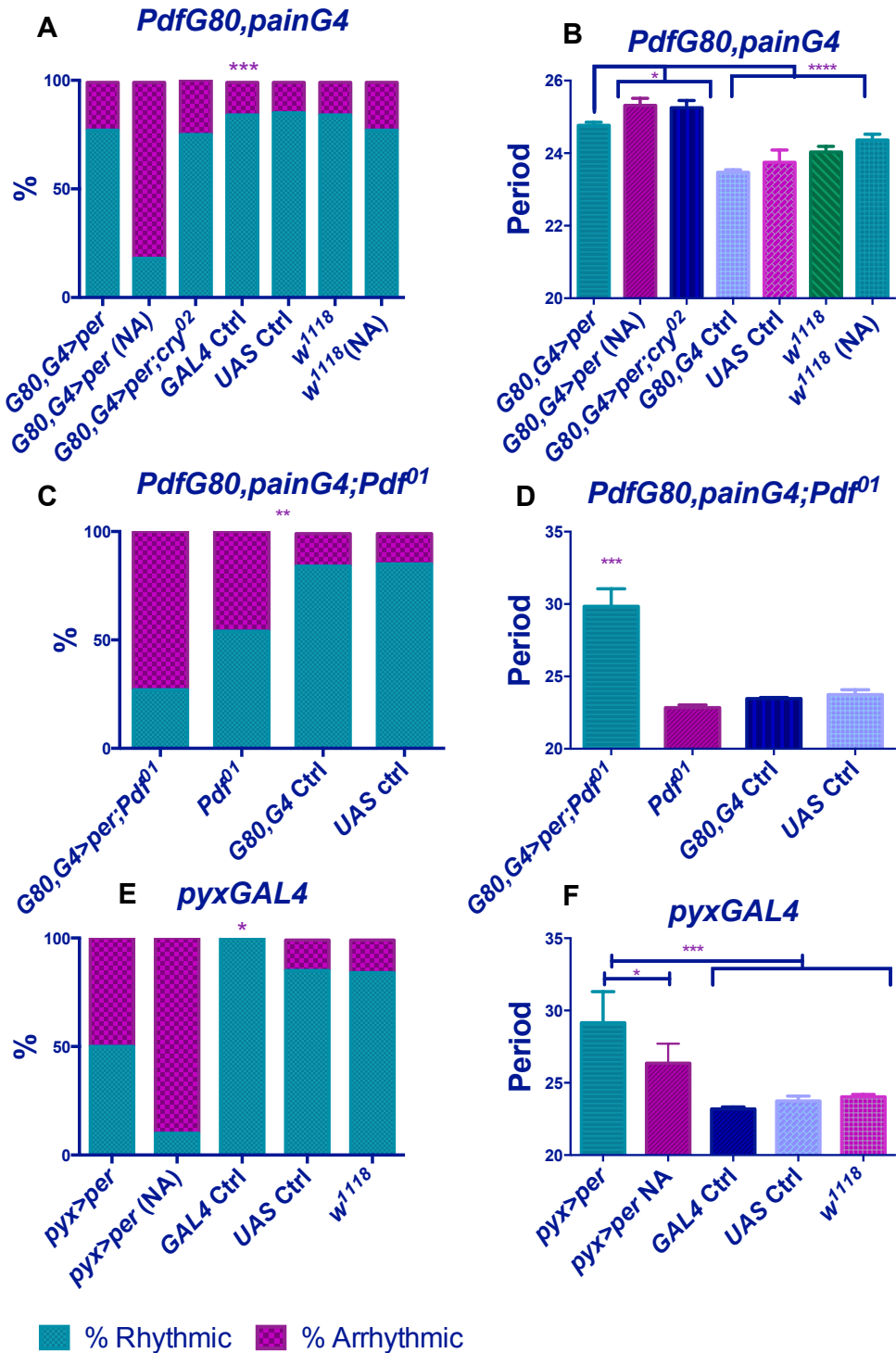


Figure 7-2 Expression of *per* in the antennae rescues *per⁰¹* locomotor rhythms.

A-B Expression of *per* with *PdfG80,painG4*. C-D PDF is required for maintaining rhythmicity levels. E-F Expression of *per* with *pyxGAL4*. Both drivers rescued rhythmicity levels and exhibited longer periods. All the genotypes are in a *per⁰¹* background with the exclusion of GAL4, UAS, *Pdf⁰¹* and *w¹¹¹⁸* controls. *UAS Ctrl* indicates *UASper* control crossed to *w¹¹¹⁸*, whereas *GAL4 Ctrl* indicates the corresponding driver crossed to *w¹¹¹⁸*. NA= No Antennae. Mean \pm SEM (Newman-Keuls post hoc test *p<0.05, **p<0.01, ***p<0.001). For period and Ns please refer to Table 7-2.

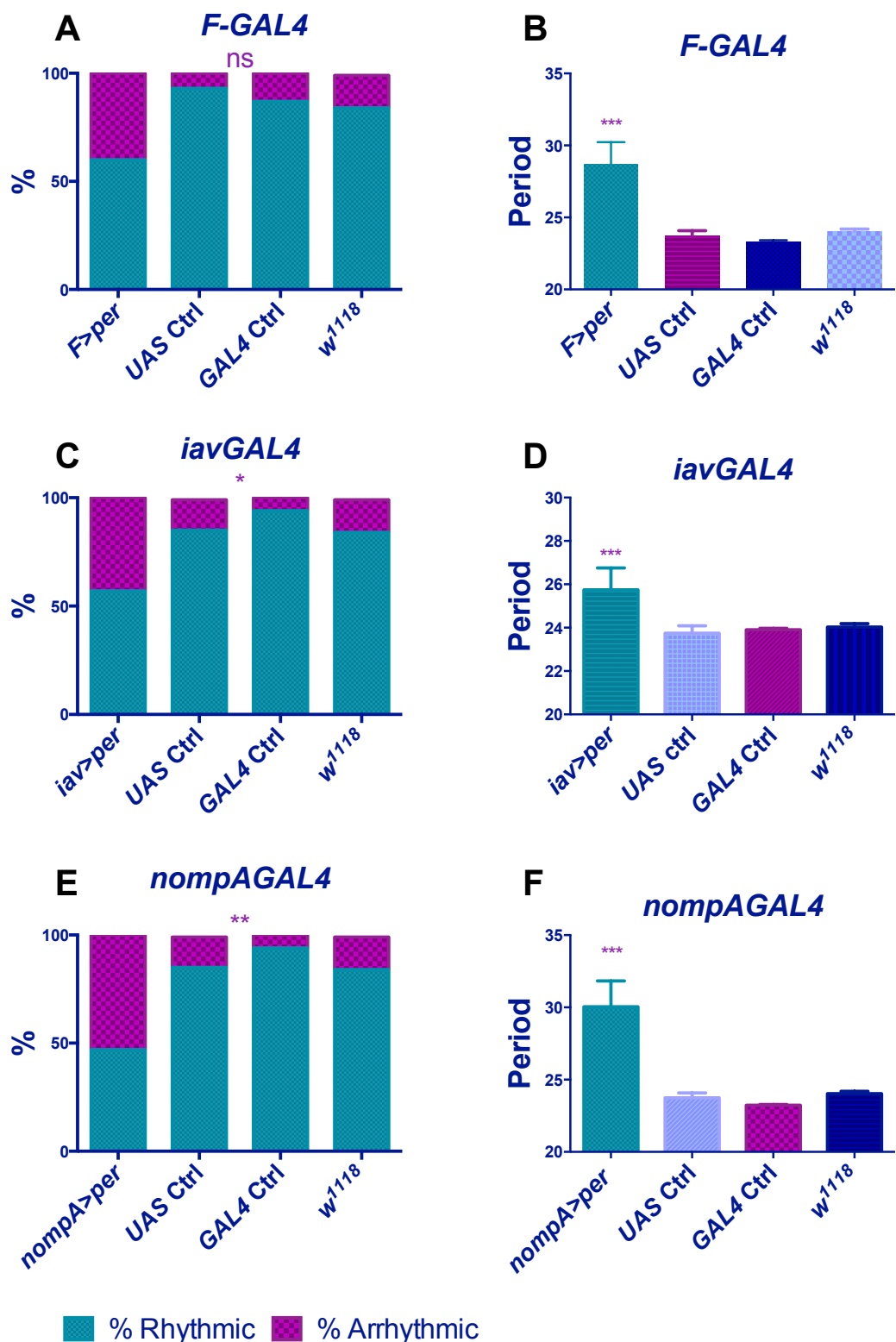


Figure 7-3 Expression of *per* in TRP channels rescues *per⁰¹* arrhythmia.

A-B *nanchung* driver. A Expression of *per* with *FGAL4* restores rhythmicity to ~60%, which is not significantly different from wild type levels ($\chi^2_{(3)}=5.64$, $p = 0.13$). B Rhythmic flies exhibit longer period compared to controls (ANOVA $F_{(3, 61)}=8.45$, $p<0.001$).

C-D *inactive* driver. C Expression of *per* with *iavGAL4* increased rhythmicity levels but not to wild-type levels ($\chi^2_{(3)}=8.21$, $p < 0.05$). D Rhythmic flies exhibit longer period compared to controls (ANOVA $F_{(3, 56)}=3.83$, $p < 0.05$). E-F *nompA* driver. E although rhythmicity levels are significantly different from *per⁰¹*, expression with *nompAGAL4* is not sufficient to restore rhythmicity to wild type levels ($\chi^2_{(3)}=11.45$, $p < 0.01$). F Rhythmic flies exhibit longer period compared to controls (ANOVA $F_{(3, 51)}=23.53$, $p < 0.001$). genotypes are in a *per⁰¹* background with the exclusion of GAL4, UAS and *w¹¹¹⁸* controls. *UAS* Ctrl indicates *UASper* control crossed to *w¹¹¹⁸*, whereas *GAL4* Ctrl indicates the corresponding driver crossed to *w¹¹¹⁸*. Mean \pm SEM (Newman-Keuls *post hoc* test * $p < 0.05$, ** $p < 0.01$, *** $p < 0.001$). For period and Ns please refer to Table 7-2.

Similar results were obtained for flies expressing *per* in the *JO15G4* pattern, a *Hobo* enhancer trap line that expresses mostly in the antennae (Sharma *et al.*, 2000; Kamikouchi, Shimada & Ito, 2006) *JO15>per* significantly rescued the rhythmicity of *per⁰¹* flies to 79% (Figure 7-1) to almost wild type levels ($\chi^2_{(6)}=42.36$, $p < 0.0001$; Figure 7-4A) whereas surgical ablation of the antennae resulted in 22% rhythmicity ($\chi^2_{(1)}=64.99$, $p < 0.0001$ compared to intact *per⁰¹;;JO>per*; ; Figure 7-4A), further confirming the importance of the antennae in providing information to the central clock. Again, the period of *per*-expressing flies was significantly longer compared to wild-type controls (ANOVA $F_{(6, 95)} = 14.06$, $p < 0.0001$; ; Figure 7-4B) and there was again no reduction in rhythmicity in the background of *per⁰¹;;cry⁰²* (; Figure 7-4A).

So far, the evidence suggest that expression of *per* in Johnston's organ is able to rescue the *per⁰¹* phenotype. However, it is not clear whether this feature is shared among ChOs only, or is common to other peripheral clocks as well. Consequently, *per* was expressed using *gmr>GAL4*, which expresses GAL4 under control of *glass* promoter, which affects mainly the eyes (Damulewicz, Rosato & Pyza, 2013). A strong rescue was observed (80%; Figure 7-1 and $\chi^2_{(4)}=33.17$, $p < 0.0001$ compared to controls; ; Figure 7-4C) in a *cry⁺* background but this was significantly reduced in the *per⁰¹;;cry⁰²* background ($\chi^2_{(1)}=76.06$, $p < 0.0001$ compared to *per⁰¹;gmr>per*; ; Figure 7-4C). Flies expressing *per* in the eyes also showed longer rhythms compared to controls (ANOVA $F_{(4, 59)} = 13.25$, $p < 0.0001$; ; Figure 7-4D).

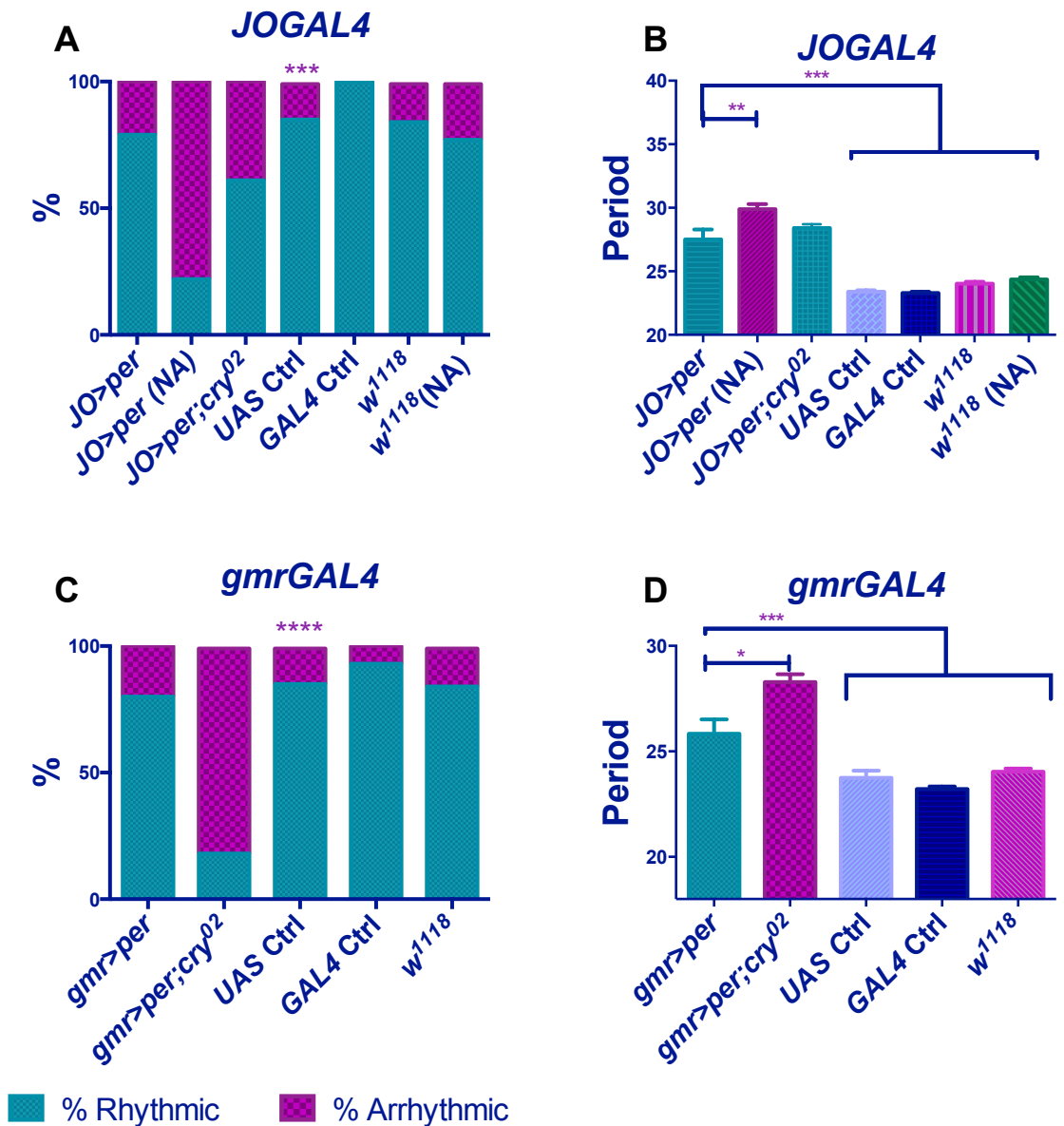


Figure 7-4 Expression of *per* in the antennae and in the eyes restores rhythmicity.

A-B *JOGAL4* driver. A rhythmicity levels. B Rhythmic flies exhibit longer period compared to controls (ANOVA $F_{(3, 61)}=8.45, p<0.001$). C-D *gmrGAL4*. C Rhythmicity levels are significantly decreased in *per⁰¹;cry⁰²* double mutants. D Rhythmic flies exhibit longer period compared to controls. Mean \pm SEM (Newman-Keuls *post hoc* test * $p<0.05$, ** $p<0.01$, *** $p<0.001$). genotypes are in a *per⁰¹* background with the exclusion of GAL4, UAS and *w¹¹¹⁸* controls. *UAS Ctrl* indicates *UASper* control crossed to *w¹¹¹⁸*, whereas *GAL4 Ctrl* indicates the corresponding driver crossed to *w¹¹¹⁸*. NA= No Antennae For period and Ns please refer to Table 7-2.

7.3.2 DBT MUTANTS AS A TOOL FOR STUDYING HOW PERIPHERAL CLOCKS AFFECT THE “CENTRAL PACEMAKER”

To farther evaluate the role of eyes and antennae in the regulation of the circadian clock, I overexpressed *UASdbt* mutations, *dbt^S* and *dbt^L* (Preuss *et al.*, 2004; Muskus *et al.*, 2007) on a wild type background using the same drivers tested above.

A significant difference in period of flies expressing *dbt^S* and *dbt^L* (Preuss *et al.*, 2004; Muskus *et al.*, 2007) with *PdfG80*, *painG4* was observed compared to the controls, ($F_{(4, 49)}= 7.44$, $p<0.0001$; Figure 7-5A), with the period of *dbt^S* (23.01 ± 0.09 h) expressing flies being significantly shorter compared to *dbt^L* (24.03 ± 0.13 h) and the driver control (23.47 ± 0.13 h). These effects were also reflected with all the other antennal drivers (*FGAL4*, *pyxGAL4*, *iavGAL4*, *nompAGAL4* and *JOGAL4*; Figure 7-5 C-F).

Interestingly, expression of both *dbt* variants with *gmr>GAL4* did not show a significant difference between the short and long mutants (ANOVA $F_{(4,56)}=0.84$, $p=0.5$; Figure 7-6).

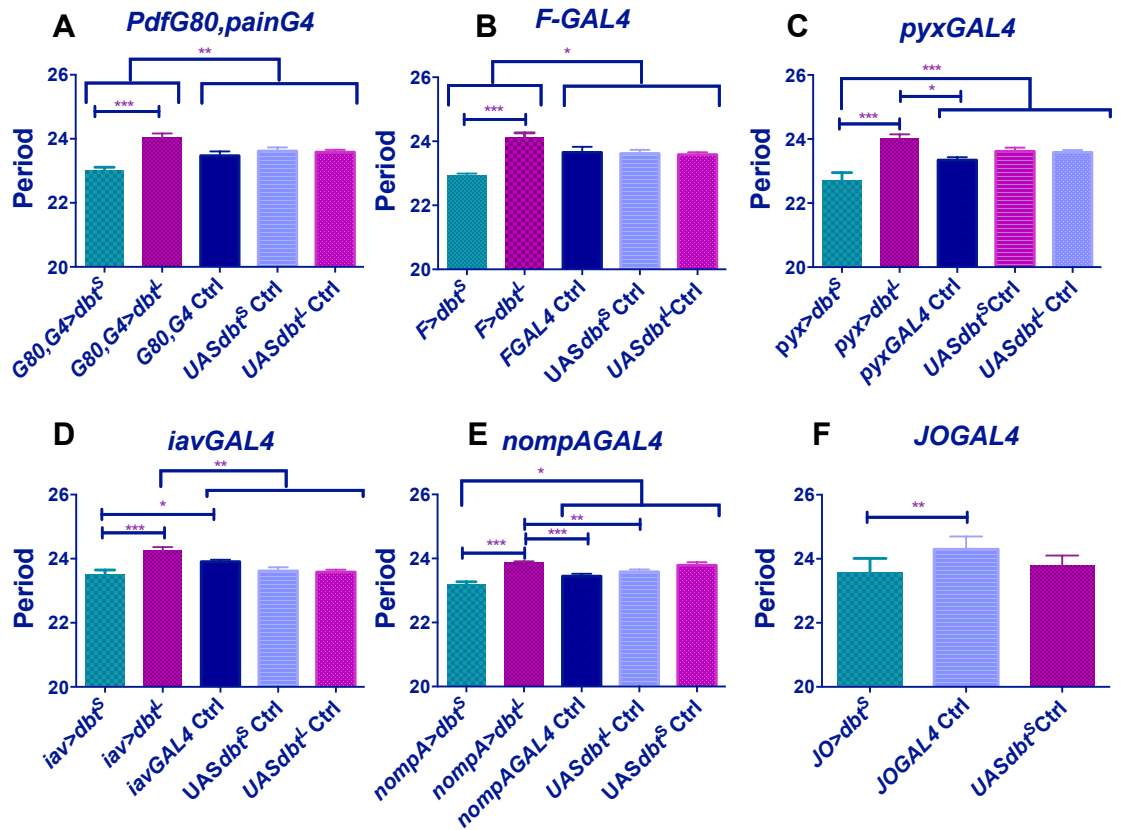


Figure 7-5 Expression of DBT mutants in the antennae is sufficient to trigger period changes.

A *PdfG80,painG4*. B *FGAL4* ($F_{(4, 66)} = 13.95$, $p < 0.0001$). C *pyxGAL4* ($F_{(4, 59)} = 10.78$, $p < 0.0001$) however flies expressing *dbt^L* did not show a significant difference with the two UAS controls. D *iavGAL4* ($F_{(4, 61)} = 9.070$, $p < 0.0001$) *iav>dbt^S* did not exhibit a significantly shorter period compared to the two UAS controls. E *nompAGAL4* ($F_{(4, 63)} = 14.28$, $p < 0.0001$). *nompA>dbt^L* flies did not show a significant difference with the two *UASdbt^S* control. F *JOGAL4* ($F_{(2, 41)} = 14.30$, $p < 0.001$). Flies expressing *dbt^S* did not show a significant difference with the *UASdbt^S* control. Unfortunately, *JO>dbt^L* was not tested before the submission of this study. *GAL4* Ctrl indicates the corresponding driver crossed to *w¹¹¹⁸*. Mean \pm SEM (Newman-Keuls *post hoc* test * $p < 0.05$, ** $p < 0.01$, *** $p < 0.001$). For period and Ns please refer to Table 7-2.

gmrGAL4

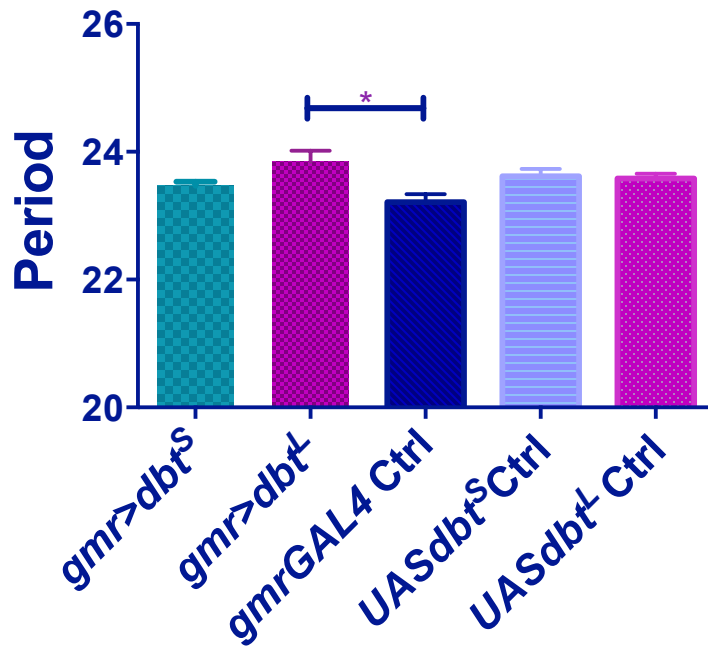


Figure 7-6 Expression of *dbt*-variants in the eyes does not trigger period changes. Mean \pm SEM (Newman-Keuls *post hoc* test * $p<0.05$, ** $p<0.01$, *** $p<0.001$). For period and Ns please refer to Table 7-2.

Additionally, the *UASdbt^{K/R}* mutant was also tested which lacks kinase activity due to a K88R missense mutation (Mus�us *et al.*, 2007), and is known to induce arrhythmia and longer periods by antagonizing the phosphorylation and degradation of PER (Mus�us *et al.*, 2007). I therefore decided to test it with the drivers that gave the most pronounced response with the other *dbt* mutants, *i.e.* *FGAL4*, *painGAL4* and *pyxGAL4*, and of *gmrGAL4*. *F>dbt^{K/R}* resulted in a significant decrease in the proportion of rhythmic flies ($\chi^2_{(2)} = 7.17$, $p < 0.05$; Figure 7-7A) but no period differences were observed (ANOVA $F_{(2,27)}=0.99$, $p=0.38$; Figure 7-7B). Expression of *dbt^{K/R}* under *pyrexia* control resulted in a significant increase of arrhythmic flies compared to controls ($\chi^2_{(2)} = 11.83$, $p < 0.01$; Figure 7-7A). The remaining flies showed a period slightly longer than controls (ANOVA $F_{(2,24)}=4.57$, $p < 0.05$; Figure 7-7C). Interestingly, *PdfG80,painG4>dbt^{K/R}* did not show increased arrhythmia ($\chi^2_{(2)} = 3.604$, $p = 0.15$; Figure 7-7A) but the period was longer than controls (ANOVA $F_{(2,34)}=5.06$, $p < 0.05$; Figure 7-7D) probably due to higher levels of expression (Mus�us *et al.*, 2007). Similarly, *gmrGAL4* flies did not show

a reduced rhythmicity ($\chi^2_{(2)} = 1.83$, $p= 0.4$; Figure 7-7A) but did reveal a longer period (ANOVA $F_{(2,29)}=4.47$, $p<0.05$; Figure 7-7E).

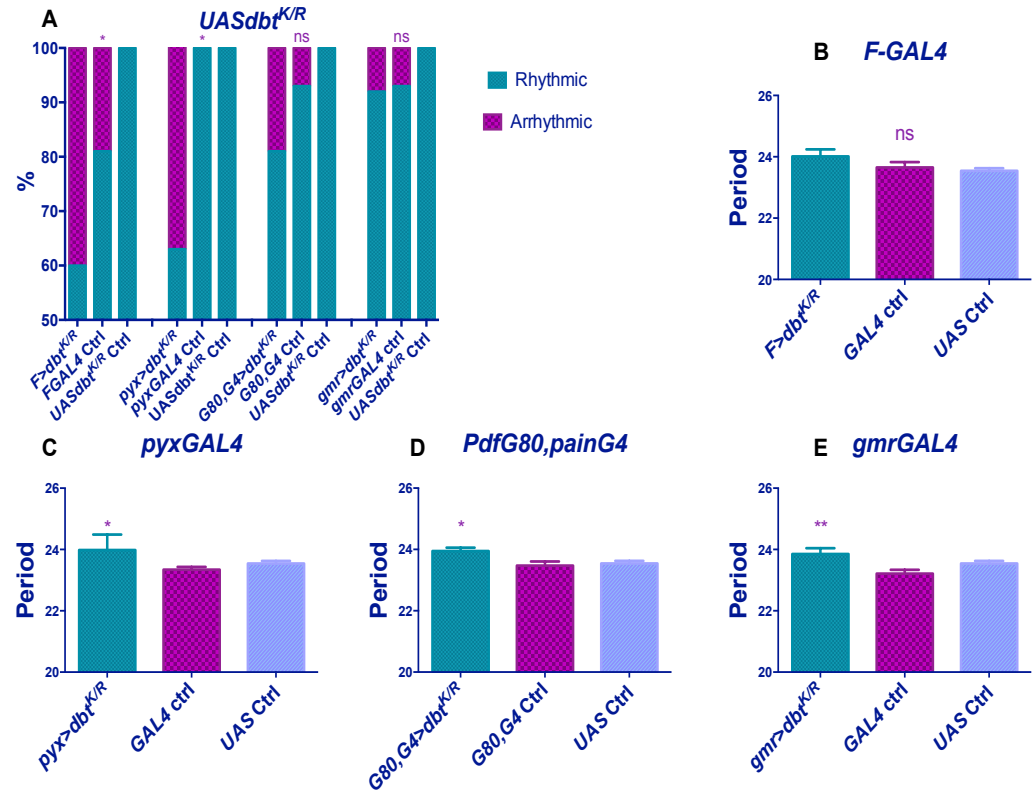


Figure 7-7 A Overexpression of *dbt^{K/R}* induces arrhythmia. B-E expression of *dbt^{K/R}* lengthens the period in all but *FGAL4* flies. Ctrl refers to *UASdbt^{K/R}* control crossed to *w¹¹¹⁸*. Mean \pm SEM (Newman-Keuls *post hoc* test * $p<0.05$, ** $p<0.01$, *** $p<0.001$). Mean \pm SEM (Newman-Keuls *post hoc* test * $p<0.05$, ** $p<0.01$, *** $p<0.001$). For period and Ns please refer to Table 7-2.

Table 7-2 Mean period \pm SEM and Ns for all the strains tested in this chapter.
NA=no antennae.

Genotype	Period	SEM	N	% Rhythmic	% Arrhythmic
<i>FGAL4</i> Ctrl	23.3	0.12	14	87	13
<i>F>dbt^{K/R}</i>	24.01	0.23	6	60	40
<i>F>dbt^L</i>	23.99	0.16	17	72	27
<i>F>dbt^S</i>	22.92	0.07	19	100	0
<i>gmr>dbt^{K/R}</i>	23.85	0.19	7	92	8
<i>gmr>dbt^L</i>	23.84	0.17	8	100	0
<i>gmr>dbt^S</i>	23.47	0.07	17	100	0
<i>gmrGAL4</i> ctrl	23.21	0.13	14	93	7
<i>iav>dbt^L</i>	24.25	0.11	26	96	4
<i>iav>dbt^S</i>	23.51	0.14	13	87	13
<i>iavGAL4</i> Ctrl	23.91	0.06	15	94	6
<i>Jo>dbt^S</i>	23.57	0.11	16	94	6
<i>JoGAL4</i> Ctrl	23.3	0.10	16	100	0
<i>nompA</i> Ctrl	23.23	0.05	14	94	6
<i>nompA>dbt^L</i>	23.87	0.04	19	100	81
<i>nompA>dbt^S</i>	23.19	0.08	13	87	13
<i>PdfG80,painG4</i> ctrl	23.47	0.07	13	84	16
<i>PdfG80,painG4>dbt^{K/R}</i>	23.95	0.11	13	81	19
<i>PdfG80,painG4>dbt^L</i>	23.89	0.10	12	100	0
<i>PdfG80,painG4>dbt^S</i>	23.01	0.10	7	85	14
<i>per^{D1};F>per</i>	28.67	1.56	18	60	40
<i>per^{D1};nompA>per</i>	30.05	1.78	8	47	53
<i>per^{D1};PdfG80,painG4>per;Pdf^{D1}</i>	26.51	1.21	11	27	73
<i>pyx>dbt^{K/R}</i>	23.98	0.50	3	63	37
<i>pyxGAL4</i> Ctrl	23.19	0.14	13	100	0
<i>UASdbt^{K/R}</i> Ctrl	23.54	0.08	11	100	0
<i>UASdbt^L</i> Ctrl	23.58	0.07	10	87	12
<i>UASdbt^S</i> Ctrl	23.79	0.10	12	80	20
<i>UASper</i> Ctrl	23.4	0.10	15	85	14
<i>w,per^{D1}</i>	NA	NA	32	0	100
<i>w,per^{D1};gmr>per</i>	25.84	0.68	14	80	20
<i>w,per^{D1};gmr>per;cry^{D2}</i>	28.29	0.36	3	18	81
<i>w,per^{D1};iav>per</i>	25.75	1.00	12	57	43
<i>w,per^{D1};Jo>per</i>	27.5	0.80	29	79	21
<i>w,per^{D1};JO>per (NA)</i>	29.9	0.40	5	22	78
<i>w,per^{D1};JO>per;cry^{D2}</i>	28.41	0.30	9	61	39
<i>w,per^{D1};PdfG80,painG4>per</i>	24.77	0.08	42	77	22
<i>w,per^{D1};PdfG80,painG4>per (NA)</i>	25.32	0.20	15	18	81
<i>w,per^{D1};PdfG80,painG4>per;cry^{D2}</i>	25.25	0.20	15	75	25
<i>w,per^{D1};pyx>per</i>	29.14	2.15	5	50	50
<i>w,per^{D1};pyx>per (NA)</i>	26.35	1.3	2	17	83
<i>w;;Pdf^{D1}</i>	23.25	0.18	13	54	46
<i>w;;pyx>dbt^{K/R}</i>	23.65	0.17	7	62	37
<i>w;;pyx>dbt^L</i>	23.89	0.15	17	100	0
<i>w;;pyx>dbt^S</i>	22.71	0.25	12	92	7
<i>w¹¹¹⁸</i>	24.03	0.15	21	86	14
<i>w¹¹¹⁸ (NA)</i>	24.36	0.16	7	77	22

7.3.3 ARE THESE DRIVERS EXPRESSED IN CANONICAL CLOCK NEURONS?

The drivers used in this experiments were chosen based on their expression patterns as published in the literature, with little or no staining in the central brain (Sun *et al.*, 2009). Nevertheless, additional expression controls were performed by crossing each driver to *UASgfp* (all IHC were performed by Dr Celia Hansen). Surprisingly, and in contrast to the literature, she found that some of the drivers (*PdfG80*, *painG4*, *pyxGAL4* and *FGAL4*) expressed in at least one I-LN_V (Figure 7-8). However, when a GFP-negative control was performed by crossing *UASGFP* to CS, I observed that also in this case, one or more I-LN_Vs were labelled, indicating that either the antisera is non-specific or the reporter line has some leakage. When this chapter was written no further controls had been performed and therefore it was not possible to rule out whether there was any expression of the antennal drivers in the I-LN_Vs.

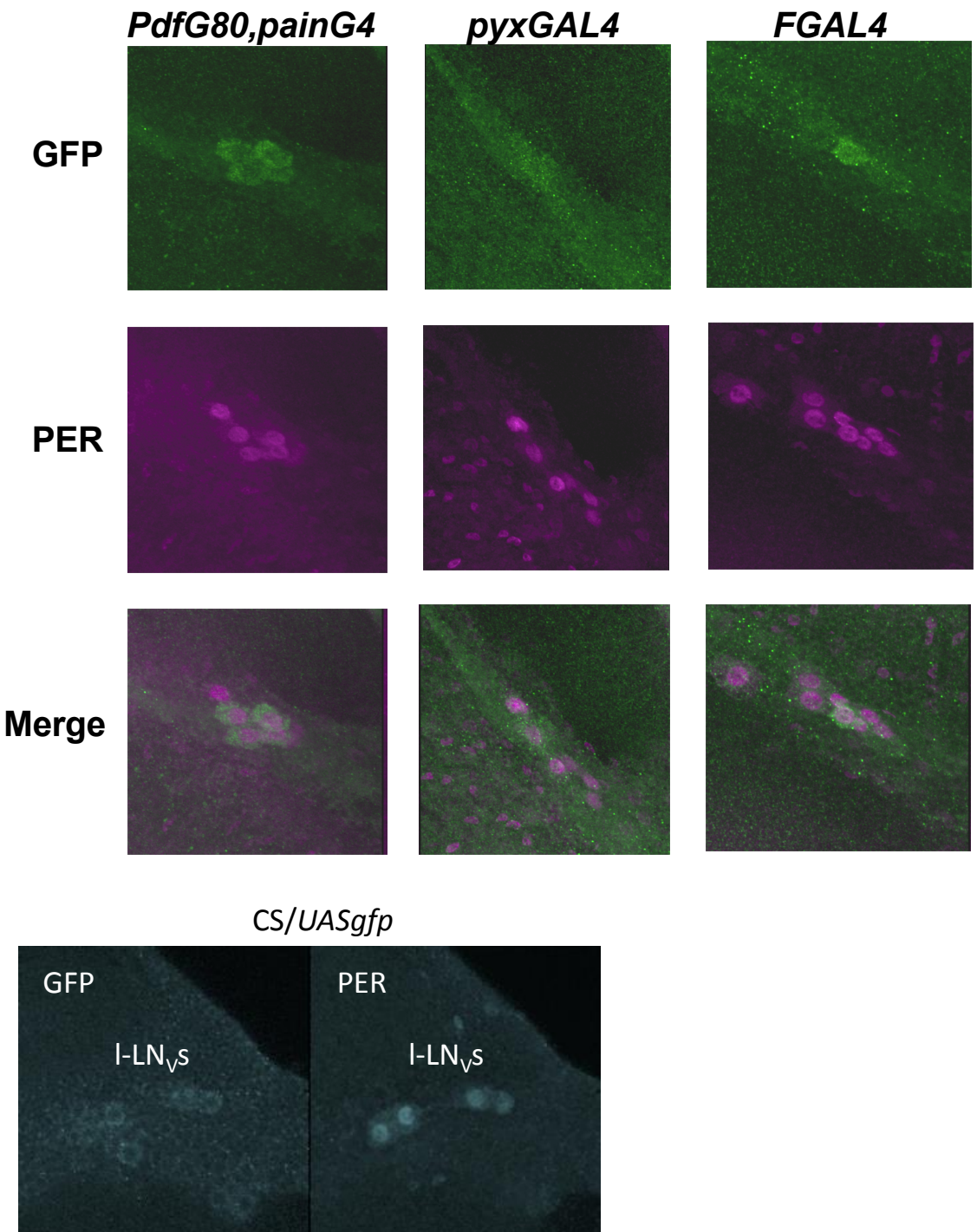


Figure 7-8 IHC showing I-LN_Vs labelled by GFP in *PdfG80,painG4*, *pyxGAL4* and *FGAL4* lines. In all these drivers at least one large PDF cell was labelled. Expression in I-LN_Vs of *FGAL4* was also described in Sehadova *et al.*, 2009. Bottom pictures represent expression of GFP in CS flies crossed to *UASGFP*. A weak GFP labelling can be observed in 3 I-LN_Vs neurons. Courtesy of Dr Hansen.

Interestingly however, I observed that *gmrGAL4*, that was reported to express in some ‘dorsal neurons’ (Vosshall & Young, 1995) did not in my hands label any dorsal clock cells. (Figure 7-9)

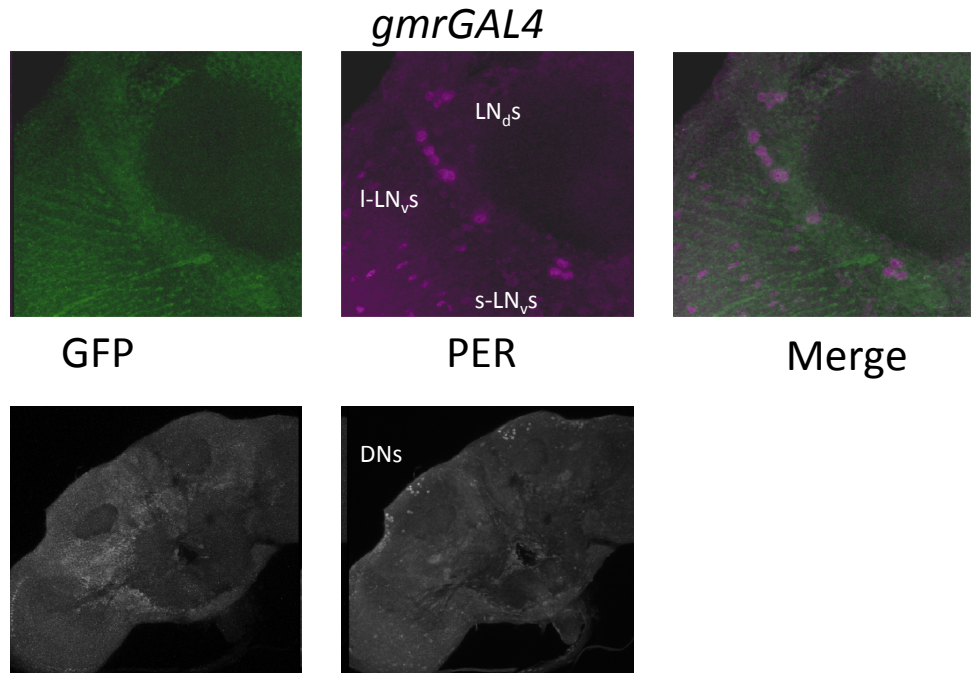


Figure 7-9 Expression of *gfp* driven by *gmrGAL4*. One I-LN_V was labelled (Top) whereas no dorsal neurons were labelled (Bottom) by GFP. Courtesy of Dr Hansen.

The GFP labelling detected in CS/UASGFP flies is comparable to the levels of expression detected in *pyxGAL4* and *gmrGAL4* therefore I can speculate that none of these drivers actually express in the I-LN_Vs whereas *FGAL4* expresses only in one of the large PDF-expressing cells, as already described in Sehadova *et al.*, (2009). A different situation has been observed in *painGAL4* flies where the expression of GFP in the I-LN_Vs seems stronger than in the negative controls.

GFP fluorescence labelling was checked and confirmed in the antennae of *PdfG80,painG4>GFP*, and *FGAL4>GFP* flies (Figure 7-11), whereas immunostaining on cryostat slices was performed for *nompAGAL4>GFP* and *iavGAL4>GFP* flies (Figure 7-11). Unfortunately, at the time this report was written, labelling in *JOGAL4* driver had not been tested.

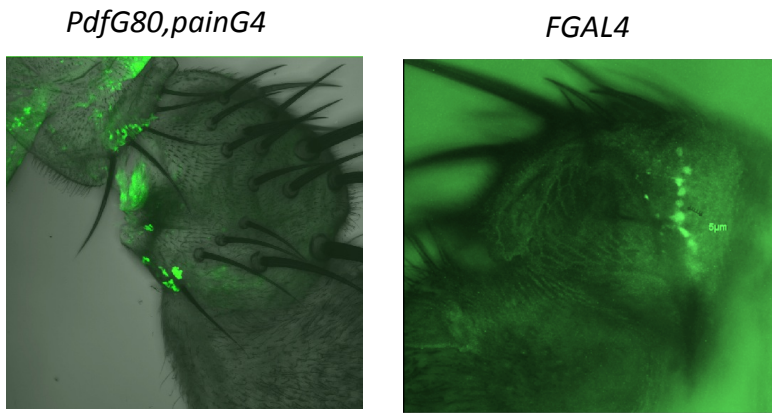


Figure 7-10 GFP-labelling in the antennae of *PdfG80,painG4* and *FGAL4*.

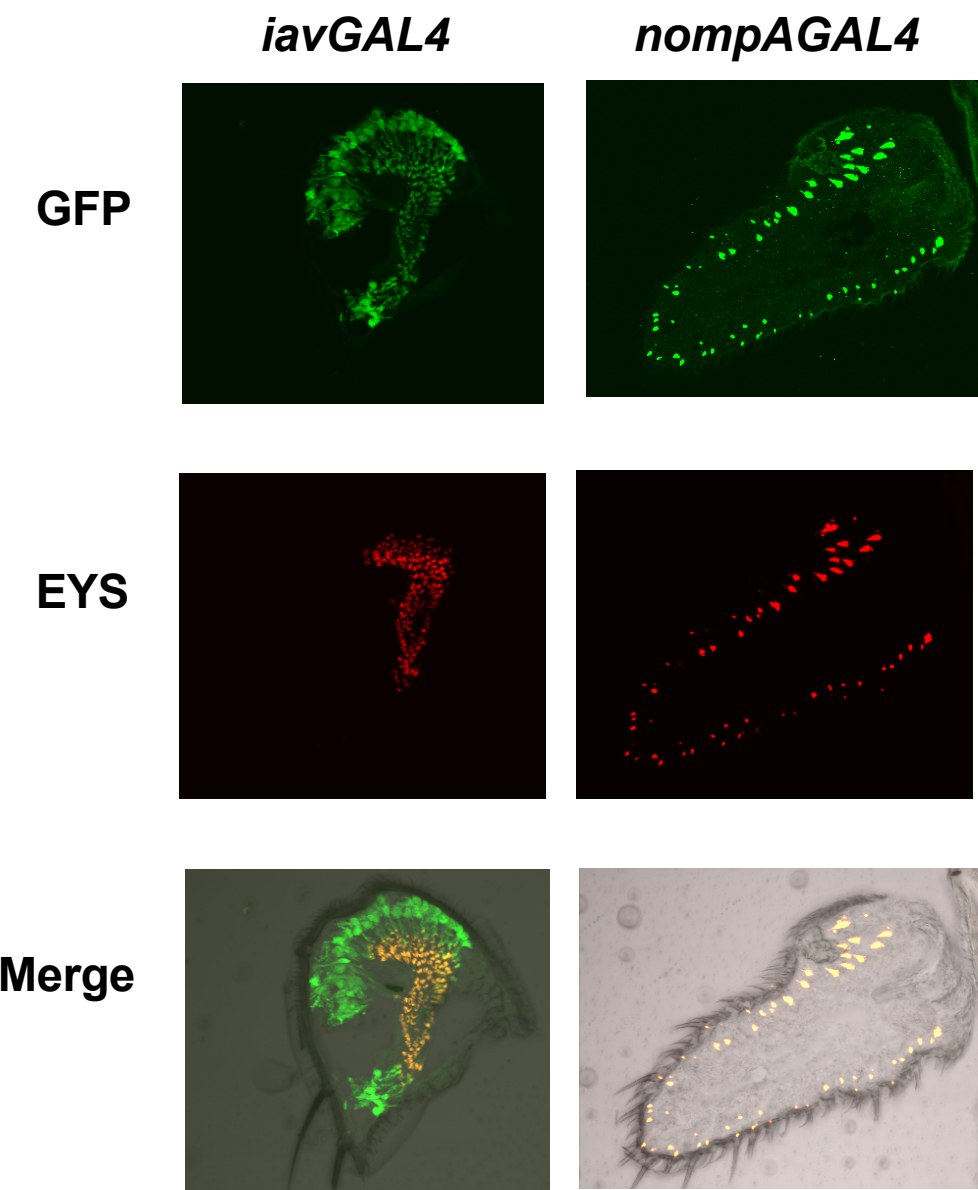


Figure 7-11 Cryostat sections of the antennae in *iavGAL4* and *nompAGAL4*. Images are reported as stacks.

7.4 DISCUSSION

In this chapter I focused my attention on how peripheral clocks might interact with the central “pacemaker”. Restricted expression of *per* in ChOs was sufficient to rescue the *per⁰¹* arrhythmic phenotype to at least 50% in all the tested lines. These striking and dramatic results further support the idea that circadian organization is a flexible and plastic network rather than a fixed system (Dissel *et al.*, 2014). Moreover, I observed that surgical removal of the antennae resulted in a highly significant fall of rhythmicity. This residual rhythmicity observed could be explained either by a non-complete removal of the antennae or by PER expression in some of the large PDF expressing cells. Interestingly, the resulting periods were all significantly longer than controls. This period lengthening could be explained by the fact that the majority of the drivers used might also expressed in one (or 3) I-LN_V. because the PDF expressing cells have a natural longer period (Dissel *et al.*, 2014). However, based on the expression of GFP in the negative controls (CS crossed to *UASGFP*) I can conclude that neither *pyxGAL4* or *gmrGAL4* seem to express in the I-LN_Vs, whereas *FGAL4* expresses in one large PDF cell (Sehadova *et al.*, 2009) and *painGAL4* does express in the large cells. Whether or not this expression is real or an artefact I can speculate that the activation of the large PDF-expressing cells in the latter, releases PDF, which will activate the nearby s-LN_Vs which have an endogenously greater than 24 h period (Dissel *et al.*, 2014).

This further supports the idea that the circadian clock is a plastic network rather than a fixed pacemaker, as there is no evidence that rhythms can be driven by a single (or 3 =maximum) large PDF expressing cells. These cells are involved in maintaining visual input rhythms (Helfrich-Förster *et al.*, 2007), in sleep/arousal behaviours and late night phase shifting (Shang, Griffith & Rosbash, 2008), but they are not required for rhythmic behaviour in DD (Grima *et al.*, 2004). However, if the staining observed in the I-LN_Vs is an artefact then the period lengthening could be due to an intercellular communication between the periphery and the CNS through yet unidentified pathways.

Nevertheless, the antennal (and eye) clocks are likely working through the canonical clock neuronal network because rhythmicity is lost in a *Pdf*⁰¹ background. Additionally, *per*⁰¹;:*cry*⁰² double mutants did not reduce the number of rhythmic flies when *per* was expressed in the antennae but did lead to longer rhythms. CRY is therefore not a canonical clock component in the antennae as implied by Krishnan *et al.* (Krishnan *et al.*, 2001a), but must play a role in the output of the antennal physiological cycles. In the eyes however, where the levels of CRY are abundant, the absence of *cry* triggered a significant drop in rhythmicity levels supporting its role as transcriptional repressor as previously suggested (Ivanchenko *et al.*, 2001; Collins *et al.*, 2006).

In addition, I also observed that overexpression of *dbt* variants in the antennae in a wild-type background, was sufficient to change the period in a predictable manner. In the eye however, expression of *dbt*^S does not shorten the period whereas expression of both *dbt*^L and *dbt*^{K/R} significantly lengthens the circadian rhythm. Thus it appears that both peripheral tissues may be normally contributing to the clock network in generating behavioural rhythms.

Taken together these observations reveal that the peripheral tissues are not only required for synchronization to environmental changes (*i.e.* vibration, heat etc (Sehadova *et al.*, 2009; Simoni *et al.*, 2014)) but also contribute to generating the behavioural circadian rhythm at central levels via intercellular communication, through as yet unidentified pathways. Indeed, one could reasonably now consider the antennae and the eye as part of the central clock. Interestingly, similar results were observed by Vosshall and Young in 1995, where circadian rhythms could be driven by a restricted group of neuronal cells, including some dorsal cells, using the *glass* promoter (Vosshall & Young, 1995). In this original study, expression of *per* in a *per*⁰¹ background using the *glass* promoter not only restored some rhythmicity but also exhibited period lengthening compared to controls (Vosshall & Young, 1995). In my study I observed a similar response when using *gmrGAL4* therefore but no expression in dorsal neurons was observed. I can speculate that this period lengthening could be mediated by the projections from the I-LN_s to the optic lobe (Helfrich-Forster *et al.*,

2007a); in other words, electrical activity from the eyes could reach the central clock therefore restoring a circadian rhythm (Dissel *et al.*, 2014).

In conclusion, these results have revealed an even more complex neuronal organization of the circadian clock in *D.melanogaster* that does not seem to simply rely on the canonical clusters of neurons (Morning and Evening neurons Allada & Chung, 2011) but confirm the idea of multiple oscillators coupled together in a plastic network (Dissel *et al.*, 2014).

8. FINAL CONCLUSIONS

In these studies we have investigated the role of the flavoprotein CRYPTOCHROME, in mediating EMF sensitivity *via* a quantum-chemical process known as the Radical Pair Mechanism (Ritz, Adem & Schulten, 2000; Rodgers & Hore, 2009).

A circadian paradigm was developed based on a previous publication (Yoshii, Ahmad & Helfrich-Förster, 2009) where weak circadian rhythms (*i.e.* under constant dim blue light) were modulated by exposure to 300 µT static field resulting in an overall lengthening of period suggesting a synergistic effect of EMF and light. In our circadian assay, using a more controlled exposure system, to avoid any form of artificial artefacts due to field heterogeneity, vibrations and temperature changes (Schuderer *et al.*, 2004), we observed a consistent and robust period shortening in wild type flies under a variety of field intensities (0, 3 and 50 Hz) and frequencies (90, 300 and 1000 µT). These responses were abolished under red light and in *cry*-null flies, whereas they were rescued by *cry* overexpression.

In addition, flies have been tested for their negative geotaxis, a complex trait which requires a functional CRY (Toma *et al.*, 2002; Rakshit & Giebultowicz, 2013). Flies showed a significant reduction in climbing ability in the presence of EMF compared to Sham exposure, but only under blue and not red light, suggesting a CRY-dependent EMF sensitivity (Fedele *et al.*, 2014). Further analysis revealed that these responses are modulated by the C-terminal tail (CT) of CRY and are independent of the classical Trp triad. In fact, under EMF exposure, *tim>cryΔ;cry⁰²*, flies failed to shorten their circadian rhythms and their climbing abilities were unaffected. In contrast, both the expression of the last 55 amino acid of the CT (*tim>cryCT;cry⁰²*) and of a CRY construct carrying a Trp to Phe amino acid substitution in position 342 (*tim>cryW342F;cry⁰²*, the final Trp involved in the electron transfer (Dodson, Hore & Wallace, 2013)) rescued the circadian EMF response (*tim>cryCT;cry⁰²* have not been tested for negative geotaxis).

These results suggest a role for CRY in EMF detection, but do not fit with the classical RPM model (Ritz *et al.*, 2000; Rodgers & Hore, 2009). First of all, it is not clear how the CT on its own could be EMF-sensitive since the FAD binding pocket is missing (Czarna *et al.*, 2013) and second, the results obtained with the W342F mutant can only be explained if other radicals from the hypothesized Trp-FAD (Ritz *et al.*, 2000, 2009), are involved in the REDOX reactions of FAD. While a clear explanation for the first problem is still missing, more and more evidence collected recently *in vivo* (Geegear *et al.*, 2010; Engels *et al.*, 2014) has opened the possibility that other yet unidentified radicals are equally important for an EMF-mediated response.

In particular, it has been shown that the same amino acid substitution (W342F) does not affect the light-dependent EMF sensitivity of flies in a conditioning assay (Geegear *et al.*, 2010) nor the ability of CRY to respond to light *in vitro* (Ozturk *et al.*, 2013). Moreover, it has been observed that *E. rubecula*, the European robin, is disoriented by a broadband of RF fields ranging from 2kHz to 9 MHz rather than a single 1.315 MHz radio frequency matching the Larmor frequency (Ritz *et al.*, 2004), providing a rationale for multiple radical partners. Molecular oxygen, tyrosine residues and ascorbic acid are among the most likely candidates (Müller & Ahmad, 2011; Biskup *et al.*, 2013; Engels *et al.*, 2014; Lee *et al.*, 2014). Further experiments will be required in order to identify these putative interactors and we suggest that a mutagenic screening of all possible residues of CRY capable of donating electrons to the FAD should be performed both *in vivo*, possibly using *Drosophila*, and *in vitro* exploiting purified CRY protein and performing EPR experiments to constantly monitor REDOX state (Timmel & Henbest, 2004).

An initial genetic dissection revealed that a generalized ectopic expression of CRY is not sufficient to rescue EMF phenotypes (both circadian and climbing). Among the clock neurons (Ozkaya & Rosato, 2012) only some CRY⁺ cells retain the ability to respond to the field, in particular the 3 CRY⁺ LN_ds and the 5th -sLN_v seem good candidates (see *Mai*¹⁷⁹>*cry*; *cry*⁰² response). These neurons are in fact able to retain rhythmicity under constant dim light (Rieger *et al.*, 2009). While with both phenotypes, expression of CRY driven by *PdfGAL4* did not show any EMF response, we cannot exclude the I-LN_vs playing a role due to the neuronal organization of the circadian

clock. The small PDF neurons strongly express PDFR, whereas the large do not (Im & Taghert, 2011), in this way we could speculate that the production of PDF from both large and small cells will further activate the latter. Therefore the activation of the small lateral cells could mask any effects coming from the large PDF expressing cells (Dissel *et al.*, 2014). Additionally, we also observed that expression of CRY in peripheral tissues (eyes and antennae) generates the EMF responses of period shortening and reduced climbing activity. It is worth noting, however, that these peripheral drivers may express GAL4 in 1 or 3 I-LN_s (see below), therefore providing a rationale for a putative role of these cells in also contributing to the EMF response.

Further analyses of our circadian assay also revealed a novel locomotor phenotype, which is not strictly related to the circadian period but is once again CRY-dependent, *i.e.* the hyperactivity of exposed flies. In wild type flies, Canton-S exposure to EMF significantly enhanced the levels of activity regardless of the frequency and intensity of the field (although the effect was abolished at 1 mT). Interestingly, this phenotype appears to be mediated by the N-terminal activity of CRY. Furthermore, CRY has been shown to be a neuronal activator (Fogle *et al.*, 2011; Dissel *et al.*, 2014): *tim>cryΔ;cry⁰²* flies which failed to manifest any other EMF induced response, nevertheless increased the activity levels, in contrast to *tim>cryCT;cry⁰²* flies..

Our circadian activity data seemed initially to contradict the results of Yoshii and coworkers, whose study suggested that exposure to EMF was increasing the effect of dim constant light, resulting in an overall period lengthening. This apparent contradiction has been resolved by exposing the flies to longer wavelengths 500±20 nm instead of 450±20 nm that was used in all our assays. This longer wavelength better overlaps the light wavelength used in (Yoshii *et al.*, 2009) (475 ± 20nm Helfrich-Forster personal communication) and exposure to such lighting conditions showed an overall period lengthening rather than period shortening in EMF exposed flies. This “antagonistic” response, previously observed and described in *Drosophila* (Phillips & Sayeed, 1993; Phillips, Jorge & Muheim, 2010a), is explained by the fact that at longer wavelengths the initial ratio of Singlet-Triplet states is altered, therefore resulting in a different product yield after the RPM reaction (Phillips *et al.*, 2010a) leading to equal but opposite responses. Interestingly similar effects were also observed in the

conditioning paradigm (Gegear *et al.*, 2008), although not mentioned by these authors but replicated in my studies, where wild type flies switched their naïve preference for the field, moving away under shorter wavelengths (<420 nm) and showing a preference for the field under longer ones (>420 nm). The biochemical basis for this intriguing result is unknown but will be one of the main focuses for future research in our laboratory.

Finally, preliminary biochemical assays (*in vitro* partial proteolysis and Co-IP) have shown interesting differences in CRY conformation and in its putative binding partners under EMF exposure that further support a role of CRY as a direct magnetoreceptor. A different conformational change induced by exposure to EMF could disrupt the normal CRY activity and/or binding ability, therefore modifying the downstream signals, explaining the observed phenotypes. If these observations could be replicated systematically, they would provide almost definitive proof that CRY is the magnetoreceptor.

Taken together all these observations seem to support a crucial role of CRY in mediating magnetosensing in *D.melanogaster*. None of our results, or any other published data, unambiguously confirm this function, and CRY could just as easily play a role upstream or downstream of the actual magnetoreceptor. While we acknowledge the difficulties of obtaining definitive proof for CRY as a magnetoreceptor we suggest a few experiments that might provide more insights.

First of all, a more detailed study of the role of magnetite in *Drosophila* needs to be assessed both *in vivo* and *in vitro*. Light responsive cation channels (TRPL for instance) or CRY itself might be linked to magnetite and trigger an EMF response only in the presence of favourable lighting conditions (Venkatachalam & Montell, 2007; Cadiou & McNaughton, 2010). The fact that both light-dependent and magnetic based EMF responses coexists in birds (Wiltschko *et al.*, 2007, 2010), and other animals such as Red spotted newts (Phillips *et al.*, 2010a), is suggestive. Additionally, recent evidence from European robins under RF fields has cast some doubt on the RPM. The fact that a broadband RF rather than the postulated Larmor frequency is capable of disorienting migratory birds, could be explained either by several other interacting

radicals (Engels *et al.*, 2014; Lee *et al.*, 2014), or by an iron clusters capable of detecting small electric and magnetic vectors from the RF radiation (Kirschvink, Winklhofer & Walker, 2010; Engels *et al.*, 2014; Kirschvink, 2014).

One possibility to test the effects of magnetite could be to feed flies with mercury which has a high affinity for magnetite (Wiatrowski *et al.*, 2009). If under strictly controlled conditions, we observe disrupted EMF behaviour, then we could assume that magnetite, not CRY is responsible. On the other hand, creating a light-responsive/EMF-unresponsive CRY (without affecting conformation and stability) should provide more biochemical hints to further understand CRYs role in the EMF responding pathway.

Again, more sophisticated *in vitro* studies should focus on the conformations assumed by CRY during EMF exposure. This could be achieved by partial trypsination assays similar to those described in our study. Moreover, the experiments we performed should be repeated with the addition of RF fields, both in broadband ranges or using the Larmor frequency (these experiments have been planned in collaboration with Prof Peter Hore, Oxford University). Also, a more detailed dose-response curve must be investigated. According to the RPM model, EMF field effects should be abolished at frequencies faster than the radical pair lifetime (ms) such as using frequencies above 50-60 Hz (Kato, 2006). Likewise, higher magnetic field intensities should also disrupt any response, as observed in (Yoshii *et al.*, 2009) with 500 µT. In fact, if the magnetic field is weaker than the hyperfine interaction, then the Zeeman splitting favours the interconversions between [S] to [T], whereas if the field is stronger, then the equilibrium between the two states is pushed toward the triplet, which has a net magnetic moment, and away from the singlet (Ritz *et al.*, 2000; Wang & Ritz, 2006; Abeyrathne, Halgamuge & Farrell, 2010; Ma & Ritz, 2014). In this respect, our 1 mT experiment showed a weaker circadian effect compared to the experiments performed at 90 or 300 µT, whereas no increased activity levels were observed, suggesting that probably 1 mT is at the edge of the sensitivity spectrum.

Finding the real magnetoreceptor molecule is only one of the two unanswered questions about magnetoreception in animals: nothing is said about the ecological

implications of sensing the geomagnetic field for a non-migratory animal like *Drosophila*. One possibility could be that the ability to sense a magnetic field could generate a 3D coordinate-system that helps to encode a variety of spatial information deriving from different inputs (Phillips, Muheim & Jorge, 2010b). Studying natural variation of EMF responsiveness should be one of the main focuses for future studies; if magnetoreception has evolved in *Drosophila* as the result of selective pressure then populations from different latitudes should in principle exhibit different response when tested under fixed conditions.

In addition, we have performed some preliminary studies investigating the role of peripheral clocks in controlling the central pacemaker and we observed that rhythms could be partially restored by expressing PER either in the antennae or in the eyes. However some of the antennal drivers used in this study seem to express also in the large PDF-expressing neurons, although this may represent an artefact due either to non-specific hybridization of the antibody or leakage in the *UASGFP* reporter line. There is no evidence that rhythms can be driven by a single (or 3 maximum) large PDF expressing cells and indeed removing the antennae reduced rhythmicity to almost *per*⁰ levels suggesting that any expression of PER in the large PDF cells, artefactual or bnot, was not functional. Either way, these fascinating results are in accordance with recent evidence that suggests that the circadian clock in *Drosophila* is a plastic neuronal network,

More importantly, for the first time we have demonstrated that the antennae and eyes are functional components of the central clock and should be considered so for future circadian studies, for example, by adopting the newly developed activity reporter system CaLexA (Calcium-dependent nuclear import of LexA) (Masuyama *et al.*, 2012).

In conclusion, this study has supported the evidence for a CRY-dependent magneto-sensitivity in fruit flies and hopefully will provide the bases for future studies aimed at the better understanding of this fascinating animal behaviour.

9 APPENDIX

Table 9-1 Buffer Formulation

Buffer	Final Concentration
10% SDS-page (for large gels 14x12 cm, run overnight at 12mA)	Resolving Gel: Acrylamide/bis-acrylamide 10% Tris-HCl 0.4 M pH 8.8 SDS 0.1 % APS 25% (Added Fresh) Temed 0.75% Double Distilled H ₂ O up to 40 mL
	Stacking Gel: Acrylamide/bis-acrylamide 4.5% Tris-HCl 0.1 M pH 6.8 SDS 0.1% APS 25% (Added Fresh) Temed 0.75% Double Distilled H ₂ O up to 15 mL
10X Laemli Running Buffer	Tris 25 mM Glycine 192 mM SDS 1% pH 8.4-8.9 Double Distilled H ₂ O up to 1L
10X TBS (Tris-Buffered Saline)	Tris 0.1 M pH 7.6

	NaCl 1.5 M
	Double Distilled H ₂ O up to 1L
	Tris 25 mM
10X Towbin Transfer Buffer (Wet)	Glycine 192 mM
(mA< 3.3 mA/cm ² for big gels or < 5.5 mA/cm ² for small gels)	Methanol 20% (v/v) pH 8.4-8.9
	Double Distilled H ₂ O up to 1L
	KH ₂ PO ₄ 10.58 mM
	Na ₂ HPO ₄ (H ₂ O) ₇ 29.66 mM
10XPBS (Phosphate-Buffered Saline)	NaCl 1.5 M
	pH 7.4
	Double Distilled H ₂ O up to 1L
	Tris 48 mM
	Glycine 39 mM
1X Bjerrum and Schafer-Nielsen transfer buffer (Semi Dry transfer)	Methanol 20% (v/v) SDS 1.3 mM (0.0375%)
	pH 9.2
	Double Distilled H ₂ O up to 1L
	Hepes 20 mM pH 7.5,
	KCl 100 mM
	EDTA 2.5 mM pH 8
1X Extraction Buffer (EB)	Glycerol 5%
	Triton X-100 0.5%
	DTT 1 mM

Protease Inhibitors (Roche)

Double Distilled H₂O up to 10 mL

SDS 4%

β-mercaptoethanol 10%

Glycerol 20%

2X Laemli Sample Buffer

Bromophenol blue 0.004%

Tris-HCl 0.125 M pH 6.5

Double Distilled H₂O up to 50 mL

5X KAPA Reaction Buffer 3 with MgCl²

5X PCR Buffer

KAPA dNTPs 10 μM (each)

Double Distilled H₂O up to 1 mL

Tris 250 mM, pH 6.8

EDTA 25 mM

SDS 10%

5X SDS Loading Buffer

β-mercaptoethanol 5%

Glycerol 30%

Bromophenol blue 0.004%

Double Distilled H₂O up to 50 mL

Tris-Cl 10 mM pH 8.2

EDTA 1 mM

Squishing Buffer (SB)

NaCl 25 mM

Double Distilled H₂O up to 100 mL

Table 9-2 Primers used for genotyping. All primers were designed using Primer3 Software.

Primers	Sequence	Tm (°C)	Size
	Common Forward		
	<i>CAGGTCTCTTCTGCCATC</i>		
<i>cry⁰²</i> genotyping	Reverse <i>cry⁺</i> <i>GCCCTCTTCCATTTCACA</i>	64	911 bp
	Reverse <i>cry⁰²</i> <i>CTCAAATGGTCCGAGTGGT</i>		956 bp
	Forward (for deletion) <i>TTAGTTGGACCCTCGGCTAA</i>		480 bp
<i>eya²</i> genotyping	Forward (flanking deletion) <i>CACTTAAGGATAAAATCGCAGTT</i>	62	377 bp in <i>eya²</i>
	Reverse <i>GGAGGATTCCATGTCCTCGG</i>		699 bp in wild type
GAL4 genotyping	Forward <i>CATTGGGCTTGAATAGGGA</i>	64	393 bp
	Reverse <i>TTAGAGCGGTGGTGGAAAT</i>		
GAL80 genotyping	Forward <i>TTCCCACTTAGAGTCATTGC</i>	64	385 bp
	Reverse <i>CCGTTCCCGATTCATAGA</i>		
<i>ls/s-tim</i> genotyping	LSTM Forward <i>TGGAATAATCAGAACTTGA</i>	55	631 bp
	STIM Forward		

	TGGAATAATCAGAACCTTTAT
	TIM Reverse
	AGATTCCACAAGATCGTGT
	TIM Control Forward
	CATTCATTCCAAGCAGTATC
	TIM Control Reverse
	TATTCATGAACTTGTGAATC
	397 bp

<i>Pdf</i> ⁰¹ genotyping	Forward		
	TGCTGCCAGTGGGGATAA	66	265 bp
	Reverse		
	CTTACTTGCCCCGCATCGT		
UAS genotyping	Forward		
	TGTCCCTCCGAGCAGGAGACTCTAG	64	238 bp
	Reverse		
	TTCTTGGCAGATTTCAGTAGTTGCAG		

9.1 EXPRESSION OF *UASGFPCRYCT*, *UASCRYW342F* AND *UASHCRY1* DRIVEN BY TIMGAL4.

Western blots of *tim>cryW342F; cry⁰²*, *tim>cryCT; cry⁰²* and *tim>hCRY1; cry⁰²* fly heads using anti-dCRY and anti-MYC (for *hCRY1* only) showing that the constructs are expressed and detectable. HSP70 and αTUB were used as loading control.

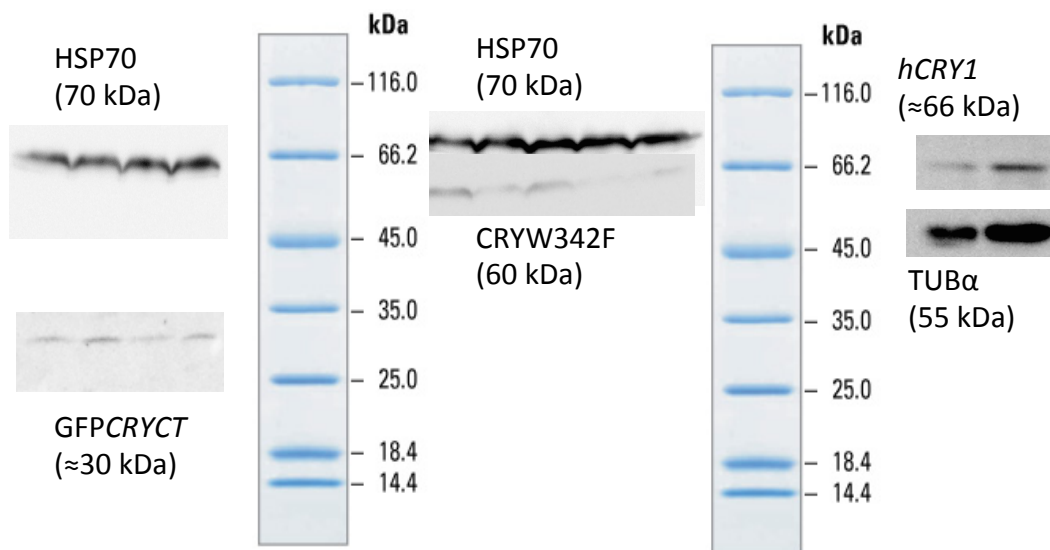


Table 9-3 Period Averages and Ns. ^a Mean difference Preexposure-Exposure for all flies. ^b Number of flies that showed period shortening. ^c Number of flies showing period lengthening during exposure. ^d Chi-square test for number of flies showing period shortening (Red values represent significance, dF = 1). Data presented in Chapters 3 and 4.

Genotype	Field	Exposure	Preexposure			Exposure			Δ Period ^a	SEM	N Short ^b	N Long ^c	% Short	% Long	χ^2 ^d	p		
			Period	SEM	N	% Rhythmic	Period	SEM										
CS	300 μ T 0Hz	EMF	28.86	0.81	22.00	68.8	26.91	0.55	27.00	84.4	1.95	0.83	13	9	59.1	40.9	2.44	0.12
		Sham	27.92	0.30	20.00	62.5	29.76	0.65	20.00	62.5	-1.84	0.91	7	13	35.0	65.0		
	300 μ T 50Hz	EMF	27.72	0.66	8.00	50.0	26.50	0.52	6.00	42.9	1.22	1.14	4	2	66.7	33.3	2.40	0.13
		Sham	28.08	0.94	6.00	37.5	30.23	1.31	5.00	35.7	-2.15	1.27	1	4	20.0	80.0		
	300 μ T 3Hz	EMF	27.28	0.24	49.00	77.7	26.39	0.20	50.00	80.6	0.90	0.33	25	16	61.0	39.0	7.53	0.01
		Sham	27.04	0.27	50.00	83.3	28.44	0.29	43.00	74.1	-1.40	0.34	13	29	31.0	69.0		
	90 μ T 3Hz	EMF	28.23	0.45	12.00	37.5	26.44	0.42	12.00	37.5	1.79	0.70	10	2	83.3	16.7	3.00	0.08
		Sham	28.55	0.51	12.00	37.5	28.80	0.58	12.00	37.5	-0.25	0.70	6	6	50.0	50.0		
cry ⁰²	1000 μ T 3Hz	EMF	28.55	0.45	11	68.8	27.33	0.43	13	81.3	1.22	0.61	8	4	66.7	33.3	1.65	0.20
		Sham	28.24	0.40	12	75.0	29.19	0.55	8	50.0	-0.95	0.68	3	5	37.5	62.5		
	300 μ T 3Hz Green	EMF	26.07	0.19	41.00	87.2	27.13	0.30	33.00	70.2	-1.06	0.36	11	22	33.3	66.7	0.80	0.36
		Sham	25.76	0.26	37.00	82.2	26.25	0.54	34.00	75.6	-0.49	0.37	15	19	44.1	55.9		
	DD 300 μ T 3Hz	EMF	23.81	0.15	16.00	100.0	24.39	0.14	16.00	100.0	-0.58	0.19	4	12	25.00	75.00	0.01	0.9
		Sham	23.80	0.11	13.00	92.86	24.23	0.11	13.00	92.86	-0.50	0.20	3	10	23.08	76.92		
	300 μ T 3Hz	EMF	23.92	0.13	16	100.0	24.43	0.14	16	100.0	-0.49	0.19	3	13	18.8	81.3	0.02	0.89
		Sham	24.12	0.13	12	85.7	24.49	0.18	12	85.7	-0.57	0.21	2	10	16.7	83.3		
tim>cry	300 μ T 3Hz	EMF	26.25	0.56	22.00	56.41	24.80	0.36	29.00	74.36	1.45	0.62	14	4	77.8	22.2	6.85	0.01
		Sham	26.69	0.52	20.00	55.56	27.75	0.40	12.00	33.33	-1.06	0.80	2	9	18.2	81.8		
	300 μ T 3Hz; cryW342F;cry ⁰²	EMF	24.45	0.09	15.00	93.8	24.03	0.16	15.00	93.8	0.43	0.22	9	6	60.0	40.0	0.85	0.36
		Sham	24.48	0.13	14.00	87.5	24.72	0.22	14.00	87.5	-0.24	0.22	6	8	42.9	57.1		
	tim>cry Δ ;cry ⁰²	EMF	26.35	0.21	45.00	75.0	26.64	0.20	48.00	80.0	-0.13	0.75	10	8	55.6	44.4	7.53	0.01
		Sham	26.62	0.39	44.00	73.3	27.42	0.37	41.00	70.7	-0.50	0.74	6	12	33.3	66.7		
	300 μ T 3Hz; tim>cryCT;cry ⁰²	EMF	24.32	0.12	31.00	96.9	24.24	0.09	31.00	96.9	0.08	0.15	16	15	51.6	48.4	3.98	0.04
		Sham	24.52	0.12	30.00	93.8	24.91	0.09	30.00	93.8	-0.39	0.15	8	22	26.7	73.3		
	DD 300 μ T 3Hz	EMF	23.87	0.11	23.00	88.46	24.18	0.10	23.00	88.46	-0.31	0.18	8	15	34.78	65.22	0.15	0.39
		Sham	24.02	0.14	19.00	79.17	24.27	0.19	21.00	87.50	-0.24	0.26	4	10	28.57	71.43		
tim>hCRY1;cry ⁰²	300 μ T 3Hz	EMF	24.42	0.12	14.00	43.8	24.43	0.17	14.00	43.8	-0.01	0.20	6	7	46.2	53.8	1.21	0.27
		Sham	24.16	0.17	12.00	37.5	24.48	0.11	14.00	43.8	-0.33	0.22	3	9	25.0	75.0		

(To be continued on the next page)

(Continued)

Genotype	Field	Exposure	Preexposure				Exposure				Δ Period ^a	SEM	N Short ^b	N Long ^c	% Short	% Long	χ^2 ^d	p
			Period	SEM	N	% Rhythmic	Period	SEM	N	% Rhythmic								
<i>tim>hCRY2;cry</i> ⁰²	300 μ T 3Hz	EMF	24.42	0.18	14	93.3	24.38	0.17	14	93.3	0.04	0.21	8	6	57.1	42.9	0.85	0.36
		Sham	24.05	0.11	15	93.8	24.16	0.12	16	100.0	-0.11	0.20	6	9	40	60.0		
<i>cry>cry;cry</i> ⁰²	300 μ T 3Hz	EMF	27.53	1.06	7	43.75	25.96	0.60	10	62.50	1.57	1.04	5	2	71.43	28.57	1.27	0.18
		Sham	26.26	0.69	8	50.00	28.93	0.65	7	43.75	-2.67	1.09	3	5	37.50	62.50		
<i>timG4cryG80>cry;cry</i> ⁰²	300 μ T 3Hz	EMF	25.74	0.88	15	93.75	27.88	1.52	7	43.75	-2.13	1.54	3	2	60.00	40.00	0.78	0.88
		Sham	26.10	1.00	12	75.00	28.49	0.77	6	37.50	-2.39	1.69	2	4	33.33	66.67		
<i>Pdf>cry;cry</i> ⁰²	300 μ T 3Hz	EMF	27.08	1.20	8	57.1	27.14	0.82	10	71.4	-0.06	1.47	4	4	50.00	50.00	0.48	0.48
		Sham	26.36	1.29	10	71.4	28.91	0.61	9	64.3	-2.55	1.42	3	6	33.33	66.67		
<i>Clk9>cry;cry</i> ⁰²	300 μ T 3Hz	EMF	24.69	0.72	9	64.29	24.57	0.26	12	85.71	0.12	0.69	5	4	55.56	44.44	2.81	0.09
		Sham	23.54	0.71	8	88.89	24.71	0.37	7	77.78	-1.16	0.82	1	6	14.29	85.71		
<i>tim>cry;cry</i> ⁰²	300 μ T 3Hz	EMF	26.37	0.40	5	41.7	24.00	0.76	10	83.3	2.37	0.91	7	1	87.50	12.50	7.53	0.01
		Sham	25.93	0.27	6	50.0	27.49	0.36	4	33.3	-1.56	1.08	0	5	0.00	100.00		
<i>tim>SGG</i>	300 μ T 3Hz	EMF	25.80	4.34	9	33.33	25.25	4.58	7	31.82	0.55	1.91	1	0	100.00	0.00	0.75	0.38
		Sham	25.52	2.18	7	25.93	28.19	2.49	3	13.64	-2.67	2.62	1	1	50.00	50.00		
<i>gmr>cry;cry</i> ⁰²	300 μ T 3Hz	EMF	27.34	0.55	7	50.0	26.72	0.42	11	78.6	0.62	0.67	5	1	83.33	16.67	4.41	0.04
		Sham	27.03	0.66	7	50.0	28.73	0.31	8	57.1	-1.70	0.72	1	4	20.00	80.00		
<i>R7>cry;cry</i> ⁰²	300 μ T 3Hz	EMF	24.13	0.16	30	93.75	23.90	0.18	31	96.88	0.23	0.25	13	16	44.83	55.17	9.69	0.01
		Sham	24.03	0.16	26	81.25	24.63	0.24	22.00	68.75	-0.60	0.28	1	20	4.76	95.24		
<i>glass</i> ⁰⁰	300 μ T 3Hz	EMF	24.63	0.21	10	62.50	23.71	0.17	9	56.25	0.93	0.35	6	2	75.00	25.00	2.26	0.13
		Sham	25.15	0.26	12	75.00	25.38	0.32	8	50.00	-0.22	0.35	3	5	37.50	62.50		
<i>pain>cry;cry</i> ⁰²	300 μ T 3Hz	EMF	24.67	0.25	16	61.54	23.10	0.62	20	76.92	1.57	0.75	8	4	66.67	33.33	2.29	0.10
		Sham	24.95	0.52	18	75.00	25.75	0.71	12	50.00	-0.81	0.83	3	6	33.33	66.67		
<i>Jo>cry;cry</i> ⁰²	300 μ T 3Hz	EMF	26.74	0.57	9	75.00	28.45	1.02	5	41.67	-1.71	0.90	1	4	20.00	80.00	0.90	0.30
		Sham	28.02	0.41	6	54.55	31.94	0.43	4	36.36	-3.92	1.04	0	4	0.00	100.00		
<i>N.vitripennis</i>	300 μ T 3Hz	EMF	23.58	0.08	27	84.38	23.92	0.11	25	78.13	-0.34	0.14	7	18	43.75	56.25	1.04	0.33
		Sham	23.63	0.06	28	87.50	23.99	0.13	25	78.13	-0.36	0.14	4	21	30.77	69.23		
<i>tim>cryΔ;cry</i> ⁰²	DD	NA	25.30	0.14	20.00	83.33												
<i>tim>cryW342F;cry</i> ⁰²	DD	NA	23.99	0.19	14	100												
<i>tim>cryCT;cry</i> ⁰²	DD	NA	23.95	0.12	14.00	93.33												
<i>UAScryCT/w</i> ¹¹⁸	DD	NA	23.41	0.08	23.00	95.83												
<i>tim>hCRY1;cry</i> ⁰²	DD	NA	24.28	0.18	15.00	93.75												
<i>tim>hCRY2;cry</i> ⁰²	DD	NA	24.30	0.11	16.00	100.00												
<i>tim>cryΔ;cry</i> ⁰²	LL	NA	26.50	0.40	16.00	100.00												
<i>tim>cryW342F;cry</i> ⁰²	LL	NA	24.51	0.08	23.00	92.00												
<i>tim>cryCT;cry</i> ⁰²	LL	NA	24.42	0.08	40.00	88.89												
<i>tim>hCRY1;cry</i> ⁰²	LL	NA	24.29	0.10	26.00	81.25												
<i>tim>hCRY2;cry</i> ⁰²	LL	NA	24.22	0.11	29.00	90.63												

Table 9-4 Mean Activity levels and Ns. Data presented in Chapters 3 and 4.

Genotype	Field	Exposure	Activity	SEM	N	% Rhythmic	Activity	SEM	N	% Rhythmic
CS	300 µT 0Hz	EMF	13.11	0.79	22.00	68.8	16.82	0.59	27.00	84.4
		Sham	14.03	1.14	20.00	62.5	12.30	1.56	20.00	62.5
	300 µT 50Hz	EMF	13.02	0.59	8.00	50.0	18.10	1.38	6.00	42.9
		Sham	12.59	0.55	6.00	37.5	12.79	0.63	5.00	35.7
	300 µT 3Hz	EMF	18.57	0.72	49.00	77.7	22.89	0.91	50.00	80.6
		Sham	18.65	0.80	50.00	83.3	19.09	0.81	43.00	74.1
	90 µT 3Hz	EMF	18.27	0.61	12.00	37.5	22.41	1.00	12.00	37.5
		Sham	19.00	0.56	12.00	37.5	17.93	1.31	12.00	37.5
	1000 µT 3Hz	EMF	17.15	1.97	11	68.8	20.11	1.77	13	81.3
		Sham	15.78	1.27	12	75.0	18.63	2.25	8	50.0
	300 µT 3Hz Green	EMF	11.74	1.29	41.00	87.2	5.99	0.63	33.00	70.2
		Sham	9.74	1.27	37.00	82.2	5.77	0.74	34.00	75.6
<i>cry</i> ⁰²	300µT 3Hz	EMF	9.16	1.31	16	100.0	6.98	1.23	16	100.0
		Sham	10.34	1.92	12	85.7	8.38	1.60	12	85.7
	<i>tim>cry</i>	EMF	14.25	0.96	22.00	56.41	16.60	1.11	29.00	74.36
		Sham	14.03	1.56	20.00	55.56	11.13	1.22	12.00	33.33
	<i>tim>cryW342F; cry</i> ⁰²	EMF	13.84	1.71	15.00	93.8	21.13	1.78	15.00	93.8
		Sham	14.33	1.66	14.00	87.5	10.74	1.73	14.00	87.5
<i>tim>cryΔ; cry</i> ⁰²	300µT 3Hz	EMF	11.16	1.12	45.00	75.0	14.90	0.66	48.00	80.0
		Sham	11.16	0.97	44.00	73.3	9.13	0.52	41.00	70.7
	<i>tim>cryCT; cry</i> ⁰²	EMF	20.53	1.87	31.00	96.9	18.07	1.11	31.00	96.9
		Sham	14.47	1.34	30.00	93.8	9.96	1.26	30.00	93.8
	DD 300µT 3Hz	EMF	23.71	2.36	23.00	88.5	17.41	1.76	23.00	88.5
		Sham	21.18	3.03	19.00	79.2	16.41	2.03	21.00	87.5
<i>tim>hCRY1; cry</i> ⁰²	300µT 3Hz	EMF	14.45	1.83	14.00	43.8	17.42	2.80	14.00	43.8
		Sham	15.29	2.41	12.00	37.5	15.55	2.17	14.00	43.8
	300µT 3Hz	EMF	15.66	1.46	14	93.3	20.66	1.52	14	93.3
		Sham	14.83	1.58	15	93.8	12.96	1.31	16	100.0
	<i>cry>cry; cry</i> ⁰²	EMF	15.85	1.90	7	43.75	24.20	2.10	10	62.50
		Sham	16.42	1.49	8	50.00	13.17	2.45	7	43.75
<i>timG4cryG80>cry; cry</i> ⁰²	300µT 3Hz	EMF	11.70	1.40	15	93.75	12.71	2.38	7	43.75
		Sham	7.73	1.24	12	75.00	10.67	1.99	6	37.50
	<i>Pdf>cry; cry</i> ⁰²	EMF	12.00	1.48	8	57.1	12.90	1.71	10	71.4
		Sham	12.23	1.74	10	71.4	8.98	1.29	9	64.3
	<i>Clk9>cry; cry</i> ⁰²	EMF	13.10	3.50	9	64.3	6.31	1.11	12	85.7
		Sham	17.93	2.45	8	88.9	9.31	1.06	7	77.8
<i>tim>cry; cry</i> ⁰²	300µT 3Hz	EMF	13.80	0.92	5	31.3	17.90	1.34	10	71.4
		Sham	13.93	1.19	6	37.5	10.75	1.49	4	25.0
	<i>tim>SGG</i>	EMF	12.32	2.68	9	33.33	13.58	6.08	7	31.82
		Sham	12.94	6.00	7	25.93	3.54	2.70	3	13.64
	<i>gmr>cry; cry</i> ⁰²	EMF	9.29	0.81	7	50.0	11.09	0.96	11	78.6
		Sham	9.20	0.93	7	50.0	7.28	0.53	8	57.1
<i>R7>cry; cry</i> ⁰²	300µT 3Hz	EMF	10.90	1.38	30	93.8	6.94	1.01	31	96.9
		Sham	11.17	1.22	26	81.3	7.60	1.02	22	68.8
	<i>glass</i> ^{60j}	EMF	15.89	2.36	10	62.50	20.59	2.66	9	56.25
		Sham	16.12	1.30	12	75.00	12.14	1.35	8	50.00
	<i>Pain>cry; cry</i> ⁰²	EMF	8.16	0.77	16	61.54	6.84	1.05	20	76.92
		Sham	6.74	0.83	18	75.00	4.88	1.00	12	50.00
<i>JO>cry; cry</i> ⁰²	300µT 3Hz	EMF	15.72	1.70	9	75.0	13.11	0.84	5	41.7
		Sham	14.60	1.49	6	54.5	13.61	0.78	4	36.4
	<i>N.vitripennis</i>	EMF	12.33	7.83	27	84.4	12.62	7.77	25	78.1
		Sham	11.30	4.29	28	87.5	12.25	6.68	25	78.1

9.2 REPLICATING REPPERT'S EXPERIMENTS

In order to increase the statistical power of our experiments, we decided to test individual flies instead of a population and so I designed a maze consisting of a rack where 20 glass tubes are held horizontally, one above the other (Figure 9-1). The sides of the vials are left open and they fit into specific holes in the rack, thereby communicating with the external surface of the rack. On each side of the rack, two sliding panels are placed (Figure 9-1). The panels are split into two vertical regions: one with bowls, where will be placed the sucrose reward, and the other is empty allowing me to expose food reward to the flies only on one side of the rack by sliding manually the panels back and forth. This configuration permits me to change the food position from one side to the other, during the conditioning. Between each tube an opaque plastic slide is placed in order to avoid any biasing the fly's behaviour due to imitation of other flies' movements. All the rack parts are metal-free.

The webcams, plugged into a laptop, are placed in front of the maze allowing filming of flies' movements inside each tube. The tracking software from Actual Analytics (University of Edinburgh) is used to track the flies in each tube. The software's output can be analyzed statistically to investigate which regions of the tube the flies prefer to spend their time, an index of previous associations. Webcams and LEDs are placed at a distance greater than the coil's radius to avoid any perturbation of the magnetic field. The entire apparatus has been put in a temperature-controlled room (25°C) and away from any other electrical appliances that may interfere with the magnetic field.

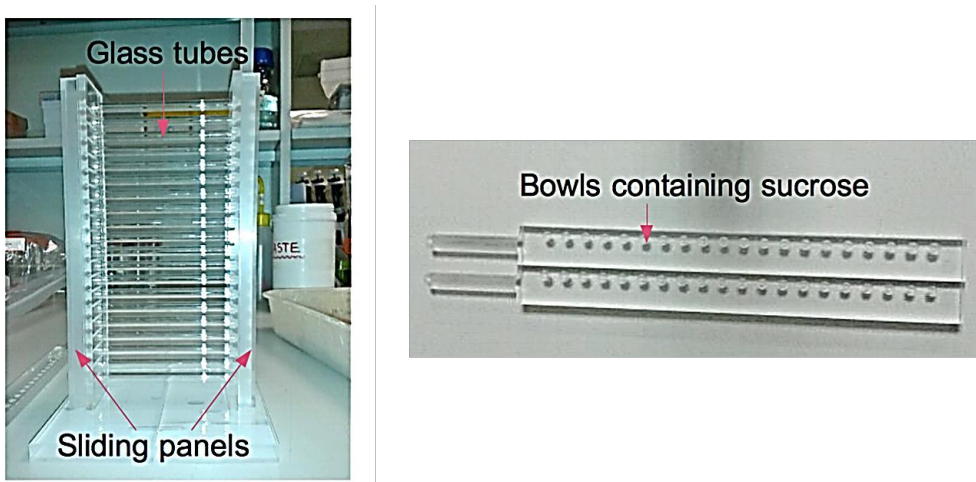


Figure 9-1 Rack and sliding panels.

Unfortunately, we were not able to obtain a decent trace of the flies and therefore their EMF response resulted completely random.

10 BIBLIOGRAPHY

- Abeyrathne, C., Halgamuge, M. & Farrell, P. (2010). Effect of Magnetic Field on the Biological Clock through the Radical Pair Mechanism. *World Acad. Sci. Eng. Technol.* **4**, 141–146.
- Acosta-Avalos, D., Wajnberg, E., Oliveira, P., Leal, I., Farina, M. & Esquivel, D. (1999). Isolation of magnetic nanoparticles from pachycondyla marginata ants. *J. Exp. Biol.* **202**, 2687–2692.
- Ahmad, M., Galland, P., Ritz, T., Wiltschko, R. & Wiltschko, W. (2007). Magnetic intensity affects cryptochrome-dependent responses in *Arabidopsis thaliana*. *Planta* **225**, 615–24.
- Akten, B., Jauch, E., Genova, G.K., Kim, E.Y., Edery, I., Raabe, T. & Jackson, F.R. (2003). A role for CK2 in the *Drosophila* circadian oscillator. *Nat. Neurosci.* **6**, 251–7.
- Allada, R. & Chung, B.Y. (2010). Circadian organization of behavior and physiology in *Drosophila*. *Annu. Rev. Physiol.* **72**, 605–24.
- Allada, R. & Chung, B.Y. (2011). NIH Public Access 605–624.
- Allada, R., White, N.E., So, W.V., Hall, J.C. & Rosbash, M. (1998a). A mutant *Drosophila* homolog of mammalian Clock disrupts circadian rhythms and transcription of period and timeless. *Cell* **93**, 791–804.
- Allada, R., White, N.E., So, W.V., Hall, J.C. & Rosbash, M. (1998b). A mutant *Drosophila* homolog of mammalian Clock disrupts circadian rhythms and transcription of period and timeless. *Cell* **93**, 791–804.
- Allebrandt, K. V., Amin, N., Müller-Myhsok, B., Esko, T., Teder-Laving, M., Azevedo, R.V.D.M., Hayward, C., van Mill, J., Vogelzangs, N., Green, E.W., Melville, S.A., Lichtner, P., Wichmann, H.-E., Oostra, B.A., Janssens, A.C.J.W., Campbell, H., Wilson, J.F., Hicks, A.A., Pramstaller, P.P., Dogas, Z., Rudan, I., Merrow, M., Penninx, B., Kyriacou, C.P., Metspalu, A., van Duijn, C.M., Meitinger, T. & Roenneberg, T. (2013). A K(ATP) channel gene effect on sleep duration: from genome-wide association studies to function in *Drosophila*. *Mol. Psychiatry* **18**, 122–32.
- Ashworth, S.H. (2012). Molecular Quantum Mechanics, 5th edn, by Peter Atkins and Ronald Friedman. *Contemp. Phys.* **53**, 372–373.
- Bargiello, T.A., Jackson, F.R. & Young, M.W. (1984). Restoration of circadian behavioural rhythms by gene transfer in *Drosophila*. *Nature* **312**, 752–754.

- Benito, J., Houl, J.H., Roman, G.W. & Hardin, P.E. (2008). The blue-light photoreceptor CRYPTOCHROME is expressed in a subset of circadian oscillator neurons in the *Drosophila* CNS. *J. Biol. Rhythms* **23**, 296–307.
- Berndt, A., Kottke, T., Breitkreuz, H., Dvorsky, R., Hennig, S., Alexander, M. & Wolf, E. (2007). A novel photoreaction mechanism for the circadian blue light photoreceptor *Drosophila* cryptochromes. *J. Biol. Chem.* **282**, 13011–21.
- Biskup, T., Paulus, B., Okafuji, A., Hitomi, K., Getzoff, E.D., Weber, S. & Schleicher, E. (2013). Variable electron transfer pathways in an amphibian cryptochromes: tryptophan versus tyrosine-based radical pairs. *J. Biol. Chem.* **288**, 9249–60.
- Blakely, R. (1998). *Introduction to geomagnetic fields. Eos, Trans. Am. Geophys. Union.*
- Blakemore, R. (1975). Magnetotactic bacteria. *Science (80-.)* **190**, 377–379.
- Blau, J. & Young, M.W. (1999). Cyclin vrille expression is required for a functional *Drosophila* clock. *Cell* **99**, 661–71.
- Bogdanov, A.M., Mishin, A.S., Yampolsky, I. V., Belousov, V. V., Chudakov, D.M., Subach, F. V., Verkhusha, V. V., Lukyanov, S. & Lukyanov, K. a. (2009). Green fluorescent proteins are light-induced electron donors. *Nat. Chem. Biol.* **5**, 459–61.
- Bouly, J.-P., Schleicher, E., Dionisio-Sese, M., Vandenbussche, F., Van Der Straeten, D., Bakrim, N., Meier, S., Batschauer, A., Galland, P., Bittl, R. & Ahmad, M. (2007). Cryptochromes blue light photoreceptors are activated through interconversion of flavin redox states. *J. Biol. Chem.* **282**, 9383–91.
- Brand, A.H. & Perrimon, N. (1993). Targeted gene expression as a means of altering cell fates and generating dominant phenotypes. *Development* **118**, 401–15.
- Cadiou, H. & McNaughton, P. a. (2010). Avian magnetite-based magnetoreception: a physiologist's perspective. *J. R. Soc. Interface* **7 Suppl 2**, S193–205.
- Campbell, W. H. (2003). Introduction to Geomagnetic Fields, Second Edition, pp. 350. ISBN 0521822068. Cambridge, UK: Cambridge University Press, July 2003.
- Cashmore, A.R. (2003). Cryptochromes. *Cell* **114**, 537–543.
- Chang, D.C. (2006). Neural circuits underlying circadian behavior in *Drosophila melanogaster*. *Behav. Processes* **71**, 211–25.
- Chaves, I., Pokorny, R., Byrdin, M., Hoang, N., Ritz, T., Brettel, K., Essen, L.-O., van der Horst, G.T.J., Batschauer, A. & Ahmad, M. (2011). The cryptochromes: blue light photoreceptors in plants and animals. *Annu. Rev. Plant Biol.* **62**, 335–64.

- Chen, K.F., Peschel, N., Zavodska, R., Sehadova, H. & Stanewsky, R. (2011). QUASIMODO, a Novel GPI-anchored zona pellucida protein involved in light input to the Drosophila circadian clock. *Curr. Biol.* **21**, 719–29.
- Chen, Y., Akin, O., Nern, A., Tsui, C.Y.K., Pecot, M.Y. & Zipursky, S.L. (2014). Cell-type-specific labeling of synapses *in vivo* through synaptic tagging with recombination. *Neuron* **81**, 280–93.
- Chiu, J.C., Ko, H.W. & Edery, I. (2011). NEMO/NLK phosphorylates PERIOD to initiate a time-delay phosphorylation circuit that sets circadian clock speed. *Cell* **145**, 357–70.
- Collins, B., Mazzoni, E.O., Stanewsky, R. & Blau, J. (2006). Drosophila CRYPTOCHROME is a circadian transcriptional repressor. *Curr. Biol.* **16**, 441–9.
- Czarna, A., Berndt, A., Singh, H.R., Grudziecki, A., Ladurner, A.G., Timinszky, G., Kramer, A. & Wolf, E. (2013). Structures of Drosophila cryptochrome and mouse cryptochrome1 provide insight into circadian function. *Cell* **153**, 1394–405.
- Dalle-Donne, I., Rossi, R., Giustarini, D., Milzani, A. & Colombo, R. (2003). Protein carbonyl groups as biomarkers of oxidative stress. *Clin. Chim. Acta* **329**, 23–38.
- Damulewicz, M. & Pyza, E. (2011). The clock input to the first optic neuropil of *Drosophila melanogaster* expressing neuronal circadian plasticity. *PLoS One* **6**, e21258.
- Damulewicz, M., Rosato, E. & Pyza, E. (2013). Circadian regulation of the Na⁺/K⁺-ATPase alpha subunit in the visual system is mediated by the pacemaker and by retina photoreceptors in *Drosophila melanogaster*. *PLoS One* **8**, e73690.
- Demorest, P. (2001). *Dynamo Theory and Earth's Magnetic Field*.
- Deutschlander, M.E.M., Phillips, J.B. & Borland, C.S. (1999). The case for light-dependent magnetic orientation in animals. *J. Exp. Biol.* **202**, 891–908.
- Dissel, S., Codd, V., Fedic, R., Garner, K.J., Costa, R., Kyriacou, C.P. & Rosato, E. (2004). A constitutively active cryptochrome in *Drosophila melanogaster*. *Nat. Neurosci.* **7**, 834–40.
- Dissel, S., Hansen, C.N., Özkaya, Ö., Hemsley, M., Kyriacou, C.P. & Rosato, E. (2014). The Logic of Circadian Organization in *Drosophila*. *Curr. Biol.*
- Dodson, C. a, Hore, P.J. & Wallace, M.I. (2013). A radical sense of direction: signalling and mechanism in cryptochrome magnetoreception. *Trends Biochem. Sci.* **38**, 435–46.

- Dolezelova, E., Dolezel, D. & Hall, J.C. (2007). Rhythm defects caused by newly engineered null mutations in *Drosophila*'s cryptochrome gene. *Genetics* **177**, 329–45.
- Dommer, D.H., Gazzolo, P.J., Painter, M.S. & Phillips, J.B. (2008). Magnetic compass orientation by larval *Drosophila melanogaster*. *J. Insect Physiol.* **54**, 719–26.
- Dormy, E. & Le Mouël, J.-L. (2008). Geomagnetism and the dynamo: where do we stand? *Comptes Rendus Phys.* **9**, 711–720.
- Dunlap, J.C. (1999). Molecular Bases for Circadian Clocks. *Cell* **96**, 271–290.
- Eberl, D.F. & Boekhoff-Falk, G. (2007). Development of Johnston's organ in *Drosophila*. *Int. J. Dev. Biol.* **51**, 679–87.
- Eder, S.H.K., Cadiou, H., Muhamad, A., McNaughton, P. a, Kirschvink, J.L. & Winklhofer, M. (2012). Magnetic characterization of isolated candidate vertebrate magnetoreceptor cells. *Proc. Natl. Acad. Sci. U. S. A.* **109**, 12022–7.
- Edery, I., Rutila, J.E. & Rosbash, M. (1994). Phase shifting of the circadian clock by induction of the *Drosophila* period protein. *Science* **263**, 237–40.
- Emery, P., So, W.V., Kaneko, M., Hall, J.C. & Rosbash, M. (1998). CRY, a *Drosophila* Clock and Light-Regulated Cryptochrome, Is a Major Contributor to Circadian Rhythm Resetting and Photosensitivity. *Cell* **95**, 669–679.
- Emery, P., Stanewsky, R., Hall, J.C. & Rosbash, M. (2000). A unique circadian-rhythm photoreceptor. *Nature* **404**, 456–7.
- Engels, S., Schneider, N.-L., Lefeldt, N., Hein, C.M., Zapka, M., Michalik, A., Elbers, D., Kittel, A., Hore, P.J. & Mouritsen, H. (2014). Anthropogenic electromagnetic noise disrupts magnetic compass orientation in a migratory bird. *Nature* **509**, 353–6.
- Fedele, G., Green, E.W., Rosato, E. & Kyriacou, C.P. (2014). An electromagnetic field disrupts negative geotaxis in *Drosophila* via a CRY-dependent pathway. *Nat. Commun.* **5**, 4391.
- Fleissner, G.G., Holtkamp-Rötzler, E., Hanzlik, M., Winklhofer, M., Petersen, N. & Wiltschko, W. (2003). Ultrastructural analysis of a putative magnetoreceptor in the beak of homing pigeons. *J. Comp. Neurol.* **458**, 350–60.
- Fogle, K.J., Parson, K.G., Dahm, N. a & Holmes, T.C. (2011). CRYPTOCHROME is a blue-light sensor that regulates neuronal firing rate. *Science* **331**, 1409–13.
- Foley, L.E., Gegear, R.J. & Reppert, S.M. (2011). Human cryptochrome exhibits light-dependent magnetosensitivity. *Nat. Commun.* **2**, 356.

- Gegear, R., Casselman, A., Waddell, S. & Reppert, S. (2008). Cryptochrome mediates light-dependent magnetosensitivity in *Drosophila*. *Nature* **454**, 1014–1019.
- Gegear, R.J., Foley, L.E., Casselman, A. & Reppert, S.M. (2010). Animal cryptochromes mediate magnetoreception by an unconventional photochemical mechanism. *Nature* **463**, 804–7.
- Giebultowicz, J.M., Stanewsky, R., Hall, J.C. & Hege, D.M. (2000). Transplanted *Drosophila* excretory tubules maintain circadian clock cycling out of phase with the host. *Curr. Biol.* **10**, 107–110.
- Gould, J.L. (1984). Magnetic field sensitivity in animals. *Annu. Rev. Physiol.* **46**, 585–9.
- Gould, J.L. (2010). Magnetoreception. *Curr. Biol.* **20**, R431–5.
- Gould, J.L., Kirschvink, J.L. & Deffeyes, K.S. (1978). Bees have magnetic remanence. *Science* **201**, 1026–8.
- Gould, S. & Vrba, E. (1982). Exaptation- A missing term in the science of form. *Paleobiology* **8**, 4–15.
- Grima, B., Chélot, E., Xia, R. & Rouyer, F. (2004). Morning and evening peaks of activity rely on different clock neurons of the *Drosophila* brain. *Nature* **431**, 869–73.
- Guerra, P. a, Gegear, R.J. & Reppert, S.M. (2014). A magnetic compass aids monarch butterfly migration. *Nat. Commun.* **5**, 1–8.
- Guo, F., Cerullo, I., Chen, X. & Rosbash, M. (2014). PDF neuron firing phase-shifts key circadian activity neurons in *Drosophila*. *Elife* e02780.
- Hardin, P.E., Hall, J.C. & Rosbash, M. (1990). Feedback of the *Drosophila* period gene product on circadian cycling of its messenger RNA levels. *Nature* **343**, 536–40.
- Hardin, P.E., Hallt, J.C., Rosbash, M. & Hall, J.C. (1992). Circadian oscillations in period gene mRNA levels are transcriptionally regulated. *Proc. Natl. Acad. Sci. U. S. A.* **89**, 11711–11715.
- Hares, J. (2013). Unravelling the function of the novel gene , day , in *Drosophila melanogaster*.
- Hege, D.M., Stanewsky, R., Hall, J.C. & Giebultowicz, J.M. (1997). Rhythmic Expression of a PER-Reporter in the Malpighian Tubules of Decapitated *Drosophila*: Evidence for a Brain-Independent Circadian Clock. *J. Biol. Rhythms* **12**, 300–308.
- Helfrich-Förster, C., Shafer, O.T., Wülbeck, C., Grieshaber, E.V.A., Rieger, D., Taghert, P., Helfrich-fo, C. & Wu, C. (2007a). Development and Morphology of the Clock-Gene-Expressing Lateral Neurons of *Drosophila melanogaster*. *J. Comp. Neurol.* **70**, 47–70.

- Helfrich-Förster, C., Winter, C., Hofbauer, a, Hall, J.C. & Stanewsky, R. (2001). The circadian clock of fruit flies is blind after elimination of all known photoreceptors. *Neuron* **30**, 249–61.
- Helfrich-Förster, C., Yoshii, T., Wülbeck, C., Grieshaber, E., Rieger, D., Bachleitner, W., Cusamano, P. & Rouyer, F. (2007b). The lateral and dorsal neurons of *Drosophila melanogaster*: new insights about their morphology and function. *Cold Spring Harb. Symp. Quant. Biol.* **72**, 517–25.
- Hemsley, M.J., Mazzotta, G.M., Mason, M., Dissel, S., Toppo, S., Pagano, M. a, Sandrelli, F., Meggio, F., Rosato, E., Costa, R. & Tosatto, S.C.E. (2007). Linear motifs in the C-terminus of *D. melanogaster* cryptochrome. *Biochem. Biophys. Res. Commun.* **355**, 531–7.
- Henbest, K.B., Kukura, P., Rodgers, C.T., Hore, P.J. & Timmel, C.R. (2004). Radio frequency magnetic field effects on a radical recombination reaction: a diagnostic test for the radical pair mechanism. *J. Am. Chem. Soc.* **126**, 8102–3.
- Hoang, N., Schleicher, E., Kacprzak, S. & Bouly, J. (2008). Human and *Drosophila* cryptochromes are light activated by flavin photoreduction in living cells. *PLoS Biol.* **6**, 1559–1569.
- Hsu, C.-Y., Ko, F.-Y., Li, C.-W., Fann, K. & Lue, J.-T. (2007). Magnetoreception system in honeybees (*Apis mellifera*). *PLoS One* **2**, e395.
- Husain, N., Pellikka, M., Hong, H., Klimentova, T., Choe, K.-M., Clandinin, T.R. & Tepass, U. (2006). The agrin/perlecan-related protein eyes shut is essential for epithelial lumen formation in the *Drosophila* retina. *Dev. Cell* **11**, 483–93.
- Im, S.H., Li, W. & Taghert, P.H. (2011). PDFR and CRY signaling converge in a subset of clock neurons to modulate the amplitude and phase of circadian behavior in *Drosophila*. *PLoS One* **6**, e18974.
- Im, S.H. & Taghert, P.H. (2010). PDF receptor expression reveals direct interactions between circadian oscillators in *Drosophila*. *J. Comp. Neurol.* **518**, 1925–45.
- Im, S.H. & Taghert, P.H. (2011). Neuroscience. A CRY to rise. *Science* **331**, 1394–5.
- Ivanchenko, M., Stanewsky, R. & Giebultowicz, J.M. (2001). Circadian Photoreception in *Drosophila*: Functions of Cryptochrome in Peripheral and Central Clocks. *J. Biol. Rhythms* **16**, 205–215.
- Jogler, C. & Schüler, D. (2009). Genomics, genetics, and cell biology of magnetosome formation. *Annu. Rev. Microbiol.* **63**, 501–21.
- Johard, H.A.D., Yoishii, T., Dirksen, H., Cusumano, P., Rouyer, F., Helfrich-Förster, C. & Nässel, D.R. (2009). Peptidergic clock neurons in *Drosophila*: ion transport peptide

- and short neuropeptide F in subsets of dorsal and ventral lateral neurons. *J. Comp. Neurol.* **516**, 59–73.
- Johnsen, S. & Lohmann, K.J. (2008). Magnetoreception in animals. *Phys. Today* **61**, 29.
- Johnston, L.A., Ostrow, B.D., Jasoni, C. & Blochlinger, K. (1998). The homeobox gene *cut* interacts genetically with the homeotic genes *proboscipedia* and *Antennapedia*. *Genetics* **149**, 131–42.
- Kadener, S., Stoleru, D., McDonald, M., Nawathean, P. & Rosbash, M. (2007). Clockwork Orange is a transcriptional repressor and a new *Drosophila* circadian pacemaker component. *Genes Dev.* **21**, 1675–86.
- Kalmijn, a J. (1982). Electric and magnetic field detection in elasmobranch fishes. *Science* **218**, 916–8.
- Kamikouchi, A., Shimada, T. & Ito, K. (2006). Comprehensive classification of the auditory sensory projections in the brain of the fruit fly *Drosophila melanogaster*. *J. Comp. Neurol.* **499**, 317–56.
- Kaneko, H., Head, L.M., Ling, J., Tang, X., Liu, Y., Hardin, P.E., Emery, P. & Hamada, F.N. (2012). Circadian rhythm of temperature preference and its neural control in *Drosophila*. *Curr. Biol.* **22**, 1851–7.
- Kato, M. (2006). *Electromagnetics in Biology*. Tokyo: Springer Japan.
- Kavlie, R.G. & Albert, J.T. (2013). Chordotonal organs. *Curr. Biol.* **23**, R334–5.
- Kilman, V.L. & Allada, R. (2009). Genetic analysis of ectopic circadian clock induction in *Drosophila*. *J. Biol. Rhythms* **24**, 368–78.
- Kim, J., Chung, Y.D., Park, D.-Y., Choi, S., Shin, D.W., Soh, H., Lee, H.W., Son, W., Yim, J., Park, C.-S., Kernan, M.J. & Kim, C. (2003). A TRPV family ion channel required for hearing in *Drosophila*. *Nature* **424**, 81–4.
- Kirschvink, J.L. (1992). Uniform magnetic fields and double-wrapped coil systems. *Bioelectromagnetics* 401–411.
- Kirschvink, J.L. (2014). Sensory biology: Radio waves zap the biomagnetic compass. *Nature* **509**, 296–7.
- Kirschvink, J.L., Walker, M.M. & Diebel, C.E. (2001). Magnetite-based magnetoreception. *Curr. Opin. Neurobiol.* **11**, 462–7.
- Kirschvink, J.L., Winklhofer, M. & Walker, M.M. (2010). Biophysics of magnetic orientation: strengthening the interface between theory and experimental design. *J. R. Soc. Interface* **7 Suppl 2**, S179–91.

- Kistenpfennig, C., Hirsh, J., Yoshii, T. & Helfrich-Förster, C. (2012). Phase-shifting the fruit fly clock without cryptochrome. *J. Biol. Rhythms* **27**, 117–25.
- Kloss, B., Price, J.L., Saez, L., Blau, J., Rothenfluh, a, Wesley, C.S. & Young, M.W. (1998). The Drosophila clock gene double-time encodes a protein closely related to human casein kinase epsilon. *Cell* **94**, 97–107.
- Ko, H.W., Kim, E.Y., Chiu, J., Vanselow, J.T., Kramer, A. & Edery, I. (2010). A hierarchical phosphorylation cascade that regulates the timing of PERIOD nuclear entry reveals novel roles for proline-directed kinases and GSK-3beta/SGG in circadian clocks. *J. Neurosci.* **30**, 12664–75.
- Koh, K., Zheng, X. & Sehgal, A. (2006). JETLAG resets the Drosophila circadian clock by promoting light-induced degradation of TIMELESS. *Science* **312**, 1809–12.
- Komeili, A. (2007). Molecular mechanisms of magnetosome formation. *Annu. Rev. Biochem.* **76**, 351–66.
- Konopka, R.J. & Benzer, S. (1971). Clock mutants of *Drosophila melanogaster*. *Proc. Natl. Acad. Sci. U. S. A.* **68**, 2112–6.
- Krishnan, B., Levine, J.D., Lynch, M.K., Dowse, H.B., Funes, P., Hall, J.C., Hardin, P.E. & Dryer, S.E. (2001a). A new role for cryptochrome in a Drosophila circadian oscillator. *Nature* **411**, 313–7.
- Krishnan, B., Levine, J.D., Lynch, M.K.S., Dowse, H.B., Funes, P., Hall, J.C., Hardin, P.E. & Dryer, S.E. (2001b). A new role for cryptochrome in a Drosophila circadian oscillator **374**, 313–317.
- Kume, K., Zylka, M.J., Sriram, S., Shearman, L.P., Weaver, D.R., Jin, X., Maywood, E.S., Hastings, M.H. & Reppert, S.M. (1999). mCRY1 and mCRY2 are essential components of the negative limb of the circadian clock feedback loop. *Cell* **98**, 193–205.
- Lee, A.A., Lau, J.C.S., Hogben, H.J., Biskup, T., Kattnig, D.R. & Hore, P.J. (2014). Alternative radical pairs for cryptochrome-based magnetoreception Alternative radical pairs for cryptochrome- based magnetoreception. *J. R. Soc. Interface* **11**.
- Lee, C., Bae, K. & Edery, I. (1998). The Drosophila CLOCK protein undergoes daily rhythms in abundance, phosphorylation, and interactions with the PER-TIM complex. *Neuron* **21**, 857–67.
- Lefeldt, N., Heyers, D., Schneider, N.-L., Engels, S., Elbers, D. & Mouritsen, H. (2014). Magnetic field-driven induction of ZENK in the trigeminal system of pigeons (*Columba livia*). *J. R. Soc. Interface* **11**, 20140777–.
- Lin, J., Kilman, V., Keegan, K. & Paddock, B. (2002). A role for casein kinase 2 α in the Drosophila circadian clock. *Nature* **420**, 816–820.

- Lin, J.-M., Schroeder, A. & Allada, R. (2005). In vivo circadian function of casein kinase 2 phosphorylation sites in Drosophila PERIOD. *J. Neurosci.* **25**, 11175–83.
- Lindsley, D.L. & Zimm, G.G. (1992). *The Genome of Drosophila melanogaster*. Academic Press.
- Ling, J., Dubruille, R. & Emery, P. (2012). KAYAK- α modulates circadian transcriptional feedback loops in Drosophila pacemaker neurons. *J. Neurosci.* **32**, 16959–70.
- Lohmann, K. & Johnsen, S. (2000). The neurobiology of magnetoreception in vertebrate animals. *Trends Neurosci.* **23**, 153–159.
- Lowenstam, H.A. (1967). Lepidocrocite, an Apatite Mineral, and Magnetite in Teeth of Chitons (Polyplacophora). *Science (80-)* **156**, 1373–1375.
- Lucano, M.J., Cernicchiaro, G., Wajnberg, E. & Esquivel, D.M.S. (2006). Stingless bee antennae: a magnetic sensory organ? *Biometals* **19**, 295–300.
- Ma, T. & Ritz, T. (2014). Magnetoreception Review Earth's Magnetic Field Biology & Possible Mechanisms.
- Maeda, K., Henbest, K.B., Cintolesi, F., Kuprov, I., Rodgers, C.T., Liddell, P. a., Gust, D., Timmel, C.R. & Hore, P.J. (2008). Chemical compass model of avian magnetoreception. *Nature* **453**, 387–390.
- Martinek, S., Inonog, S., Manoukian, A.S. & Young, M.W. (2001). A Role for the Segment Polarity Gene shaggy/GSK-3 in the Drosophila Circadian Clock. *Cell* **105**, 769–779.
- Masuyama, K., Zhang, Y., Rao, Y. & Wang, J.W. (2012). Mapping neural circuits with activity-dependent nuclear import of a transcription factor. *J. Neurogenet.* **26**, 89–102.
- Meissner, R.-A., Kilman, V.L., Lin, J.-M. & Allada, R. (2008). TIMELESS is an important mediator of CK2 effects on circadian clock function in vivo. *J. Neurosci.* **28**, 9732–40.
- Merlin, C., Gegear, R.J. & Reppert, S.M. (2009). Antennal circadian clocks coordinate sun compass orientation in migratory monarch butterflies. *Science* **325**, 1700–4.
- Mishra, M. (2014). A quick method to investigate the Drosophila Johnston's organ by confocal microscopy. *J. Microsc. Ultrastruct.*
- Miyasako, Y., Umezaki, Y. & Tomioka, K. (2007). Separate sets of cerebral clock neurons are responsible for light and temperature entrainment of Drosophila circadian locomotor rhythms. *J. Biol. Rhythms* **22**, 115–26.

- Mollereau, B., Wernet, M.F., Beaufils, P., Killian, D., Pichaud, F., Kühnlein, R. & Desplan, C. (2000). A green fluorescent protein enhancer trap screen in *Drosophila* photoreceptor cells. *Mech. Dev.* **93**, 151–160.
- Molteno, T.C. a & Kennedy, W.L. (2009). Navigation by induction-based magnetoreception in elasmobranch fishes. *J. Biophys.* **2009**, 380976.
- Mouritsen, H. (2012). Sensory biology: Search for the compass needles. *Nature* **484**, 320–1.
- Müller, P. & Ahmad, M. (2011). Light-activated cryptochrome reacts with molecular oxygen to form a flavin-superoxide radical pair consistent with magnetoreception. *J. Biol. Chem.* **286**, 21033–21040.
- Murad, A., Emery-Le, M. & Emery, P. (2007). A subset of dorsal neurons modulates circadian behavior and light responses in *Drosophila*. *Neuron* **53**, 689–701.
- Muskus, M.J., Preuss, F., Fan, J.-Y., Bjes, E.S. & Price, J.L. (2007). *Drosophila* DBT lacking protein kinase activity produces long-period and arrhythmic circadian behavioral and molecular rhythms. *Mol. Cell. Biol.* **27**, 8049–64.
- Myers, E.M., Yu, J. & Sehgal, A. (2003). Circadian Control of Eclosion. *Curr. Biol.* **13**, 526–533.
- Myers, M.P., Wager-Smith, K., Wesley, C.S., Young, M.W. & Sehgal, A. (1995). Positional cloning and sequence analysis of the *Drosophila* clock gene, timeless. *Science* **270**, 805–8.
- Nässel, D.R. & Winther, A.M.E. (2010). *Drosophila* neuropeptides in regulation of physiology and behavior. *Prog. Neurobiol.* **92**, 42–104.
- Nawathean, P. & Rosbash, M. (2004). The doubletime and CKII kinases collaborate to potentiate *Drosophila* PER transcriptional repressor activity. *Mol. Cell* **13**, 213–23.
- Nießner, C., Denzau, S., Stappert, K., Ahmad, M., Peichl, L., Wiltschko, W. & Wiltschko, R. (2013). Magnetoreception: activated cryptochrome 1a concurs with magnetic orientation in birds. *J. R. Soc. Interface* **10**, 20130638.
- Nitabach, M.N. & Taghert, P.H. (2008). Organization of the *Drosophila* circadian control circuit. *Curr. Biol.* **18**, R84–93.
- Nitabach, M.N., Wu, Y., Sheeba, V., Lemon, W.C., Strumbos, J., Zelensky, P.K., White, B.H. & Holmes, T.C. (2006). Electrical hyperexcitation of lateral ventral pacemaker neurons desynchronizes downstream circadian oscillators in the fly circadian circuit and induces multiple behavioral periods. *J. Neurosci.* **26**, 479–89.
- North, G. & Greenspan, R. (2007). Invertebrate neurobiology.

- Okamura, H., Miyake, S., Sumi, Y., Yamaguchi, S., Yasui, A., Muijtjens, M., Hoeijmakers, J.H. & van der Horst, G.T. (1999). Photic induction of mPer1 and mPer2 in cry-deficient mice lacking a biological clock. *Science* **286**, 2531–4.
- De Oliveira, J.F., Wajnberg, E., Esquivel, D.M.D.S., Weinkauf, S., Winklhofer, M. & Hanzlik, M. (2010). Ant antennae: are they sites for magnetoreception? *J. R. Soc. Interface* **7**, 143–52.
- Ozkaya, O. & Rosato, E. (2012). *The circadian clock of the fly: a neurogenetics journey through time*. *Adv. Genet.*
- Ozturk, N., Selby, C., Annayev, Y., Zhong, D. & Sancar, A. (2011). Reaction mechanism of Drosophila cryptochrome. *Proc. Natl. Acad. Sci. U. S. A.* **108**, 516–521.
- Ozturk, N., Selby, C.C.P., Zhong, D. & Sancar, A. (2013a). Mechanism of Photosignaling by Drosophila Cryptochrome: Role of the Redox Status of the Flavin Chromophore. *J. Biol. Chem.* **289**, 4634–42.
- Oztürk, N., Song, S.-H., Selby, C.P. & Sancar, A. (2008). Animal type 1 cryptochromes. Analysis of the redox state of the flavin cofactor by site-directed mutagenesis. *J. Biol. Chem.* **283**, 3256–63.
- Ozturk, N., VanVickle-Chavez, S.J., Akileswaran, L., Van Gelder, R.N. & Sancar, A. (2013b). Ramshackle (Brwd3) promotes light-induced ubiquitylation of Drosophila Cryptochrome by DDB1-CUL4-ROC1 E3 ligase complex. *Proc. Natl. Acad. Sci. U. S. A.* **110**, 4980–5.
- Painter, M.S., Dommer, D.H., Altizer, W.W., Muheim, R. & Phillips, J.B. (2013). Spontaneous magnetic orientation in larval Drosophila shares properties with learned magnetic compass responses in adult flies and mice. *J. Exp. Biol.* **216**, 1307–16.
- Paulin, M. (1995). Electroreception and the compass sense of sharks. *J. Theor. Biol.* 325–339.
- Peschel, N., Chen, K.F., Szabo, G. & Stanewsky, R. (2009). Light-Dependent Interactions between the Drosophila Circadian Clock Factors Cryptochrome, Jetlag, and Timeless. *Curr. Biol.* **19**, 241–247.
- Peschel, N. & Helfrich-Förster, C. (2011). Setting the clock--by nature: circadian rhythm in the fruitfly Drosophila melanogaster. *FEBS Lett.* **585**, 1435–42.
- Peschel, N., Veleri, S. & Stanewsky, R. (2006). Veela defines a molecular link between Cryptochrome and Timeless in the light-input pathway to Drosophila's circadian clock. *Proc. Natl. Acad. Sci. U. S. A.* **103**, 17313–8.

- Phillips, J.B. & Borland, S.C. (1992a). Wavelength specific effects of light on magnetic compass orientation of the eastern red-spotted newt *Notophthalmus viridescens*. *Ethol. Ecol. Evol.* **4**, 33–42.
- Phillips, J.B. & Borland, S.C. (1992b). Behavioural evidence for use of a light-dependent magnetoreception mechanism by a vertebrate. *Nature* **359**, 142–144.
- Phillips, J.B., Jorge, P.E. & Muheim, R. (2010a). Light-dependent magnetic compass orientation in amphibians and insects: candidate receptors and candidate molecular mechanisms. *J. R. Soc. Interface* **7 Suppl 2**, S241–56.
- Phillips, J.B., Muheim, R. & Jorge, P.E. (2010b). A behavioral perspective on the biophysics of the light-dependent magnetic compass: a link between directional and spatial perception? *J. Exp. Biol.* **213**, 3247–55.
- Phillips, J.B. & Sayeed, O. (1992). Wavelength-dependent effects of light on magnetic compass in drosophila.pdf. *J. Comp. Physiol. A. Neuroethol. Sens. Neural. Behav. Physiol.* **172**, 303–308.
- Phillips, J.B. & Sayeed, O. (1993). Wavelength-dependent effects of light on magnetic compass orientation in *Drosophila melanogaster*. *J. Comp. Physiol. A.* **172**, 303–8.
- Plautz, J.D., Straume, M., Stanewsky, R., Jamison, C.F., Brandes, C., Dowse, H.B., Hall, J.C. & Kay, S.A. (1997). Quantitative Analysis of *Drosophila* period Gene Transcription in Living Animals. *J. Biol. Rhythms* **12**, 204–217.
- Preuss, F., Fan, J.-Y., Kalive, M., Bao, S., Schuenemann, E., Bjes, E.S. & Price, J.L. (2004). Drosophila doubletime mutations which either shorten or lengthen the period of circadian rhythms decrease the protein kinase activity of casein kinase I. *Mol. Cell. Biol.* **24**, 886–98.
- Rakshit, K. & Giebultowicz, J.M. (2013). Cryptochrome restores dampened circadian rhythms and promotes healthspan in aging *Drosophila*. *Aging Cell* **12**, 752–62.
- Randall D, Burggren W, French K (2002) Eckert Animal Physiology. Macmillan S, editor.
- Reddy, P., Zehring, W.A., Wheeler, D.A., Pirrotta, V., Hadfield, C., Hall, J.C. & Rosbash, M. (1984). Molecular analysis of the period locus in *Drosophila melanogaster* and identification of a transcript involved in biological rhythms. *Cell* **38**, 701–710.
- Renn, S.C., Park, J.H., Rosbash, M., Hall, J.C. & Taghert, P.H. (1999). A pdf Neuropeptide Gene Mutation and Ablation of PDF Neurons Each Cause Severe Abnormalities of Behavioral Circadian Rhythms in *Drosophila*. *Cell* **99**, 791–802.
- Richier, B., Michard-Vanhée, C., Lamouroux, A., Papin, C. & Rouyer, F. (2008). The clockwork orange *Drosophila* protein functions as both an activator and a repressor of clock gene expression. *J. Biol. Rhythms* **23**, 103–16.

- Rieger, D., Wülbeck, C., Rouyer, F. & Helfrich-Förster, C. (2009). Period gene expression in four neurons is sufficient for rhythmic activity of *Drosophila melanogaster* under dim light conditions. *J. Biol. Rhythms* **24**, 271–82.
- Ritz, T., Adem, S. & Schulten, K. (2000). A model for photoreceptor-based magnetoreception in birds. *Biophys. J.* **78**, 707–18.
- Ritz, T., Ahmad, M., Mouritsen, H., Wiltschko, R. & Wiltschko, W. (2010). Photoreceptor-based magnetoreception: optimal design of receptor molecules, cells, and neuronal processing. *J. R. Soc. Interface* **7 Suppl 2**, S135–46.
- Ritz, T., Thalau, P., Phillips, J.B., Wiltschko, R. & Wiltschko, W. (2004). Resonance effects indicate a radical-pair mechanism for avian magnetic compass. *Nature* **429**, 177–80.
- Ritz, T., Wiltschko, R., Hore, P.J., Rodgers, C.T., Stapput, K., Thalau, P., Timmel, C.R. & Wiltschko, W. (2009). Magnetic compass of birds is based on a molecule with optimal directional sensitivity. *Biophys. J.* **96**, 3451–7.
- Roberts, D.H., Lehar, J. & Dreher, J.W. (1987). Time series analysis with CLEAN. I. Derivation of a spectrum. *Astron. J.* **93**, 968–989.
- Rodgers, C.T. & Hore, P.J. (2009). Chemical magnetoreception in birds: the radical pair mechanism. *Proc. Natl. Acad. Sci. U. S. A.* **106**, 353–60.
- Rosato, E., Codd, V., Mazzotta, G., Piccin, a, Zordan, M., Costa, R. & Kyriacou, C.P. (2001). Light-dependent interaction between *Drosophila* CRY and the clock protein PER mediated by the carboxy terminus of CRY. *Curr. Biol.* **11**, 909–17.
- Rosato, E. & Kyriacou, C.P. (2006). Analysis of locomotor activity rhythms in *Drosophila*. *Nat. Protoc.* **1**, 559–68.
- Rutila, J.E., Suri, V., Le, M., So, W. V, Rosbash, M. & Hall, J.C. (1998). CYCLE is a second bHLH-PAS clock protein essential for circadian rhythmicity and transcription of *Drosophila* period and timeless. *Cell* **93**, 805–14.
- Sandrelli, F., Tauber, E., Pegoraro, M., Mazzotta, G., Cisotto, P., Landskron, J., Stanewsky, R., Piccin, A., Rosato, E., Zordan, M., Costa, R. & Kyriacou, C.P. (2007). A molecular basis for natural selection at the timeless locus in *Drosophila melanogaster*. *Science* **316**, 1898–900.
- Schuderer, J., Oesch, W., Felber, N., Spät, D. & Kuster, N. (2004). In vitro exposure apparatus for ELF magnetic fields. *Bioelectromagnetics* **25**, 582–91.
- Sehadova, H., Glaser, F.T., Gentile, C., Simoni, A., Giesecke, A., Albert, J.T. & Stanewsky, R. (2009). Temperature entrainment of *Drosophila*'s circadian clock involves the gene nocte and signaling from peripheral sensory tissues to the brain. *Neuron* **64**, 251–66.

- Sehgal, A., Rothenfluh-Hilfiker, A., Hunter-Ensor, M., Chen, Y., Myers, M.P. & Young, M.W. (1995). Rhythmic expression of timeless: a basis for promoting circadian cycles in period gene autoregulation. *Science* **270**, 808–10.
- Shang, Y., Griffith, L.C. & Rosbash, M. (2008). Light-arousal and circadian photoreception circuits intersect at the large PDF cells of the Drosophila brain. *Proc. Natl. Acad. Sci. U. S. A.* **105**, 19587–94.
- Sharma, Y., Cheung, U., Larsen, E.W. & Eberl, D.F. (2000). PPTGAL, a convenient Gal4 P-element vector for testing expression of enhancer fragments in drosophila. *Genesis* **34**, 115–8.
- Sheeba, V., Fogle, K.J. & Holmes, T.C. (2010). Persistence of morning anticipation behavior and high amplitude morning startle response following functional loss of small ventral lateral neurons in Drosophila. *PLoS One* **5**, e11628.
- Simoni, A., Wolfgang, W., Topping, M.P., Kavlie, R.G., Stanewsky, R. & Albert, J.T. (2014). A mechanosensory pathway to the Drosophila circadian clock. *Science* **343**, 525–8.
- Solov'yov, I. a, Chandler, D.E. & Schulten, K. (2007). Magnetic field effects in *Arabidopsis thaliana* cryptochrome-1. *Biophys. J.* **92**, 2711–26.
- Solov'yov, I. & Greiner, W. (2013). Light-Activated Magnetic Compass in Birds.
- Solov'yov, I. & Schulten, K. (2011). Mechanism of magnetic field effect in cryptochrome. *arXiv Prepr. arXiv1102.5359* 1–28.
- Stanewsky, R., Kaneko, M., Emery, P., Beretta, B., Wager-Smith, K., Kay, S.A., Rosbash, M. & Hall, J.C. (1998). The cryb Mutation Identifies Cryptochrome as a Circadian Photoreceptor in Drosophila. *Cell* **95**, 681–692.
- Stanley, S. (2014). Biological nanoparticles and their influence on organisms. *Curr. Opin. Biotechnol.* **28**, 69–74.
- Stapput, K., Güntürkün, O., Hoffmann, K.-P., Wiltschko, R. & Wiltschko, W. (2010). Magnetoreception of directional information in birds requires nondegraded vision. *Curr. Biol.* **20**, 1259–62.
- Stapput, K., Thalau, P., Wiltschko, R. & Wiltschko, W. (2008). Orientation of birds in total darkness. *Curr. Biol.* **18**, 602–6.
- Stoleru, D., Nawathean, P., Fernández, M. de la P., Menet, J.S., Ceriani, M.F. & Rosbash, M. (2007). The Drosophila circadian network is a seasonal timer. *Cell* **129**, 207–19.

- Stoleru, D., Peng, Y., Nawathean, P. & Rosbash, M. (2005). A resetting signal between *Drosophila* pacemakers synchronizes morning and evening activity. *Nature* **438**, 238–42.
- Stoneham, a M., Gauger, E.M., Porfyrakis, K., Benjamin, S.C. & Lovett, B.W. (2012). A new type of radical-pair-based model for magnetoreception. *Biophys. J.* **102**, 961–8.
- Sun, Y., Liu, L., Ben-Shahar, Y., Jacobs, J.S., Eberl, D.F. & Welsh, M.J. (2009). TRPA channels distinguish gravity sensing from hearing in Johnston's organ. *Proc. Natl. Acad. Sci. U. S. A.* **106**, 13606–11.
- Szabó, A., Papin, C., Zorn, D., Ponien, P., Weber, F., Raabe, T. & Rouyer, F. (2013). The CK2 kinase stabilizes CLOCK and represses its activity in the *Drosophila* circadian oscillator. *PLoS Biol.* **11**, e1001645.
- Tahayato, A., Sonneville, R., Pichaud, F., Wernet, M.F., Papatsenko, D., Beaufils, P., Cook, T. & Desplan, C. (2003). Otd/Crx, a Dual Regulator for the Specification of Ommatidia Subtypes in the *Drosophila* Retina. *Dev. Cell* **5**, 391–402.
- Tanoue, S., Krishnan, P., Krishnan, B., Dryer, S.E. & Hardin, P.E. (2004). Circadian clocks in antennal neurons are necessary and sufficient for olfaction rhythms in *Drosophila*. *Curr. Biol.* **14**, 638–49.
- Tauber, E., Zordan, M., Sandrelli, F., Pegoraro, M., Osterwalder, N., Breda, C., Daga, A., Selmin, A., Monger, K., Benna, C., Rosato, E., Kyriacou, C.P. & Costa, R. (2007). Natural selection favors a newly derived timeless allele in *Drosophila melanogaster*. *Science* **316**, 1895–8.
- Tian, Y., Hu, W., Tong, H. & Han, J. (2012). Phototransduction in *Drosophila*. *Sci. China. Life Sci.* **55**, 27–34.
- Timmel, C.R. & Henbest, K.B. (2004). A study of spin chemistry in weak magnetic fields. *Philos. Trans. A. Math. Phys. Eng. Sci.* **362**, 2573–89.
- Toma, D.P., White, K.P., Hirsch, J. & Greenspan, R.J. (2002). Identification of genes involved in *Drosophila melanogaster* geotaxis, a complex behavioral trait. *Nat. Genet.* **31**, 349–53.
- Treiber, C.D., Salzer, M.C., Riegler, J., Edelman, N., Sugar, C., Breuss, M., Pichler, P., Cadiou, H., Saunders, M., Lythgoe, M., Shaw, J. & Keays, D.A. (2012). Clusters of iron-rich cells in the upper beak of pigeons are macrophages not magnetosensitive neurons. *Nature* **484**, 367–70.
- Vácha, M., Půžová, T. & Drštková, D. (2008). Ablation of Antennae Does Not Disrupt Magnetoreceptive Behavioural Reaction of the American Cockroach to Periodically Rotated Geomagnetic Field. *435*.

- Vácha, M., Puzová, T. & Kvícalová, M. (2009). Radio frequency magnetic fields disrupt magnetoreception in American cockroach. *J. Exp. Biol.* **212**, 3473–7.
- Vaidya, A.T., Top, D., Manahan, C.C., Tokuda, J.M., Zhang, S., Pollack, L., Young, M.W. & Crane, B.R. (2013). Flavin reduction activates *Drosophila* cryptochrome. *Proc. Natl. Acad. Sci. U. S. A.* **110**, 20455–60.
- VanVickle-Chavez, S.J. & Van Gelder, R.N. (2007). Action spectrum of *Drosophila* cryptochrome. *J. Biol. Chem.* **282**, 10561–6.
- Venkatachalam, K. & Montell, C. (2007). TRP channels. *Annu. Rev. Biochem.* **76**, 387–417.
- Vieira, J., Jones, A.R., Danon, A., Sakuma, M., Hoang, N., Robles, D., Tait, S., Heyes, D.J., Picot, M., Yoshii, T., Helfrich-Förster, C., Soubigou, G., Coppee, J.-Y., Klarsfeld, A., Rouyer, F., Scrutton, N.S. & Ahmad, M. (2012). Human cryptochrome-1 confers light independent biological activity in transgenic *Drosophila* correlated with flavin radical stability. *PLoS One* **7**, e31867.
- Voolstra, O., Oberhauser, V., Sumser, E., Meyer, N.E., Maguire, M.E., Huber, A. & von Lintig, J. (2010). NinaB is essential for *Drosophila* vision but induces retinal degeneration in opsin-deficient photoreceptors. *J. Biol. Chem.* **285**, 2130–9.
- Vosshall, L.B. & Young, M.W. (1995). Circadian rhythms in drosophila can be driven by period expression in a restricted group of central brain cells. *Neuron* **15**, 345–360.
- Walker, M.M., Diebel, C.E. & Kirschvink, J.L. (2003). Detection and use of earth's magnetic field by aquatic vertebrates. In *Sensory processing in aquatic environments*: 53–74. Springer-Verlag (Ed). New York.
- Wang, J. & Pantopoulos, k. (2011). Regulation of cellular iron metabolism.
- Wang, K. & Ritz, T. (2006). Zeeman resonances for radical-pair reactions in weak static magnetic fields. *Mol. Phys.* **104**, 1649–1658.
- Wehner, R. & Labhart, T. (1970). Perception of the geomagnetic field in the fly *Drosophila melanogaster*. *Experientia* 967–968.
- Wernet, M.F., Labhart, T., Baumann, F., Mazzoni, E.O., Pichaud, F. & Desplan, C. (2003). Homothorax Switches Function of *Drosophila* Photoreceptors from Color to Polarized Light Sensors. *Cell* **115**, 267–279.
- Wever, R. (1973). Human circadian rhythms under the influence of weak electric fields and the different aspects of these studies. *Int. J. Biometeorol.* **17**, 227–32.
- Wiatrowski, H.A., Das, S., Kukkadapu, R., Ilton, E.S., Barkay, T. & Yee, N. (2009). Reduction of Hg(II) to Hg(0) by Magnetite. *Environ. Sci. Technol.* **43**, 5307–5313.

- Wiegmann, B.M., Yeates, D.K., Thorne, J.L. & Kishino, H. (2003). Time Flies, a New Molecular Time-Scale for Brachyceran Fly Evolution Without a Clock. *Syst. Biol.* **52**, 745–756.
- Wiltschko, R., Dehe, L., Gehring, D., Thalau, P. & Wiltschko, W. (2013). Interactions between the visual and the magnetoreception system: Different effects of bichromatic light regimes on the directional behavior of migratory birds. *J. Physiol. Paris* **107**, 137–146.
- Wiltschko, R., Denzau, S., Gehring, D., Thalau, P. & Wiltschko, W. (2011a). Magnetic orientation of migratory robins, *Erithacus rubecula*, under long-wavelength light. *J. Exp. Biol.* **214**, 3096–101.
- Wiltschko, R., Stappert, K., Bischof, H.-J. & Wiltschko, W. (2007a). Light-dependent magnetoreception in birds: increasing intensity of monochromatic light changes the nature of the response. *Front. Zool.* **4**, 5.
- Wiltschko, R., Stappert, K., Ritz, T., Thalau, P. & Wiltschko, W. (2007b). Magnetoreception in birds: different physical processes for two types of directional responses. *HFSP J.* **1**, 41.
- Wiltschko, R., Stappert, K., Thalau, P. & Wiltschko, W. (2010). Directional orientation of birds by the magnetic field under different light conditions. *J. R. Soc. Interface* **7 Suppl 2**, S163–77.
- Wiltschko, R. & Wiltschko, W. (2006). Magnetoreception. *Bioessays* **28**, 157–68.
- Wiltschko, W., Moller, A., Gesson, M., Noll, C. & Wiltschko, R. (2004). Light-dependent magnetoreception in birds: analysis of the behaviour under red light after pre-exposure to red light. *J. Exp. Biol.* **207**, 1193–1202.
- Wiltschko, W., Munro, U., Ford, H. & Wiltschko, R. (2006a). Bird navigation: what type of information does the magnetite-based receptor provide? *Proc. Biol. Sci.* **273**, 2815–20.
- Wiltschko, W., Munro, U., Wiltschko, R. & Kirschvink, J.L. (2002). Magnetite-based magnetoreception in birds: the effect of a biasing field and a pulse on migratory behavior. *J. Exp. Biol.* **205**, 3031–7.
- Wiltschko, W., Stappert, K., Thalau, P. & Wiltschko, R. (2006b). Avian magnetic compass: fast adjustment to intensities outside the normal functional window. *Naturwissenschaften* **93**, 300–4.
- Wiltschko, W. & Wiltschko, R. (1972). Magnetic compass of European robins. *Science* **176**, 62–4.

- Wiltschko, W. & Wiltschko, R. (2005). Magnetic orientation and magnetoreception in birds and other animals. *J. Comp. Physiol. A. Neuroethol. Sens. Neural. Behav. Physiol.* **191**, 675–93.
- Wiltschko, W., Wiltschko, R. & Ritz, T. (2011b). The mechanism of the avian magnetic compass. *Procedia Chem.* **3**, 276–284.
- Winklhofer, M. (2010). Magnetoreception. *J. R. Soc. Interface* **7 Suppl 2**, S131–4.
- Yao, Z. & Shafer, O.T. (2014). The Drosophila Circadian Clock Is a Variably Coupled Network of Multiple Peptidergic Units. *Science (80-.).* **343**, 1516–1520.
- Yorozu, S., Wong, A., Fischer, B.J., Dankert, H., Kernan, M.J., Kamikouchi, A., Ito, K. & Anderson, D.J. (2009). Distinct sensory representations of wind and near-field sound in the Drosophila brain. *Nature* **458**, 201–5.
- Yoshii, T., Ahmad, M. & Helfrich-Förster, C. (2009). Cryptochrome mediates light-dependent magnetosensitivity of Drosophila's circadian clock. *PLoS Biol.* **7**, e1000086.
- Yoshii, T., Todo, T., Wülbeck, C., Stanewsky, R. & Helfrich-Förster, C. (2008). Cryptochrome is present in the compound eyes and a subset of Drosophila's clock neurons. *J. Comp. Neurol.* **508**, 952–66.
- Yu, W., Houl, J.H. & Hardin, P.E. (2011). NEMO kinase contributes to core period determination by slowing the pace of the Drosophila circadian oscillator. *Curr. Biol.* **21**, 756–61.
- Yu, W., Zheng, H., Price, J.L. & Hardin, P.E. (2009). DOUBLETIME plays a noncatalytic role to mediate CLOCK phosphorylation and repress CLOCK-dependent transcription within the Drosophila circadian clock. *Mol. Cell. Biol.* **29**, 1452–8.
- Yuan, Q., Metterville, D., Briscoe, A.D. & Reppert, S.M. (2007). Insect cryptochromes: gene duplication and loss define diverse ways to construct insect circadian clocks. *Mol. Biol. Evol.* **24**, 948–55.
- Zhang, L., Chung, B.Y., Lear, B.C., Kilman, V.L., Liu, Y., Mahesh, G., Meissner, R.-A., Hardin, P.E. & Allada, R. (2010). DN1(p) circadian neurons coordinate acute light and PDF inputs to produce robust daily behavior in Drosophila. *Curr. Biol.* **20**, 591–9.
- Zhu, H., Yuan, Q., Briscoe, A.D., Froy, O., Casselman, A. & Reppert, S.M. (2005). The two CRYs of the butterfly. *Curr. Biol.* **15**, R953–4.
- Zimmerman, J.E., Bui, Q.T., Liu, H. & Bonini, N.M. (2000). Molecular genetic analysis of Drosophila eyes absent mutants reveals an eye enhancer element. *Genetics* **154**, 237–46.

11 PAPERS PUBLISHED

CORRESPONDENCE

COMPETING FINANCIAL INTERESTS

The authors declare no competing financial interests.

Mingliang Ye¹⁻³, Yanbo Pan¹⁻³, Kai Cheng^{1,2} & Hanfa Zou^{1,2}

¹Key Laboratory of Separation Sciences for Analytical Chemistry, National Chromatographic Research and Analysis Center, Dalian Institute of Chemical Physics, Chinese Academy of Sciences, Dalian, China. ²University of Chinese Academy of Sciences, Beijing, China. ³These authors contributed equally to this work.
e-mail: mingliang@dicp.ac.cn or hanfazou@dicp.ac.cn

1. Fonslow, B.R. et al. *Nat. Methods* **10**, 54–56 (2013).
2. Siepen, J.A., Keevil, E.J., Knight, D. & Hubbard, S.J. *J. Proteome Res.* **6**, 399–408 (2007).
3. Rodriguez, J., Gupta, N., Smith, R.D. & Pevzner, P.A. *J. Proteome Res.* **7**, 300–305 (2008).
4. Agard, N.J. et al. *Proc. Natl. Acad. Sci. USA* **109**, 1913–1918 (2012).
5. Crooks, G.E. et al. *Genome Res.* **14**, 1188–1190 (2004).

Editor's note: For the response by Fonslow et al., please see the Addendum to their Brief Communication (Fonslow, B.R. et al., *Nat. Methods* **11**, 347–348, 2014).

A *Drosophila* RNAi collection is subject to dominant phenotypic effects

To the Editor: The transgenic RNA interference (RNAi)-inducing lines from the Vienna *Drosophila* RNAi Center's (VDRC) libraries¹ have been used to elucidate gene function in both candidate gene experiments and a number of high-profile whole-genome reverse genetics screens. The first 'GD' library was generated by P element-mediated transformation of short hairpin RNA (shRNA) constructs into the fly genome, a technique susceptible to both false positive results (through insertional mutagenesis) and false negative results (including insertion into transcriptionally silent genomic regions). The VDRC's newer 'KK' collection of 10,740 lines instead used a two-step transformation in which flies were first transformed with vector pKC43 to generate a 'target' line (VDRC stock 60100, site VIE260B). Gene-specific shRNA sequences within the pKC26 vector could then be integrated into this pKC43 target using attP/B site, phiC31-mediated integration². This strategy is thought to eliminate the risk of insertional mutagenesis, and the genetic homogeneity among lines makes the KK collection particularly appropriate for screens of complex or subtle phenotypes such as behavior.

While using the KK library, we observed recurrent phenotypes not reconcilable with knockdown of the genes being targeted. Specifically, on crossing 39 randomly selected KK lines to the pan-neuronal driver *elav-GAL4^{c155}*, nine of them produced F₁ progeny unable to properly inflate their wings (**Fig. 1a**). Furthermore, crossing these same nine lines to the constitutive driver *actin-GAL4* caused pupal lethality.

Intrigued by these observations, we sequenced the genome of a recombinant line derived from the KK line targeting CG2913 (*yin*; VDRC line 104181; see **Supplementary Methods**). To our surprise, we found that this line harbored not one but two copies of the pKC43 target into which the pKC26 vector (carrying the shRNA sequences) could integrate: the annotated insertion reported by the VDRC (position chr2L: 22019296, cytological band 40D3; **Fig. 1e**) and a previously non-annotated insertion (position chr2L: 9437482, cytological band 30B3; **Fig. 1f**).

We developed a PCR-based diagnostic assay to interrogate these pKC43 insertion sites (**Supplementary Fig. 1**) and found that both were present in the VIE260B genetic background used to generate the KK collection (**Fig. 1d**). Indeed we found that the main integra-

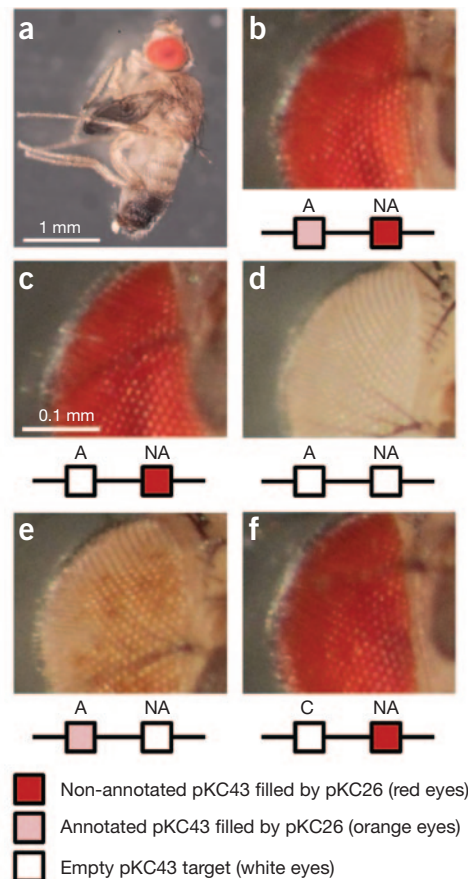


Figure 1 | Eye color of VDRC 'KK' lines with differing site occupancy. (a) The non-inflating wing phenotype of F₁ flies carrying a pKC26 integration at the annotated pKC43 site crossed to *elav-GAL4^{c155}*. (b,c) The eye color of VDRC line 104181 with the indicated integration sites. (d–f) Eye color of recombinant lines; backcrossing VDRC line 104181 to the white-eyed VDRC genetic background (d) generates the indicated recombinations (e,f).

tion site for pKC26 in the KK library is the non-annotated pKC43 target (occupied in all 39 lines tested), whereas only the nine lines displaying the *elav-GAL4^{c155}*-dependent non-inflating wing phenotype were found to have a pKC26 integration into the annotated pKC43 insertion (**Supplementary Table 1**).

After separating the two occupied pKC43 targets by recombination (**Supplementary Methods** and **Supplementary Fig. 2**), we found that occupancy of the non-annotated site resulted in saturating expression of the split *mini-white* (*w^{+mc}*) transgenesis marker, making it impossible to phenotypically distinguish lines with single or double pKC26 integrations (compare **Fig. 1b,c**). We observed some variability in *mini-white* expression from pKC26 integrations at the annotated site (**Supplementary Fig. 3**). Molecular analyses revealed that this site could be occupied by at least three different pKC26 derived sequences: (i) a pKC26 vector containing a normal hairpin sequence, (ii) an empty pKC26 vector containing no hairpin and (iii) a truncated pKC26 in which sequence-specific recombination between the *hsp70* elements used to drive expression of both the shRNA and the *mini-white* marker had deleted an ~1.1-kilobase vector fragment. Each of the three types of annotated site insertions was sufficient to cause the non-inflating wing phenotype when crossed to *elav-GAL4^{c155}* in the absence of any integration at the non-annotated pKC43 target.

Given that the annotated insertion of the pKC43 target vector is within the 5' untranslated region of the gene *tiptop* (*tio*), we hypothesize that integration of pKC26 into this site might cause Gal4-mediated toxicity through misexpression of *tio*. In fact, overexpression of *tio* (using *c724-GAL4*)³ generates flies with a similarly abnormal wing posture (N. Hu and B. Denholm, Cambridge University, personal communication), and general overexpression of *tio* (using *actin-GAL4*) results in lethality, albeit at an earlier stage than pupal lethality we observed.

In conclusion, the dominant Gal4-dependent toxicity we describe represents a substantial source of both false positive and negative results in assays of gene function when using the VDRC's KK collection. We strongly encourage researchers to validate their lines. Strains found to carry two integrations can be identified using our simple diagnostic PCR can and be 'cleaned' through a recombination scheme that maintains genetic isogeneity (**Supplementary Methods**), thereby enhancing the value of this extremely convenient and widely used resource.

Note: Any Supplementary Information and Source Data files are available in the online version of the paper (doi:10.1038/nmeth.2856).

ACKNOWLEDGMENTS

We are grateful to E. Spana for comments and advice on *Drosophila* transgenesis. E.W.G. was supported by grants from the Biotechnology and Biological Sciences Research Council (BBSRC) (BB/J005169/1) to C.P.K. and the Cure Huntington's Disease Initiative (CHDI) Foundation (A-3267) to F.G. G.F. was supported by a grant from the Electromagnetic Field (EMF) Biological Research Trust (BRT 10/38) to C.P.K. This research used the Special Computational Teaching and Research Environment (SPECTRE) High Performance Computing Facility at the University of Leicester.

AUTHOR CONTRIBUTIONS

E.W.G. conceived of the project, performed the *Drosophila* experiments and wrote the manuscript; G.F. performed PCR reactions; and F.G. and C.P.K. edited the manuscript.

COMPETING FINANCIAL INTERESTS

The authors declare no competing financial interests.

Edward W Green, Giorgio Fedele, Flaviano Giorgini & Charalambos P Kyriacou

Department of Genetics, University of Leicester, Leicester, UK.
e-mail: cpk@le.ac.uk

1. Dietzl, G. et al. *Nature* **448**, 151–156 (2007).
2. Groth, A.C., Fish, M., Nusse, R. & Calos, M.P. *Genetics* **166**, 1775–1782 (2004).
3. Denholm, B. et al. *Development* **140**, 1100–1110 (2013).

ARTICLE

Received 24 Jan 2014 | Accepted 13 Jun 2014 | Published 14 Jul 2014

DOI: 10.1038/ncomms5391

OPEN

An electromagnetic field disrupts negative geotaxis in *Drosophila* via a CRY-dependent pathway

Giorgio Fedele¹, Edward W. Green¹, Ezio Rosato¹ & Charalambos P. Kyriacou¹

Many higher animals have evolved the ability to use the Earth's magnetic field, particularly for orientation. *Drosophila melanogaster* also respond to electromagnetic fields (EMFs), although the reported effects are quite modest. Here we report that negative geotaxis in flies, scored as climbing, is disrupted by a static EMF, and this is mediated by cryptochrome (CRY), the blue-light circadian photoreceptor. CRYs may sense EMFs via formation of radical pairs of electrons requiring photoactivation of flavin adenine dinucleotide (FAD) bound near a triad of Trp residues, but mutation of the terminal Trp in the triad maintains EMF responsiveness in climbing. In contrast, deletion of the CRY C terminus disrupts EMF responses, indicating that it plays an important signalling role. CRY expression in a subset of clock neurons, or the photoreceptors, or the antennae, is sufficient to mediate negative geotaxis and EMF sensitivity. Climbing therefore provides a robust and reliable phenotype for studying EMF responses in *Drosophila*.

¹ Department of Genetics, University of Leicester, Leicester LE1 7RH, UK. Correspondence and requests for materials should be addressed to C.P.K. (email: cpk@leicester.ac.uk).

Many organisms have evolved the ability to sense and exploit the Earth's magnetic field, particularly for navigation and orientation¹. Three main models for magnetosensing have been promoted. Magnetic induction, which can only be applied to marine creatures, owing to the high conductivity of salt water^{1,2}, the magnetite hypothesis that proposes a process mediated by crystals of permanently magnetic material (magnetite)¹ and finally the radical pair mechanism (RPM), which relies on a chemical reaction involving specialized photoreceptors^{3,4}.

In the RPM, the first step of the reaction requires absorption of a photon by the pigment molecule, leading to the transient formation of a radical pair of electrons in an overall singlet state (antiparallel spin orientation), in which the two unpaired electrons are at a suitable distance to undergo transition to the triplet state (parallel orientation). This transition may be sensitive to an electromagnetic field (EMF), altering the singlet-triplet balance. Return to the ground state can only occur from the singlet state, hence EMFs may alter the lifetime of the radical pair and any signal that it generates^{3,4}. So far, the only photopigments proposed as putative candidates for the RPM are the cryptochromes (CRYs). These blue-light-sensing flavoproteins evolved from photolyases and are highly conserved across many different taxa⁵. CRYs are expressed in the eyes of mammals⁶ and migratory birds⁷, which are putative sites for magnetoreceptors in vertebrates⁸. In animals, CRYs also function as circadian photoreceptors in the *Drosophila* brain, mediating the light resetting of the 24 h clock⁹, but in vertebrates, the CRYs act as the main negative regulators for the circadian feedback loop¹⁰. The major difference between fly and vertebrate CRYs is that the former (type 1) are photosensitive, whereas the latter (type 2) are not¹¹. Non-drosophilid insects can also encode CRY1 and CRY2's, but CRY1s retain their light-sensing properties, whereas the CRY2s act as vertebrate-like negative regulators¹².

Previous genetic analyses in *Drosophila* have suggested a CRY-dependent ability for magnetosensing^{13,14}, whereas other fly studies have done so indirectly by utilizing wavelengths of light to which CRYs are sensitive^{15–17}. The two experimental paradigms that utilized *cry* mutations in flies include a conditioning^{13,18} and a circadian behavioural assay¹⁴. In these studies, CRYs have been implicated as mediators of the fly's EMF responses in a wavelength-dependent manner. Surprisingly, fly transformants carrying the *hCry2* transgene can also detect EMFs in the conditioning assay, suggesting that in the fly's cellular environment, hCRY2 can be activated by light¹⁹. In addition, mutations of the terminal Trp residue, which forms the Trp triad believed to be important for mediating radical pair formation²⁰, does not disrupt the EMF conditioning response, indicating that an unorthodox CRY-dependent EMF-sensing mechanism may be responsible¹⁸. Finally, although the CRYs implicate the circadian clock in magnetosensitivity, a working clock is not required for EMF responses in the fly conditioning assay¹⁸.

In the conditioning assay, the EMF behavioural effects are modest but consistent^{13,18,19}, whereas the circadian period changes induced by EMF under blue constant light are highly variable, leading to shorter or longer periods in half the flies, and no response at all in the other half¹⁴. We therefore sought a different fly behavioural assay that might respond to EMFs with more marked and robust changes. Negative geotaxis in flies (their ability to climb against gravity) has been studied by both traditional quantitative genetic and modern genomic methods²¹. Artificial selection for flies that show high and low levels of geotaxis has been allied to transcriptomic analyses to reveal that CRY may play a significant role in this phenotype²¹, and CRY's role in fly climbing behaviour has recently been confirmed²². We

therefore suspected that this phenotype could be wavelength dependent and if so, might be compromised by applying an EMF. We show here that negative geotaxis is blue-light and CRY dependent and is significantly compromised by the application of a static EMF. We further reveal that the CRY C terminus is critical for mediating the effects of the EMF, and that CRY expression in specific clock neurons, eyes and antennae contribute to the EMF phenotype. We conclude that negative geotaxis provides a reliable method for studying behavioural responses to EMFs.

Results

Climbing is wavelength- and CRY-dependent. We examined climbing ability as the percentage of flies that could climb 15 cm in 15 s at different wavelengths using a custom-made apparatus (see Methods and Fig. 1). We used either a sham exposure or a static EMF of 500 μ T, which although an order of magnitude greater than the Earth's magnetic field, is an intensity comparable with that used in previous genetic studies of fly EMF sensitivity^{13,14}. Figure 2a reveals that under blue light (450 nm), the proportion of wild-type Canton-S sham 'climbers' is significantly higher than in corresponding EMF exposed flies ($P = 0.0004$), whereas in red light (635 nm) climbing is substantially reduced under sham exposure, to levels similar to those of EMF-exposed flies under blue light. We also investigated the *cry-null* mutant, *cry⁰²* in blue light, which reveals responses similar to wild-type flies in red light. We conclude that negative geotaxis requires both blue-light activation and the presence of CRY, and that climbing can be disrupted by a static EMF.

Overexpressing CRY rescues EMF responses. We overexpressed fly CRY under GAL4 control, using various circadian clock drivers on a *cry⁰²* background. We observe that expressing CRY in most of the major clock neurons, using either the *timgal4* driver or in a more restricted *crygal4* pattern, restores high levels of climbing in sham, which was significantly reduced in EMF conditions, as in the wild type (Figs 2b and 3a). We also tested the climbing of all the gal4 driver and UAS lines that are used in this study, and all generate normal EMF responses (Fig. 3b). However, when CRY expression is restricted further using the *Pdfgal4* driver, which

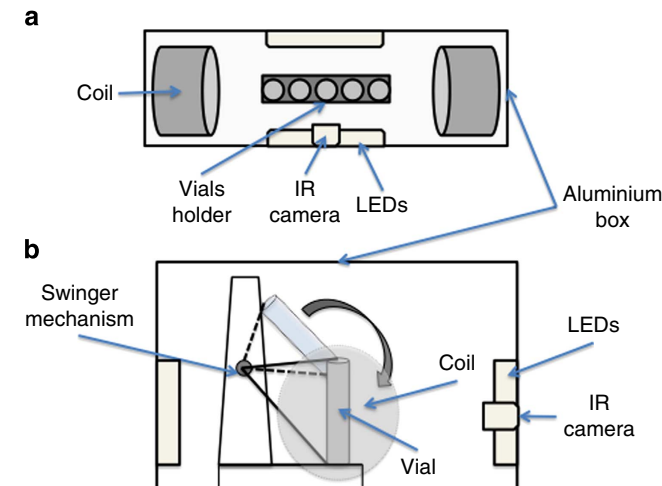


Figure 1 | Measuring negative geotaxis under a static EMF. The delivery system for EMFs consists of a double-wrapped coil system (a, top view), and a custom-made swinger apparatus (b, side view) that allows tapping three vials simultaneously with equal force so the flies fall to the bottom of the tube. IR, infrared.

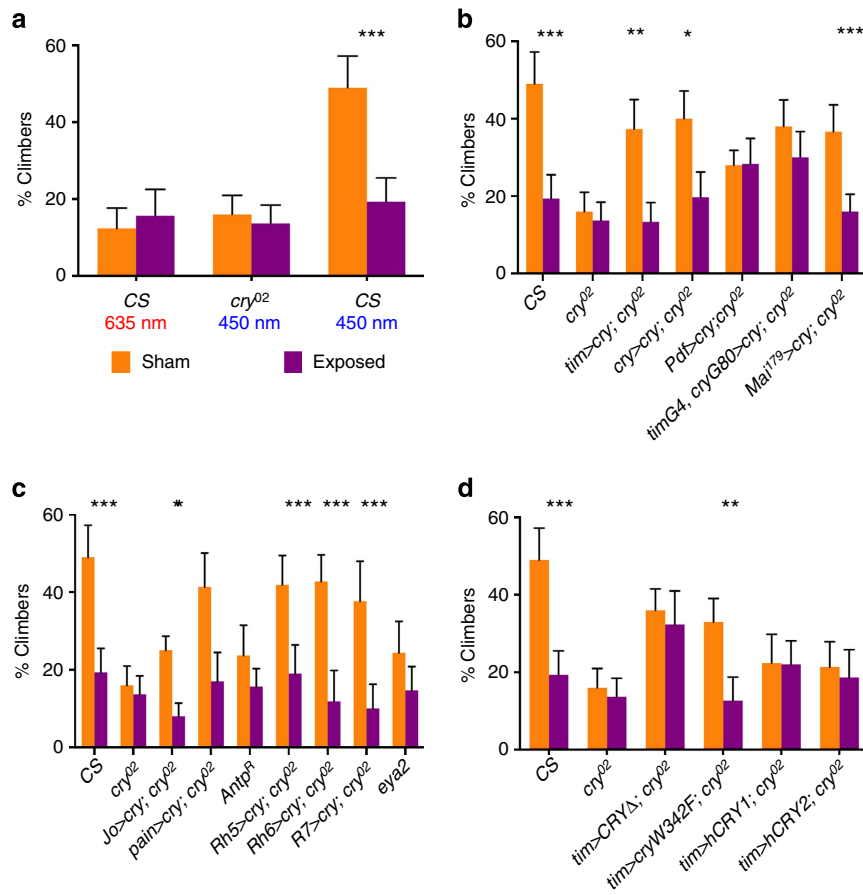


Figure 2 | Negative geotaxis is CRY dependent and is sensitive to EMFs. Mean geotactic responses \pm s.e.m. based on three biological replicates. Orange bars, sham exposed; purple bars, EMF exposed. Asterisks denote results of Duncan's *a posteriori* test within genotype after analysis of variance (ANOVA), $*P < 0.05$, $**P < 0.01$, $***P < 0.001$. The results from Canton-S (CS) and *cry⁰²* were used as positive and negative controls for all analyses and **b-d** represent experiments performed only at 450 nm. **(a)** Response of CS and *cry⁰²* exposed to different wavelengths of light. (ANOVA, genotype $F_{2,12} = 16.48$, $P = 0.00036$, exposure $F_{1,12} = 8.67$, $P = 0.012$, G \times E interaction $F_{2,12} = 9.86$, $P = 0.002$). Post hoc tests revealed significant differences only between CS in blue light under sham compared with all the other conditions ($P < 0.001$). **(b)** Responses of clock *gal4*/80>UAScry genotypes on a *cry⁰²* background (ANOVA, genotype $F_{6,28} = 3.98$, $P = 0.005$, exposure $F_{1,28} = 36.1$, $P = 2 \times 10^{-6}$, G \times E interaction $F_{6,28} = 3.08$, $P = 0.019$). Post hoc tests reveal no significant differences between sham *timgal4*/UAScry or *crygal4*/UAScry compared with CS, nor for EMF exposure. For sham, *Pdfgal4*>UAScry vs *cry⁰²* $P = 0.1$, vs CS $P = 0.009$ *timgal4*/*crygal80*>UAScry vs *cry⁰²* $P = 0.007$, vs CS $P = 0.12$; for EMF *Pdfgal4*>UAScry vs *cry⁰²* $P = 0.06$, vs CS $P = 0.22$, *timgal4*/*crygal80*>UAScry vs *cry⁰²* $P = 0.039$, vs CS $P = 0.16$. **(c)** Responses of eye and antennal genotypes (*gal4*/UAScry on *cry⁰²* background) (ANOVA, genotype $F_{8,36} = 5.45$, $P = 0.00016$, exposure $F_{1,36} = 99.4$, $P < 0$, G \times E interaction $F_{8,36} = 3.25$, $P = 0.007$). Post hoc for sham, CS was not significantly different from sham *pain*, *rh5*, *rh6*, *R7gal4*>UAScry, but *JOgal4*>UAScry vs *cry⁰²* $P = 0.18$, vs CS $P = 0.0005$. For EMF, none of the genotypes were significantly different from CS or *cry⁰²*. **(d)** Responses of *cry* variants driven by *timgal4* (ANOVA, genotype $F_{5,24} = 6.89$, $P = 0.0004$, exposure $F_{1,24} = 16.8$, $P = 0.0005$ and G \times E interaction $F_{5,24} = 4.13$, $P = 0.008$). Post hoc sham *timgal4*>*cry1* vs *cry⁰²* $P = 0.007$, vs CS $P = 0.04$, *timgal4*>*cryW342F* vs *cry⁰²* $P = 0.02$, vs CS $P = 0.017$; for EMF *timgal4*>*cry1* vs *cry⁰²* $P = 0.01$, vs CS $P = 0.06$, *timgal4*>*cryW342F* vs *cry⁰²* $P = 0.2$, vs CS $P = 0.33$.

expresses in the lateral ventral (LNv) subset of clock neurons, intermediate levels of climbing are observed that are not further disrupted by EMF (Figs 2b and 3). A similar scenario prevails when the *timgal4*/*crygal80* combination is used to drive CRY expression predominantly in the dorsal neurons plus three normally CRY-negative lateral dorsal neurons (LNd)s²³ with again, levels of climbing observed that are similar to those obtained with the *timgal4* and *crygal4* drivers, but with no significant reduction of geotaxis under EMF (Figs 2b and 3). In contrast to these restricted patterns of CRY expression, the *Mai¹⁷⁹gal4* driver that expresses in the LNvs and three CRY-positive LNd neurons^{23,24} generated intermediate levels of climbing, which are nevertheless susceptible to an EMF. Consequently, it appears that among the canonical clock neurons, it is the three CRY-expressing LNd cells that are required to generate a robust EMF response.

We also investigated whether major peripheral tissues in the head, namely the eyes and antennae that normally express CRY, could also contribute to EMF sensitivity. The *rh5*, *rh6* and *R7gal4* eye-specific rhodopsin drivers all restore normal levels of climbing to *cry⁰²* mutants that are significantly reduced under EMF (Figs 2c and 3). To complement these results, the eyes-absent mutant, *eya²*, which has a complete absence of eyes, shows a significant reduction in climbing and no further reduction under EMF (Figs 2c and 3a). The antennal drivers *JOgal4* and *painlessgal4* also rescue the sham/EMF response on a *cry⁰²* background, in spite of the fact that in *JOgal4*, the sham level of climbing is significantly reduced compared with Canton-S flies ($P = 0.0005$, Figs 2c and 3a) and no higher than that of *eya²*. Furthermore, the *Antp^R* mutant, in which antennae are transformed to mesothoracic legs, significantly reduces the climbing score under sham, but does

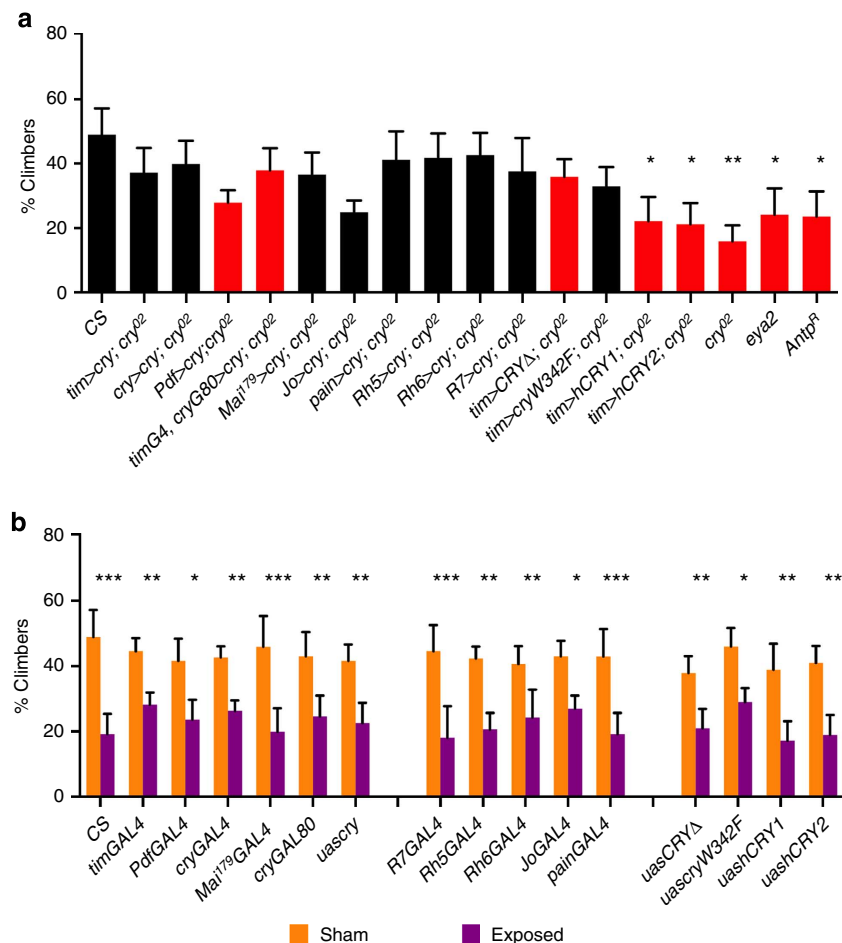


Figure 3 | Control genotype responses to sham and EMFs. (a) Sham controls are shown to illustrate which genotypes did not respond (red bars) or did respond (black bars) to EMFs. Mean climbing scores (\pm s.e.m.) under blue light based on three biological replicates. Repeated measure analysis of variance (ANOVA) ($F_{(17,36)} = 4.41, P = 0.001$) and Duncan's *post hoc* analysis (* $P < 0.05$, ** $P < 0.01$), further reveal which genotypes differ significantly in their sham responses to CS wild type. Note that *JO>cry; cry⁰²* have intermediate levels of climbing under sham, yet show an EMF response (Fig. 2c), whereas genotypes with higher levels of sham climbing (*Pdf>cry; cry⁰²*, *timgal4, crygal80>cry; cry⁰²*, *tim>cryΔ; cry⁰²*) do not respond to EMF (Fig. 2b,d). (b) GAL4/UAS controls strains show normal EMF responses. Mean climbing scores (\pm s.e.m.) under blue light based on three biological replicates. Repeated measures ANOVA revealed a significant exposure ($F_{(1,64)} = 217.52, P = 0.0004$) but no effect of genotype ($F_{(15,64)} = 0.818, P = 0.65$) nor a G \times E interaction ($F_{(15,64)} = 0.60, P = 0.86$), so all genotypes responded in the same way to the EMF. All strains are in a *w¹¹¹⁸* genetic background. Duncan's *post hoc* * $P < 0.05$, ** $P < 0.01$, *** $P < 0.001$.

not reduce it further under EMF (Figs 2c and 3a). These results suggest that the eyes and antennae also play significant roles in climbing and in the response to EMFs.

Finally, we expressed a number of *cry* variants on the *cry⁰²* background using *timgal4*, including human *hCry1* and *hCry2* transgenes, the latter having been reported to rescue the EMF effect on a conditioning paradigm¹⁹. Neither of these transgenes appears capable of rescuing the climbing phenotype beyond that of *cry⁰²*, so they are not competent to respond to EMF (Fig. 2d). In contrast, a Trp to Phe mutation (*cryW342F*) of the terminal Trp of CRYs putative 'Trp triad', generates intermediate levels of climbing, which are significantly further reduced on EMF exposure (Figs 2d and 3). We also examined the sham/EMF response of the CRY C-terminal deletion mutant *CRYΔ*, which is constitutively active in both darkness and light^{25,26}. Interestingly, under both sham and EMF conditions, this mutant shows intermediate levels of climbing but with no difference between the two conditions. Therefore, like *cryW342F*, *timgal4>cryΔ* retains the ability to climb but in contrast, is not responsive to an EMF, revealing a role for the CRY C terminus in magnetosensing (Figs 2d and 3a).

Discussion

We have observed that *Drosophila* requires a functional CRY molecule to climb against gravity, confirming the results of two earlier studies that used different measures of negative geotaxis^{21,22}. We have extended these observations by revealing that under blue light, the climbing of wild-type flies exposed to a 500- μ T static EMF is significantly reduced compared with sham exposure. The pass/fail nature of our behavioural assay clearly differentiates between the two exposure conditions. In red light, flies exposed to sham or EMF show significantly reduced climbing, very similar to the levels observed under blue light with EMF exposure. Consequently, negative geotaxis is blue-light dependent, thereby implicating the fly's dedicated circadian photoreceptor, CRY. As red light does not activate CRY, our results imply that EMFs compromise the photoreceptor's response to blue light. Consistent with this, the *cry-null* mutant fails to climb in sham conditions, but this ability can be partially or almost fully rescued by overexpressing CRY in a number of different neuronal types that include clock neurons, antennae and eyes. These results suggest that CRY mediates the effects of EMFs, as also revealed in two other behavioural paradigms, a conditioning and a circadian assay^{13,14,18}.

There is, nevertheless, a logical problem in the inference that CRY is the sensor for EMF taken only from the *cry-null* mutant data, in that the phenotype of climbing is itself CRY dependent, so any mutant that does not climb cannot show a reduction in climbing due to EMF. The same is true for the circadian EMF phenotype, where a change of period under constant dim blue light, which is CRY dependent, has been reported to be further modulated by EMF¹⁴. However, in *cry* mutants, as there is no initial circadian period change in blue light, there is no behavioural substrate for the EMF to modify. Thus *cry-null* mutants, in themselves, are not informative in these two assays. In contrast, in the conditioning assay, flies of various genetic backgrounds show both positive or negative naive preferences to an EMF, and this can be modulated by association with sucrose leading to an enhanced preference for EMF after training^{13,18}. *cry-null* flies do not show any preference in the first place indicating they cannot sense the EMF, so they cannot be trained, thus there is no net change in preference after training. Yet a strong indication for the role of *cry* in this phenotype is provided by the *cry-null* mutant's initial inability to sense the EMF, which is independent of the type of *cry-null* allele and the flies' genetic background^{13,18}.

With this reservation in mind, perhaps the most convincing support for the CRY-EMF hypothesis in our climbing assay requires a mutant that climbs in sham conditions to near wild-type levels, so that the CRY molecule retains basic geotactic function, yet would climb to similar levels under EMF, reflecting a mutant, suppressed EMF response. One mutation that fulfils this requirement is CRYΔ, which although producing an unstable CRY, retains some residual molecular response to light^{25,26}. This mutant shows intermediate levels of climbing between *cry*⁰² and wild type under sham conditions, but does not respond to the EMF by reducing its climbing. The CRY C-terminal region may therefore play a pivotal role in the intracellular signalling of the CRY response to EMF, possibly by modulating downstream protein–protein interactions.

Another mutation *cryW342F* that substitutes a Phe for the terminal Trp in the putative 'Trp triad' that is a candidate for mediating radical pair formation, shows similar levels of climbing to *cry4*, but in sharp contrast, is responsive to EMF. This result echoes the observation that *cryW342F* is also able to retain EMF sensitivity in the conditioning assay¹⁸. Consequently, the terminal CRY Trp342 may not be the critical residue that is a prerequisite for the RPM, and perhaps another residue within that local conformation is involved, perhaps a tyrosine²⁷. While both the climbing and conditioning assays reveal consistent effects for the terminal Trp mutant, the same could not be stated for hCRY2. In the conditioning test, hCRY2 is EMF-sensitive¹⁹, but in the climbing assay, hCRY1 and hCRY2 behave very similarly to *cry*⁰², suggesting that they are not blue-light responsive, revealing that the ability of hCRY to rescue an EMF response is phenotype dependent.

We also obtained EMF phenotypes when we varied the expression patterns of CRY. Under the control of different clock drivers, we observed that as we reduced expression from *timgal4* (expressed in nearly all clock cells) to *crygal4* (only CRY-expressing cells), to *Pdfgal4* (expressed in LNvs) and *timgal4; crygal80* (predominantly dorsal neurons, DNs and three LNdS that do not normally express high levels of CRY), we noticed that under sham conditions the proportion of climbers was generally either intermediate between the mutant and wild-type values or not statistically different from the value of the wild type. For example, *timgal4; crygal80* gave 38% climbers compared with *cry*⁰² 16% and wild type, 49%. Yet for the *Pdfgal4* and *timgal4; crygal80* drivers there were no significant differences between the sham and EMF conditions, so the EMF response had been lost. However, the *Mai*¹⁷⁹*gal4* driver, which expresses in the LNvs and

three strongly CRY-positive LNd cells^{23,24}, restored the intermediate levels of climbing under sham control as well as the EMF suppression. Comparing this result with that of the *timgal4; crygal80* combination and *Pdfgal4* drivers, it would appear that CRY expressed in the three CRY-positive LNd neurons could be sufficient for restoring both climbing and the EMF responses. The LNd cluster is involved in circadian locomotor responses under light conditions²⁸, providing a rationale for why they may play an important role in the climbing phenotype under blue light. Our results thus provide a new, non-circadian function for the CRY-positive LNds.

The clock neurons are not the only relevant cells for mediating the effects of EMFs. CRY expression in the R8 photoreceptors of pale ommatidia (via *rh5gal4*), or in the R8 yellow ommatidia²⁹ and the Hofbauer-Buchner eyelet (*rh6gal4*)³⁰ or in the R7 cell, is sufficient for robust climbing and EMF responses. Johnston's organ (JO), which is located in the second antennal segment, has been previously implicated in negative geotaxis³¹ and our results with *JOgal4*, which expresses specifically in JO^{31,32}, and *paingal4*, which is more widely expressed in the antennae and some central neurons³³, suggest that CRY expression in JO is sufficient for mediating the effects of EMF. Consequently, there are three separate anatomical foci (LNds, eyes and antennae), where CRY expression in any one is sufficient to restore EMF sensitivity to *cry* mutants. While this might suggest some type of cellular redundancy, severe mutations of the eyes or the antenna, which reduce the climbing response to ~30% do not give a significant further reduction in geotaxis when exposed to EMF. While this might reflect the general behavioural effects of neurological damage in structures that might be required to be intact (even if CRY negative) to generate normal geotactic responses, a similar level of sham climbing is observed in *JO>cry; cry*⁰² flies, which are nevertheless significantly disrupted in climbing on EMF exposure (Fig. 2c). Thus an integrative scenario is suggested, where in the anatomical absence of one structure, CRY expression in the other two cannot compensate to generate an EMF response.

In other insects such as the Monarch butterfly, the antennae play a prominent role in orientation and migration^{34–36}, but it remains to be seen whether *Drosophila*'s ability to respond to magnetic fields has any adaptive function. One well-known switch in geotactic behaviour occurs in the late larval stage, whereby larvae that have spent most of their development digging down into food (positive geotaxis) become negatively geotactic in the late 3rd larval instar before they pupate. The adult's escape response also involves negative geotaxis, yet whether the Earth's magnetic field (or CRY) plays any role in these adaptive phenotypes has not been studied, to our knowledge. In conclusion, our results have identified a novel and robust CRY-dependent behavioural phenotype in *Drosophila* that responds to EMFs, and which may be extremely useful for further neurogenetic dissection of the cellular and molecular basis of magnetosensitivity.

Methods

Fly strains. Flies were maintained in LD 12:12 at 25 °C. Canton-S flies, *cry*⁰² and all *gal4* drivers and mutants (including UAS transgenes) were backcrossed into a *w¹1¹⁸* background for 5–7 generations. *timGAL4*, *UAScry24b* and *UASHAcry* and CRYΔ mutants (refs 26,37) were further crossed into a *cry*⁰² background³⁸ using standard balancing techniques. *JOgal4* and *crygal80* were recombined onto the third chromosome carrying *cry*⁰². *UASmychCRY1/2* and *cryW342F* strains were obtained from Steven Reppert (University of Massachusetts). *R7gal4*, *rh5gal4*, *rh6gal4*, *R7gal4*, *Antp*^R, *paingal4* and *eya*² strains were obtained from the Bloomington stock centre (IN, USA). *Mai*¹⁷⁹*gal4* was obtained from Francois Rouyer (Gif, Paris).

Behavioural apparatus. An EMF delivery system was designed consisting of an aluminium box placed in a temperature-controlled room, containing two double-wrapped (50 windings each) Helmholtz coils³⁹ that allow sham and EMF

exposures to be generated. A constant static magnetic field of 500 μT was produced by the coils through a power pack (Fig. 1a). Ten, 2–3-day-old males were placed in a plastic vial and tapped to the bottom by means of a custom-made ‘swinger’ that allowed three vials to be tapped to the bottom simultaneously with exactly equal force (Fig. 1b). An infrared webcam (Logitech) was used to film the flies. Flies that were able to reach a vertical height of 15 cm in 15 s were counted as ‘climbers’, and each tube was tested 10 times, with 30 s between each of the first 5 trials, then after a 15-min rest, another 5 trials were performed. The EMF or sham was applied at random after every group of 10 trials. Each set of 10 trials on the swinger ran three different genotypes simultaneously in the three tubes. Experiments were run at 25 °C either in dim blue (450 nm, 40 nm range) or dim red light (635 nm, 20 nm range) using light-emitting diodes with an intensity at the surface of the vials of 0.25 $\mu\text{W cm}^{-2}$. Three biological replicates were used for each genotype, and data were analysed using a multifactorial analysis of variance with repeated measures⁴⁰. All statistical analyses in this study were performed using GraphPad Prism version 6.00 for Windows, (GraphPad Software, La Jolla, CA, USA) and STATISTICA (data analysis software system, version 8.0, StatSoft Inc. 2008).

References

- Gould, J. L. Magnetoreception. *Curr. Biol.* **20**, R431–R435 (2010).
- Johnsen, S. & Lohmann, K. J. Magnetoreception in animals. *Phys. Today* **61**, 29–35 (2008).
- Ritz, T., Adem, S. & Schulten, K. A model for photoreceptor-based magnetoreception in birds. *Biophys. J.* **78**, 707–718 (2000).
- Ritz, T., Ahmad, M., Mouritsen, H., Wiltschko, R. & Wiltschko, W. Photoreceptor-based magnetoreception: optimal design of receptor molecules, cells, and neuronal processing. *J. R. Soc. Interface* **7**(Suppl 2): S135–S146 (2010).
- Chaves, I. *et al.* The cryptochromes: blue light photoreceptors in plants and animals. *Annu. Rev. Plant Biol.* **62**, 335–364 (2011).
- Ruan, G. X., Zhang, D. Q., Zhou, T., Yamazaki, S. & McMahon, D. G. Circadian organization of the mammalian retina. *Proc. Natl Acad. Sci. USA* **103**, 9703–9708 (2006).
- Moller, A., Sagasser, S., Wiltschko, W. & Schierwater, B. Retinal cryptochrome in a migratory passerine bird: a possible transducer for the avian magnetic compass. *Naturwissenschaften* **91**, 585–588 (2004).
- Niessner, C. *et al.* Magnetoreception: activated cryptochrome 1a concurs with magnetic orientation in birds. *J. R. Soc. Interface* **10**, 20130638 (2013).
- Stanewsky, R. *et al.* The *cry^b* mutation identifies cryptochrome as a circadian photoreceptor in *Drosophila*. *Cell* **95**, 681–692 (1998).
- Shearman, L. P. *et al.* Interacting molecular loops in the mammalian circadian clock. *Science* **288**, 1013–1019 (2000).
- Froy, O., Chang, D. C. & Reppert, S. M. Redox potential: differential roles in dCRY and mCRY1 functions. *Curr. Biol.* **12**, 147–152 (2002).
- Yuan, Q., Metterville, D., Briscoe, A. D. & Reppert, S. M. Insect cryptochromes: gene duplication and loss define diverse ways to construct insect circadian clocks. *Mol. Biol. Evol.* **24**, 948–955 (2007).
- Gegear, R. J., Casselman, A., Waddell, S. & Reppert, S. M. Cryptochrome mediates light-dependent magnetosensitivity in *Drosophila*. *Nature* **454**, 1014–1018 (2008).
- Yoshii, T., Ahmad, M. & Helfrich-Forster, C. Cryptochrome mediates light-dependent magnetosensitivity of *Drosophila*'s circadian clock. *PLoS Biol.* **7**, e1000086 (2009).
- Phillips, J. B. & Sayeed, O. Wavelength-dependent effects of light on magnetic compass orientation in *Drosophila melanogaster*. *J. Comp. Physiol. A* **172**, 303–308 (1993).
- Wehner, R. & Labhart, T. Perception of the geomagnetic field in the fly *Drosophila melanogaster*. *Experientia* **26**, 967–968 (1970).
- Painter, M. S., Dommer, D. H., Altizer, W. W., Muheim, R. & Phillips, J. B. Spontaneous magnetic orientation in larval *Drosophila* shares properties with learned magnetic compass responses in adult flies and mice. *J. Exp. Biol.* **216**, 1307–1316 (2013).
- Gegear, R. J., Foley, L. E., Casselman, A. & Reppert, S. M. Animal cryptochromes mediate magnetoreception by an unconventional photochemical mechanism. *Nature* **463**, 804–807 (2010).
- Foley, L. E., Gegear, R. J. & Reppert, S. M. Human cryptochrome exhibits light-dependent magnetosensitivity. *Nat. Commun.* **2**, 356 (2011).
- Dodson, C. A., Hore, P. J. & Wallace, M. I. A radical sense of direction: signalling and mechanism in cryptochrome magnetoreception. *Trends Biochem. Sci.* **38**, 435–446 (2013).
- Toma, D. P., White, K. P., Hirsch, J. & Greenspan, R. J. Identification of genes involved in *Drosophila melanogaster* geotaxis, a complex behavioral trait. *Nat. Genet.* **31**, 349–353 (2002).
- Rakshit, K. & Giebultowicz, J. M. Cryptochrome restores dampened circadian rhythms and promotes healthspan in aging *Drosophila*. *Aging Cell* **12**, 752–762 (2013).
- Yoshii, T., Todo, T., Wulbeck, C., Stanewsky, R. & Helfrich-Forster, C. Cryptochrome is present in the compound eyes and a subset of *Drosophila*'s clock neurons. *J. Comp. Neurol.* **508**, 952–966 (2008).
- Grima, B., Chelot, E., Xia, R. & Rouyer, F. Morning and evening peaks of activity rely on different clock neurons of the *Drosophila* brain. *Nature* **431**, 869–873 (2004).
- Rosato, E. *et al.* Light-dependent interaction between *Drosophila* CRY and the clock protein PER mediated by the carboxy terminus of CRY. *Curr. Biol.* **11**, 909–917 (2001).
- Dissel, S. *et al.* A constitutively active cryptochrome in *Drosophila melanogaster*. *Nat. Neurosci.* **7**, 834–840 (2004).
- Biskup, T. *et al.* Variable electron transfer pathways in an amphibian cryptochrome: tryptophan versus tyrosine-based radical pairs. *J. Biol. Chem.* **288**, 9249–9260 (2013).
- Stoleru, D. *et al.* The *Drosophila* circadian network is a seasonal timer. *Cell* **129**, 207–219 (2007).
- Montell, C. *Drosophila* visual transduction. *Trends Neurosci.* **35**, 356–363 (2012).
- Szular, J. *et al.* Rhodopsin 5- and Rhodopsin 6-mediated clock synchronization in *Drosophila melanogaster* is independent of retinal phospholipase C-beta signaling. *J. Biol. Rhythms* **27**, 25–36 (2012).
- Kamikouchi, A. *et al.* The neural basis of *Drosophila* gravity-sensing and hearing. *Nature* **458**, 165–171 (2009).
- Kamikouchi, A., Shimada, T. & Ito, K. Comprehensive classification of the auditory sensory projections in the brain of the fruit fly *Drosophila melanogaster*. *J. Comp. Neurol.* **499**, 317–356 (2006).
- Sun, Y. *et al.* TRPA channels distinguish gravity sensing from hearing in Johnston's organ. *Proc. Natl Acad. Sci. USA* **106**, 13606–13611 (2009).
- Reppert, S. M., Gegear, R. J. & Merlin, C. Navigational mechanisms of migrating monarch butterflies. *Trends Neurosci.* **33**, 399–406 (2010).
- Merlin, C., Gegear, R. J. & Reppert, S. M. Antennal circadian clocks coordinate sun compass orientation in migratory monarch butterflies. *Science* **325**, 1700–1704 (2009).
- de Oliveira, J. F. *et al.* Ant antennae: are they sites for magnetoreception? *J. R. Soc. Interface* **7**, 143–152 (2010).
- Emery, P., So, W. V., Kaneko, M., Hall, J. C. & Rosbash, M. CRY, a *Drosophila* clock and light-regulated cryptochrome, is a major contributor to circadian rhythm resetting and photosensitivity. *Cell* **95**, 669–679 (1998).
- Dolezelova, E., Dolezel, D. & Hall, J. C. Rhythm defects caused by newly engineered null mutations in *Drosophila*'s *cryptochrome* gene. *Genetics* **177**, 329–345 (2007).
- Kirschvink, J. L. Uniform magnetic fields and double-wrapped coil systems: improved techniques for the design of bioelectromagnetic experiments. *Bioelectromagnetics* **13**, 401–411 (1992).
- Winer, B. J. in *Statistical Principles in Experimental Design* 2nd edn (McGraw-Hill, 1971).

Acknowledgements

We are grateful to the Electromagnetic Field Biological Trust for supporting this work. E.W.G. was funded by a BBSRC grant to C.P.K. We thank Jim Metcalfe for his comments on the manuscript and for his advice and encouragement throughout this project. We also thank David Jones in the Biomedical Joint Workshop for his help in designing and building the apparatus.

Author contributions

G.F. performed the experiments; E.W.G. and G.F. designed the apparatus; E.R. and C.P.K. supervised the work; C.P.K. and G.F. analysed the data and co-wrote the manuscript.

Additional information

Competing financial interests: The authors declare no competing financial interests.

Reprints and permissions information is available online at <http://npg.nature.com/reprintsandpermissions/>

How to cite this article: Fedele, G. *et al.* An electromagnetic field disrupts negative geotaxis in *Drosophila* via a CRY-dependent pathway. *Nat. Commun.* 5:4391 doi: 10.1038/ncomms5391 (2014).

 This work is licensed under a Creative Commons Attribution 4.0 International License. The images or other third party material in this article are included in the article's Creative Commons license, unless indicated otherwise in the credit line; if the material is not included under the Creative Commons license, users will need to obtain permission from the license holder to reproduce the material. To view a copy of this license, visit <http://creativecommons.org/licenses/by/4.0/>



Genetic Analysis of Circadian Responses to Low Frequency Electromagnetic Fields in *Drosophila melanogaster*

Giorgio Fedele¹, Mathew D. Edwards², Supriya Bhutani^{1✉a}, John M. Hares^{1✉b}, Manuel Murbach^{3,4}, Edward W. Green^{1✉c}, Stephane Dissel^{1✉d}, Michael H. Hastings², Ezio Rosato¹, Charalambos P. Kyriacou^{1*}

1 Department of Genetics, University of Leicester, Leicester, United Kingdom, **2** Division of Neurobiology, Medical Research Council Laboratory of Molecular Biology, Cambridge, United Kingdom, **3** ITIS Foundation, Zurich, Switzerland, **4** Institute for Biomedical Engineering, University and ETH Zurich, Zurich, Switzerland

Abstract

The blue-light sensitive photoreceptor cryptochrome (CRY) may act as a magneto-receptor through formation of radical pairs involving a triad of tryptophans. Previous genetic analyses of behavioral responses of *Drosophila* to electromagnetic fields using conditioning, circadian and geotaxis assays have lent some support to the radical pair model (RPM). Here, we describe a new method that generates consistent and reliable circadian responses to electromagnetic fields that differ substantially from those already reported. We used the Schuderer apparatus to isolate *Drosophila* from local environmental variables, and observe extremely low frequency (3 to 50 Hz) field-induced changes in two locomotor phenotypes, circadian period and activity levels. These field-induced phenotypes are CRY- and blue-light dependent, and are correlated with enhanced CRY stability. Mutational analysis of the terminal tryptophan of the triad hypothesised to be indispensable to the electron transfer required by the RPM reveals that this residue is not necessary for field responses. We observe that deletion of the CRY C-terminus dramatically attenuates the EMF-induced period changes, whereas the N-terminus underlies the hyperactivity. Most strikingly, an isolated CRY C-terminus that does not encode the Tryptophan triad nor the FAD binding domain is nevertheless able to mediate a modest EMF-induced period change. Finally, we observe that *hCRY2*, but not *hCRY1*, transformants can detect EMFs, suggesting that *hCRY2* is blue light-responsive. In contrast, when we examined circadian molecular cycles in wild-type mouse suprachiasmatic nuclei slices under blue light, there was no field effect. Our results are therefore not consistent with the classical Trp triad-mediated RPM and suggest that CRYs act as blue-light/EMF sensors depending on trans-acting factors that are present in particular cellular environments.

Citation: Fedele G, Edwards MD, Bhutani S, Hares JM, Murbach M, et al. (2014) Genetic Analysis of Circadian Responses to Low Frequency Electromagnetic Fields in *Drosophila melanogaster*. PLoS Genet 10(12): e1004804. doi:10.1371/journal.pgen.1004804

Editor: Paul H. Taghert, Washington University Medical School, United States of America

Received May 22, 2014; **Accepted** October 3, 2014; **Published** December 4, 2014

Copyright: © 2014 Fedele et al. This is an open-access article distributed under the terms of the Creative Commons Attribution License, which permits unrestricted use, distribution, and reproduction in any medium, provided the original author and source are credited.

Data Availability: The authors confirm that all data underlying the findings are fully available without restriction. All summary data are within the paper and its Supporting Information files. Raw data are available from DRYAD (<http://datadryad.org>) with the doi: 10.5061/dryad.j56n4.

Funding: This work was carried out with the aid of Electromagnetic Field Biological Research Trust grants to CPK/ER and to MHH (<http://www.emfbrt.org/>). European Community 6th Framework (EU CLOCK 018741) to CPK (http://ec.europa.eu/research/fp6/index_en.cfm), Biotechnology and Biological Sciences Research Council grant (BB/J005169/1) to CPK and ER (<http://www.bbsrc.ac.uk/home/home.aspx0>) and a BBSRC studentship to JMH. The funders had no role in study design, data collection and analysis, decision to publish, or preparation of the manuscript.

Competing Interests: The authors have declared that no competing interests exist.

* Email: cpk@leicester.ac.uk

^{✉a} Current address: Department of Molecular and Cellular Neurosciences, National Brain Research Centre, Manesar, Haryana, India

^{✉b} Current address: Alliance Pharmaceuticals Limited, Chippenham, United Kingdom

^{✉c} Current address: German Cancer Research Center (DKFZ), Heidelberg, Germany

^{✉d} Current address: Department of Anatomy and Neurobiology, Washington University School of Medicine, St. Louis, Missouri, United States of America

Introduction

A wide range of animals are able to detect and exploit the Earth's magnetic field, particularly for the purposes of orientation and navigation [1–3]. The biological basis for the detection of electromagnetic fields (EMFs) is not understood but two main theories have been presented. The first involves crystals of magnetite (iron oxide, Fe_3O_4) that can be found in the upper beaks of birds [4] or in the nasal regions of salmonid fish [5]. The second suggests that photoreceptors may play a significant role through the radical pair mechanism (RPM) whereby biochemical reactions generate radical pairs that become sensitive to EMFs [6].

One class of photoreceptors that meets the requirements for the RPM is cryptochrome (CRY), a blue-light photoreceptor that in *Arabidopsis* is proposed to mediate the effects of EMFs through electron transfer between a triad of Tryptophan residues and the flavin cofactor FAD [7,8]. In *Drosophila melanogaster*, CRY is the deep-brain photoreceptor that mediates circadian responses to light [9–11], making it a suitable model for studying any link between circadian clock and magnetoreception. In non-drosophilid insects, there can be two CRY homologues, one which plays the circadian photoreceptor role, type 1 CRY, and another, type 2, that acts as the main negative autoregulator for the circadian clock and does not apparently respond to light [12,13]. In

Author Summary

Low frequency electromagnetic fields (EMFs) are associated with electrical power lines and have been implicated in the development of childhood leukemias. However, the Earth also has a natural EMF that animals can detect and which they use in order to navigate and orient themselves, particularly during migrations. One way they might do this is by using specialised photoreceptors called cryptochromes, which when activated by light, generate changes within the molecule that are susceptible to EMFs. Cryptochromes are important components of animal circadian clocks, the 24 hour timers that determine daily behavioral and physiological cycles. We have studied the circadian behavior of the fruitfly and have observed some novel and robust effects of EMFs on the fly's sleep-wake cycle that are mediated by cryptochrome. By using cryptochrome mutants we find that our results do not support the classic model for how this molecule might respond to EMFs. We also show that mammalian cryptochromes can respond to EMF when placed into transgenic *Drosophila*, whereas in mammalian clock neurons, they cannot. Consequently, the EMF responsiveness of cryptochrome is determined by its intracellular environment, suggesting that other, unknown molecules that interact with cryptochrome are also very important.

mammals, there are no Type 1 CRYs but two paralogues of Type 2 CRY, which both act as negative autoregulators of the circadian clock [14,15], but can retain light responsiveness under some conditions [16].

D. melanogaster responds to low intensity EMFs under wavelengths of light to which CRYs are sensitive, but the adaptive implications of these magnetic effects on fly orientation are unclear [17–19]. Recently, the genetic and molecular basis of fly magnetosensitivity has been explored using four different experimental paradigms that have converged on the finding that CRY plays a key role in the EMF response [20,21,29]. In the first paradigm, naïve responses of populations of flies to a static EMF are enhanced by associating the field with sucrose and this conditioned response is eliminated in *cry* mutants [20]. Mutagenesis of tryptophan within the triad (residues Trp-342, Trp-397 and Trp-420 in *Drosophila* CRY) in the FAD chromophore domain, however, did not disrupt the ability of type 1 *cry* transgenes from the Monarch butterfly or *Drosophila* to rescue the EMF response in *cry-null* mutants [22]. Thus it may be that a mechanism other than radical pairs involving the Trp triad is used by Type 1 CRY molecules to sense EMFs. Indeed superoxide radicals and ascorbic acid have been proposed as suitable candidates for forming a radical pair with the FAD [23,24]. Furthermore, Type 2 human hCRY2 was also able to rescue the fly's EMF response in blue light, suggesting that in a *Drosophila* cellular environment, hCRY2 may be photosensitive [25].

In the second paradigm, responses to EMF are explicitly clock-dependent and rely on the observation that in constant dim blue light (LL), circadian periods are usually significantly lengthened beyond 24 h due to constitutive activation of CRY [26]. On applying a static EMF for a number of days, about 50% of wild-type flies either lengthened or shortened their circadian period [21]. This alteration in period on EMF exposure is not observed in *cry* mutants, but as the initial period lengthening due to dim blue light is CRY-dependent, there is no period change for the subsequent EMF exposure to modify. Nevertheless, a relevant observation from this study is that overexpression of CRY in clock neurons leads to a significant decrease in rhythmicity and a

variable enhancement of the period changes during EMF exposure in the few animals that were reported to remain rhythmic under these conditions [21]. In both the conditioning and circadian paradigms, the sensing of EMF by flies is wavelength dependent and focused on the action spectra and absorption characteristics of CRY, which is in the blue and UV range [20,21].

The third paradigm, involves negative geotaxis of adult flies, and is the fly's tendency to walk upwards against gravity. This phenotype is CRY mediated [27,28] and is susceptible to disruption by static EMFs under blue light [29]. In addition, key CRY-expressing structures such as the eyes, the antennae and a subset of circadian clock neurons, contribute to the EMF geotactic phenotype [29]. The fourth paradigm involves a CRY-mediated increase in the recovery time of *Drosophila* larvae from electric shock when they are exposed to a static EMF under blue light [30]. In our study we sought to re-examine the effects of EMF on circadian behavior using the Schuderer apparatus, in which responses to EMF can be studied without interference from the Earth's natural magnetic field or from other local magnetic/radiofrequency fields [31]. Under these more controlled and stringent conditions, there is a highly robust and consistent CRY-dependent period response to extremely low frequency and static EMFs as well as an additional novel locomotor phenotype. Further use of *cry* variants reveals some surprising results, which are difficult to explain with the current RPM. Finally we reveal that the cellular environment of mammalian CRY2 determines whether it is light-sensitive and can respond to EMFs, suggesting that trans-acting factors are critical for CRYs mediation of field effects.

Results

We primarily used 300 μT for our experiments, as this was the intensity used in Yoshii *et al.*, (2009), but we also studied two additional intensities, 90 μT (closer to the Earth's ambient magnetic field) and 1 mT (1000 μT). The minimum frequency possible in the Schuderer apparatus was initially 3 Hz [31] but we also tested 50 Hz (the common frequency in Europe). A subsequent upgrade of the equipment allowed us to also test a static field. Thus the frequencies we used fell within the range of background frequency called the Schumann Resonance [32]. The experimental design was as follows: two groups of flies of the same genotype were studied for seven days under constant dim blue light (LL, hereafter termed pre-exposure) followed by eight days under the same illumination but exposed either to an EMF (EMF exposure) or a sham EMF (sham exposure). The circadian locomotor period was then calculated separately for the pre-exposure and exposure days for each fly and compared (see Methods section for more details). We examined the EMF responses of flies using a standard field intensity of 300 μT with stationary, 3 Hz or 50 Hz frequencies (Figure 1A–C), or using a standard 3 Hz frequency with field intensities of 90, 300 or 1000 μT (1 mT, Figure 1C–E). Irrespective of frequency or intensity of the field, sham-exposed Canton-S (CS) exhibited a lengthening in period between the initial LL pre-exposure and the sham exposure due to the constitutive activation of CRY [26], whereas the EMF-exposed flies showed a significantly shorter period compared to the corresponding sham-exposed flies and to their own pre-exposure (Figure 1, 2A). A three way ANOVA revealed significant effects for EMF frequency ($F_{(2,294)} = 37.28$, $p \sim 0$), exposure to EMF/sham ($F_{(1,294)} = 14.81$, $p < 0.001$), and for the two-way interaction between pre-exposure and EMF/sham ($F_{(1,294)} = 21.73$, $p < 0.01$). Importantly, there was no significant three-way interaction ($F_{(2,294)} = 1.01$, $p = 0.36$), revealing that a

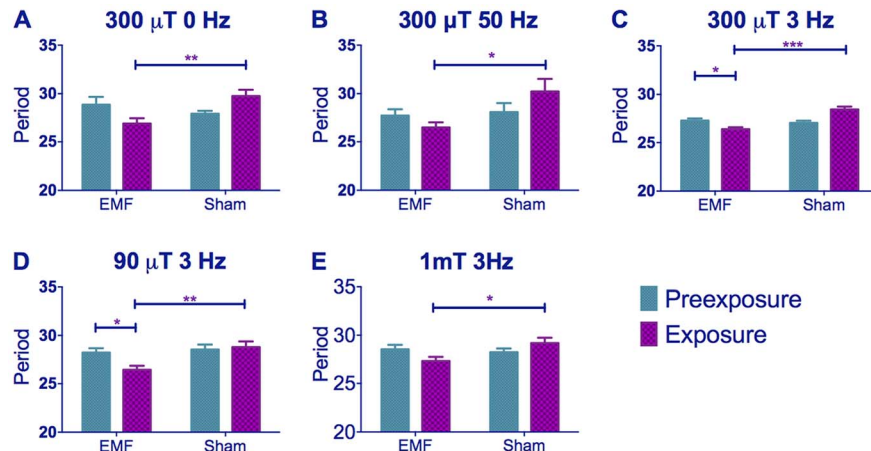


Figure 1. EMF exposure shortens free-running circadian periods in dim blue light. Mean circadian periods (h) \pm SEM are shown for the EMF and sham-exposed groups. Note how periods are considerably longer than 24 h. (A–C) period changes in CS flies under static, 50 and 3 Hz field respectively at 300 μ T (C–E) period changes in CS flies under 300, 90 and 1000 μ T (1 mT) field respectively at 3 Hz. EMF-exposed flies show significant period shortening. For period and N see Table S1. (post-hoc * p <0.05, ** p <0.01, *** p <0.001).

doi:10.1371/journal.pgen.1004804.g001

similar pattern is revealed at all three frequencies at 300 μ T (Figure 1A–C). Three way ANOVA also revealed significant effects for intensity ($F_{(2, 272)} = 23.59$, p <0.001) exposure to EMF/sham ($F_{(1, 272)} = 16.69$, p <0.001) and for the pre-exposure x EMF/sham interaction ($F_{(1, 272)} = 19.38$, p <0.001). There was no significant 3-way interaction ($F_{(2, 272)} = 0.04$, p =0.96) showing that the flies were responding in a similar manner to these exposures at 3 Hz (Figure 1C–E, Table S1).

To study whether any of these effects associated with EMF exposure could be due to artefacts, particularly those caused by any vibration produced by the electric current flowing through the coils or the turning of the fans in each chamber, we performed a number of additional control experiments. However, manipulating the putative sources of vibration did not reveal any effects that could have contributed to our behavioral results (Figure S1).

We therefore pursued our analyses using a 3 Hz/300 μ T EMF to study any effect of the *cry*⁰² null mutation [33]. The response to the EMF was abolished in *cry*⁰² flies (Figure 2B, 3A, Table S1), consistent with a possible role for CRY in determining this phenotype (pre-exposure x EMF/sham exposure interaction $F_{(1, 52)} = 2.93$, p =0.09). However, as mentioned earlier, CRY is required in order to generate the initial blue light-dependent lengthening of period and so these results are not informative in determining whether CRY is the magnetoreceptor. *cry*⁰² flies did show a slight lengthening of period between the pre- and exposure conditions of about 0.5 h ($F_{(1, 52)} = 108.4$, p <0.001, Table S1) suggesting an ageing effect over the ~15 day observation [28]. Indeed we observed a similar period lengthening in CS flies exposed to DD for the same number of days during which CRY would not be light-activated ($F_{(1, 54)} = 14.40$, p <0.001, Figure 3A, Table S1). ANOVA revealed no significant three-way interaction when we compared CS in DD to *cry*⁰² in LL (genotype x pre-exposure x EMF/sham exposure, $F_{(2, 106)} = 0.07$, p =0.79), supporting the view that the slight lengthening of period was due to ageing. This experiment also clearly shows how the period-shortening of CS flies under EMF is light-dependent (Compare Figure 3A in DD with Figure 1C). Consequently the more dramatic lengthening in period of 1–2 h (Figure 1A–E) observed in CS flies in sham conditions under dim blue LL will also include a small ageing component in addition to that generated by constitutive CRY expression (Table S1). The shortening of period

in wild-type flies exposed to EMF is therefore observed in spite of a natural tendency of the flies to increase their period over the duration of the experiment due to ageing (Figure 1, Table S1).

We then overexpressed *cry* in clock cells using *timgal4* and observed that ~55% of the *timgal4>cry* flies in the wild-type background became arrhythmic during the initial LL pre-exposure interval, consistent with a hyper-activation of CRY (Figure 2C, 3B, Table S1). EMF-exposure, however, abrogated arrhythmicity to ~25%, suggesting a disruption of CRY signalling under these conditions, whereas sham-exposed flies showed 67% arrhythmicity ($\chi^2_{(3)} = 13.96$, p <0.05, Figure 3B, 2C, Table S1). Furthermore, the flies that stayed rhythmic throughout the *timgal4>cry* experiment again revealed a significant shortening in period under EMF compared to the sham controls (pre-exposure x EMF/sham exposure interaction $F_{(1, 79)} = 6.23$, p =0.015, Figure 3C, Table S1).

We next examined the responses of the *UAScryW342F* mutant under *timgal4* control in a *cry*⁰² background (Figure S2) [22]. This mutant carries a Trp to Phe substitution in the final Trp forming the Trp triad that is responsible for donating the required electron to the cascade during light activation [34]. Nevertheless, this mutant is light responsive and significantly lengthens its period in dim blue light (Figure S3A, Table S1). We observed a significant period shortening in EMF exposed compared to sham flies (pre-exposure x EMF/sham exposure interaction $F_{(1, 54)} = 4.15$, p <0.05, Figure 3D, Table S1). Consequently mutation of Trp-342 in the triad believed to be necessary for the RPM does not significantly disrupt the circadian response to EMF.

We also used the *UAScryΔ* mutation (Figure S2), again under control of *timgal4*, in which residues 521–540 of the C-terminal have been deleted [26]. *timgal4>cryΔ* flies have a long free-running period in DD as if CRY is constitutively active, but CRYΔ can be further activated by blue light [26,35]. We confirmed this observation by showing that flies carrying *timgal4>cryΔ* in a *cry*-null background showed a lengthening of period of 1.2 h under dim blue light compared to DD ($F_{(1, 34)} = 6.53$, p <0.01, Figure S3B). Surprisingly, however, they did not show any significant period changes under EMF exposure (pre-exposure x EMF/sham Exposure $F_{(1, 174)} = 0.74$, p =0.39, Figure 2D, 3E, Table S1) implicating the C-terminal of CRY (CT) in the response to EMF. We therefore tested flies expressing a

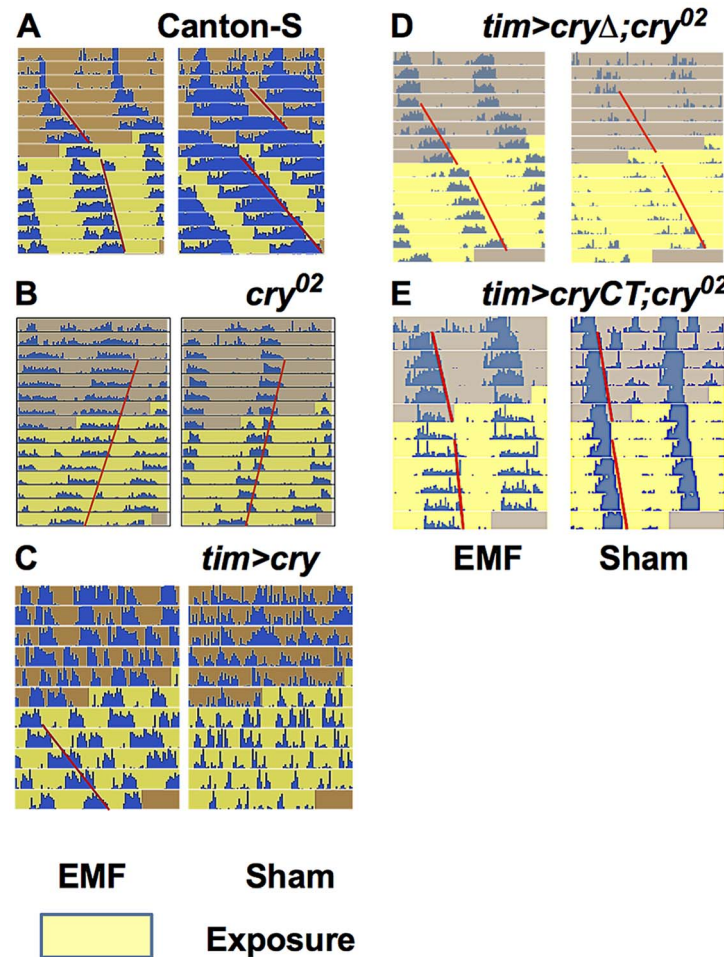


Figure 2. EMF exposure shortens circadian period. Representative free-running locomotor rhythms in dim blue, constant LL before and during the exposure to EMF (300 μ T, 3 Hz). A. Exposed Canton-S flies showed a significant period shortening compared to sham. B. *cry*⁰² flies did not show any EMF effect and maintain their free-run during the exposure period. C. Most exposed *tim>cry* flies showed arrhythmia before, but a well-defined period during the EMF exposure. D. *tim>cryΔ;cry*⁰² are not EMF sensitive. E. *tim>cryCT;cry*⁰² show an EMF effect with a slight period shortening compared to sham exposed flies. Each horizontal line show activity events (blue) double plotted for two successive 24 hour periods, day 1 and 2 on the top line, day 2 and 3 on the second line and so on. The red line outlines the activity offset.

doi:10.1371/journal.pgen.1004804.g002

GFP-CRY-CT (Figure S2) fusion in a *cry*⁰² genetic background (*UASGFPcryCT;timGAL4;cry*⁰²). This construct carries only the CRY C-terminal residues 491–542 fused to GFP (see Methods). Remarkably, these flies were still able to respond to light (Figure S3C) and also show a modest response to the EMF ($F_{(1,118)} = 4.9$, $p < 0.02$; Figure 2E, 3F, Table S1) confirming the importance of the CRY-CT in the EMF response. We also performed the same experiment in DD but we did not observe any significant EMF effect (pre-exposure x EMF/sham exposure $F_{(1,82)} = 0.1$, $p = 0.81$) although we did find the ageing effect on period (pre-exposure vs exposure $F_{(1,82)} = 4.2$, $p < 0.05$). Consequently, for *UASGFP-cryCT;timGAL4;cry*⁰² flies, the slight reduction in period between the pre- and EMF exposure occurs in spite of the ageing effect which would tend to increase period between the two conditions. We should also note here that pre-exposed *UASGFPcryCT;tim-GAL4;cry*⁰² flies have periods very close to 24 h and only 0.4 h longer than their DD controls (Table S1), so there is little room to reduce this period further given that CRY is not a canonical clock molecule. Consequently, it would be difficult to see how any CRY manipulation could yield periods shorter than the DD

free-running period via changes in CRYs light-mediated TIM interactions and consequent input to the clock.

A novel locomotor phenotype is sensitive to EMF

When we scrutinised further our locomotor activity records we observed that exposure to low frequency EMF not only shortened circadian period but it also caused significant hyperactivity in wild-type flies. Comparison of static to 3 and 50 Hz at 300 μ T fields revealed significant Frequency ($F_{(2,294)} = 42.35$, $p \sim 0$), sham/EMF $F_{(1,294)} = 6.75$, $p < 0.01$, pre-exposure/exposure ($F_{(1,294)} = 7.98$, $p < 0.01$) and pre-exposure x EMF/sham exposure interaction ($F_{(1,294)} = 7.93$, $p < 0.001$), but no significant three-way interaction ($F_{(2,294)} = 0.17$, $p = 0.83$) illustrating that all frequencies gave a similar pattern of EMF mediated hyperactivity (Figure 4A–C, Table S2). When we compared 90, 300 and 1000 μ T at 3 Hz we did not observe a significant Intensity effect ($F_{(2,272)} = 2.14$, $p = 0.1$), but sham/EMF ($F_{(1,272)} = 4.66$, $p < 0.05$), pre-exposure/exposure ($F_{(1,272)} = 8.133$, $p < 0.05$) and pre-exposure x EMF/sham exposure interactions ($F_{(1,2272)} = 3.71$, $p = 0.05$) were all significant (Figure 4C–E, Table S2). Post-hoc tests revealed a significant

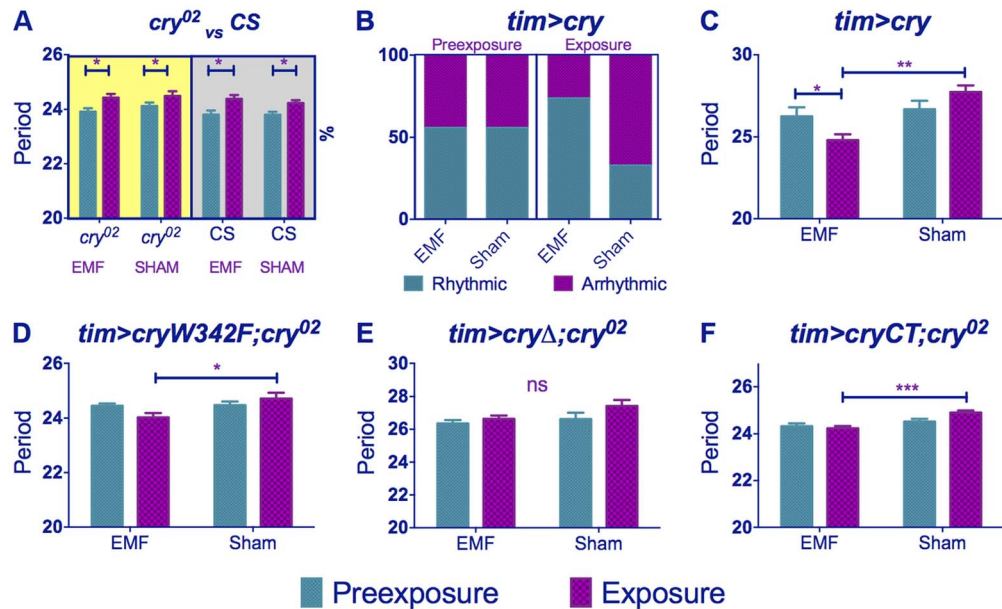


Figure 3. *cry* variants alter normal circadian responses to EMFs. Circadian periods (h) in dim blue LL are shown for EMF and sham-exposed groups. Mean periods \pm sem. (A) *cry⁰²* flies exposed to EMF show only ageing effects on period (yellow shaded box). Wild-type flies kept in DD (grey shaded box) show similar ageing effects (B) *tim>cry* % rhythmic/arrhythmic flies during pre-exposure and exposure to EMF or sham. Exposure to EMF dramatically increases the proportion of rhythmic flies ($\chi^2_{(3)} = 12.78$, $p < 0.01$). (C) *tim>cry* period for EMF exposed and sham flies before and during exposure (D) *tim>cryW342F; cry⁰²* (E) *tim>cryΔ; cry⁰²*. (F) *tim>cryCT; cry⁰²*. (See Table S1, post-hoc * $p < 0.05$, ** $p < 0.01$, *** $p < 0.001$).

doi:10.1371/journal.pgen.1004804.g003

hyperactivity in EMF exposed flies compared to sham at 90 and 300 μ T, but not at 1 mT, but this difference was not sufficient to generate a significant three-way interaction ($F_{(2,272)} = 0.71$, $p = 0.5$).

Similar results were obtained for *timgal4>cry* overexpressing flies (pre-exposure x EMF/sham exposure interaction ($F_{(1,79)} = 4.021$, $p < 0.05$, Figure 5A, Table S2) revealing that EMF-exposed flies showed enhanced hyperactivity compared to sham and pre-exposed flies. More surprisingly, *timgal4>cryΔ* flies also expressed this hyperactivity under EMF exposure (pre-exposure x EMF/sham Exposure interaction $F_{(1,174)} = 11.28$,

$p < 0.01$, Figure 5B, Table S2) whereas no locomotor differences were detected in *cry⁰²* (pre-exposure x EMF/sham exposure interaction, $F_{(1, 52)} = 0.04$, $p = 0.95$, Figure 5C, Table S2) nor in *UASGFPcryCT; timGAL4; cry⁰²* (pre-exposure x EMF/sham interaction, $F_{(1, 118)} = 0.51$, $p = 0.46$, Figure 5D, Table S2). Furthermore flies expressing the *cryW342F* mutation also exhibited the hyperactivity associated with EMF exposure ($F_{(1,54)} = 11.9$ $p < 0.01$, Figure 5E, Table S2). We therefore conclude that while robust EMF-induced shortening of circadian period requires the CRY C-terminus, the hyperactivity appears to be determined via the N-terminal photolyase-like domain and is not susceptible to

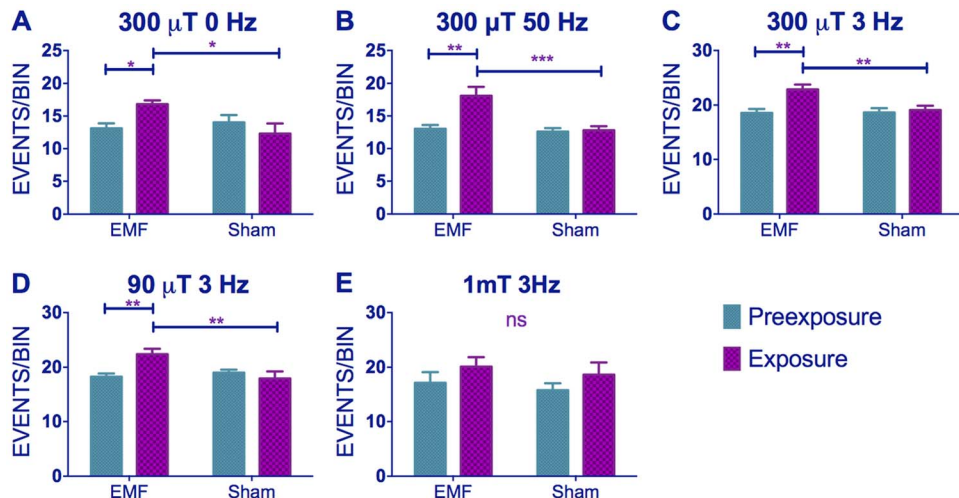


Figure 4. EMFs increase activity levels in wild-type flies. (A-C) Hyperactivity in EMF-exposed CS under static, 50 and 3 Hz field respectively at 300 μ T. (C-E) Hyperactivity in CS flies under 300, 90 and 1000 μ T field respectively at 3 Hz. N's are the same as in Figure 1. Mean activity events per 30 min time bin (\pm sem). For average activity and N refer to Table S2 (post-hoc * $p < 0.05$, ** $p < 0.01$, *** $p < 0.001$).

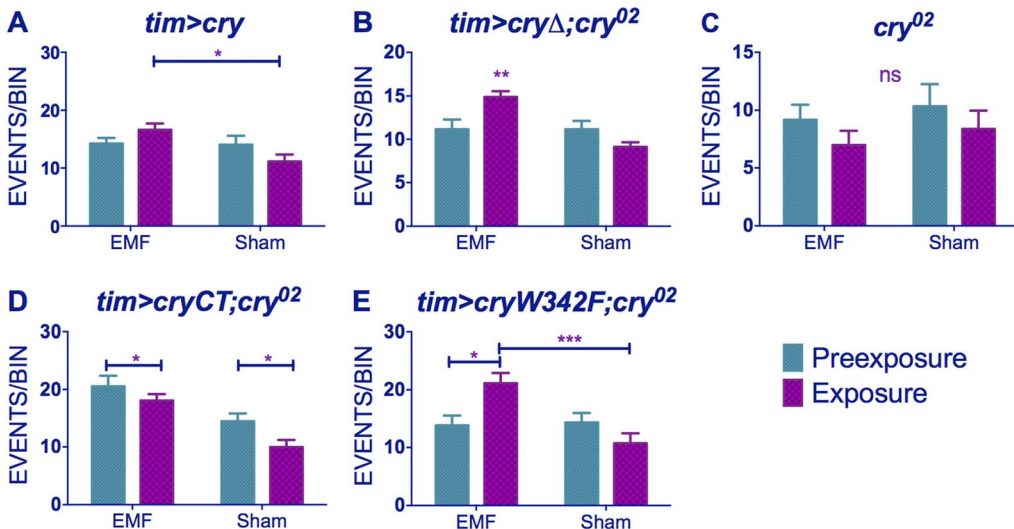


Figure 5. EMF-induced hyperactivity in *cry* variants. (A) *tim>cry* (B) *tim>cryΔ;cry⁰²* (C) *cry⁰²* (D) *tim>cryCT;cry⁰²* (E) *tim>cryW342 F;cry⁰²* N's are the same as in Figure 3. Mean \pm sem. (see Table S2, post-hoc *p<0.05, **p<0.01, ***p<0.001).

doi:10.1371/journal.pgen.1004804.g005

disruption by the Trp-342 mutation, indicating that alternative routes are available for the RPM.

hCRY and magnetoreception

Flies expressing vertebrate non-photoreceptor *hCRY2* are reported to exhibit light-dependent magnetoreception in a conditioning assay [25]. By separately expressing *tim-GAL4>hCRY1* or *hCRY2* on a *cry⁰²* background, we observed no significant differences in period between exposed and sham flies (Figure 6A, B, Table S1). Indeed, the *hCRY1/2* flies behaved as if they did not respond to dim blue LL because their circadian period does not lengthen in LL compared to DD (Figure 6C), although hCRY proteins have been shown to be light degraded in flies [16] (Fig. S3) and *hCRY2* has been implicated in mediating EMF response in a light dependent manner [25]. Nevertheless and somewhat surprisingly, flies expressing *hCRY2* but not *hCRY1* showed the EMF-induced hyperactivity phenotype (*hCRY2* pre-exposure x sham interaction $F_{(1,54)} = 5.69$ p<0.05, Figure 6D, E, Table S2).

Drosophila CRY is stabilised by EMF

Western analysis revealed, that levels of CRY in DD were significantly elevated compared to sham in dim blue light as expected [11], but we also observed that under EMF exposure, CRY was significantly more abundant compared to sham (p<0.001, Figure 7). EMF therefore appears to reduce CRY degradation, which in turn would suggest that CRY signalling is compromised.

Molecular circadian rhythms in mouse SCN slices do not respond to EMFs

Given that the EMF hyperactivity response could be rescued in fly transformants carrying *hCRY2*, we asked whether mammalian type 2 CRYs could also be EMF responsive in a circadian context. We therefore used the Schuderer apparatus to expose SCN slices to EMFs ranging from 50 to 500 μ T at 50 Hz and examined the rhythmic bioluminescence of the PER2:LUC reporter (Figure S4A, B). We have shown previously that these rhythms are dependent on CRY1 and CRY2 [36] SCN slices were housed in

exposure chambers for 5 days with field exposure strengths of 50, 150, 300 and 500 μ T, followed by 5 days in sham conditions of 0 μ T or vice versa in a paired crossover design. All slices generated very clear and sustained circadian cycles of bioluminescence (Figure S4B). No significant differences were observed, however, in period, period error or relative amplitude error (see Methods) between exposed and sham conditions under any of the EMF intensities (Figure S4 C–H). We also compared the effects of blue versus red light with a 300 μ T, 50 Hz field, but again, no significant differences in the three rhythm measures were observed between sham and EMF exposed slices (Figure S5). Thus, if mammalian CRY1 and/or CRY2 have the intrinsic capacity to mediate light-dependent sensing of EMF, the specific CRY-dependent response and/or the intracellular context of the protein may be critical in determining its function.

Discussion

We have identified two light-dependent and robust behavioral responses to EMF in the fly; shortening of circadian period and locomotor hyperactivity. Our findings are consistent with an underlying CRY-dependent magneto-response and importantly confirm and extend the most relevant observation of Yoshii et al (2009), which was that overexpression of CRY in clock neurons enhances the circadian response to EMF. This was observed in two ways in our study, by an increase in the proportion of rhythmicity under EMF in flies overexpressing CRY (55 v. 76%) as well as in an enhanced shortening of circadian period between sham- and EMF-exposed conditions of wild-type versus CRY overexpressing flies (2.07 h \pm 0.34 versus 2.95 h \pm 0.75, respectively Figure 1C, 3C, Table S1). However, these results contrast sharply with those of Yoshii et al [21], who observed a significant decrease in the proportion of rhythmic CRY-overexpressing flies under EMF and a predominant lengthening of period. While both sets of results indirectly support the role of CRY in magnetosensitivity it is unlikely that these differences are solely due to the more controlled EMF environment generated by the Schuderer apparatus.

This contradiction may conceivably be resolved by considering the action spectrum of CRY [16,37] and the ‘antagonistic effect’ of the magnetic field in response to light [38,39]. Under this

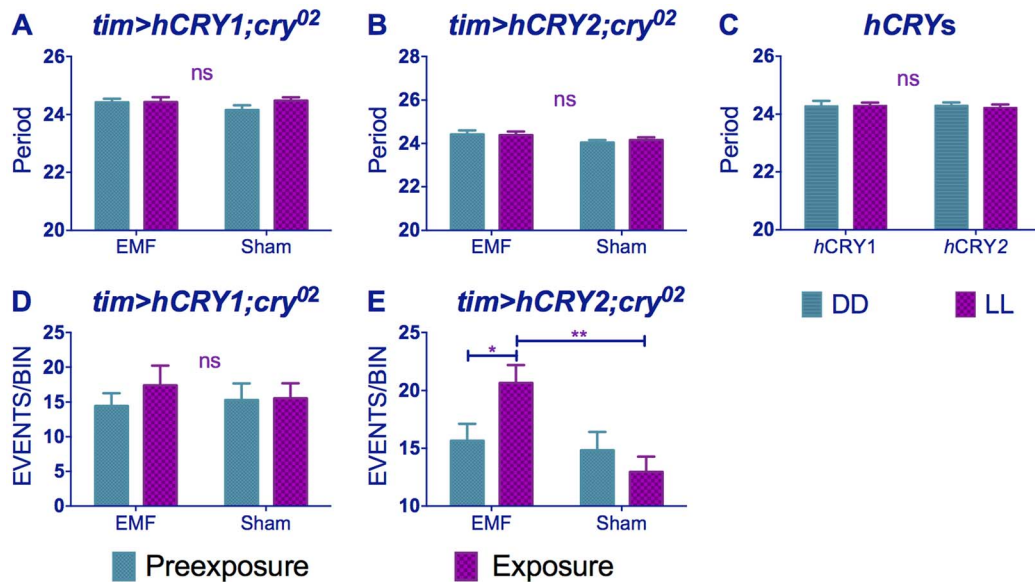


Figure 6. *hCRY2* but not *hCRY1* reveals a sensitivity to EMFs. (A) *tim>hCRY1; cry⁰²* or (B) *tim>hCRY2; cry⁰²* transformants do not show period shortening under EMF (pre-exposure*EMF/sham interaction *hCRY1* $F_{(1,48)}=1.41$, $p=0.3$ *hCRY2* $F_{(1,54)}=0.2$, $p=0.63$ (see Table S1). (C) *hCRY1/2* flies do not show period increase in dim blue LL compared to DD ($F_{(1,82)}=0.125$, $p=0.72$) (D) *hCRY1* are not hyperactive under EMF ($F_{(1,48)}=0.33$, $p=0.56$). (E) *hCRY2* are hyperactive under EMF exposure. Mean \pm sem (see Table S2, post hoc * $=p<0.05$, ** $=p<0.01$).

proposal, the alignment of the magnetic field would produce inverse or complementary responses under different wavelengths that are dependent on the initial ratio of singlet-triplet states of the radical. This antagonistic effect of wavelength was observed in experiments on magnetic compass orientation in *Drosophila*, which under green light (500 nm) showed a 90° shift in their alignment compared to flies tested under violet light (365 nm)

[18]. This wavelength-dependent effect was also proposed to explain why in the EMF conditioning experiments of Geegar *et al.* (2008), flies failed to exhibit a response to EMF under full spectrum light when wavelengths below 420 nm were filtered out [38]. As pointed out by Phillips and co-workers, this failure could be due to a change in the nature of the response rather than an inability of the flies to sense the field. Indeed, the response of naïve

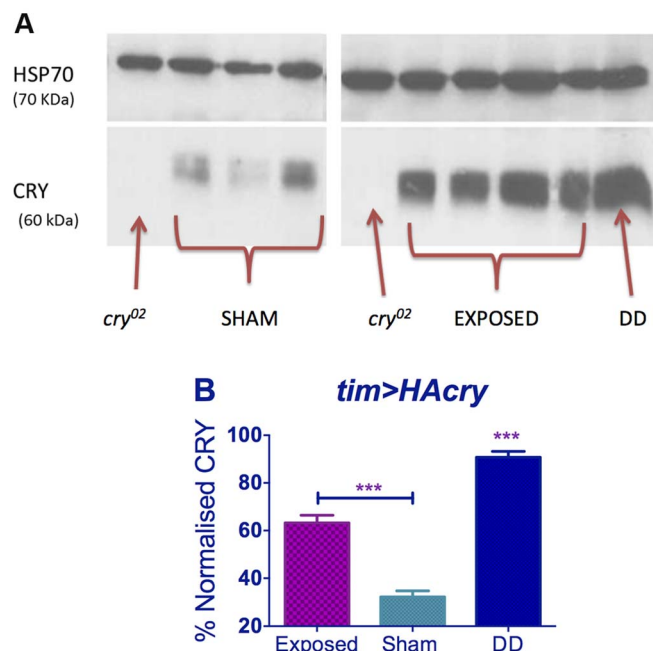


Figure 7. EMF exposure increases CRY stability. Top panel. Western blots for CRY using anti-dCRY in wild-type flies exposed to EMF or sham in dim blue LL with *cry⁰²* and DD control. HSP is used as loading control. Bottom panel. Quantification based on 3 biological replicates each with 3 technical replicates (repeated measures ANOVA $F_{(2,6)}=113.1$, $p<0.001$, post hoc *** $p<0.001$). Mean \pm sem.

flies to EMF under full spectrum and full spectrum >420 nm has opposite directions [20]. However, the wavelengths used in our study (430–470 nm) compared to the previous work (445–495 nm [21] and Helfrich-Forster, pers comm)) would initially not appear to be sufficiently different to engage any such antagonistic effect, so the opposite features of the results of the two studies remains puzzling. In an attempt to solve this conundrum, we exposed flies to 500 nm (+/-20 nm) in the Schuderer apparatus, and were surprised to observe that EMF exposed flies revealed a *period lengthening* rather than the period-shortening we had observed at 450 nm (EMF/Sham Exposure $F_{(1,141)} = 5.12$, $p < 0.05$ and pre-exposure/exposure $F_{(1,141)} = 8.77$, $p < 0.01$, Figure 8). Taken together these results at the different wavelengths favor the RPM and the antagonistic model mentioned above, whereby small changes in wavelengths may result in a different Triplet-Singlet ratio and therefore the S-T interconversions would strongly affect the CRY product yield [38]. This striking result nicely explains why the results of Yoshii *et al.* (2009) are in the opposite direction to ours.

Dim LL lengthens circadian period because activation of CRY alters PER and TIM dynamics, so that nuclear accumulation of these proteins is delayed in s-LNv pacemaker neurons, generating a longer period [26]. The shortening of circadian period observed under EMF thus suggests a partial inactivation of CRY. This interpretation is strongly supported by the results of the western blots, which showed a more stable/abundant CRY under EMF. Upon light absorption, CRY undergoes conformational changes leading to its activation and ultimately to its degradation, which is mediated by E3-ubiquitin ligases [9,11,35,40,41]. Displacement of the CRY C-terminal (CT) induced by light may increase the binding affinity of CRY to its partners, generating more extended positively and negatively charged regions [42]. Thus significantly more abundant CRY under EMF is likely to be due to CRY maintaining a more inactive conformation that attenuates its light-mediated degradation and prevents period-lengthening [43].

The Trp triad has for some years been considered to be indispensable for the photo-induction of CRY by electron transfer to the FAD, and in the *Drosophila* CRY structure, these are Trp342, Trp397 and Trp420 [42,44,45]. A further residue, Trp536 was initially suggested to lie near the FAD binding pocket, potentially representing an electron donor [44] but more recent dCRY structural analyses have residue Phe534 at this location [42,45]. Nevertheless double mutant W397F/W536F proteins remain photo-inducible as measured by light induced proteolysis in a cell assay [46]. In addition, the W397F CRY mutant protein

was effective in light induced TIM proteolysis even at fluences that do not photoreduce flavin [46]. Furthermore, the redox state of flavin played no significant role in light induced CRY conformational changes nor in downstream interactions with JET (but see [43]). These startling results reveal that photoreduction of flavin may not be the primary mechanism that provides CRY light signalling, even though FAD binding is essential [46]. These results have clear implications for the RPM and provide a rationale for why the W342F mutant retains EMF sensitivity in both our circadian and the conditioning assay. However we should add that there is considerable debate at present on the relevance of the redox status of FAD for CRY light signalling [37,42,43,46,47]. We also cannot exclude the possibility that another residue such as tyrosine may complete the electron transfer [48], or that a photolyase-like photocycle could be involved [35,47].

The use of the CRY Δ construct allowed us to decouple the two phenotypic effects of EMF. The period-shortening is significantly attenuated by deletion of the CRY C-terminal, whereas the hyperactivity can be mediated by the N-terminal sequences. According to recent structural analyses of dCRY [42], the deletion of Cys523 in CRY Δ could conceivably alter the photoreduction state of the FAD via Met421 which lies close to Trp397 thereby disrupting electron transfer and, presumably, the EMF-induced period-shortening phenotype. Yet CRY Δ leaves the hyperactivity phenotype intact, suggesting that period-shortening might be more sensitive to disruption of the RPM than hyperactivity. However, this is unlikely because the GFP-CRY-CT construct was competent for inducing modest but significant EMF-induced period shortening compared to its corresponding sham control, if not to the pre-exposed flies, but it did not mediate hyperactivity. As none of the Trp residues of the triad are included in this construct, this result raises further difficulties with the RPM as mediated by the triad. GFP is capable of absorbing blue photons and may trigger an electron transfer [49] so it could be that a GFP-mediated transfer to the CRY-C-terminus required by the RPM is mimicking the wild-type CRY response to EMF, albeit somewhat weakly. Such a model would require the GFP-CRY-CT peptide to have a FAD binding pocket, which is unlikely. Alternatively if there is no electron transfer between GFP and CT, then perhaps the CRY-CT is actually the effector for EMFs and represents the domain capable of transmitting the magnetic information by interactions with downstream molecules not yet identified. This would require another light-sensing molecule because the isolated CRY-CT would not have this ability. Such a model would have the CRY-CT mediating the period shortening EMF phenotype via this unknown light-sensor and disrupting interactions with downstream clock molecules, TIM, JETLAG and RAMSHACKLE [40,41]. The N-terminal could mediate hyperactivity, perhaps via dCRY's known role in mediating light-dependent neuronal firing [50]. However, even though we have demonstrated that a mutation of one of the Tryptophans forming the Trp-triad is not sufficient to abolish the response, we cannot rule out that the Trp-triad is not required for the RPM without simultaneously mutating all three Trp residues.

Finally, of the two hCRYs, both of which have conserved N-terminals but diverged C-terminals compared to dCRY, expression of hCRY2 exhibited the EMF-induced hyperactivity even though neither hCRY responded to LL by increasing period. This result suggests that the C-terminal of hCRYs cannot mediate the downstream events required for period lengthening, which requires interactions with CRYs known *Drosophila* clock partners. However, the hyperactivity phenotype generated by hCRY2 must require a different downstream pathway that requires the more conserved N-terminal sequences. At the primary sequence level,

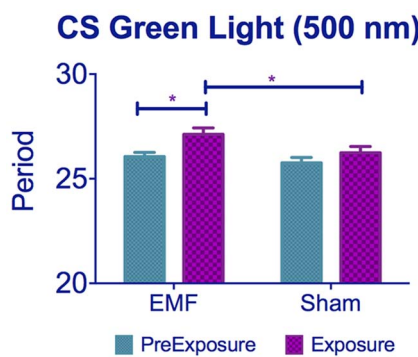


Figure 8. Exposure to 500 nm green light lengthens circadian period under EMF. CS flies kept under 500 nm show period lengthening when exposed to EMF compared to sham flies. See Table S1, post-hoc * $p < 0.05$, *** $p < 0.001$). Mean \pm sem.
doi:10.1371/journal.pgen.1004804.g008

hCRY2 is only marginally more similar to dCRY than hCRY1 (40.4% v 39.4%) in the N-terminal 500 residues, but whether this translates to more similarity in functional features of protein structure to dCRY is not known [42]. Given hCRY2's responsiveness to an EMF in flies, we subsequently examined whether a circadian assay in mouse SCN slices mediated by the endogenous type 2 mCRY1 and mCRY2 could also respond to EMFs. We were unable to demonstrate any significant effects using a number of different field intensities, in both the presence and absence of suitable illumination for CRY photoactivation. These results suggest that mCRY1 and mCRY2 are not photosensitive during the period that they are active as repressors, at least in the context of SCN neurons. There is some debate concerning the photosensitivity of vertebrate CRYs, which can show photoreduction *in vitro* [16]. Indeed, as mentioned earlier, hCRY2 shows a photosensitivity in both the conditioning [25] and our hyperactivity assay (but not in our period-lengthening LL assay), so within a *Drosophila* cellular environment, mammalian CRYs can retain light responses. Within the SCN environment, however, the endogenous mammalian CRYs show no evidence for direct sensitivity to light or EMF. As light information from the retina is transmitted to the SCN by the retinohypothalamic tract [51], perhaps the use of mouse retina, in which CRYs are also expressed at high levels may provide a more appropriate cellular milieu in which to study putative mammalian CRY-mediated responses to EMF.

In conclusion, our results have revealed that under stringently controlled conditions, circadian locomotor behavior can be used to detect two robust CRY-dependent responses to very low frequency EMFs in *Drosophila*. Our results cast further doubt on the RPM for mediating CRY EMF responses in its conventional form via the Trp triad, yet our results with 500 nm resonate with the antagonistic hypothesis, providing further support for the RPM. New putative radical partners have recently been hypothesised such as ascorbic acid [24], so while the RPM retains its validity, it is not yet clear what is the identity of all the essential players. Our future work will aim to identify the neurons and the associated molecular mechanisms that are responsible for these intriguing EMF-mediated phenotypes.

Methods

Drosophila strains

Flies were raised at 25°C on standard yeast-maize medium under a light-dark (LD 12:12) cycle. All strains, mutants, GAL4 and UAS transgenes were backcrossed into a *w¹¹¹⁸* background for 5–7 generations. *UASmychCRY1/2* and *UAScryW342F* were obtained from Steven Reppert (UMass). *timGAL4*, *UAScry24b* [11], *UASHAcry* and *UAScryA14.6* have been described elsewhere [26]. *UAS-GFP-C-terminal-CRY* (*UASGFPcryCT*) flies were crossed into a *cry⁰²* background, using standard balancing techniques.

***UASGFPcryCT* cloning.** This chimeric *cry* construct contains the C-terminal CRY residues 491–542 fused downstream of the GFP gene with an N-terminus tagged with Strep(II). This was generated by amplifying the GFP sequences using a forward primer (*primer-Af*) containing a start codon and the Strep(II) tag and a reverse primer possessing the relevant GFP sequence plus an additional stretch of bases complementary to the *cry* C-terminal sequence. A second amplification used a forward primer encoding a tract of complementary GFP nucleotides and the start of the *cry*-C-terminus with the reverse primer (*primer-Br*) completing the *cry* sequences plus stop codons to terminate translation. The products of the two amplifications were added together after gel-extraction

with *primer-Af* and *primer-Br* to generate the chimeric construct. This was sequenced to check for errors before being inserted into pUAST and outsourced for injection (BestGene, CA, USA).

Behavioral analyses. Circadian locomotor activity was recorded with *Drosophila* Trikinetics Monitors (Waltham, MA) and analysed using spectral analysis and autocorrelograms [52]. To test the effects of EMF on the free-running circadian period of locomotor activity, we used a modified version of the Schuderer apparatus [31], which consists of two independent double-wrapped coils [53] placed inside two μ-metal boxes within a commercial incubator. The shielded, four quadratic Helmholtz coil systems produce a homogenous, linearly polarized *B* field (static or oscillating) with perpendicular orientation to the horizontal plane of the Trikinetics monitors (Figure S6, or the Petri dishes carrying the SCN slices, Figure S4A). Each coil is formed with a pair of wires with the current passing in the same direction through both wires for EMF exposure but in opposite directions to provide a sham exposure condition. A PC randomly selects which of the two chambers receives either the EMF or the sham exposure so the operator is blind to which is the experimental chamber. For the fly experiments we initially chose a 300 μT EMF, the intensity at which the maximal responses had been previously observed [21], oscillating at 3 Hz and in constant blue light (LL) at an intensity of 0.25 μWcm⁻² (LED wavelength 450 nm, 40 nm broad range, RS Component). This LL intensity was operationally selected because 60% of flies remained rhythmic under these conditions so any putative effects of EMF on rhythmicity could be observed in both directions (Figure S7A). In addition, the free-running period of the rhythmic flies in dim blue light was 27.5±0.6 h compared to 24.1±0.4 h in DD (p<0.01, Figure S7B). For the 500 nm experiment the same light intensity was used.

One to three day old flies were first entrained at 25°C in the apparatus under a LD12:12 cycle for three days using white light, before being pre-exposed to continuous dim blue light for seven days, followed by exposure to an EMF or sham for a further eight days under the same blue lighting conditions. Experiments were performed using a static field 3 Hz, 50 Hz each at 300 μT, and also at 90 μT and 1 mT at 3 Hz. Under the RPM, the effect of a superimposed EMF should not be different for static or extremely low frequency fields at the same field intensity, since the oscillations of the field are longer by several orders of magnitude than the radicals' lifetime, which is in the order of microseconds [1]. We observed that under 0.25 μWcm⁻² a 50 Hz oscillating field exposure led to a rate of arrhythmicity in the flies well above 50% and so we reduced the blue light intensity to 0.09 μWcm⁻². The 50 Hz EMF interfered with the circuit for the LEDs causing them to flicker and thereby raising their effective intensity. A radiometer (ILT1400 Lot Oriel) was not able to detect any flickering under static or 3 Hz EMF.

The period was determined during the pre-exposure and during the EMF or sham exposure. Statistical analyses were performed on flies that were rhythmic throughout the experiment, however for some experiments, especially when only a few flies were rhythmic both before and after the exposure, all flies that were rhythmic either before or after the exposure were included in the analysis. General activity levels were calculated for every 30 min bin regardless of period, but only rhythmic flies were included.

dCRY antibody and Western blots

A dCRY anti-serum was generated in guinea-pig against the N-terminal 188 residues of *Drosophila* CRY fused to GST. In three diagnostic CRY tests, western blots of fly heads revealed that the reagent detected a high level of endogenous CRY from wild-type

flies maintained in darkness, which was dramatically reduced in the *cry^b* nearly-null mutant [10], in the *cry⁰²* mutant (Figure 7A) as well as in wild-type flies maintained in both under normal laboratory lighting and in constant dim blue light (Fig. 7 sham condition, [11]). For the EMF or sham blots, flies were harvested after 5 days under constant dim blue light and constant darkness (DD) controls were generated by using flies in vials wrapped in aluminium foil and placed inside the same boxes so exposed to the same EMF or sham conditions. A pool of 100 heads, collected at ZT14, was homogenized in 1.5 volume of extraction buffer (20 mM Hepes, pH 7.5, 100 mM KCl, 2.5 mM EDTA, pH 8, 5% glycerol, 0.5% Triton X-100, 1 mM DTT, complete protease inhibitors tablets from Roche). After quantification *via* Bradford (Sigma) assay, proteins were loaded on a 10% SDS-page and transferred to Nitrocellulose Membrane (GE HealthCare). The following primary antisera were used: mouse Guinea Pig anti-CRY (1:1,000) and mouse anti-HSP70 (Sigma, 1:50,000). Secondary horseradish peroxidase-conjugated antisera were goat anti-guinea pig (ABCam Ltd, 1:10,000) and goat anti-mouse (Sigma, 1:6,000). Signals were obtained by chemiluminescence (ECL, GE HealthCare) and quantified with GelAnalyser 2010 (GelAnalyser.com, Dr Istvan Lazar). Three biological replicates with three technical replicates (ca 30 heads each) were performed.

Western blots on the *UAS-GFP-C-terminal-CRY*, *UAS-cryW342F* and *UASmychCRYI* crossed to *timGAL4* were performed as followed: Ten to fifteen flies were kept in DD for 3 days and during the fourth subjective night (ZT 20–22) were collected. Proteins were extracted as described above. The following primary antisera were used: mouse Guinea Pig anti-CRY (1:1,000, used for *UAS-GFP-C-terminal-CRY*, *UAS-cryW342F*), mouse anti-MYC (Invitrogen, 1:3000, used for *UASmychCRYI*), mouse anti-HSP70 (Sigma, 1:50,000) and mouse anti-TUB α (Sigma, 1:10000, used for *UASmychCRYI*). Secondary horseradish peroxidase-conjugated antisera were goat anti-guinea pig (ABCam Ltd, 1:10,000) and goat anti-mouse (Sigma, 1:6,000). Signals were obtained by chemiluminescence (ECL, GE HealthCare) and quantified with GelAnalyser 2010 (GelAnalyser.com, Dr Istvan Lazar). Three biological replicates with three technical replicates (ca 30 heads each) were performed.

Mouse SCN slices

All animal work carried out in these studies was licensed under the UK Animals (Scientific Procedures) Act 1986, with Local Ethical Review by the MRC. Sacrifice was by cervical dislocation. Wild type (WT) *Per2:Luc* mice, generated by J. Takahashi (University of Texas Southwestern Medical Center, Dallas), were housed under a 12 h light:12 h dark cycle. Brains were removed from pups (P7–P10) and SCN organotypic slices were prepared as previously described [54]. After at least 7 days, SCN slices were transferred to a photon multiplier tube assembly (PMT) for bioluminescence recordings.

EMF exposure for SCN slices

SCN slices were incubated in a Schuderer apparatus-based system, within a light-tight incubator at 37°C, with fibre-optic transmission of bioluminescence signals to a PMT assembly housed outside the incubator to avoid interference with the EMF (Figure S4A). For light exposure, SCN slices were exposed to either 405 nm (blue) or 625 nm (red) light from high-power LEDs (Thorlabs, UK) at 1 μ W/cm² coupled to the fibre-optics used for bioluminescence transmission. Automated control of LEDs and PMT allowed a cycle of intermittent light and bioluminescent recordings consisting of 23 min light exposure, 30 s delay, 6 min

PMT capture, 30 s delay, providing bioluminescence data acquisition every 30 min.

Statistical analyses

Statistical analyses of *Drosophila* locomotor rhythms were performed using spectral analysis implemented in the custom-written BeFly! package [52,55]. Further analyses were carried out using GraphPad Prism version 6.00 for Windows, (GraphPad Software, La Jolla California USA, www.graphpad.com) and STATISTICA (data analysis software system, version 8.0 StatSoft, Inc. 2008, www.statsoft.com). Rhythmic bioluminescence was analysed in BioDare software (A. Millar, University of Edinburgh, UK). A repeated-measure two-way ANOVA was used to test for significant influences of magnetic field exposure and order of field application on circadian period. Period error (a measure of cycle to cycle variability) and relative amplitude error (RAE, an index of the rhythmic coherence of the slice) of SCN bioluminescence was also analysed.

Supporting Information

Figure S1 Period changes are not caused by mechanical vibration. A. When one of the two fans was unplugged from the mains to reduce vibration in one chamber, there were no differences observed in period under dim blue light between wild-type flies in the two chambers ($F_{(1,31)} = 0.17$, $p = 0.68$, $N = 16$ for both conditions) B. When both fans were plugged in for a sham exposure condition, there were no differences observed in period under dim blue light ($F_{(1, 36)} = 1.7$, $p = 0.27$, $N = 18$ and 19). Mean \pm sem.
(TIFF)

Figure S2 Representation of CRY variants used. Bold residues symbolise the position of the mutation: the red-circled “W” indicates that the Trp342 has been substituted with Phe. Red plus green residues indicate the residues used for making the *GFPcryCT* construct whereas green shows the residues deleted in CRY Δ . red zig-zag represents H-alpha and other helices, green arrows are E-beta strand or bridge and blue bars show C-coil.
(TIF)

Figure S3 Light responsiveness of CRY variants. Mean \pm sem and Table S1 shows the periods and Ns. A *tim>cryW342F*; *cry⁰²* flies still show a light responsiveness ($F_{(1,35)} = 3.30$, $p < 0.05$) B *tim>cry4; cry⁰²* overexpressing *cry4* leads to a period-lengthening in dim blue LL compared to DD. C *tim>cryCT; cry⁰²* flies show light responsiveness ($F_{(2,74)} = 32.29$, $p < 0.001$) (post hoc * $p < 0.5$, ** $p < 0.01$, *** $p < 0.001$). D Western blots of *tim>cryW342F; cry⁰²*, *tim>cryCT; cry⁰²* and *tim>hCRYI; cry⁰²* fly heads using anti-dCRY and anti-MYC (for *hCRYI* only) showing that the constructs are expressed and detectable.
(TIFF)

Figure S4 SCN exposure to EMF. (A) Schematic representation of exposure system. Within the incubator are two μ -metal shield boxes that hold up to four SCN each. EMF is generated within the μ -metal shield chambers and SCN bioluminescence is transmitted to a PMT assembly house outside the incubator. Arrows indicate air flow. There are 2 chambers within the incubator holding 4 samples each. (B) Representative recording of *Per2::Luc* bioluminescence from a WT SCN explant. Shading indicates exposure to an oscillating 50 Hz 300 μ T field. (C–E) Paired circadian periods of slices in sham and exposure conditions ($n = 10$ for each exposure strength). (F–H) Grouped data of period (F), period error (G) and relative amplitude error (H) of SCN explants under exposure to different strength, oscillating 50 Hz fields. Error bars = SEM,

$n=10$ for each field strength, except $n=5$ for 150 μT . There are no significant differences between groups.
(TIFF)

Figure S5 No EMF-induced effects by blue or red light on SCN. (A) Representative recording of Per2::Luc bioluminescence from SCN explants under intermittent blue light. Shading indicates duration of field and light exposure. (B) Intermittent blue light exposure alone does not have any effect on the period of SCN slices. (C, D) Paired circadian periods of slices in sham and exposure conditions under blue or red intermittent light. (E-F) Period error and (G-H) relative amplitude error of SCN explants under exposure to different strength oscillating 50 Hz fields. Hatched bars = field exposure, clear bars = sham exposure, +SEM. There are no significant differences between groups, $n=12$ for each condition in C-H.
(TIF)

Figure S6 Schematic representation of the Schuderer Apparatus for flies [31]. The blue arrows represent the air flow through the chambers.
(TIFF)

Figure S7 Rhythmicity of wild-type under different intensities of constant blue light. (A) % of rhythmic CS under different blue light intensities. Heterogeneity $\chi^2_{(4)}=16.19$, $p=0.0028$. (B) Period

lengthening of CS flies under different blue light intensities. $F_{(4,53)}=6.79$, $p<0.001$. $0.16 \mu\text{Wcm}^{-2}=26.80 \pm 0.35$, $N=14$, $0.18 \mu\text{Wcm}^{-2}=26.97 \pm 0.44$, $N=16$; $0.25 \mu\text{Wcm}^{-2}=27.53 \pm 0.64$, $N=12$; $0.40 \mu\text{Wcm}^{-2}=29.04 \pm 1.10$, $N=8$; DD = 24.1 ± 0.40 , $N=8$. (post-hoc * $p<0.05$, ** $p<0.01$, *** $p<0.001$). Mean \pm sem.
(TIFF)

Table S1 Summary of circadian behavior.
(TIFF)

Table S2 Summary of hyperactivity.
(TIFF)

Acknowledgments

We thank the Mechanical Workshop, MRC LMB, especially David Cattermole, Martin Kyte and Philip Heard for adapting the PMT assembly housing for the bioluminescence experiments. We thank Prof. Jim Metcalfe for his advice, encouragement and comments on the manuscript. GF, ER and CPK also thank Dr. Carlo Breda for scientific discussion.

Author Contributions

Conceived and designed the experiments: GF MDE MHH CPK. Performed the experiments: GF MDE. Analyzed the data: GF MDE MHH EWG CPK. Contributed reagents/materials/analysis tools: SB JMH MM SD ER. Wrote the paper: GF MDE MHH CPK.

References

- Kato M (2006) In: Kato M, ed. Electromagnetics in Biology. Tokyo: Springer Japan.
- Johnsen S, Lohmann KJ (2008) Magnetoreception in animals. *Phys Today* 61: 29.
- Gould JL (2010) Magnetoreception. *Curr Biol* 20: R431–5.
- Wiltschko R, Wiltschko W (2013) The magnetite-based receptors in the beak of birds and their role in avian navigation. *J Comp Physiol A* 198: 89–98.
- Eder SHK, Cadiou H, Muhamad A, McNaughton P a, Kirschvink JL, et al. (2012) Magnetic characterization of isolated candidate vertebrate magnetoreceptor cells. *Proc Natl Acad Sci U S A* 109: 12022–12027.
- Ritz T, Adem S, Schulten K (2000) A model for photoreceptor-based magnetoreception in birds. *Biophys J* 78: 707–718.
- Solov'yov I a, Chandler DE, Schulten K (2007) Magnetic field effects in *Arabidopsis thaliana* cryptochrome-1. *Biophys J* 92: 2711–2726.
- Ahmad M, Galland P, Ritz T, Wiltschko R, Wiltschko W (2007) Magnetic intensity affects cryptochrome-dependent responses in *Arabidopsis thaliana*. *Planta* 225: 615–624.
- Emery P, Stanewsky R, Hall JC, Rosbash M (2000) A unique circadian-rhythm photoreceptor. *Nature* 404: 456–457.
- Stanewsky R, Kaneko M, Emery P, Beretta B, Wager-Smith K, et al. (1998) The cryb Mutation Identifies Cryptochrome as a Circadian Photoreceptor in *Drosophila*. *Cell* 95: 681–692.
- Emery P, So WV, Kaneko M, Hall JC, Rosbash M (1998) CRY, a *Drosophila* Clock and Light-Regulated Cryptochrome, Is a Major Contributor to Circadian Rhythm Resetting and Photosensitivity. *Cell* 95: 669–679.
- Zhu H, Yuan Q, Briscoe AD, Froy O, Casselman A, et al. (2005) The two CRYs of the butterfly. *Curr Biol* 15: R953–4.
- Yuan Q, Metterville D, Briscoe AD, Reppert SM (2007) Insect cryptochromes: gene duplication and loss define diverse ways to construct insect circadian clocks. *Mol Biol Evol* 24: 948–955.
- Kume K, Zylka MJ, Sriram S, Shearman LP, Weaver DR, et al. (1999) mCRY1 and mCRY2 are essential components of the negative limb of the circadian clock feedback loop. *Cell* 98: 193–205.
- Okamura H, Miyake S, Sumi Y, Yamaguchi S, Yasui A, et al. (1999) Photic induction of mPer1 and mPer2 in cry-deficient mice lacking a biological clock. *Science* 286: 2531–2534.
- Hoang N, Schleicher E, Kacprzak S, Bouly J (2008) Human and *Drosophila* cryptochromes are light activated by flavin photoreduction in living cells. *PLoS Biol* 6: 1559–1569.
- Wehner R, Labhart T (1970) Perception of the geomagnetic field in the fly *Drosophila melanogaster*. *Experientia*: 967–968.
- Phillips JB, Sayeed O (1992) Wavelength-dependent effects of light on magnetic compass in *drosophila*. *J Comp Physiol A Neuroethol Sens Neural Behav Physiol* 172: 303–308.
- Painter MS, Dommer DH, Altizer WW, Muheim R, Phillips JB (2013) Spontaneous magnetic orientation in larval *Drosophila* shares properties with learned magnetic compass responses in adult flies and mice. *J Exp Biol* 216: 1307–1316.
- Gege R, Casselman A, Waddell S, Reppert S (2008) Cryptochrome mediates light-dependent magnetosensitivity in *Drosophila*. *Nature* 454: 1014–1019.
- Yoshii T, Ahmad M, Helfrich-Förster C (2009) Cryptochrome mediates light-dependent magnetosensitivity of *Drosophila*'s circadian clock. *PLoS Biol* 7: e1000086.
- Gege R, Foley LE, Casselman A, Reppert SM (2010) Animal cryptochromes mediate magnetoreception by an unconventional photochemical mechanism. *Nature* 463: 804–807.
- Müller P, Ahmad M (2011) Light-activated cryptochrome reacts with molecular oxygen to form a flavin-superoxide radical pair consistent with magnetoreception. *J Biol Chem* 286: 21033–21040.
- Lee AA, Lau JCS, Hogben HJ, Biskup T, Kattnig DR, et al. (2014) Alternative radical pairs for cryptochrome-based magnetoreception Alternative radical pairs for cryptochrome-based magnetoreception. *J R Soc Interface* 11: 20131063.
- Foley LE, Gege R, Reppert SM (2011) Human cryptochrome exhibits light-dependent magnetosensitivity. *Nat Commun* 2: 356.
- Disse S, Codd V, Fedir R, Garner KJ, Costa R, et al. (2004) A constitutively active cryptochrome in *Drosophila melanogaster*. *Nat Neurosci* 7: 834–840.
- Toma DP, White KP, Hirsch J, Greenspan RJ (2002) Identification of genes involved in *Drosophila melanogaster* geotaxis, a complex behavioral trait. *Nat Genet* 31: 349–353.
- Rakshit K, Giebelowicz JM (2013) Cryptochrome restores damped circadian rhythms and promotes healthspan in aging *Drosophila*. *Aging Cell* 12: 752–762.
- Fedele G, Green EW, Rosato E, Kyriacou CP (2014) An electromagnetic field disrupts negative geotaxis in *Drosophila* via a CRY-dependent pathway. *Nat Commun* 5: 4391.
- Marley R, Giachello CNG, Scrutton NS, Baines RA, Jones AR (2014) Cryptochrome-dependent magnetic field effect on seizure response in *Drosophila* larvae. *Sci Rep* 4: 5799.
- Schuderer J, Oesch W, Felber N, Spät D, Kuster N (2004) In vitro exposure apparatus for ELF magnetic fields. *Bioelectromagnetics* 25: 582–591.
- Volland H (1995) Handbook of Atmospheric Electrodynamics, Volume 1. CRC Press.
- Dolezelova E, Dolezel D, Hall JC (2007) Rhythm defects caused by newly engineered null mutations in *Drosophila*'s cryptochrome gene. *Genetics* 177: 329–345.
- Dodson C a, Hore PJ, Wallace MI (2013) A radical sense of direction: signalling and mechanism in cryptochrome magnetoreception. *Trends Biochem Sci* 38: 435–446.
- Ozturk N, Selby C, Annayev Y, Zhong D, Sancar A (2011) Reaction mechanism of *Drosophila* cryptochrome. *Proc Natl Acad Sci U S A* 108: 516–521.
- Maywood ES, Chesham JE, O'Brien JA, Hastings MH (2011) A diversity of paracrine signals sustains molecular circadian cycling in suprachiasmatic nucleus circuits. *Proc Natl Acad Sci U S A* 108: 14306–14311.
- Berndt A, Kottke T, Breitkreuz H, Dvorsky R, Hennig S, et al. (2007) A novel photoreaction mechanism for the circadian blue light photoreceptor *Drosophila* cryptochrome. *J Biol Chem* 282: 13011–13021.

38. Phillips JB, Jorge PE, Muheim R (2010) Light-dependent magnetic compass orientation in amphibians and insects: candidate receptors and candidate molecular mechanisms. *J R Soc Interface* 7 Suppl 2: S241–56.
39. Nießner C, Denzau S, Stappert K, Ahmad M, Peichl L, et al. (2013) Magnetoreception: activated cryptochrome 1a concurs with magnetic orientation in birds. *J R Soc Interface* 10: 20130638.
40. Peschel N, Chen KF, Szabo G, Stanewsky R (2009) Light-Dependent Interactions between the *Drosophila* Circadian Clock Factors Cryptochrome, Jetlag, and Timeless. *Curr Biol* 19: 241–247.
41. Ozturk N, VanVickle-Chavez SJ, Akileswaran L, Van Gelder RN, Sancar A (2013) Ramshackle (Brwd3) promotes light-induced ubiquitylation of *Drosophila* Cryptochrome by DDB1-CUL4-ROC1 E3 ligase complex. *Proc Natl Acad Sci U S A* 110: 4980–4985.
42. Czarna A, Berndt A, Singh HR, Grudziecki A, Ladurner AG, et al. (2013) Structures of *Drosophila* cryptochrome and mouse cryptochromel provide insight into circadian function. *Cell* 153: 1394–1405.
43. Vaidya AT, Top D, Manahan CC, Tokuda JM, Zhang S, et al. (2013) Flavin reduction activates *Drosophila* cryptochrome. *Proc Natl Acad Sci U S A* 110: 20455–20460.
44. Zoltowski BD, Vaidya AT, Top D, Widom J, Young MW, et al. (2011) Structure of full-length *Drosophila* cryptochrome. *Nature* 480: 396–399.
45. Levy C, Zoltowski BD, Jones AR, Vaidya AT, Top D, et al. (2013) Updated structure of *Drosophila* cryptochrome. *Nature* 495: E3–4.
46. Ozturk N, Selby CCP, Zhong D, Sancar A (2013) Mechanism of Photosignaling by *Drosophila* Cryptochrome: Role of the Redox Status of the Flavin Chromophore. *J Biol Chem* 289: 4634–4642.
47. Ozürk N, Song S-H, Selby CP, Sancar A (2008) Animal type 1 cryptochromes. Analysis of the redox state of the flavin cofactor by site-directed mutagenesis. *J Biol Chem* 283: 3256–3263.
48. Biskup T, Paulus B, Okafuji A, Hitomi K, Getzoff ED, et al. (2013) Variable electron transfer pathways in an amphibian cryptochrome: tryptophan versus tyrosine-based radical pairs. *J Biol Chem* 288: 9249–9260.
49. Bogdanov AM, Mishin AS, Yampolsky IV, Belousov V V, Chudakov DM, et al. (2009) Green fluorescent proteins are light-induced electron donors. *Nat Chem Biol* 5: 459–461.
50. Fogle KJ, Parson KG, Dahm N a, Holmes TC (2011) CRYPTOCHROME is a blue-light sensor that regulates neuronal firing rate. *Science* 331: 1409–1413.
51. Foster RG, Hankins MW (2007) Circadian vision. *Curr Biol* 17: R746–51.
52. Rosato E, Kyriacou CP (2006) Analysis of locomotor activity rhythms in *Drosophila*. *Nat Protoc* 1: 559–568.
53. Kirschvink JL (1992) Uniform magnetic fields and double-wrapped coil systems. *Bioelectromagnetics* 13: 401–411.
54. Hastings MH, Reddy AB, McMahon DG, Maywood ES (2005) Analysis of circadian mechanisms in the suprachiasmatic nucleus by transgenesis and biolistic transfection. *Methods Enzymol* 393: 579–592.
55. Allebrandt K V, Amin N, Müller-Myhsok B, Esko T, Teder-Laving M, et al. (2013) A K(ATP) channel gene effect on sleep duration: from genome-wide association studies to function in *Drosophila*. *Mol Psychiatry* 18: 122–132.